Fall 2016

Adaptive consensus based formation control of unmanned vehicles

Haci Mehmet Guzey

Follow this and additional works at: https://scholarsmine.mst.edu/doctoral_dissertations

Part of the Electrical and Computer Engineering Commons

Department: Electrical and Computer Engineering

Recommended Citation

Guzey, Haci Mehmet, "Adaptive consensus based formation control of unmanned vehicles" (2016). *Doctoral Dissertations*. 2537.

https://scholarsmine.mst.edu/doctoral_dissertations/2537

ADAPTIVE CONSENSUS BASED FORMATION CONTROL OF UNMANNED

VEHICLES

by

HACI MEHMET GUZEY

A DISSERTATION

Presented to the Faculty of the Graduate School of the

MISSOURI UNIVERSITY OF SCIENCE AND TECHNOLOGY

In Partial Fulfillment of the Requirements for the Degree

DOCTOR OF PHILOSOPHY

In

Electrical Engineering

2016

Approved by:
Dr. Jagannathan Sarangapani, Advisor
Dr. Levent Acar, Co-advisor
Dr. Maciej Zawodniok
Dr. Kelvin Todd Erickson
Dr. Cihan Dagli

PUBLICATION DISSERTATION OPTION

This dissertation consists of the following four articles that have been submitted for publication. The papers are formatted according to Missouri University of Science and Technology specifications.

Pages 13-60: The article entitled "Neural Network-based Finite Horizon Optimal Adaptive Consensus Control of Mobile Robot Formation" was published in the International Journal of Optimal Control Applications and Methods in Nov. 2015.

Pages 61-107: The article entitled "Hybrid Consensus-based Control of Nonholonomic Mobile Robot Formations" is submitted to the Journal of Intelligent and Robotic Systems.

Pages 108-158: The article entitled "Distributed Consensus-based Event-triggered Approximate Control of Nonholonomic Mobile Robot Formations" is submitted to IEEE Transactions on System Man and Cybernetics.

Pages 159-210: The article entitled "Consensus-based Output Feedback Control of Quadrotor UAV Formations Using Neural Networks" will be submitted to the International Journal of Advanced Robotic Systems.

ABSTRACT

Over the past decade, the control research community has given significant attention to formation control of multiple unmanned vehicles due to a variety of commercial and defense applications. Consensus-based formation control is considered to be more robust and reliable when compared to other formation control methods due to scalability and inherent properties that enable the formation to continue even if one of the vehicles experiences a failure. In contrast to existing methods on formation control where the dynamics of the vehicles are neglected, this dissertation in the form of four papers presents consensus-based formation control of unmanned vehicles-both ground and aerial, by incorporating the vehicle dynamics.

First, neural networks (NN)-based optimal adaptive consensus-based formation control over finite horizon is presented for networked mobile robots or agents in the presence of uncertain robot/agent dynamics and communication. In the second paper, a hybrid automaton is proposed to control the nonholonomic mobile robots in two discrete modes: a regulation mode and a formation keeping mode in order to overcome well-known stabilization problem. The third paper presents the design of a distributed consensus-based event-triggered formation control of networked mobile robots using NN in the presence of uncertain robot dynamics to minimize communication. All these papers assume state availability.

Finally, the fourth paper extends the consensus effort by introducing the development of a novel nonlinear output feedback NN-based controller for a group of quadrotor UAVs.

ACKNOWLEDGEMENTS

TABLE OF CONTENTS

LIST OF ILLUSTRATIONS

1. INTRODUCTION

Over the last few decades, the control research community has given significant attention to formation control of multiple unmanned vehicles. These vehicles can be very beneficial for numerous tasks when compared to a single, heavily equipped vehicle, which may require much more power and lack the robustness needed to avoid failure. For example, in military missions, a group of autonomous vehicles are required to keep in a specified formation for area coverage and reconnaissance; hence, multiple vehicles can complete tasks requiring a large area coverage much faster than a single vehicle. Therefore, the coordination of multiple wheeled robots, unmanned air/ocean vehicles, satellites, aircraft and spacecraft [1]–[8] have been investigated as applications of vehicle formation control.

Consensus-based formation control [4]–[8] is considered to be more robust and reliable when compared to other formation control methods due to scalability [4], [7] and inherent properties that enable the formation to continue even if one of the robots experiences a failure. In consensus-based formation control, the robots share information regarding their position errors from their respective goal positions. The shared information is then synthesized into a control law which seeks to achieve the same position error for all robots until each robot has reached its goal position. The desired formation is achieved and maintained by reaching and maintaining consensus on the position errors. Therefore, the main tasks in consensus-based formation control are described as: i) given an initial state, achieve a desired formation, and ii) maintain this formation while the robots move through

the environment to reach their desired goal position. Completing task ii) is equivalent to solving the regulation problem for the formation.

In earlier works [1]–[4], consensus-based schemes have been studied for generalized linear systems with known system dynamics and applied to systems with time varying communication graphs [8], bounded disturbances [9], and communication delays during state information sharing [4]. In addition, the majority of consensus-based formation control methods for mobile robots [10]–[12] also takes into consideration linearized robot dynamics for a controller design. In contrast, nonlinear robot dynamics play a vital role [13] in maintaining a predefined formation as shown before.

The consensus-based optimal formation control scheme was also introduced in [14]. Similar to the aforementioned approaches [4]–[8], optimal control [14] was designed for linearized robot dynamics in a backward-in-time manner and requires complete knowledge of the robots' system dynamics. The backward-in-time solution for optimal control is not suitable for practical implementation.

Various schemes [15]–[17] are now available in the literature to solve the optimal control online and the forward in time movements with complete or partial knowledge of the system dynamics. These online approaches, referred to as adaptive dynamics programming (ADP) [16], [17], require a significant number of iterations [18] to maintain stability. However, to control the robot formation, both iterative [16] and backward-in-time techniques [19] are unsuitable [18] because an insufficient number of iterations can lead to instability.

In the event-sampled framework [20]–[23], the measured state vector is sampled based on certain state dependent criteria referred to as the event-triggering condition, and

the controller is executed at these aperiodic sampling instants. The event-triggering condition is designed by taking into account the stability and the closed-loop performance, and hence, it's proven to be advantageous over its periodic counterpart.

Initially, the event-triggered techniques from [20],[22],[23] were designed for ensuring stable operations of the closed-loop system by assuming that a stabilizing controller exists for the system under consideration. Developing an event-triggering condition and establishing the existence of positive inter-event time with the proposed event-sampling condition was the main focus in these works [20],[22],[23]. An event-sampled adaptive controller design was presented in [21] for physical systems with uncertain dynamics.

Quadrotor UAVs are easier to build and maintain when compared to conventional helicopters [24]. However, the dynamics of the quadrotor UAVs are not only nonlinear, but also coupled and under-actuated. They have six degree of freedom and can be modeled as having four independent control inputs; one for elevation adjustments and three rotational control inputs. Many controller schemes are proposed in the literature for trajectory tracking problems of quadrotors [25]-[26], where the control objective is to track the Cartesian position and a yaw angle. Others research focused on ways to control a group of quadrotor UAVs [24]-[35].

The quadrotor UAV leader-follower formation controller design was introduced in [27] while considering the fourth order linearized dynamics of quadrotors. A relative distance approach is utilized for adaptive leader-follower formation keeping when the GPS signal lost in [31]. The nonlinear quadrotor dynamics are assumed to both be known [27],[31] . An NN based adaptive formation controller is developed for quadrotor UAVs

in [24]. The availability of position, orientation and velocities of the follower as well as the leader for the leader-follower based formation controller design in [24] is quite a strong assumption as it may not be practical. Further, there are several limitations of leader-follower based formation control over the consensus-based approach.

1.1   ORGANIZATION OF THE DISSERTATION

The dissertation is organized as it is shown in Figure 1.1. For nonholonomic systems, the regulation problem is not straightforward due to nonholonomic constraints and Brockett's theorem. In [36], the robot kinematics were transformed into polar coordinates to satisfy Brockett's theorem, and control velocities were developed to solve the regulation problem. However, the work in [36] assumed perfect velocity tracking and did not consider the robot dynamics. In addition, several others [4]–[8] have considered consensus-based formation control but failed to consider velocity tracking error dynamics in their controller design.

Motivated by the aforementioned limitations of existing stabilizing consensus [4]–[8] controllers, adaptive dynamic programming (ADP) controllers [15]–[17] and the optimal consensus controller [14] , a novel online, forward-in-time, finite horizon optimal adaptive formation control is proposed for mobile robots by modeling the robots as nonlinear continuous-time systems in affine form in the first paper. A novel value function is introduced as a quadratic function of consensus-based formation keeping, regulation errors of each individual robot and control inputs.

The ADP is utilized to solve the optimal control by using two neural networks (NNs). One NN is used to identify the unknown mobile robot formation dynamics and the

other is utilized to approximate the time varying value function, which becomes the solution of the HJB equation.

Both the NN estimation error and the Hamiltonian estimation convergence have been proven to show that the estimated value function becomes the solution of the HJB equation. The identified formation dynamics and the approximated time-varying value function were subsequently utilized for designing the optimal control policy for each robot. The NN weights were updated by using a novel update law, which is derived by using both the Lyapunov stability technique and to minimize formation keeping regulation and terminal constraint errors. An initial admissible controller is not needed.

In the second paper, the limitations of existing stabilizing consensus [4]–[8] and regulation controllers [36] are considered and a novel time-varying velocity tracking error system is designed to solve the formation regulation control problem with guaranteed performance for nonholonomic wheeled mobile robots. A hybrid automaton is proposed to control the nonholonomic mobile robots with nonlinear dynamics in two discrete modes: a regulation mode and a formation keeping mode. The regulation mode drives each robot to a constant goal position while the formation-keeping mode ensures that the robots achieve and maintain a specified geometric formation *prior* to reaching their goal position to solve the formation regulation problem.

In order to avoid hard switches between regulation and formation keeping modes, a novel blended time-varying velocity tracking error approach is developed. The blended error approach ensures the robots' velocity tracking errors and control torques are continuous at the switching conditions. Time-varying Lyapunov functions are used in conjunction with multiple Lyapunov methods [37] to provide stability of the hybrid system.

Unlike current approaches available in [4]-[7], this work considers the kinematics and dynamics of each mobile robot as well as the formation.

The third paper describes the development of an adaptive event-based distributed formation control of mobile robots wherein the dynamics of the individual robot and the controlled formation are explicitly taken into account. The NN are utilized as function approximators to learn the dynamics of each mobile robot in the formation. Traditionally, adaptive NN controllers require more computations when compared to the proportional-integral-derivative (PID) controllers whereas event sampling of feedback reduces computations for adaptive formation control. Moreover, since the mobile robots need location and velocity information from neighborhood robots to reach consensus, they share their information with each other through a resource-limited communication network. Therefore, utilizing the communication network in an event sampled context can lead to minimizing network congestion and undesired performance of the controller.

However, event-based sampling can make stability analysis complex and a suitable adaptive sampling condition is needed to obtain consensus-based formation errors. These formation errors are then utilized to obtain the desired velocities for each robot in order to drive the robots to a predefined formation as a tracking problem. Further, to determine the formation error, a unique virtual cart is defined using the regulation errors of the neighborhood robots in the network. However, due to the dynamics of each robot, a persistent velocity tracking error continues to exist. Using the NN-based representation of the mobile robot dynamics, the control inputs can be obtained to minimize this velocity tracking error with event-sampled feedback.

It is worth mentioning that the velocity tracking errors of each robot acts as a virtual subsystem for the formation error subsystem. Thus, by using the distributed back-stepping controller design, the velocity tracking errors are reduced leading to fewer formation errors and the robots reach a desired formation. The overall control scheme is distributed since the controllers for each robot are designed using a consensus-based formation error, which is a function of the position and velocity of all the robots.

Since the unknown NN weights are tuned at the event-sampled instants, computations were reduced when compared to traditional NN and adaptive control schemes, but the innovation also introduced aperiodic weight tuning. A novel event-sampling condition was derived, in such a way that the robots use locally available information and previous information from others to determine the feedback instants thereby reducing communication costs and ensuring stability and performance of the overall formation due to this intermittent feedback. In other words, the event-sampling mechanism enables asynchronous broadcast of position and velocity information, reducing network congestion. Finally, the extension of the Lyapunov direct method is used to prove the local uniform ultimate boundedness (UUB) of the tracking and the parameter estimation errors with event-sampled feedback.

The fourth paper presents the development of a novel consensus-based output feedback formation controller for a group of quadrotor UAVs in the presence of uncertain quadrotor dynamics. The leader quadrotor UAV is assumed to track a pre-defined desired trajectory while the others have no knowledge of the desired trajectory. Since the NN-based output feedback controller has already been developed for a single UAV in [35], it was briefly introduced in the fourth paper and utilized to demonstrate the control of a leader

UAV. In this UAV leader controlled setup, follower UAVs only need the position and orientation of the quadrotor UAVs in the neighborhood, thereby relaxing the need for linear and angular velocities.
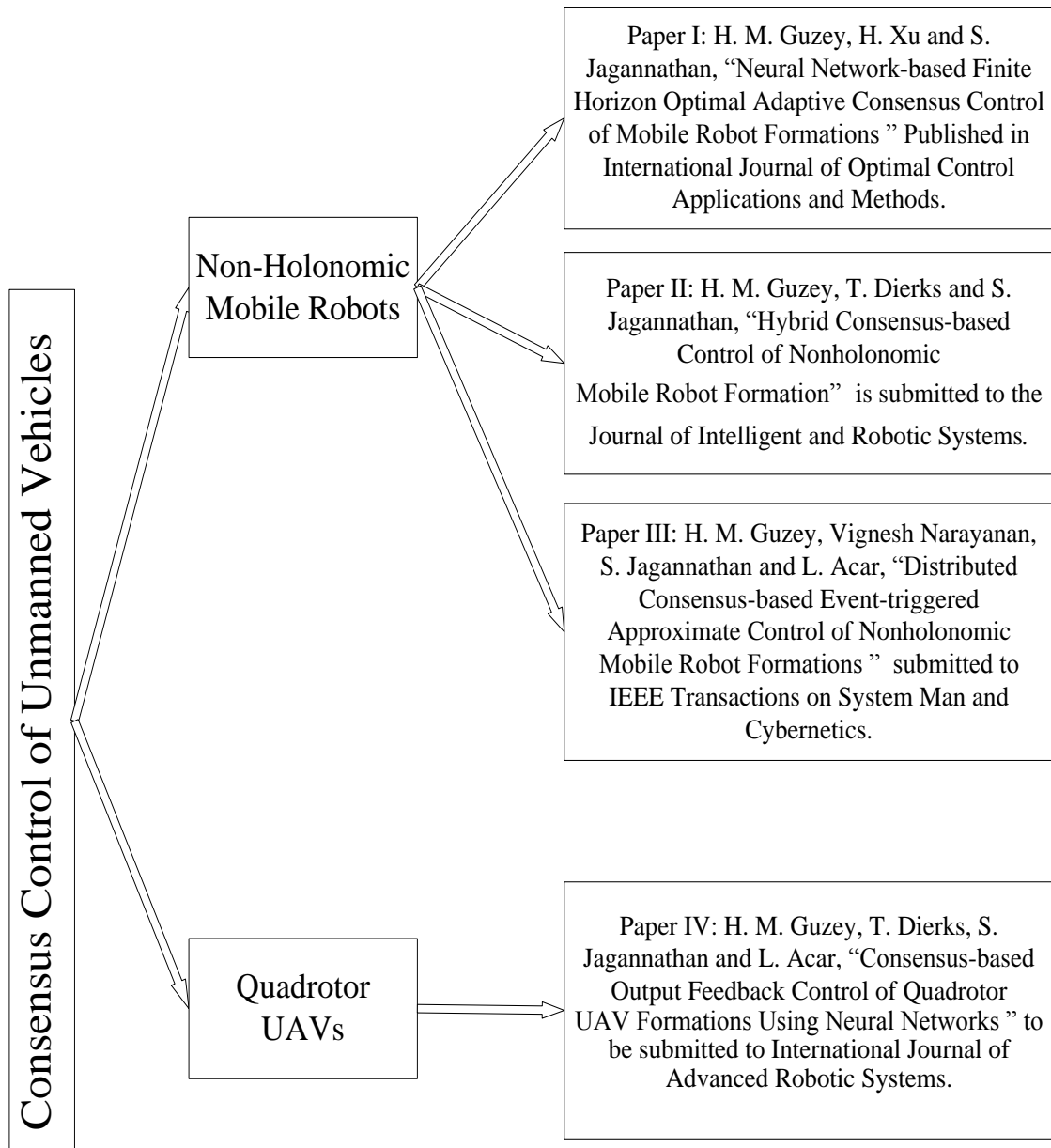
Figure 1.1 Flowchart of the dissertation.

The position and velocities were designed to be shared among the UAVs enabling each UAV to obtain information about position and velocities of neighbor UAVs through local sensors when communications are not available. A novel NN-based extended observer was developed in this dissertation research allowing each follower UAV to estimate its own velocities as well as that of its neighbors. To support UAVs joining or leaving a formation or neighborhood, a novel size reduction matrix was defined to remove the zero elements in the observer design corresponding to the states of a UAV that has left the formation. The size reduction matrix provides a method to ensure that an invertible observer matrix is always available.

By using the position, orientation, reference location and estimated velocities of neighbors, each UAV determines its consensus-based formation errors. Since the under-actuated quadrotor UAVs have no control over the position error along x and y directions, novel desired pitch and roll angles were developed in this research to reach consensus on position errors in those directions, the author also utilized as a virtual controller in the controller design. An elevation controller was also developed by considering the formation error along z direction and other position and orientation errors.

1.2 CONTRIBUTIONS OF THE DISSERTATION

The consensus-based formation controllers [4]–[8] mainly dealt with linear systems prior to the research developed in this dissertation. Developing controllers for nonholonomic unmanned systems had it its own challenges, which were met and are presented here in as objectives achieved. The achievements include defining the consensus error of each unmanned vehicle, deriving the error dynamics and contribution to the

understanding of nonlinear under-actuated error dynamics. Each chapter of this dissertation provides contributions to the consensus control and unmanned vehicle control research community.

In the first paper, a novel consensus-based finite horizon optimal formation control is presented. It was developed for the mobile robots in the presence of uncertain nonlinear dynamics by using a novel cost function. By doing so, a group of nonholonomic mobile robots can now reach consensus on their regulation error and reach their desired location thereby minimizing a cost function that is based on consensus error and regulation error as well as the control torque in a given finite time. The ideal cost function which enhances the Hamiltonian zero and the robot formation dynamics are approximated by using novel NN weights adaptation laws derived in the first paper. By using the Lyapunov's stability theorem, the closed loop robot formation dynamics, and regulation dynamics are shown to be bounded and the overall formation errors are also shown to be bounded.

In real life applications, unmanned vehicles may be expected to form a desired shape first and move to a desired location in the given desired shape. Therefore, the combined regulation-formation controller developed in the first paper may not be suitable for all applications. In the second paper, a novel hybrid method is designed for nonholonomic mobile robots to take care of the consensus seeking and regulation problems sequentially. In order to avoid the hard switches between the regulation and consensus seeking tasks, a novel blending of velocity tracking errors was developed which improves transactions between different modes of the hybrid system. Additionally, analysis of the nonlinear hybrid system's stability using time-varying Lyapunov functions to prove the guaranteed performance of the approach is another contribution of the second paper. Two

separate Lyapunov functions were separately assigned for both regulation and consensus seeking tasks. It is shown that each Lyapunov function dies while the corresponding task is being taken care of by the controller. The initial values of each Lyapunov function at the time of its corresponding time period is also shown to be decreasing. This provides the stability of the hybrid system.

In the first two papers, it is assumed that each robot broadcasts its state information continuously, and others use it to obtain their consensus error and learn where they stand currently. However, this may cause communication over traffic in real applications. Therefore, the author considered reducing communication as possible by using a novel event trigger condition that can be triggered by each robot individually. To accomplish this, in the third paper, a novel distributed adaptive consensus-based formation control of mobile robots is presented, which was developed by taking into account the uncertain dynamics of each robot and its formation. A novel adaptive event-sampling condition was determined through the Lyapunov analysis using both current information of the robot under consideration and previous information from neighborhood robots to determine the feedback instants, which in turn resulted in asynchronous communication. At the end of the paper, overall stability of the robot formation was demonstrated even if the state information was only broadcasted when the event was triggered by using the Lyapunov stability theory.

The controllers in the first three papers were developed for nonholonomic mobile robots formation. The fourth paper deals with formation control of quadrotor UAVs which is also under-actuated in the same manner as that done for the nonholonomic mobile robots. The first contribution of the fourth paper is the design of a novel NN-based nonlinear

extended observer to estimate the velocity of the UAV under consideration and its neighbors which enables the quadrotors to maintain any desired formation shape even without communication among each other. By using the observer, each UAV is able to observe their neighbors' velocities through their positions and orientations. Secondly, the development of a nonlinear consensus based output feedback adaptive formation controller for a group of quadrotor UAVs is one of the major contributions of the fourth paper. Finally, showing that any number of quadrotors can form any given desired shape in the presence of switching communication topologies through Lyapunov analysis is a contribution to the research community and the state of the art.

PAPER

I. NEURAL NETWORK-BASED FINITE HORIZON OPTIMAL ADAPTIVE CONSENSUS CONTROL OF MOBILE ROBOT FORMATIONS

ABSTRACT

In this paper, a novel NN-based optimal adaptive consensus-based formation control scheme over finite horizon is presented for networked mobile robots or agents in the presence of uncertain robot/agent dynamics. The uncertain robot formation dynamics are approximated online by using an NN-based identifier and a suitable weight tuning law. In addition, a novel time-varying value function is derived by using the augmented error vector, which consists of the regulation and consensus-based formation errors of each robot. By using the value function approximation and the identified dynamics, the near optimal control input over finite horizon is derived. This finite horizon optimal control leads to a time varying value function, which becomes the solution of the Hamilton-Jacobi-Bellman (HJB) equation, and control input is approximated by a second NN with time varying activation function. A novel weight update law for the NN value function is developed to tune the value function, satisfy the terminal constraint, and relax an initial admissible controller requirement. The Lyapunov stability method is utilized to demonstrate the consensus of the overall formation. Finally, simulation results are given to verify theoretical claims.

NOMENCLATURE

x : x Cartesian position of the robot

y : y Cartesian position of the robot

ϕ : Bearing angle of the robot

x_r : x position of the robot with respect to robot frame

y_r : y position of the robot with respect to robot frame

$\bar{v}$: State vector of the robot

τ : Controller torque of the robot

$\bar{f}$: Internal dynamics of robot velocities

$\bar{g}$: Controller input matrix of robot velocity dynamics

$\bar{f}_r$: Internal dynamics of the robot

$\bar{g}_r$: Input matrix of the robot

$\bar{v}_d$: Desired robot states

$\tilde{v}$: Regulation error of robot states

f_r : Internal regulation error dynamics of robot

g_r : Regulation error dynamics matrix of robot

δ : Consensus based formation error of the robot

ζ : Augmented error vector of robot

f : Internal formation dynamics of robot

g : Formation control input matrix of the robot

1. INTRODUCTION

Formation control of multi-agent systems has been studied broadly [1]- [6] in recent times and various formation control techniques have been in the literature, which have traditionally favored the consensus based approach [1], 0, [4], [6]-[8]. This consensus approach 0 continues to receive increased attention since it is more robust and scalable when compared to other methods. The aim of consensus-based formation control is to guarantee that the state information of each agent in the network converges to a common value.

In earlier works [1]-[4], consensus-based schemes have been studied for generalized linear systems with known system dynamics and applied to systems with time varying communication graphs [8], bounded disturbances [9], and communication delays during state information sharing [4]. In addition, the majority of consensus-based formation control methods for mobile robots [10]-[12] also takes into consideration linearized robot dynamics for a controller design. In contrast, nonlinear robot dynamics play a vital role [13] in maintaining a predefined formation as shown before.

The consensus-based optimal formation control scheme was also introduced in [14]. Similar to the aforementioned approaches, optimal control [14] was designed for linearized robot dynamics in a backward-in-time manner and requires complete knowledge of the robots' system dynamics. The backward-in-time solution for optimal control is not suitable for practical implementation.

Various schemes [15]-[17] are now available in the literature to solve the optimal control online and forward in time with complete or partial knowledge of the system

dynamics. These online approaches, referred to as adaptive dynamics programming (ADP) [16], [17], require a significant number of iterations [18] to maintain stability. However, to control the robot formation, both iterative [16] and backward-in-time techniques [19] are unsuitable [18] because an insufficient number of iterations can lead to instability.

A novel ADP-based online optimal control over infinite horizon of mobile robots is presented in [18], which does not require value and /or policy iterations. Therefore, the problem of solving the consensus-based optimal formation control problem of mobile robots or agents with uncertain nonlinear dynamics in an online and forward-in-time manner within a finite time horizon remains open. The objective of adaptive optimal consensus based finite horizon controller is to regulate the robot state vector in an optimal manner from an arbitrary initial position and orientation to a desired target position and orientation while maintaining the formation. The finite horizon optimal control is more practical for formation control. Because of the terminal constraint, the value function, which is the solution of the Hamilton-Jacobi-Bellman (HJB) equation, becomes time varying [15],[19] and involved, and the closed-loop system becomes non-autonomous.

Motivated by the aforementioned challenges, a novel online, forward-in-time, finite horizon optimal adaptive formation control is proposed for mobile robots by modeling the robots as nonlinear continuous-time systems in affine form. A novel value function is introduced as a quadratic function of consensus-based formation keeping, regulation errors of each individual robot and control inputs.

The ADP is utilized to solve the optimal control by using two neural networks (NNs). One NN is used to identify the unknown mobile robot formation dynamics and the other is utilized to approximate the time varying value function, which becomes the

solution of the HJB equation. Both the neural network estimation error and the Hamiltonian estimation convergence have been proven to show that the estimated value function becomes the solution of the HJB equation. The identified formation dynamics and the approximated time-varying value function are subsequently utilized for designing the optimal control policy for each robot. The NN weights are updated by using a novel update law, which is derived by using both the Lyapunov stability technique and to minimize formation keeping regulation, and terminal constraint errors. An initial admissible controller is not needed.

The main contributions of this paper include: 1) the design of a consensus based optimal formation control of mobile robots or agents in finite time in the presence of uncertain nonlinear dynamics by using a novel cost function; 2) the derivation of novel adaptation laws for the NN weights to approximate the robot dynamics and the value function; and 3) demonstration of the boundedness of the closed-loop robot dynamics and overall formation stability.

The remainder of the paper is organized as follows. Section 2 presents a brief background on consensus based control of mobile robots. The problem formulation is given in Section 3. Section 4 discusses the design of the finite horizon optimal controller design. Before offering conclusions in Section 6, simulation results are presented to support our theoretical work in Section 5. An appendix gives detailed proofs for the theorems and the lemmas.

2. BACKGROUND AND PRELIMINARIES

In this section, the dynamics of an individual robot is formulated in an affine form, and a brief background on the consensus-based formation control is discussed. Later, the finite horizon optimal control design for nonlinear affine systems is revisited.

2.1 MOBILE ROBOT DYNAMICS

The dynamics of an individual mobile robot [20] are functions of the Cartesian positions and the bearing angle. In Figure 2.1, x_r, y_r denote Cartesian positions with respect to the robot frame. They are also subject to non-holonomic constraints and represented by

$$\bar{M}(\bar{v}_1)\dot{\bar{v}}_2 + \bar{C}\bar{v}_2 + \bar{F}(\bar{v}_2) + \bar{G}(\bar{v}_1) + \tau_d = \bar{B}(\bar{v}_1)\tau - \bar{A}^T\Lambda, \tag{1}$$

where $\bar{v}_1 = \begin{bmatrix} x & y & \phi \end{bmatrix}^T$ and $\bar{v}_2 = \begin{bmatrix} \dot{x} & \dot{y} & \dot{\phi} \end{bmatrix}^T$ with x, y, and $\dot{x}$, $\dot{y}$ represent the Cartesian positions and velocities, ϕ and $\dot{\phi}$, denote bearing angles and angular velocity, respectively as shown in Figure 2.1 The matrices $\bar{B}(\bullet) \in \mathbb{R}^{3 \times 2}$, $\bar{M}(\bullet) \in \mathbb{R}^{3 \times 3}$, $\bar{C} \in \mathbb{R}^{3 \times 3}$, and $\bar{A} \in \mathbb{R}^{3 \times 2}$ represent input transformation, inertial, Coriolis, and constraints matrices, respectively. The vectors $\tau \in \mathbb{R}^{2 \times 1}$, $\tau_d \in \mathbb{R}^{3 \times 1}$, $\Lambda \in \mathbb{R}^{2 \times 1}$, $\bar{G}(\bullet) \in \mathbb{R}^{3 \times 1}$ and $\bar{F}(\bullet) \in \mathbb{R}^{3 \times 1}$ are, respectively, the control torque, bounded disturbance, constraint forces, and gravitational and friction vectors [20] . By using the fact that the inertia matrix, $\bar{M}(\bar{v}_1)$, is invertible [21], equation (1) can be rewritten as

$$\dot{\bar{v}}_2 = \bar{M}(\bar{v}_1)^{-1}\left(\bar{C}\bar{v}_2 - \bar{F}(\bar{v}_2) - \bar{G}(\bar{v}_1) - \tau_d - \bar{A}^T\Lambda\right) + \bar{M}(\bar{v}_1)^{-1}\bar{B}(\bar{v}_1)\tau. \tag{2}$$
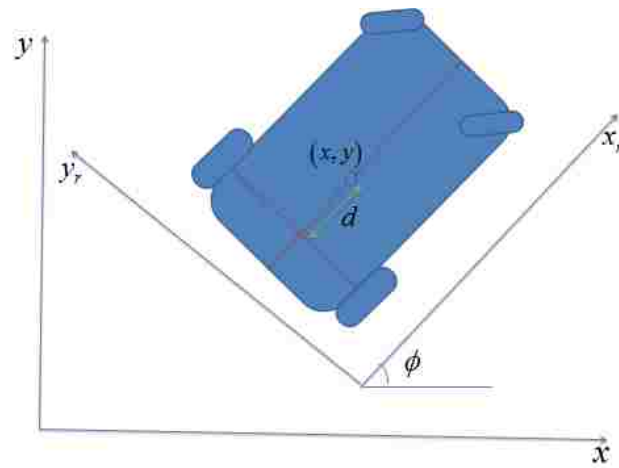
Figure 2.1 Differentially riven mobile robots.
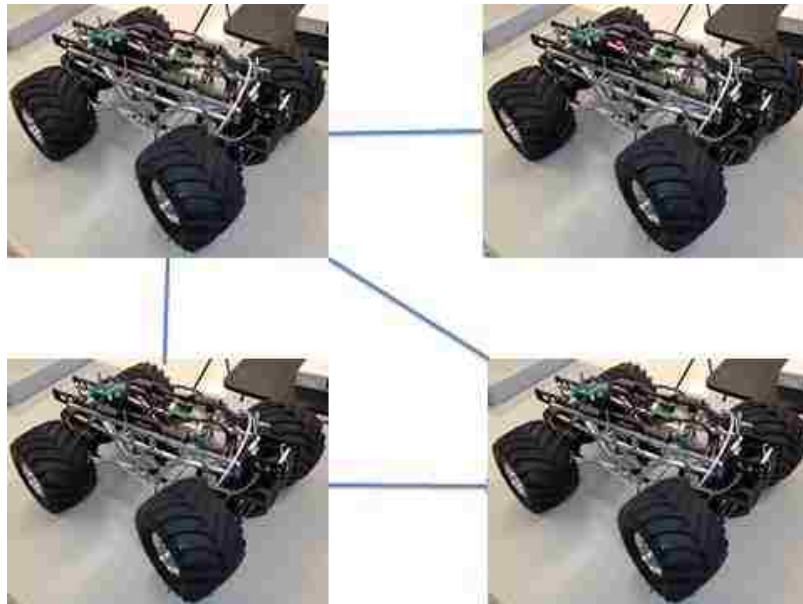
Figure 2.2 Communication topology among robots.

In terms of state space representation, equation (2) can be expressed as

$$\dot{\bar{v}}_1 = \bar{v}_2$$
$$\dot{\bar{v}}_2 = \bar{f}\left(\bar{v}\right) + \bar{g}\left(\bar{v}\right)\tau \quad (3)$$

with $\bar{v} = \begin{bmatrix} \bar{v}_1^T & \bar{v}_2^T \end{bmatrix}^T \in \mathbb{R}^{6\times 1}$, $\bar{f}(\bar{v}_2, \bar{v}_1) = \bar{M}(\bar{v}_1)^{-1}(\bar{C}\bar{v}_2 - \bar{F}(\bar{v}_2) - \bar{G}(\bar{v}_1) - \tau_d - \bar{A}^T \Lambda) \in \mathbb{R}^{3\times 1}$,

and $\bar{g}(\bar{v}_1) = \bar{M}(\bar{v}_1)^{-1} \bar{B}(\bar{v}_1) \in \mathbb{R}^{3\times 2}$ denotes the nonlinear functions representing the system

dynamics.

Alternatively, equation (3) can be expressed in affine form as

$$\dot{\bar{v}} = \bar{f}_r(\bar{v}) + \bar{g}_r(\bar{v})\tau, \tag{4}$$

where $\bar{f}_r(\bar{v}) = \begin{bmatrix} \bar{v}_2^T & \bar{f}(\bar{v})^T \end{bmatrix}^T \in \mathbb{R}^{6\times 1}$, $\bar{g}_r(\bar{v}) = \begin{bmatrix} 0_{2\times 3} & \bar{g}(\bar{v})^T \end{bmatrix}^T \in \mathbb{R}^{6\times 2}$ represents the

nonlinear internal dynamics and the control coefficient matrix, respectively. In the

formation control problem where there are n mobile robots present, the dynamics of the

i^{th} mobile robot can be written as

$$\dot{\bar{v}}_i = \bar{f}_{r,i}(\bar{v}_i) + \bar{g}_{r,i}(\bar{v}_i)\tau_i, \quad i = 1, 2, \cdots, n. \tag{5}$$

The following assumption is needed before we proceed.

Assumption 1: The state vector $\bar{v}_i$ in (5) is available and the input matrix satisfies

$\left\| \bar{g}_{r,i}(\bar{v}_i) \right\| \leq \bar{g}_{\max}$.

Without loss of generality, the system (5) is considered controllable in the sense

that there exists a continuous control policy that stabilizes the robot error dynamics (8)

with $\bar{v}_i = 0$ being a unique equilibrium point on a set $\Omega \subseteq \mathbb{R}^6$. The main objective of the

formation control problem is to reach a desired state, $\bar{v}_{i,d} \in \mathbb{R}^{6\times 1}$, by the ith mobile robot

while maintaining the formation intact.

Next, we define the regulation error as the difference between actual state, $\overline{v}_i$ and desired state vectors, $\overline{v}_{i,d}$, as

$$\tilde{v}_i = \overline{v}_i - \overline{v}_{i,d}, \tag{6}$$

where $\tilde{v}_i \in \mathbb{R}^{6 \times 1}$ is the regulation error for the ith robot. Since the desired positions and velocities are assumed to be fixed, $\dot{\overline{v}}_{i,d} = 0$, and the regulation error dynamics from (6) becomes

$$\dot{\tilde{v}}_i = \dot{\overline{v}}_i - \dot{\overline{v}}_{i,d} = \dot{\overline{v}}_i = \overline{f}_{r,i}(\overline{v}_i) + \overline{g}_{r,i}(\overline{v}_i)\tau_i. \tag{7}$$

The regulation error dynamics can be rewritten as

$$\dot{\tilde{v}}_i = f_{r,i}(\tilde{v}_i) + g_{r,i}(\tilde{v}_i)\tau_i \tag{8}$$

with $f_{r,i}(\tilde{v}_i) = \overline{f}_{r,i}(\overline{v}_i) = \overline{f}_{r,i}(\tilde{v}_i + \overline{v}_{i,d})$ and $g_{r,i}(\tilde{v}_i) = \overline{g}_{r,i}(\overline{v}_i) = \overline{g}_{r,i}(\tilde{v}_i + \overline{v}_{i,d})$.

Remark 1: From (8) it is evident that the regulation error must be forced to zero in order for the formation to reach the target. Assumption 1 ensures that $\left\| g_{r,i}(\tilde{v}_i) \right\| \leq g_{\max}$ is bounded. On the other hand, in a formation control design, a consensus has to be reached to maintain formation.

2.2   CONSENSUS BASED FORMATION CONTROL

In this subsection, the traditional consensus-based control is discussed in brief. Before introducing the consensus approach, the following assumption is needed to proceed.

Assumption 2 [27], [9]: The connectivity graph of the formation network is assumed to be undirected and connected.

The primary goal of a formation control is to reach consensus by maintaining the formation error defined as

$$\delta_i = \sum_{j \in N_i} \left[(\tilde{v}_i - \tilde{v}_j) \right] \in \mathbb{R}^{6 \times 1}, \tag{9}$$

where $\tilde{v}_i$ is the regulation error of the ith robot and $\tilde{v}_j$ is the regulation error of jth robot and N_i is the set of mobile robots in the neighborhood of the ith robot. Similar to (9), the formation error can also be defined as

$$\delta_i = \sum \left[l_{ij} (\tilde{v}_i - \tilde{v}_j) \right] \in \mathbb{R}^{6 \times 1}, \tag{10}$$

with $l_{ii} \triangleq 0$, $l_{ij} \triangleq 1$ if information flows from vehicle j to vehicle i and $l_{ij} \triangleq 0$, otherwise $\forall i \neq j$. Then, the connectivity matrix of overall network is defined as $L = \left[l_{ij} \right]$. However, for the sake of simplicity on notation, the neighboring set notation (9) is preferred during the paper.

Remark 2: To ensure consensus among the robots in the network, each robot needs to be aware of regulation errors of other robots; hence, the robots need to communicate with each other. The set of robots from which the ith robot can receive regulation error is called a neighboring set or N_i of the ith robot that is

$$\forall i = 1, \ldots, n, \quad N_i = \left\{ j = 1, \ldots, N \middle| (i, j) \in G \right\}, \tag{11}$$

where G designates the existence of a regulation error exchange between i^{th} and j^{th} robot. Additionally, all the robots have a two-way communication.

To achieve the desired formation, the difference among the regulation errors of the robots should converge to zero. Although each robot is not receiving the regulation error information from every other robot in the network, the connectedness of the network

provides consensus on regulation errors[14]. Consequently, the final regulation error of each individual robot will be in consensus [14] . In other words, even though there is no direct communication between i^{th} and k^{th} robots, since $\tilde{v}_i \rightarrow \tilde{v}_j$, $\tilde{v}_j \rightarrow \tilde{v}_k$, then $\tilde{v}_i \rightarrow \tilde{v}_k$ [14].

Traditionally, in a consensus-based formation control [22] of agents described by a linear system [14], [23], the control input for linear systems is based on the formation error by using the information of their neighbors. To design an optimal consensus-based formation control of nonlinear systems, both the regulation and formation errors need to be accounted for. Next, traditional optimal control background is discussed before introducing the proposed scheme.

2.3   OPTIMAL REGULATION OF CONTINUOUS-TIME SYSTEMS

A brief background on optimal control of general nonlinear continuous-time systems in affine form is presented in this subsection. Consider the nonlinear mobile robot regulation error dynamics (8) in affine form. The objective here is to design an optimal control policy while minimizing the cost function,

$$V_i(\tilde{v}_i, t_0) = \psi_i(\tilde{v}_i(t_f), t_f) + \int_{t_0}^{t_f} (Q(\tilde{v}_i) + \tau_i^T R \tau_i) dt , \tag{12}$$

in a finite time $\begin{bmatrix} t_0 & t_f \end{bmatrix}$ where $Q(\tilde{v}_i) \geq 0 \in \mathbb{R}$ is a positive semi-definite function to penalize the regulation error, $R \in \mathbb{R}^{2 \times 2}$, is a positive definite matrix to penalize the control input of the ith robot while the terminal constraint, $\psi_i(\tilde{v}_i(t_f), t_f)$, penalizes the terminal state at the finial time , t_f . It is important to mention here that due to fixed finite time, the cost function becomes an explicit function of time in contrast to the infinite time case where the cost

function is a time invariant function. Next, define the Hamiltonian

$$H(\tilde{v}_i, \tau_i, t) = V_{it} + Q(\tilde{v}_i) + \tau_i^T R \tau_i + V_{\tilde{v}_i}^T [f_{r,i}(\tilde{v}_i) + g_{r,i}(\tilde{v}_i)\tau_i],$$ (13)

where $V_{it} = \dfrac{\partial V_i(\tilde{v}_i, t)}{\partial t}$ and $V_{\tilde{v}_i} = \dfrac{\partial V_i(\tilde{v}_i, t)}{\partial \tilde{v}_i}$ are the gradient of the cost function, $V_i(\tilde{v}_i, t_0)$.

Equation (13) has the time-dependency term, V_{it}, in contrast with the infinite-horizon case.

The optimal control policy [18] is obtained by using the stationary condition, $\partial H(\tilde{v}_i, \tau_i, t)/\partial \tau_i = 0$, which yields

$$\tau_i^*(\tilde{v}_i, t) = -\frac{1}{2} R^{-1} g_{r,i}^T(\tilde{v}_i) V_{\tilde{v}_i}^*.$$ (14)

Substituting (14) into (13) yields the time-varying HJB equation as

$$V_{it}^* + V_{\tilde{v}_i}^{*T} f_{r,i}(\tilde{v}_i) + Q(\tilde{v}_i) - \frac{1}{4} V_{i\tilde{v}_i}^{*T} g_{r,i}(\tilde{v}_i) R^{-1} g_{r,i}^T(\tilde{v}_i) V_{\tilde{v}_i}^* = 0,$$ (15)

with V_{it}^*, $V_{\tilde{v}_i}^*$ representing the derivatives of optimal time-varying value function of ith robot, V_i^*, with respect to time and regulation error, respectively. The solution to the time varying HJB equation, which is essentially the value function, is used to obtain the optimal control input. On the other hand, finding an analytical closed form solution of the HJB equation is difficult and has been considered to be extremely difficult. Hence, approximation based ADP techniques are used to solve the solution online.

Lemma 1[18]: Consider the regulation error dynamics of ith robot (8) with value function (12) and the optimal control policy (14). Let $J(\tilde{v}_i)$ be a continuously differentiable, radially unbounded Lyapunov candidate such that $\dot{J}(\tilde{v}_i) = J_{\tilde{v}_i}^T(\tilde{v}_i)\dot{\tilde{v}}_i = J_{\tilde{v}_i}^T(\tilde{v}_i)(f(\tilde{v}_i) + g(\tilde{v}_i)\tau_i^*) < 0$ with $J_{\tilde{v}_i}(\tilde{v}_i)$ being the partial derivative of

$J(\tilde{v}_i)$ with respect to $\tilde{v}_i$. In addition, let $\bar{Q}(\tilde{v}_i) \in \mathbb{R}$ be a positive definite matrix, i.e.,

$$\forall \tilde{v}_i \neq 0, \tilde{v}_i \in \Omega, \quad \left\| \bar{Q}(\tilde{v}_i) \right\| > 0, \quad \text{and} \quad \tilde{v}_i = 0 \Rightarrow \left\| \bar{Q}(\tilde{v}_i) \right\| = 0 \quad , \quad \text{and} \quad \bar{Q}_{\min} \leq \left\| \bar{Q}(\tilde{v}_i) \right\| \leq \bar{Q}_{\max}.$$

Moreover, let $\bar{Q}(\tilde{v}_i)$ satisfy $\lim\limits_{\tilde{v}_i \to \infty} \bar{Q}(\tilde{v}_i) = \infty$ as well as

$$V_{\tilde{v}_i}^{*\mathrm{T}} \bar{Q}(\tilde{v}_i) J_{\tilde{v}_i} = r(\tilde{v}_i, \tau_i^*) = Q(\tilde{v}_i) + \tau_i^{*\mathrm{T}} R \tau_i^* \tag{16}$$

Then, the following relation holds: $J_{\tilde{v}_i}^{\mathrm{T}} (f(\tilde{v}_i) + g(\tilde{v}_i)\tau_i^*) = -J_{\tilde{v}_i}^{\mathrm{T}} \bar{Q}(\tilde{v}_i) J_{\tilde{v}_i}$.

In a consensus-based control, since the complete formation depends on both regulation and formation errors, the cost function has to be redefined. In the next section, the problem statement of the consensus-based optimal formation control is formulated.

3. PROBLEM FORMULATION

In this section, the augmented formation dynamics are derived and the near optimal control of a consensus-based formation control of mobile robots is formulated.

3.1 FORMATION DYNAMICS

The formation dynamics are derived by augmenting the regulation and the formation errors. The dynamics of formation error discussed in (9) can be derived as

$$\dot{\delta}_i = \sum_{j \in N_i} \left(f_{r,i}(\tilde{v}_i) + g_{r,i}(\tilde{v}_i)\tau_i - f_{r,j}(\tilde{v}_j) - g_{r,j}(\tilde{v}_j)\tau_j \right). \tag{17}$$

Now, augmenting the regulation and formation errors of ith robot, $\zeta_i = \begin{bmatrix} \tilde{v}_i^T & \delta_i^T \end{bmatrix}^T \in \mathbb{R}^{12 \times 1}$, the dynamics of the formation error for the ith robot by using (8) and (17) becomes

$$\dot{\zeta}_i = \begin{bmatrix} f_{r,i}(\tilde{v}_i) + g_{r,i}(\tilde{v}_i)\tau_i \\ \sum_{j \in N_i} \left(f_{r,i}(\tilde{v}_i) + g_{r,i}(\tilde{v}_i)\tau_i - f_{r,j}(\tilde{v}_j) - g_{r,j}(\tilde{v}_j)\tau_j \right) \end{bmatrix}. \tag{18}$$

In an affine form, equation (18) can be represented as

$$\dot{\zeta}_i = \begin{bmatrix} f_{r,i}(\tilde{v}_i) \\ \sum_{j \in N_i} \left(f_{r,i}(\tilde{v}_i) - f_{r,j}(\tilde{v}_j) - g_{r,j}(\tilde{v}_j)\tau_j \right) \end{bmatrix} + \begin{bmatrix} g_{r,i}(\tilde{v}_i) \\ \rho_i g_{r,i}(\tilde{v}_i) \end{bmatrix} \tau_i \tag{19}$$

where ρ_i being the number of robots in the neighborhood of the ith mobile robot. The formation dynamics of the ith mobile robot (19) can be expressed in a compact form as

$$\dot{\zeta}_i = f_i(\tilde{v}_{Ni}, \tau_{Ni}) + g_i(\tilde{v}_i)\tau_i \tag{20}$$

with $\tau_j \in \tau_{Ni}, \forall j \in N_i$, $\tilde{v}_j \in \tilde{v}_{Ni}, \forall j \in N_i$ being the control input and regulation error vector

of all robots in the network, respectively, and

$$f_i\left(\tilde{v}_{Ni}, \tau_{Ni}\right) = \begin{bmatrix} f_{r,i}(\tilde{v}_i) \\ \sum_{j \in N_i}\left(f_{r,i}\left(\tilde{v}_i\right) - f_{r,j}\left(\tilde{v}_j\right) - g_{r,j}\left(\tilde{v}_j\right)\tau_j\right) \end{bmatrix} \in \mathbb{R}^{12 \times 1}, \; g_i\left(\tilde{v}_i\right) = \begin{bmatrix} g_{r,i}(\tilde{v}_i) \\ \rho_i g_{r,i}(\tilde{v}_i) \end{bmatrix} \in \mathbb{R}^{12 \times 1}.$$

Remark 3: Note that, similar to [24], the ith robot formation dynamics (19) are

given as a function of the regulation errors and control inputs of its neighbors and its own

regulation error dynamics. The controller, τ_i, in the augmented error dynamics (20) of the

i^{th} robot is formulated in a decentralized way. These formation dynamics are not known

beforehand as they are a function of other robot dynamics in the formation. Therefore, an

NN identifier will be utilized to identify them for optimal consensus control. Next a novel

cost function is defined for the optimal control problem to achieve optimality in a finite

time by minimizing both the regulation and formation errors.

3.2   CONSENSUS-BASED VALUE FUNCTION

In order to control the consensus-based formation error dynamics (20) optimally

in finite time, a novel value function is proposed for the ith robot as

$$V_i(\zeta_i, t_0) = \vartheta_i(\zeta_i(t_f), t_f) + \int_{t_0}^{t_f}(Q(\zeta_i) + \tau_i^T R \tau_i)dt , \tag{21}$$

where t_0 and t_f are initial and final time instants, respectively, while

$Q(\zeta_i) = \chi_1 \tilde{v}_i^T Q_i \tilde{v}_i + \chi_2 \delta_i^T Q_i \delta_i$ with $Q_i \in \mathfrak{R}^{6 \times 6}$ representing positive definite matrices to

penalize regulation and formation errors, respectively. In addition, χ_1, χ_2 are positive

design parameters, R is a positive definite constant matrix, and $\vartheta_i(\zeta_i(t_f), t_f)$ serves as a

terminal constraint for each robot. Note that the design parameters χ_1, and χ_2 define how much relative penalty needs to be given to regulation and formation errors. In other words, for example, increasing χ_2 and reducing χ_1 increases priority of formation which prevents over minimization of the regulation error.

The time-varying value function (21) with augmented error, ζ_i, as its input can be expressed by using an NN with a time-varying activation function on a compact set Ω in the form [15] as

$$V_i(\zeta_i,t) = \theta_{V_i}^T \psi_{Vi}(\zeta_i, t_f - t) + \varepsilon_{V_i}(\zeta_i,t) \tag{22}$$

and the terminal constraint can be represented as

$$V_i(\zeta_i,t_f) = \theta_{V_i}^T \psi_{V_i}(\zeta_i(t_f),0) + \varepsilon_{V_i}(\zeta_i,t_f) \tag{23}$$

where $\theta_{Vi} \in \mathbb{R}^{L \times 1}$ is the target NN weight vector with L being the number of hidden-layer neurons; hence, $\psi_{V_i}(\zeta_i, t - t_f) : \mathbb{R}^{12} \times [0,\infty) \rightarrow \mathbb{R}^L$ is the bounded time-dependent activation function of augmented errors of each robot, while $\varepsilon_{V_i}(\zeta_i,t)$ is the NN reconstruction error.

The target NN weights, θ_{V_i}, and reconstruction error, $\varepsilon_{V_i}(\zeta_i,t)$, are assumed to be bounded above such that $\left\| \theta_{V_i} \right\| \leq \theta_{VM_i}$ and $\left\| \varepsilon_{V_i}(\zeta_i,t) \right\| \leq \varepsilon_{Mi}$, where θ_{VM_i} and ε_{Mi} are positive constants [13]. In addition, it is assumed that the gradient of the NN reconstruction error with respect to ζ_i is bounded above, such that $\left\| \nabla_{\xi_i} \varepsilon_{Vi}(\zeta_i,t) \right\| \leq \varepsilon_{VMi}$ [18], where ε_{VM} is also a positive constant. The quantities $\psi_{V_i}(\zeta_i(t_f),0)$ and $\varepsilon_{V_i}(\zeta_i,t_f)$ have the same meaning but correspond to the terminal time and state. Next, an adaptive optimal consensus-based finite horizon NN-based controller scheme is derived.

4. OPTIMAL ADAPTIVE CONSENSUS CONTROL

In this section, finite horizon optimal adaptive consensus-based formation control is designed for mobile robots in the presence of unknown robot formation dynamics. First, NN-based identification of the dynamics is introduced. In the second part of this section, a novel NN-based finite horizon optimal adaptive consensus controller is proposed. In this scenario, two NNs are utilized, one for identification and the other one for estimating time varying value function.

In contrast with the traditional actor critic methods where two NNs are utilized, in the proposed approach, only one NN is utilized in an online fashion. A Novel NN weight matrix adaptation law is derived to guarantee terminal constraint as well as maintaining stability of the system. The Lyapunov stability theorem is utilized to find an optimal controller and stability analysis of the closed-loop system incorporating the identifier. Without loss of generality, i^{th} robot's adaptive optimal controller design is considered as follows. Further, the optimality and consensus ability of external robot network is demonstrated in *Theorem* 2 based on the controller defined for each robot individually. The next section introduces identification of ith mobile robot dynamics.

4.1 NN-BASED IDENTIFIER

Consider the formation dynamics of mobile robots (20) in affine form. On a compact set Ω, by using an universal function, the approximation property of NN-based identification of mobile robot formation dynamics can be expressed as [25]

$$f_i(\tilde{v}_{Ni}, \tau_{Ni}) = \theta_{fi}^T \psi_{fi}(\tilde{v}_{Ni}, \tau_{Ni}) + \varepsilon_{fi} , \; g_i(\tilde{v}_i) = \theta_{gi}^T \psi_{gi}(\tilde{v}_i) + \varepsilon_{gi} , \qquad (24)$$

where $\theta_{fi} \in \mathbb{R}^{l \times 6}$, $\theta_{gi} \in \mathbb{R}^{l \times 6}$ are NN target weight matrices with l being number of neurons,

and $\psi_{fi} : \mathbb{R}^6 \to \mathbb{R}^l$, and $\psi_{gi} : \mathbb{R}^{6 \times 2} \to \mathbb{R}^{l \times 2}$ are activation functions and $\varepsilon_{fi} \in \mathbb{R}^{6 \times 1}$, $\varepsilon_{gi} \in \mathbb{R}^{6 \times 2}$

are NN reconstruction errors. Even though the dynamics of other robots are unknown to

i^{th} robot, the regulation errors and control inputs are transmitted for identification of

formation dynamics.

Then, the mobile robot dynamics (20) can be represented by using (24) as

$$\dot{\zeta}_i = f_i(\tilde{v}_{Ni}, \tau_{Ni}) + g_i(\tilde{v}_i)\tau_i = \theta_{fi}^T \psi_{fi}(\tilde{v}_{Ni}, \tau_{Ni}) + \theta_{gi}^T \psi_{gi}(\tilde{v}_i)\tau_i + \varepsilon_{fi} + \varepsilon_{gi}\tau_i$$

$$= \begin{bmatrix} \theta_{fi} \\ \theta_{gi} \end{bmatrix}^T \begin{bmatrix} \psi_{fi}(\tilde{v}_{Ni}, \tau) & 0 \\ 0 & \psi_{gi}(\tilde{v}_i) \end{bmatrix} \begin{bmatrix} 1 \\ \tau_i \end{bmatrix} + \varepsilon_{fi} + \varepsilon_{gi}\tau_i$$

$$= \theta_{Ii}^T \psi_{Ii}(\tilde{v}_{Ni}, \tau_{Ni})\bar{\tau}_i + \varepsilon_{Ii}, \tag{25}$$

where $\theta_{Ii} = [\theta_{fi}^T \ \theta_{gi}^T]^T \in \mathbb{R}^{2l \times 6}$ and, $\psi_{Ii}(\xi_i) = diag\{\psi_{fi}(\tilde{v}_{Ni}, \tau), \psi_{gi}(\tilde{v}_i)\}$, $\psi_{Ii} : \mathbb{R}^{6 \times 3} \to \mathbb{R}^{2l \times 3}$

represent the NN identifier target weights matrix and activation function, respectively,

where $\bar{\tau}_i = [1 \ \tau_i^T]^T \in \mathbb{R}^3$ and $\varepsilon_{Ii} = \varepsilon_{fi} + \varepsilon_{gi}\tau_i$ are being the augment control input and the

NN identifier reconstruction error, respectively. Because $\psi_{Ii}(\tilde{v})$ is known, and θ_{Ii}^T is

unknown, equation (25) can be estimated as

$$\dot{\hat{\zeta}}_i = \hat{\theta}_{Ii}^T \psi_{Ii}(\tilde{v}_{Ni}, \tau_{Ni})\bar{\tau}_i + Ke_i, \tag{26}$$

with $\hat{\theta}_{Ii} \in \mathbb{R}^{2l \times 6}$ being an estimation of the NN weight matrix; furthermore, K is a design

parameter, which is used to maintain stability of the NN identifier, and $e_i = \zeta_i - \hat{\zeta}_i$ presents

the state estimation error. By substituting (26) with (25), the state estimation error

dynamics for robot i^{th} can be given as

$$\dot{e}_i = \dot{\zeta}_i - \dot{\hat{\zeta}}_i = \tilde{\theta}_{Ii}^T \psi_{Ii}(\tilde{v}_{Ni}, \tau_{Ni})\bar{\tau}_i + \varepsilon_{Ii} - Ke_i, \tag{27}$$

where $\tilde{\theta}_{Ii} = \left(\theta_{Ii} - \hat{\theta}_{Ii}\right) \in \mathbb{R}^{2l \times 6}$ is the NN weight estimation error. The update law for $\hat{\theta}_{Ii}$ is

defined to force the actual NN weights close to target NN weight in a finite time by using

the Lyapunov stability theorem as

$$\dot{\hat{\theta}}_{Ii} = -\lambda_{Ii}\hat{\theta}_{Ii} + \psi_{Ii}(\tilde{v}_{Ni}, \tau_{Ni})\bar{\tau}_i e_i, \tag{28}$$

with λ_{Ii} being the tuning parameter of the NN identifier satisfying $\lambda_{Ii} > 0$. Since $\dot{\tilde{\theta}}_{Ii} = -\dot{\hat{\theta}}_{Ii}$

, by using (28), the NN identifier weight estimation error dynamics can be written as

$$\dot{\tilde{\theta}}_{Ii} = \lambda_{Ii}\hat{\theta}_{Ii} - \psi_{Ii}(\tilde{v}_{Ni}, \tau_{Ni})\bar{\tau}_i e_i \tag{29}$$

The identification of robot formation dynamics (26) is utilized to determine the

optimal controller of robot formation which is given in the next section.

4.2 FINITE HORIZON OPTIMAL CONSENSUS CONTROLLER DESIGN

To estimate the value function, $V_i(\zeta_i, t)$, for i^{th} robot, we can define it as

$$\hat{V}_i(\zeta_i, t) = \hat{\theta}_{V_i}^T \psi_{V_i}(\zeta_i, t_f - t), \tag{30}$$

The terminal condition then becomes

$$\hat{V}_i(\zeta_i, t_f) = \hat{\theta}_{V_i}^T \psi_{V_i}(\hat{\zeta}_i, 0), \tag{31}$$

where $\hat{V}_i(\zeta_i, t)$ is the approximated value function, and $\hat{\theta}_{V_i} \in \mathfrak{R}^L$ is the actual NN weights

for the value function; additionally, $V_i(\zeta_i, t_f)$ is the approximated value function at the

terminal time t_f, and $\psi_{V_i}(\hat{\zeta}_i(t_f), 0) \in \mathbb{R}^{12} \times [0, \infty) \to \mathbb{R}^L$ is the activation function with

approximated terminal state $\hat{\zeta}_i(t_f)$. Note that term $\hat{\zeta}_i(t_f)$ is randomly chosen from a region of stability from the initial stabilizing control [26].

Using the NN approximation of value function (30), the approximated Hamiltonian is then given by

$$\hat{H}_i(\zeta_i,\tau_i,t) = \hat{\theta}_{V_i}^T \nabla_t \psi_{V_i}(\zeta_i,t_f-t) + \hat{\theta}_{V_i}^T \nabla_{\xi_i} \psi_{V_i}(\zeta_i,t_f-t)\hat{f}_i(\zeta_i)$$

$$-\frac{1}{4}\hat{\theta}_{V_i}^T \nabla_{\xi_i} \psi_{V_i}(\zeta_i,t_f-t)\hat{D}(\tilde{v}_i)\nabla_{\xi_i}^T \psi_{V_i}(\zeta_i,t_f-t)\hat{\theta}_{V_i}, \tag{32}$$

where $\hat{D}(\tilde{v}_i) = \hat{g}_i^T(\tilde{v}_i)R^{-1}\hat{g}_i(\tilde{v}_i)$ is obtained from the NN identifier. Finally, the estimated control policy is given by

$$\hat{\tau}_i(\zeta_i,t) = -\frac{1}{2}R^{-1}\hat{g}_i^T(\tilde{v}_i)\nabla_{\xi_i}\psi_{V_i}^T(\zeta_i,t_f-t)\hat{\theta}_{V_i}. \tag{33}$$

In order to derive the finite-horizon optimal control, both the time-varying nature of the value function and the terminal constraint needs to be included in a proper manner. With NN approximation, define the terminal constraint error as

$$e_{t_{fi}} = \vartheta_i(\zeta_i(t_f),t_f) - \hat{\theta}_{V_i}^T \psi_{V_i}(\hat{\zeta}_i(t_f),t_f) = \theta_{V_i}^T \tilde{\psi}_{V_i}(\zeta_i(t_f),\hat{\zeta}_i(t_f),t_f) + \tilde{\theta}_{V_i}^T \psi_{V_i}(\hat{\zeta}_i(t_f),t_f) + \varepsilon_{t_{fi}}, \tag{34}$$

where $\tilde{\psi}_{V_i}(\zeta_i(t_f),t_f) = \psi_{V_i}(\zeta_i(t_f),t_f) - \psi_{V_i}(\hat{\zeta}_i(t_f),t_f)$. The objective is to minimize the approximated Hamiltonian (23) and the terminal constraint error (25) along the system trajectory, such that the optimality can be achieved while satisfying the terminal constraint. Hence, the total error is defined as

$$e_{totali} = (\hat{H}_i(\zeta_i,\tau_i,t))^2/2 + e_{t_{fi}}^4/4. \tag{35}$$

The update law for tuning the NN weights is found by minimizing (35) using normalized gradient descent as

$$\dot{\hat{\theta}}_{V_i} = -\gamma_1 \frac{\hat{\eta}}{(1+\hat{\eta}^T\hat{\eta})^2}\hat{H}_i(\zeta_i,\tau_i,t) + \gamma_2 \frac{\hat{\mu}}{(1+\hat{\mu}^T\hat{\mu})^2}e_{t_fi}^3 + \frac{\gamma_3}{2}\nabla_{\xi_i}\psi_{V_i}(\zeta_i,t_f-t)\hat{D}(\tilde{v}_i)J_{\zeta_i}(\zeta_i) \quad (36)$$

where $-\dfrac{1}{2}\nabla_{\xi_i}\psi_{V_i}(\zeta_i,t_f-t)\hat{D}(\tilde{v}_i)\nabla_{\zeta_i}^T\psi_{V_i}(\zeta_i,t_f-t)\hat{\theta}_{V_i}$, $\gamma_1,\gamma_2,\gamma_3$ and $\hat{\mu}=\psi_{V_i}(\hat{\zeta}_i(t_f),t_f)$ are

positive design parameters and $J_{\zeta_i}(\zeta_i)$ is the partial derivative of a Lyapunov candidate

with respect to ζ_i. The last term in (36) ensures the system states remain bounded while

the NN scheme learns the optimal cost function [18].

Theorem 1: Consider the formation dynamics of the ith mobile robot (20) in a

network of robots. Assume that, each robot broadcasts its regulation errors and control

torques over the network without any communication delays; furthermore, the topological

graph of the robot in the communication network satisfies Assumptions 1 and 2 given in

the paper. Let the NN weight update law for the identifier and the value functions

approximation are given as (28), and (36), respectively, and the estimated control input is

given as (33). Then, there exists positive design constants, $\gamma_1>0,\gamma_2>0$

$\gamma_3>4+\dfrac{\gamma_1+\gamma_2}{2\gamma_2}\|\zeta_i\|^4$, $\lambda_{\min}(K)>\dfrac{3}{2}+\dfrac{\gamma_2}{4\gamma_1}$, $\lambda_{\max}(R^{-1})$, allowing all robots to have a small

bounded formation error $\|\delta_i\|$ and, they are also able to reach their desired position and

orientation with a small, bounded regulation error $\|\tilde{v}_i\|$. Additionally, identification error

$\|e_i\|$ and the NN weights estimation errors for the NN identifier, $\|\tilde{\theta}_{I_i}\|$, and the controller,

$\|\tilde{\theta}_{V_i}\|$, are bounded. Further, the bounds are the function of final time t_f, initial system state

bound $B_{J_{\zeta_i},0}$, initial identification error bound $B_{e_i,0}$ and initial weight estimation error

bound for NN identifier and controller $B_{\theta_{I_i},0}, B_{\theta_{V_i},0}$, respectively.

Proof: Refer to the appendix.

In *Theorem* 1, consensus-based formation errors were proven to be bounded for each robot. The bounded formation error is due to NN approximation error. In the literature, many papers have dealt with consensus and bounded measurement error [27] as well as bounded disturbances [9] for decentralized control systems. Since the formation error has proven to be eventually traced to bounded NN reconstruction errors, by using the assumption stated for network topology [27], we can claim that all regulation errors of the networked mobile robots are due to bounded reconstruction errors. Next, the consensus of the overall network of mobile robots will be introduced.

Theorem 2: Consider the formation dynamics (20) of the ith robot in a team of mobile robots based on the neighboring sets. Let the NN weight update laws for the identifier and the value functions be given by (28), and (36), respectively. Then, let the control inputs given by (33) of each robot minimize the cost functions (21) and also guarantee that the robots reach consensus over their regulation errors. Furthermore, the leaderless group of robots will move toward their goal position while maintaining consensus on the way and, they eventually reach close to the goal position in a finite time**.**

Proof: See appendix.

Next it is worth mentioning the benefits of the proposed consensus-based finite horizon adaptive optimal controller(33). In the traditional leader-follower based formation control [24], each follower needs to receive the controller input and the state information of its leader while the communication delays are ignored. Once the communication is lost between a leader and the follower, the follower and the robots behind the follower will lose formation. However, this is not the case in the consensus based approach. As long as the

communication graph of the robot formation is connected, which means each robot transmits its information to at least one neighbor robot and receives at least one neighbor robot's information, the consensus is preserved over the entire group.

Now, assume that i^{th} robot receives information from only part of the group. Then the formation dynamics of ith robot becomes

$$\dot{\zeta}_i = f_i(\tilde{v}_{Ni}, \tau_{Ni}, \tilde{v}_i) + g_i(\tilde{v}_i)\tau_i. \tag{37}$$

The neighboring set N_i can contain up to n robots. As mentioned before, the ith robot neighboring set should have at least one robot. To demonstrate this, let us assume that the ith robot is at the edge of the group, and it can only receive information from the jth robot. Then the formation dynamics of the ith robot will be a function of only the jth robot's regulation error and controller such as

$$\dot{\zeta}_i = f_i(\tilde{v}_i, \tilde{v}_j, \tau_j) + g_i(\tilde{v}_i)\tau_i. \tag{38}$$

Since the communication links are undirected, the formation dynamics of the jth robot needs to have i^{th} robot's information

$$\dot{\zeta}_i = f_i(\tilde{v}_{Nj}, \tau_{Nj}, \tilde{v}_j) + g_j(\tilde{v}_j)\tau_j \quad \tilde{v}_i \in \tilde{v}_{Nj} , \; \tau_i \in \tau_{Nj} , \tag{39}$$

one can realize that j^{th} robot can be considered as the leader [24] of ith robot for this case.

In the worst case, if the ith robot cannot receive any of the other robots information. Then the dynamics become

$$\dot{\zeta}_i = f_i(\tilde{v}_i, 0, 0) + g_i(\tilde{v}_i)\tau_i , \tag{40}$$

which is a function of its own regulation error. Then the ith robot runs to its goal position without considering other robots. If others get i^{th} robot's information, then every robot in

the group will align themselves with respect to i^{th} robot; otherwise, the rebel (unaligned) robots will be separated from the group and run by themselves to the goal position.

In the simulations, the performance of the controller is demonstrated for several network topologies. The proposed controller (33) not only stabilizes the formation dynamics (20) of the robots, but also minimizes a cost function in a finite time. Therefore, a novel cost function is proposed based on consensus error, regulation error and minimized in a desired finite time. Regulation and formation errors are penalized with two different penalizing matrices. In the simulation section, different penalizing matrices are utilized to inspect how it will affect the formation performance. Next, simulation results are given.

5. SIMULATION RESULTS

This section presents performance of finite horizon optimal consensus control (33) in mobile robot formation in the presence of uncertain robot dynamics. Four non-holonomic mobile robots are utilized to simulate robots that reach their desired positions as well as show how formation stability is maintained along the way. Initial robot positions and velocities are selected as

$$\begin{bmatrix} x_1(0) & x_2(0) & x_3(0) & x_4(0) \end{bmatrix}^T = \begin{bmatrix} 0 & 20 & 0 & -20 \end{bmatrix}^T,$$

$$\begin{bmatrix} y_1(0) & y_2(0) & y_3(0) & y_4(0) \end{bmatrix}^T = \begin{bmatrix} 20 & 0 & -20 & 0 \end{bmatrix}^T$$

$$\begin{bmatrix} \dot{x}_1(0) & \dot{x}_2(0) & \dot{x}_3(0) & \dot{x}_4(0) \end{bmatrix}^T = \begin{bmatrix} 0 & 0 & 0 & 0 \end{bmatrix}^T,$$

$$\begin{bmatrix} \dot{y}_1(0) & \dot{y}_2(0) & \dot{y}_3(0) & \dot{y}_4(0) \end{bmatrix}^T = \begin{bmatrix} 0 & 0 & 0 & 0 \end{bmatrix}^T.$$

Each robot is controlled by using finite horizon optimal formation control (33) and forced to achieve their desired positions and velocities by using minimum energy in 10 seconds. Desired locations are given as

$$\begin{bmatrix} x_{1d} & x_{2d} & x_{3d} & x_{4d} \end{bmatrix}^T = \begin{bmatrix} -14 & -8 & -14 & -22 \end{bmatrix}^T,$$

$\begin{bmatrix} y_{1d} & y_{2d} & y_{3d} & y_{4d} \end{bmatrix}^T = \begin{bmatrix} 21 & 15 & 9 & 15 \end{bmatrix}^T$, and desired accelerations are all set to zero.

The basis vector of value function estimation is done in two steps because of its time varying feature. In the first step, time dependent basis matrix is defined as

$\psi_{ti} = \begin{bmatrix} t_r^{49}, t_r^{48}, \cdots, 1; 1, t_r^{49}, \cdots, t_r; \cdots; t_r^{48}, t_r^{47}, \dots, 1, t_r^{49} \end{bmatrix} \in \Re^{50 \times 50}$ where $t_r = 10 - t$ representing

the time left to reach the final destination. Secondly, we show the dependent part of a basis vector for value function estimation defined as

$$\psi_{\zeta i} = \left[\varsigma_1^2, \cdots, \varsigma_{12}^2, \varsigma_1^2 \varsigma_2, ..., \varsigma_{12}^2 \varsigma_1, \varsigma_1^3 \varsigma_2^2, ..., \varsigma_{12}^3 \varsigma_1^2, \varsigma_1^4 \varsigma_2^3, ..., \varsigma_{12}^4 \varsigma_1^3, \varsigma_1^6, \varsigma_2^6\right]^T \in \mathfrak{R}^{50 \times 1} \text{ where}$$

$\left[\varsigma_1, \cdots, \varsigma_6\right]$ corresponds to the regulation error of the ith robot, and $\left[\varsigma_7, \cdots, \varsigma_{12}\right]$ corresponds

to the formation error of ith robot.

Subsequently, the basis vector of value function estimation is given as multiplication of time-dependent and state-dependent parts, $\psi_{Vi} = \psi_{ti} \psi_{\zeta i} \in \mathfrak{R}^{50 \times 1}$. For the identifier NN, activation function is selected in the same manner as the time-invariant part of the value function basis vector,

$$\psi_{fi} = \left[\varsigma_1^2, \cdots, \varsigma_{12}^2, \varsigma_1^2 \varsigma_2, ..., \varsigma_{12}^2 \varsigma_1, \varsigma_1^3 \varsigma_2^2, ..., \varsigma_{12}^3 \varsigma_1^2, \varsigma_1^4 \varsigma_2^3, ..., \varsigma_{12}^4 \varsigma_1^3, \varsigma_1^6, \varsigma_2^6\right]^T \in \mathfrak{R}^{50 \times 1},$$

$\left[\tilde{v}_{i1}^2, \tilde{v}_{i1}\tilde{v}_{i2}, ..., \tilde{v}_{i2}^2, ..., \tilde{v}_{i1}^6, \tilde{v}_{i1}^5\tilde{v}_{i2}, ..., \tilde{v}_{i2}^6\right]^T \in \mathfrak{R}^{15 \times 1}$ and $\psi_{Ii} = \begin{bmatrix} \psi_{fi} & 0_{50 \times 1} \\ 0_{15 \times 1} & \psi_{gi} \end{bmatrix} \in \mathfrak{R}^{65 \times 2}$. Initial NN

weights are selected as small random numbers as $W_{I0} \in 0.01 * \text{rand}(65,12)$ and

$W_{V0} \in 0.02 * \text{rand}(50,12)$ for both the identifier and value function NNs. The history of

NN weights for value function approximation is illustrated in Figure 5.1. Moreover, the

value function is defined as function of regulation error, formation error and control input

of each robot as

$$V(\zeta, 0) = \vartheta(\zeta(10), 10) + \int_0^{10} (Q(\zeta) + u^T R u) dt \tag{41}$$

where $R = \text{eye}(2,2)$ is identity matrix,

$$Q(\zeta) = \frac{1}{2}[\varsigma_1, \cdots, \varsigma_6]Q_1[\varsigma_1, \cdots, \varsigma_6]^T + \frac{1}{2}[\varsigma_7, \cdots, \varsigma_{12}]Q_2[\varsigma_7, \cdots, \varsigma_{12}]^T \text{ where } Q_1 \in \mathfrak{R}^{6 \times 6} \text{ and}$$

$Q_2 \in \mathfrak{R}^{6 \times 6}$ become positive definite matrices to penalize regulation error and formation

error, respectively; hence, terminal constraint is given as

$$\vartheta(\zeta(10),10) = \left[\begin{bmatrix} 1.2 & 1.2 & 1.2 & 1.2 & 1.2 & 1.2 \end{bmatrix}^T, 3*\begin{bmatrix} 1.2 & 1.2 & 1.2 & 1.2 & 1.2 & 1.2 \end{bmatrix}^T \right]^T.$$
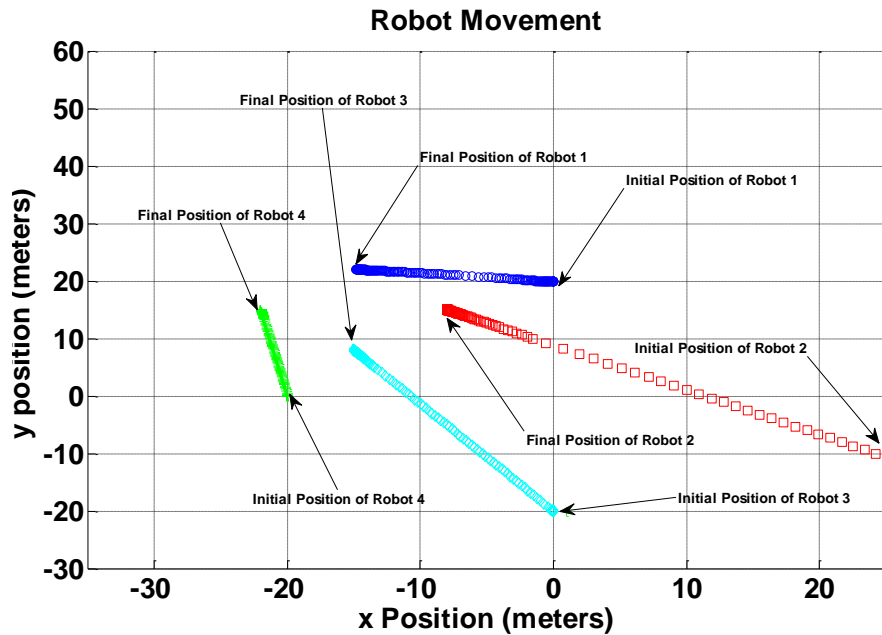
Figure 5.1 Robot movements on x-y plane.

The simulation results are given for three different communication scenarios among the four robots.

5.1   FULL CONNECTIVITY

In this case, it is assumed that each one of the four robots is able to receive the regulation errors and controller torques of all other robots, i.e., the connectivity matrix is chosen as $\quad L = \begin{bmatrix} 0 & 1 & 1 & 1 \\ 1 & 0 & 1 & 1 \\ 1 & 1 & 0 & 1 \\ 1 & 1 & 1 & 0 \end{bmatrix}.$

Figure 5.1 depicts how robots move from their initial position to their goal positions. Since the initial position of the second robot is farther away from its desired position, it moves faster to minimize the formation error and reaches the goal position at the same time as the other robots. The NN weights converge in the first couple seconds as shown in Figure 5.2.

History of value function NN weights for each robot
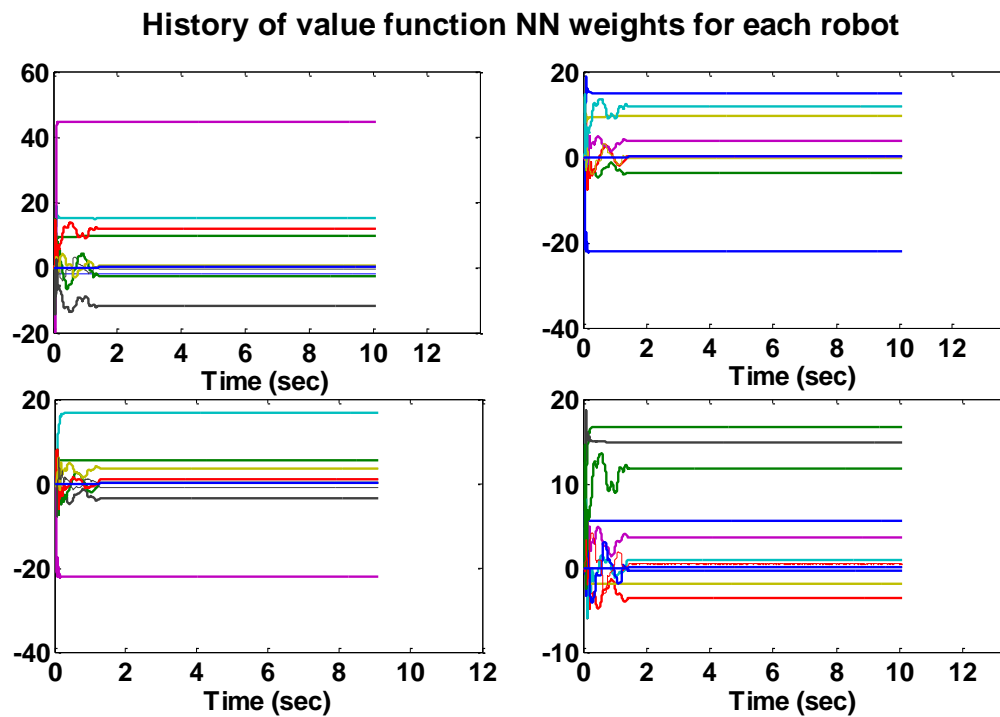
Figure 5.2 Value function estimation NN weight history.

In Figure 5.3, regulation and formation errors are depicted for all four robots. It is assumed that each robot has all the information possessed by the other three robots. In the cost function (41), the regulation and formation errors are penalized equally, $Q_1 = Q_2$.

However, Figure 5.4 shows the effect of penalizing matrices on the formation performance of robots. In Figure 5.4, performance of controller (33) with two different cost

functions is compared. The first plot illustrates how regulation errors converge when formation errors are penalized five times larger than regulation errors, $Q_1 = 0.2Q_2$, and the second plot depicts the regulation errors with equal penalizing matrices. As can be observed in Figure 5.4, the third robot moves away from its goal position initially to maintain formation; however, in the second plot, the third robot converges to the goal position directly.

Analysis of the HJB equation and terminal constraint errors have been given in Figure 5.5, which show that not only the HJB equation error but also terminal constraint errors converge close to zero within the finite time (i.e., $t \in [0, 10s]$).

According to *Theorem* 2, the proposed finite horizon optimal design can ensure the boundedness of both HJB and terminal constraint errors within finite horizon. Moreover, the convergence of the HJB and terminal constraint errors confirm that the approximated control input (33) approaches the finite horizon optimal control input over finite time.

As shown in Figure 5.3, Figure 5.6 and Figure 5.7, the proposed finite horizon optimal control can force robot states to converge close to zero within a finite horizon; or, in other words, the proposed controller scheme can maintain the boundedness even in presence of uncertain robot dynamics.
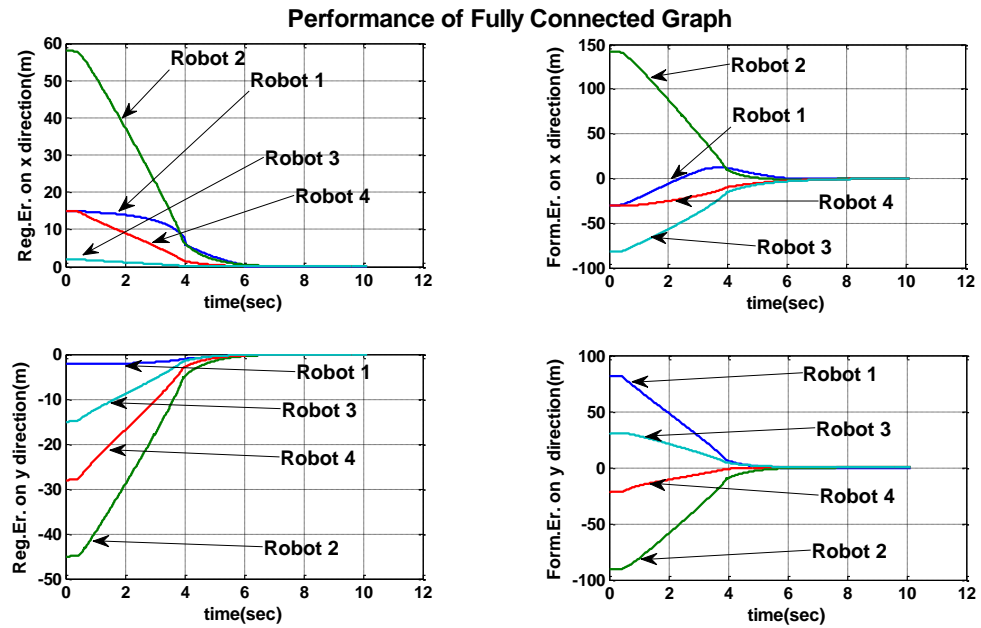
Figure 5.3 Error convergences with full communication.
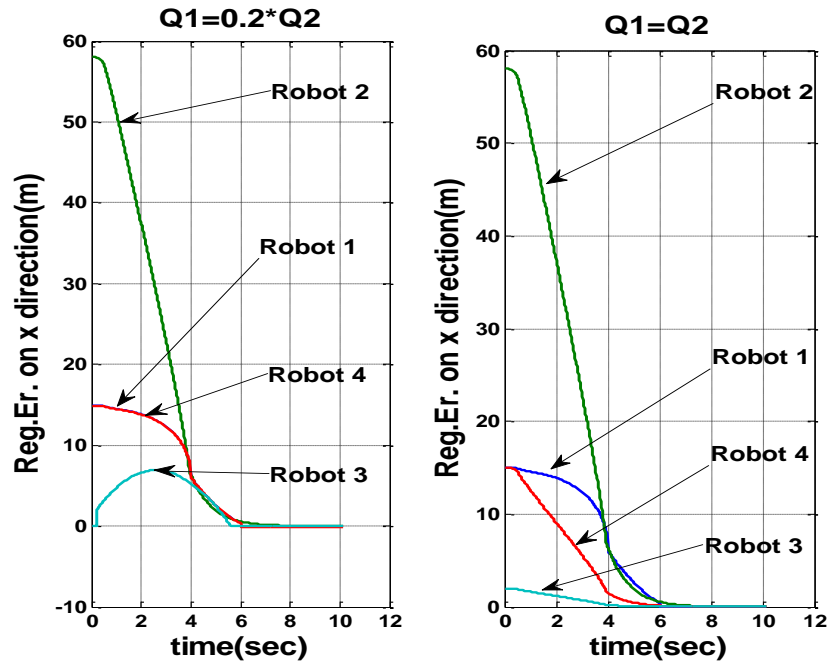
Figure 5.4 Effect of cost function on performance of controller.

5.2 PARTIAL CONNECTIVITY

In this second case, the communication graph of the robots is assumed to be similar to Figure 2.2 in terms of connectivity whereas each robot is able to receive only part of group member's information, i.e., the connectivity matrix is chosen as

$$L = \begin{bmatrix} 0 & 0 & 0 & 1 \\ 0 & 0 & 0 & 1 \\ 0 & 1 & 0 & 1 \\ 1 & 0 & 1 & 0 \end{bmatrix}.$$

Even in this case, because the graph is connected, the performance of formation controller is almost similar to the full connected case. The performance of the controller is given in Figure 5.6.
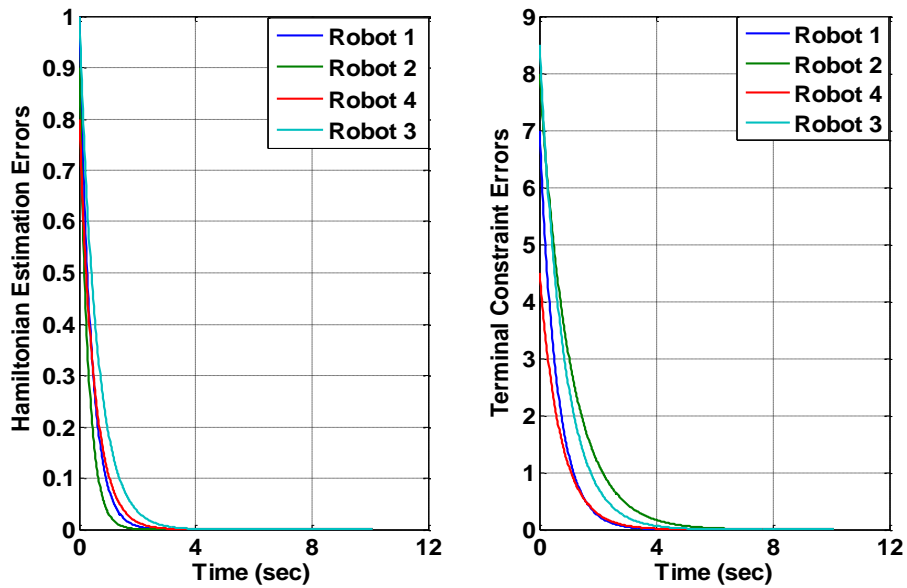
Figure 5.5 Hamiltonian and terminal constraint errors.
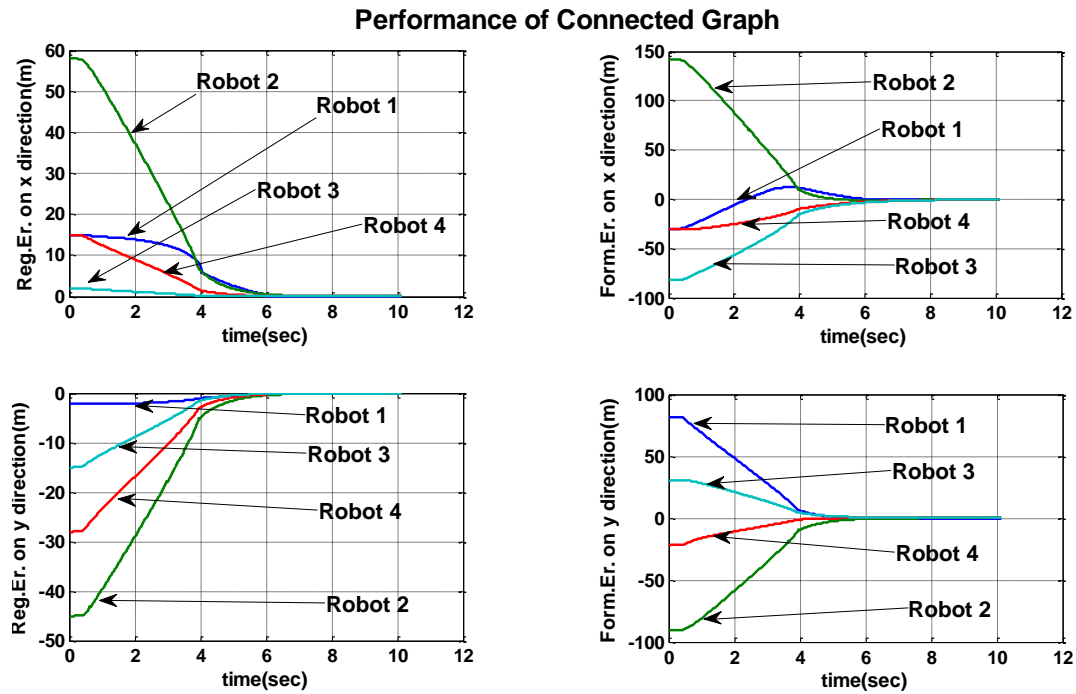
Figure 5.6 Error convergences with connected communication.

5.3 NO CONNECTIVITY

In this last case, one of the four robots (second robot) is assumed to have neither received any information from other robots nor passed its information to any other robot,

i.e., the connectivity matrix is $L = \begin{bmatrix} 0 & 0 & 1 & 1 \\ 0 & 0 & 0 & 0 \\ 1 & 0 & 0 & 1 \\ 1 & 0 & 1 & 0 \end{bmatrix}$.

From Figure 5.7, it is clear that the regulation error of the second robot converges to zero independently from others; however, the other three robots converge to the same value in the first couple of seconds.
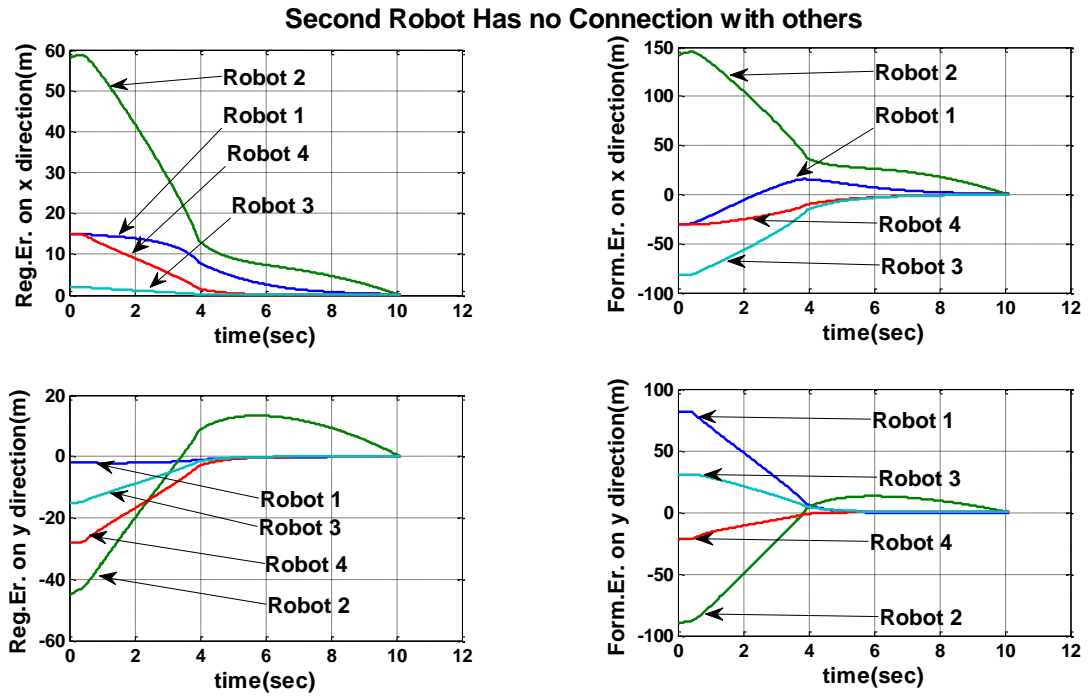
Figure 5.7 Error convergences with unconnected communication graph.

6. CONCLUSIONS

In this paper, a finite horizon optimal consensus-based formation controller was designed for mobile robot formation in the presence of uncertain robot dynamics. The consensus-based control was derived for a formation of mobile robots by taking into account their dynamics. Subsequently, the cost function derived as a function of regulation and formation errors would be able to generate optimal inputs to each robot such that the entire formation will travel in consensus from an initial position to the goal position. An NN identifier generated the formation dynamics while the time-varying value function approximated the solution to the HJB equation. Simulation results confirm the theoretical conclusions.

APPENDIX

Proof of Theorem 1: Define Lyapunov candidate function as

$$
L_i = \underbrace{\gamma_3 J_{\xi_i}(\xi_i)}_{a} + \underbrace{\frac{1}{2}tr\{\tilde{\theta}_{Vi}^T \Pi \tilde{\theta}_{Vi}\}}_{b} + \frac{1}{2}e_i^T \Xi e_i + \frac{1}{2}tr\{\tilde{\theta}_{Ii}^T \Xi \tilde{\theta}_{Ii}\} + \underbrace{\frac{\gamma_1}{4}(e_i^T \Lambda e_i)^2 + \frac{\gamma_2}{4}(tr\{\tilde{\theta}_{Ii}^T \Lambda \tilde{\theta}_{Ii}\})^2}_{c}
$$

$$(A.1)$$

First, consider the derivative of L_a as

$$
\dot{L}_{ia} = \lambda_3 J_{\xi_i}^T(\zeta_i)(f_i(\zeta_i) + g_i(\zeta_i)\tau_i.)
$$

$$(A.2)$$

$$
= \alpha_3 J_{\xi_i}^T(\zeta_i)(f_i(\zeta_i) - \frac{1}{2} g_i(\tilde{v}_i) R^{-1} \hat{g}_i(\zeta_i) \nabla_{\xi_i}^T \varphi_i(\zeta_i, t_f - t)\hat{\theta}_{Vi})
$$

Then, take the derivative of the second term, $\dot{L}_{bi}$, to get

$$
\dot{L}_{bi} = \tilde{\theta}_{Vi}^T \Pi \dot{\tilde{\theta}}_{Vi} = \|\Pi\| \left(\begin{array}{c} \gamma_1 \dfrac{\hat{\eta}}{(1+\hat{\eta}^T\hat{\eta})^2} \hat{H}_i(\zeta_i, \tau_i, t) - \gamma_2 \dfrac{\hat{\mu}}{(1+\hat{\mu}^T\hat{\mu})^2} e_{t_f i}^3 \\[4mm] -\dfrac{\gamma_3}{2} \nabla_{\xi_i} \psi_{V_i}(\zeta_i, t_f - t)\hat{D}(\tilde{v}_i) J_{\xi_i}(\zeta_i) \end{array} \right)
$$

$$
= -\gamma_1 \dfrac{\|\Pi\|\tilde{\theta}_V^T}{(1+\hat{\eta}^T\hat{\eta})^2} \left[\begin{array}{c} \nabla_t \psi_{Vi}(\zeta_i, t_f - t) + \nabla_{\xi_i}\psi_{Vi}(\zeta_i, t_f - t)f_i(\tilde{v}, \tau) \\[3mm] -\nabla_\xi \psi_{Vi}(\zeta_i, t_f - t)\tilde{f}_i(\tilde{v}, \tau) \\[3mm] -\dfrac{1}{2}\nabla_\xi \psi_{Vi}(\zeta_i, t_f - t)D(\tilde{v}_i)\nabla_{\xi_i}^T \psi_{Vi}(\zeta_i, t_f - t)\hat{\theta}_V \\[3mm] +\dfrac{1}{2}\nabla_\xi \psi_{Vi}(\zeta_i, t_f - t)\tilde{D}(\tilde{v}_i)\nabla_{\xi_i}^T \psi_{Vi}(\zeta_i, t_f - t)\hat{\theta}_V \end{array} \right]
$$

$$\times \begin{bmatrix} \tilde{\theta}_{Vi}^T \nabla_t \psi_{Vi}(\zeta_i, t_f - t) + \tilde{\theta}_{Vi}^T \nabla_{\xi_i} \psi_{Vi}(\zeta_i, t_f - t) f_i(\xi_i) \\ -\tilde{W}_V^T \nabla_{\xi_i} \psi_{Vi}(\zeta_i, t_f - t)\tilde{f}_i(\xi_i) + W_V^T \nabla_{\xi_i} \psi_{Vi}(\zeta_i, t_f - t)\tilde{f}_i(\xi_i) \\ -\dfrac{1}{2} \tilde{\theta}_{Vi}^T \nabla_{\xi_i} \psi_{Vi}(\zeta_i, t_f - t) D(\tilde{v}_i) \nabla_{\xi_i}^T \psi_{Vi}(\zeta_i, t_f - t)\hat{\theta}_{Vi} \\ +\dfrac{1}{2} \tilde{\theta}_{Vi}^T \nabla_{\xi_i} \psi_{Vi}(\zeta_i, t_f - t) \tilde{D}(\tilde{v}_i) \nabla_{\xi_i}^T \psi_{Vi}(\xi_i, t_f - t)\hat{\theta}_{Vi} \\ -\dfrac{1}{4} \theta_{Vi}^T \nabla_{\xi_i} \psi_{Vi}(\zeta_i, t_f - t) \tilde{D}(\tilde{v}_i) \nabla_{\xi_i}^T \psi_{Vi}(\zeta_i, t_f - t)\hat{\theta}_{Vi} \\ -\dfrac{1}{4} \tilde{\theta}_{Vi}^T \nabla_{\xi_i} \psi_{Vi}(\zeta_i, t_f - t) \hat{D}(\tilde{v}_i) \nabla_{\xi_i}^T \psi_{Vi}(\zeta_i, t_f - t)\tilde{\theta}_{Vi} - \varepsilon_{HJBi} \end{bmatrix}$$

$$\begin{bmatrix} +\dfrac{1}{2} \tilde{\theta}_{Vi}^T \nabla_{\xi_i} \psi_{Vi}(\zeta_i, t_f - t) \tilde{D}(\tilde{v}_i) \nabla_{\xi_i}^T \psi_{Vi}(\zeta_i, t_f - t)\hat{\theta}_{Vi} \\ -\dfrac{1}{4} \theta_{Vi}^T \nabla_{\xi_i} \psi_{Vi}(\zeta_i, t_f - t) \tilde{D}(\tilde{v}_i) \nabla_{\xi_i}^T \psi_{Vi}(\zeta_i, t_f - t)\hat{\theta}_{Vi} \\ -\dfrac{1}{4} \tilde{\theta}_{Vi}^T \nabla_{\xi_i} \psi_{Vi}(\zeta_i, t_f - t) \hat{D}(\tilde{v}_i) \nabla_{\xi_i}^T \psi_{Vi}(\zeta_i, t_f - t)\tilde{\theta}_{Vi} - \varepsilon_{HJBi} \end{bmatrix} \Bigg)$$

$$-\gamma_2 \frac{\left\| \Pi \right\| \tilde{\theta}_{Vi}^T \vartheta_i(\zeta_i(t_f), t_f)([\theta_{Vi}^T \tilde{\vartheta}_i(\zeta_i(t_f), \hat{\zeta}_i(t_f), t_f) + \tilde{\theta}_{Vi}^T \vartheta_i(\hat{\zeta}_i(t_f), t_f)]^3)^T}{(1 + \hat{\mu}^T \hat{\mu})^2}$$

$$\leq -\gamma_1 \frac{\left\| \Pi \right\| \tilde{\theta}_{Vi}^T \hat{\eta} \begin{bmatrix} \tilde{\theta}_{Vi}^T \hat{\eta} - \dfrac{1}{4} \theta_{Vi}^T \nabla_{\xi_i} \vartheta_i(\zeta_i(t_f), t_f - t) \tilde{D}(\tilde{v}_i) \nabla_{\zeta_i}^T \vartheta_i(\zeta_i(t_f), t_f) \theta_{Vi} \\ -\dfrac{1}{4} \tilde{W}_V^T \nabla_{\xi_i} \vartheta_i(\zeta_i(t_f), t_f - t) \hat{D}(\tilde{v}_i) \nabla_{\xi_i}^T \vartheta_i(\zeta_i(t_f), t_f - t) \tilde{\theta}_{Vi} \\ +\theta_{Vi}^T \nabla_{\xi_i} \vartheta_i(\zeta_i(t_f), t_f - t) \tilde{f}_i(\zeta_i) - \varepsilon_{HJBi} \end{bmatrix}^T}{(1 + \hat{\eta}^T \hat{\eta})^2}$$

$$-\gamma_2 \frac{\left\| \Pi \right\| \tilde{\theta}_{Vi}^T \hat{\mu}\left(\left[\theta_{Vi}^T \tilde{\vartheta}_i(\zeta_i(t_f), \hat{\zeta}_i(t_f), t_f - t) + \tilde{\theta}_{Vi}^T \hat{\mu} + \varepsilon_{FC} \right]^3 \right)^T}{(1 + \hat{\mu}^T \hat{\mu})^2}$$

$$-\frac{\gamma_3 \left\| \Pi \right\|}{2} \tilde{\theta}_{Vi}^T \nabla_{\xi_i} \vartheta_i(\zeta_i(t_f), t_f - t) \hat{D}(\zeta_i) J_{\xi_i}(\zeta_i)$$

$$\leq -\frac{\gamma_1 \|\Pi\|}{4} \frac{\tilde{\theta}_V^T \hat{\eta} \hat{\eta}^T \tilde{\theta}_{Vi}}{(1+\hat{\eta}^T \hat{\eta})^2} + \frac{\lambda_1 \|\Pi\|}{2} \frac{\varepsilon_{HJBi}^2}{(1+\hat{\eta}^T \hat{\eta})^2}$$

$$+ \frac{\gamma_1 \|\Pi\|}{8} \frac{(\theta_{Vi}^T \nabla_{\xi_i} \vartheta_i(\xi_i(t_f), t_f - t) \tilde{D}(\xi_i) \nabla_{\xi_i}^T \vartheta_i(\xi_i(t_f), t_f - t)\theta_{Vi})^2}{(1+\hat{\eta}^T \hat{\eta})^2}$$

$$+ \frac{\gamma_1 \|\Pi\|}{8} \frac{(\tilde{\theta}_{Vi}^T \nabla_{\xi_i} \vartheta_i(\xi_i(t_f), t_f - t) \hat{D}(\xi_i) \nabla_{\xi_i}^T \vartheta_i(\xi_i(t_f), t_f - t)\tilde{\theta}_{Vi})^2}{(1+\hat{\eta}^T \hat{\eta})^2}$$

$$- \|\Pi\| \left(\alpha_2 \frac{\tilde{\theta}_{Vi}^T \hat{\mu} \hat{\mu}^T \tilde{\theta}_{Vi}}{(1+\hat{\mu}^T \hat{\mu})^2} - \frac{1}{2}\gamma_2 \frac{\tilde{\theta}_{Vi}^T \hat{\mu} \hat{\mu}^T \tilde{\theta}_{Vi}}{(1+\hat{\mu}^T \hat{\mu})^2} - \gamma_2 \frac{\varepsilon_{FC}^2}{(1+\hat{\mu}^T \hat{\mu})^2} \right.$$

$$\left. - \alpha_2 \frac{\theta_{Vi}^T \nabla_{\xi_i} \tilde{\vartheta}_i(\xi_i(t_f), \hat{\xi}_i(t_f), t_f) \tilde{\vartheta}_i^T(\xi_i(t_f), \hat{\xi}_i(t_f), t_f)\theta_{Vi}}{(1+\hat{\mu}^T \hat{\mu})^2} \right)$$

$$(3\tilde{\theta}_{Vi}^T \hat{\mu} \hat{\mu}^T \tilde{\theta}_{Vi} + 3\theta_{Vi}^T \tilde{\vartheta}_i(\xi_i(t_f), \hat{\xi}_i(t_f), t_f) \tilde{\vartheta}_i^T(\xi_i(t_f), \hat{\xi}_i(t_f), t_f) \times \theta_{Vi} + 3\varepsilon_{FC}^2)$$

$$- \frac{\gamma_3 \|\Pi\|}{2} \tilde{\theta}_{Vi}^T \nabla_{\xi_i} \vartheta_i(\xi_i(t_f), t_f - t) \hat{D}(\xi_i) J_{\xi_i}(\xi_i)$$

$$\leq -\frac{\gamma_1 \|\Pi\|}{4} \frac{\tilde{\theta}_{Vi}^T \hat{\eta} \hat{\eta}^T \tilde{\theta}_{Vi}}{(1+\hat{\eta}^T \hat{\eta})^2} + \frac{\gamma_1 \|\Pi\|}{2} \frac{\varepsilon_{HJBi}^2}{(1+\hat{\eta}^T \hat{\eta})^2}$$

$$+ \frac{\gamma_1 \|\Pi\|}{8} \frac{(\theta_{Vi}^T \nabla_{\xi_i} \vartheta_i(\xi_i(t_f), t_f - t) \tilde{D}(\xi_i) \nabla_{\xi_i}^T \vartheta_i(\xi_i(t_f), t_f - t)\theta_{Vi})^2}{(1+\hat{\eta}^T \hat{\eta})^2}$$

$$+ \frac{\alpha_1 \|\Pi\|}{8} \frac{\gamma_1 \|\Pi\|}{8} \frac{(\tilde{\theta}_{Vi}^T \nabla_{\xi_i} \vartheta_i(\xi_i(t_f), t_f - t) \hat{D}(\tilde{v}_i) \nabla_{\xi_i}^T \vartheta_i(\xi_i(t_f), t_f - t)\tilde{\theta}_{Vi})^2}{(1+\hat{\eta}^T \hat{\eta})^2}$$

$$- \|\Pi\| \frac{\gamma_1 \alpha_2}{4} \frac{(\tilde{\theta}_{Vi}^T \hat{\eta} \hat{\eta}^T \tilde{\theta}_{Vi})^2}{(1+\hat{\eta}^T \hat{\eta})^2} + \frac{15}{2} \left(\gamma_2 \frac{\varepsilon_{FC}^2}{(1+\hat{\eta}^T \hat{\eta})^2} \right.$$

$$\left. + \frac{\theta_{Vi}^T \tilde{\vartheta}_i(\xi_i(t_f), \hat{\xi}_i(t_f), t_f) \tilde{\vartheta}_i^T(\xi_i(t_f), \hat{\xi}_i(t_f), t_f)\theta_{Vi}}{(1+\hat{\eta}^T \hat{\eta})^2} \right)^2$$

$$+3(\tilde{\vartheta}_i(\xi_i(t_f),\hat{\xi}_i(t_f),t_f)\tilde{\vartheta}_i^T(\xi_i(t_f),\hat{\xi}_i(t_f),t_f)\theta_{Vi}W_V + \varepsilon_{FC}^2)^2$$

$$-\frac{\gamma_3\|\Pi\|}{2}\tilde{\theta}_{Vi}^T\nabla_{\xi_i}\vartheta_i(\xi_i(t_f),t_f-t)\hat{D}(\xi_i)J_{\xi_i}(\xi_i)$$

$$\leq -\frac{\gamma_1\|\Pi\|}{4}\frac{\tilde{\theta}_{Vi}^T\hat{\eta}\hat{\eta}^T\tilde{\theta}_{Vi}}{(1+\hat{\eta}^T\hat{\eta})^2} - \|\Pi\|\frac{3\gamma_2}{8}\frac{(\tilde{\theta}_{Vi}^T\hat{\mu}\hat{\mu}^T\tilde{\theta}_{Vi})^2}{(1+\hat{\mu}^T\hat{\mu})^2}$$

$$+\frac{\gamma_1\|\Pi\|}{8}\frac{(\theta_{Vi}^T\nabla_{\xi_i}\vartheta_i(\xi_i(t_f),t_f-t)\tilde{D}(\tilde{v}_i)\nabla_{\xi_i}^T\vartheta_i(\xi_i(t_f),t_f-t)\theta_{Vi})^2}{(1+\hat{\eta}^T\hat{\eta})^2}$$

$$-\frac{\gamma_3\|\Pi\|}{2}\tilde{\theta}_{Vi}^T\nabla_{\xi_i}\vartheta_i(\xi_i(t_f),t_f-t)\hat{D}(\xi_i)J_{\xi_i}(\xi_i) + \varepsilon_{V1i}$$

$$\leq -\frac{\gamma_1\|\Pi\|}{4}\frac{\lambda_{\min}(\hat{\eta}\hat{\eta}^T)}{(1+\hat{\eta}^T\hat{\eta})^2}\left\|\tilde{\theta}_{Vi}\right\|^2 - \|\Pi\|\frac{3\gamma_2}{8}\frac{(\tilde{\theta}_{Vi}^T\hat{\mu}\hat{\mu}^T\tilde{\theta}_{Vi})^2}{(1+\hat{\mu}^T\hat{\mu})^2}$$

$$+\frac{\gamma_1\theta_{VMi}^4\lambda_{\max}^4(R^{-1})\nabla_{\xi_i}\vartheta_{Mi}^4\sigma_{I,Mi}^4}{2(1+\hat{\eta}^T\hat{\eta})^2}\left\|\tilde{\theta}_{Ii}\right\|^4 - \frac{\gamma_3\|\Pi\|}{2}\tilde{\theta}_{Vi}^T\nabla_{\xi_i}\vartheta_i(\xi_i(t_f),t_f-t)\hat{D}(\xi_i)J_{\xi_i}(\xi_i)$$

$$+\varepsilon_{V1} + \frac{\gamma_1\theta_{VMi}^4\lambda_{\max}^4(R^{-1})\nabla_{\xi_i}\vartheta_{Mi}^4\varepsilon_{Ii}}{2(1+\hat{\eta}^T\hat{\eta})^2}$$

$$\leq -\frac{\gamma_1\|\Pi\|}{4}\frac{\lambda_{\min}(\hat{\eta}\hat{\eta}^T)}{(1+\hat{\eta}^T\hat{\eta})^2}\left\|\tilde{\theta}_{Vi}\right\|^2 + \frac{\gamma_1\theta_{VMi}^4\lambda_{\max}^4(R^{-1})\nabla_{\xi_i}\vartheta_{Mi}^4\sigma_{IMi}^4}{2(1+\hat{\omega}^T\hat{\omega})^2}\left\|\tilde{\theta}_{Vi}\right\|^4$$

$$-\frac{\gamma_3\|\Pi\|}{2}\tilde{\theta}_{Vi}^T\nabla_{\xi_i}\vartheta_i(\xi_i(t_f),t_f-t)\hat{D}(\xi_i)J_{\xi_i}(\xi_i) + \varepsilon_{VMi}$$

where

$$0 < \gamma_1 \leq \frac{3\gamma_2(1+\hat{\eta}^T\hat{\eta})^2\lambda_{\min}^2(\hat{\mu}\hat{\mu}^T)}{\lambda_{\max}^2(\nabla_{\xi_i}\vartheta_i(\xi_i(t_f),t_f-t)\hat{D}(\xi_i)\nabla_{\xi_i}^T\vartheta_i(\xi_i(t_f),t_f-t)(1+\hat{\mu}^T\hat{\mu})^2} \quad \text{and}$$

$$\varepsilon_{Vi} = \frac{\gamma_1 \|\Pi\|}{2} \frac{\varepsilon_{HJB}^2}{(1+\hat{\eta}^T\hat{\eta})^2} + 3(\theta_{Vi}^T \tilde{\vartheta}_i(\xi_i(t_f), \hat{\xi}_i(t_f), t_f)\tilde{\vartheta}_i^T(\xi_i(t_f), \hat{\xi}_i(t_f), t_f)\theta_{Vi}$$

$$+\varepsilon_{FC}^2)^2 + \frac{15}{2}\left(\frac{\theta_{Vi}^T \tilde{\vartheta}_i(\xi_i(t_f), \hat{\xi}_i(t_f), t_f)\tilde{\vartheta}_i^T(\xi_i(t_f), \hat{\xi}_i(t_f), t_f)\theta_{Vi} + \lambda_2 \varepsilon_{FC}^2}{(1+\hat{\mu}^T\hat{\mu})^2}\right)^2$$

$$+\frac{\gamma_1 \theta_{VMi}^4 \lambda_{\max}^4(R^{-1})\nabla_{\xi_i}\vartheta_{Mi}^4 \varepsilon_{Ii}^4}{2(1+\hat{\omega}^T\hat{\omega})^2}\ .$$

Moreover, where $\lambda_{\min}(R^{-1})$ and $\lambda_{\max}(R^{-1})$ denote minimum and maximum eigenvalues of the inverse matrix R^{-1}, $\|\theta_{Vi}\| = \theta_{VMi}$, $\left\|\nabla_{\xi_i}\vartheta_i(\xi_i(t_f), t_f - t)\right\| = \nabla_{\xi_i}\vartheta_{Mi}$, $\left\|\tilde{\vartheta}_i(\xi_i(t_f), \hat{\xi}_i(t_f))\right\| = 2\vartheta_{Mi}$ with $\left\|\vartheta_i(\xi_i(t_f), \hat{\xi}_i(t_f))\right\| = \vartheta_{Mi}$, $\|\sigma_I(\xi_i)\| = \sigma_{IMi}$ .Next, consider the third term and its derivate $\dot{L}_c$ as

$$\dot{L}_c = \|\Lambda\|^2 \gamma_1(e_i^T e_i)e_i^T \dot{e}_i + \|\Lambda\|^2 \gamma_2 tr\{\tilde{\theta}_{Ii}^T \tilde{\theta}_{Ii}\}tr\{\tilde{\theta}_{Ii}^T \dot{\tilde{\theta}}_{Ii}\}$$

$$= \|\Lambda\|^2 \gamma_1(e_i^T e_i)e_i^T[\tilde{\theta}_{Ii}^T \psi_{Ii}(\xi_i)\bar{\tau}_i + \varepsilon_{Ii} - Ke_i] + \|\Lambda\|^2 \gamma_2 tr\{\tilde{\theta}_{Ii}^T \tilde{\theta}_{Ii}\}tr\{\tilde{\theta}_{Ii}^T[\gamma_{Ii}\hat{\theta}_{Ii} - \psi_{Ii}(\xi_i)\bar{\tau}_i e_i]\}$$

$$= \|\Lambda\|^2 \gamma_1(e_i^T e_i)e_i^T \tilde{\theta}_{Ii}^T \psi_{Ii}(\xi_i)\bar{\tau}_i + \|\Lambda\|^2 \gamma_1(e_i^T e_i)e_i^T \varepsilon_{Ii}$$

$$- \|\Lambda\|^2 \gamma_1(e_i^T e_i)e_i^T Ke_i + \|\Lambda\|^2 \gamma_2\gamma_{Ii} tr\{\tilde{\theta}_{Ii}^T \tilde{\theta}_{Ii}\}tr\{\tilde{\theta}_{Ii}^T \hat{\theta}_{Ii}\}$$

$$- \|\Lambda\|^2 \gamma_2 tr\{\tilde{\theta}_{Ii}^T \tilde{\theta}_{Ii}\}tr\{\tilde{\theta}_{Ii}^T \psi_{Ii}(\xi_i)\bar{\tau}_i e_i\}$$

$$\leq \frac{1}{2}\|\Lambda\|^2 \gamma_1(e_i^T e_i)^2 + \frac{1}{2}\|\Lambda\|^2 \lambda_1(e_i^T \tilde{\theta}_{Ii}^T \psi_{Ii}(\xi_i)\bar{\tau}_i)^2$$

$$+ \frac{1}{2}\|\Lambda\|^2 \gamma_1(e_i^T e_i)^2 + \frac{1}{2}\|\Lambda\|^2 \gamma_1(e_i^T \varepsilon_{Ii})^2 + \|\Lambda\|^2 \frac{\gamma_2\gamma_{Ii}}{4}\theta_{Mi}^4$$

$$- \|\Lambda\|^2 \gamma_1\lambda_{\min}(K)(e_i^T e_i)^2 + \|\Lambda\|^2 \frac{\gamma_2\gamma_{Ii}}{2}(tr\{\tilde{\theta}_{Ii}^T \tilde{\theta}_{Ii}\})^2$$

$$+\left\|\Lambda\right\|^2 \frac{\gamma_2\gamma_{Ii}}{4}(tr\{\tilde{\theta}_{Ii}^T\tilde{\theta}_{Ii}\})^2 - \left\|\Lambda\right\|^2 \gamma_2 tr\{\tilde{\theta}_{Ii}^T\tilde{\theta}_{Ii}\}tr\{\tilde{\theta}_{Ii}^T\psi_{Ii}(\xi_i)\bar{\tau}_i e_i\} - \left\|\Lambda\right\|^2 \gamma_2\gamma_I tr\{\tilde{\theta}_{Ii}^T\tilde{\theta}_{Ii}\}tr\{\tilde{\theta}_{Ii}^T\tilde{\theta}_{Ii}\}$$

$$\leq -\left\|\Lambda\right\|^2\left(\gamma_1\lambda_{\min}(K) - \frac{3}{2}\gamma_1 - \frac{\gamma_2}{4}\right)\left\|e_i\right\|^4 + \frac{\gamma_2}{2}\left\|\Lambda\right\|^2\left\|\tilde{\theta}_{Ii}\right\|^4$$

$$+\frac{\gamma_1+\gamma_2}{4}\left\|\Lambda\right\|^2\left\|\zeta_{Ii}\right\|^4\left\|\tilde{\theta}_{Ii}\right\|^4 - \frac{\gamma_2\gamma_I}{4}\left\|\Lambda\right\|^2\left\|\tilde{\theta}_{Ii}\right\|^4 + \frac{\gamma_2\gamma_{Ii}}{4}\left\|\Lambda\right\|^2\theta_{Mi}^4 + \frac{1}{4}\left\|\Lambda\right\|^2\gamma_1\left\|\varepsilon_{Ii}\right\|^4$$

$$\leq -\gamma_1\left(\lambda_{\min}(K) - \frac{3}{2} - \frac{\gamma_2}{4\lambda_1}\right)\left\|\Lambda\right\|^2\left\|e_i\right\|^4 - \frac{\gamma_2}{2}\left(\frac{\lambda_{Ii}}{2} - 1 - \frac{\gamma_1+\gamma_2}{4\gamma_2}\left\|\zeta_I\right\|^4\right)\left\|\Lambda\right\|^2\left\|\tilde{\theta}_{Ii}\right\|^4$$

$$+\frac{\gamma_2\gamma_{Ii}}{4}\left\|\Lambda\right\|^2\theta_{Mi}^4 + \frac{1}{4}\gamma_1\left\|\Lambda\right\|^2\left\|\varepsilon_{Ii}\right\|^2$$

$$\leq -\gamma_1\left(\lambda_{\min}(K) - \frac{3}{2} - \frac{\gamma_2}{4\gamma_1}\right)\left\|\Lambda\right\|^2\left\|e_i\right\|^4 - \frac{\gamma_2}{2}\left(\frac{\gamma_I}{2} - 1 - \frac{\gamma_1+\gamma_2}{4\gamma_2}\left\|\zeta_I\right\|^4\right)\left\|\Lambda\right\|^2\left\|\tilde{\theta}_{Ii}\right\|^4 + \varepsilon_{Mi} \qquad (A.3)$$

where $\gamma_1 > 0$, $\gamma_2 > 0$ and $\gamma_{Ii} > 4 + \frac{\gamma_1+\gamma_2}{2\gamma_2}\left\|\zeta_I\right\|^4$. Select K to satisfy $\lambda_{\min}(K) > \frac{3}{2} + \frac{\gamma_2}{4\gamma_1}$.

Moreover,

$$\varepsilon_{cM} = \frac{\gamma_2\gamma_I}{4}\left\|\Lambda\right\|^2\theta_{Mi}^4 + \frac{1}{4}\left\|\Lambda\right\|^2\gamma_1\left\|\varepsilon_{Ii}\right\|^2 \frac{1}{4}\left\|\Lambda\right\|^2\lambda_{1i}\left\|\varepsilon_{Ii}\right\|^2.$$

Combining (A.1), (A.2) and (A.3), the first derivative of the overall Lyapunov function candidate, $\dot{L}$, can be expressed as

$$\dot{L} = \dot{L}_a + \dot{L}_b + \dot{L}_c + \dot{L}_I$$

$$\leq \gamma_3 J_{\xi_i}^T(\xi_i)(f_i(\xi_i) - \frac{1}{2}g_i(\xi_i)R^{-1}\hat{g}_i(\xi_i)\nabla_{\xi_i}^T\vartheta_i(\xi_i, t_f - t)\hat{\theta}_{Vi})$$

$$-\frac{1}{2}\left[\gamma_1\frac{\lambda_{\min}(\hat{\eta}\hat{\eta}^T)}{(1+\hat{\eta}^T\hat{\eta})^2} + \gamma_2\frac{\lambda_{\min}(\hat{\mu}\hat{\mu}^T)}{(1+\hat{\mu}^T\hat{\mu})^2}\right]\left\|\Pi\right\|\left\|\tilde{\theta}_{Vi}\right\|^2$$

$$+\frac{\gamma_1\theta_{VMi}^4\lambda_{\max}^4(R^{-1})\nabla_{\xi_i}\vartheta_{Mi}^4\sigma_{IMi}^4}{16(1+\hat{\eta}^T\hat{\eta})^2}\left\|\Lambda\right\|\left\|\tilde{\theta}_{Ii}\right\|^4 - \frac{\gamma_{Ii}}{2}\left\|\Xi\right\|\left\|\tilde{\theta}_{Ii}\right\|^2 + \left\|\Xi\right\|b_{IMi}$$

$$-\frac{\gamma_3}{2}\tilde{\theta}_{Vi}^T\Sigma(\xi_i,\hat{\tau}_i)\nabla_{xi}^T\vartheta_i(\xi_i,t_f-t)\hat{D}(\xi_i)J_{\xi_i}^T(\xi_i)+\varepsilon_{WMi}$$

$$-\alpha_1\left(\lambda_{\min}(K)-\frac{3}{2}-\frac{\gamma_2\|\zeta_I\|^4}{8\gamma_1}\right)\|\Lambda\|^2\|e_i\|^4+\varepsilon_{IMi} \qquad\qquad\text{(A.4)}$$

$$-\frac{\gamma_2}{4}\left(\gamma_I-\frac{3}{2}-\frac{\gamma_1}{\gamma_2}\|\zeta_I\|^4\right)\|\Lambda\|^2\|\tilde{\theta}_{Ii}\|^4-\left[\lambda_{\min}(K)-\frac{1}{2}\right]\Xi\|e_i\|^2$$

$$\leq\gamma_3 J_{\xi_i}^T(\xi_i)(f_i(\xi_i)-\frac{1}{2}g_i(\tilde{v}_i)R^{-1}\hat{g}_i(\xi_i)\nabla_{\xi_i}^T\vartheta_i(\xi_i,t_f-t)\hat{\theta}_{Vi})$$

$$-\frac{\gamma_1}{4}\|\Pi\|\frac{\lambda_{\min}(\hat{\eta}\hat{\eta}^T)}{(1+\hat{\eta}^T\hat{\eta})^2}\|\tilde{\theta}_{Vi}\|^2+\frac{\gamma_1\theta_{VMi}^4\lambda_{\max}^4(R^{-1})\nabla_{\xi_i}\vartheta_{Mi}^4\sigma_{IMi}^4}{2(1+\hat{\eta}^T\hat{\eta})^2}\|\Pi\|\|\tilde{\theta}_{Ii}\|^4$$

$$-\frac{\alpha_3}{2}\tilde{W}_V^T\Sigma(\xi_i,\tau_i)\nabla_{\xi_i}^T\vartheta_i(\xi_i,t_f-t)\hat{D}(\xi_i)J_{\xi_i}(\xi_i)+\varepsilon_{WMi}-\frac{\gamma_I}{2}\|\tilde{\theta}_{Ii}\|^2$$

$$-\left[\lambda_{\min}(K)-\frac{1}{2}\right]\|e_i\|^2+\varepsilon_{IMi}-\gamma_1\left(\lambda_{\min}(K)-\frac{3}{2}-\frac{\gamma_2}{4\gamma_1}\right)\|\Lambda\|^2\|e_i\|^4$$

$$-\frac{\gamma_2}{2}\left(\frac{\gamma_I}{2}-1-\frac{\gamma_1+\gamma_2}{4\gamma_2}\|\zeta_I\|^4\right)\|\Lambda\|^2\|\tilde{\theta}_{Ii}\|^4+\varepsilon_{cMi}$$

$$\leq-\gamma_3 Q_{\min}\|J_{\xi_i}(\xi_i)\|^2+\frac{\gamma_3}{2}J_{\xi_i}^T(\xi_i)g_i(\xi_i)R^{-1}\hat{g}_i^T(\xi_i)\nabla_{\xi_i}^T\vartheta_i(\xi_i,t_f-t)\theta_{Vi}$$

$$+\frac{\gamma_3}{2}J_{\xi_i}^T(\xi_i)g_i(\xi_i)R^{-1}\hat{g}_i^T(\xi_i)\nabla_{\xi_i}^T\vartheta_i(\xi_i,t_f-t)\tilde{\theta}_{Vi}$$

$$-\frac{\gamma_3}{2}J_{\xi_i}^T(\xi_i)g_i(\xi_i)R^{-1}\hat{g}_i^T(\xi_i)\nabla_{\xi_i}^T\vartheta_i(\xi_i,t_f-t)\tilde{\theta}_{Vi}+\alpha_3 J_{\xi_i}^T(\xi_i)\varepsilon_{xMi}-\frac{\gamma_1}{4}\|\Pi\|\frac{\lambda_{\min}(\hat{\eta}\hat{\eta}^T)}{(1+\hat{\eta}^T\hat{\eta})^2}\|\tilde{\theta}_{Vi}\|^2$$

$$-\frac{\gamma_1\theta_{VMi}^4\lambda_{\max}^4(R^{-1})\nabla_{\xi_i}\vartheta_{Mi}^4\sigma_{IMi}^4}{2}\|\Pi\|\|\tilde{\theta}_{Ii}\|^4-\left[\lambda_{\min}(K)-\frac{1}{2}\right]\Xi\|e_i\|^2-\frac{\gamma_{Ii}}{2}\Xi\|\tilde{\theta}_{Ii}\|^2$$

$$-\gamma_1\left(\lambda_{\min}(K)-\frac{3}{2}-\frac{\gamma_2}{4\gamma_1}\right)\|\Lambda\|^2\|e_i\|^4+\varepsilon_{WMi}+\|\Xi\|\varepsilon_{IMi}+\varepsilon_{cMi}$$

$$\leq-\gamma_3\overline{Q}_{\min}\left\|J_{\xi_i}(\xi_i)\right\|^2+\frac{\gamma_3\overline{Q}_{\min}}{5}\left\|J_{\xi_i}(\xi_i)\right\|^2$$

$$+\frac{5\alpha_3}{16Q_{\min}}\left\|g_i(\xi_i)R^{-1}\hat{g}_i^T(\xi_i)\nabla_{\xi_i}^T\vartheta_i(\xi_i,t_f-t)\theta_{Vi}\right\|^2+\frac{\gamma_3\overline{Q}_{\min}}{5}\left\|J_{\xi_i}(\xi_i)\right\|^2$$

$$\frac{5\gamma_3}{16Q_{\min}}\left\|g_i(\xi_i)R^{-1}\hat{g}_i^T(\tilde{v}_i)\right\|^2+\frac{\gamma_3}{4}\left\|\nabla_{\xi_i}^T\vartheta_i(\xi_i,t_f-t)\tilde{\theta}_{Vi}\right\|^2$$

$$+\frac{\gamma_3Q_{\min}}{5}\left\|J_{\xi_i}(\xi_i)\right\|^2+\frac{5\gamma_3}{16Q_{\min}}\left\|\tilde{g}_i(\xi_i)R^{-1}\tilde{g}_i^T(\xi_i)\right\|^2+\frac{5\gamma_3}{4Q_{\min}}\left\|\varepsilon_{xMi}\right\|^2$$

$$+\frac{\gamma_3}{4}\left\|\nabla_{\xi_i}^T\vartheta_i(\xi_i,t_f-t)\tilde{\theta}_{Vi}\right\|^2+\frac{\gamma_3Q_{\min}}{5}\left\|J_{\xi_i}(\xi_i)\right\|^2$$

$$-\frac{\gamma_1}{4}\|\Pi\|\frac{\lambda_{\min}(\hat{\eta}\hat{\eta}^T)}{(1+\hat{\eta}^T\hat{\eta})^2}\left\|\tilde{\theta}_{Vi}\right\|^2-\left[\lambda_{\min}(K)-\frac{1}{2}\right]\|\Xi\|\|e_i\|^2$$

$$-\frac{\gamma_1\theta_{VMi}^4\lambda_{\max}^4(R^{-1})\nabla_{\xi_i}\vartheta_{Mi}^4\sigma_{IMi}^4}{2}\|\Pi\|\left\|\tilde{\theta}_{Ii}\right\|^4-\frac{\gamma_{Ii}}{2}\|\Xi\|\left\|\tilde{\theta}_{Ii}\right\|^2$$

$$-\gamma_1\left(\lambda_{\min}(K)-\frac{3}{2}-\frac{\gamma_2}{4\gamma_1}\right)\|\Lambda\|^2\|e_i\|^4+\varepsilon_{WMi}+\|\Xi\|\varepsilon_{IMi}+\varepsilon_{cMi}$$

$$\leq-\frac{\gamma_3Q_{\min}}{5}\left\|J_{\xi_i}(\xi_i)\right\|^2+\frac{5\gamma_3\theta_{IMi}^2\nabla_x\vartheta_{Mi}^2\theta_{IMi}^2\sigma_{IMi}^4\lambda_{\max}^2(R^{-1})}{16Q_{\min}}\left\|\tilde{\theta}_{Ii}\right\|^2$$

$$-\frac{\gamma_1}{4}\|\Pi\|\frac{\lambda_{\min}(\hat{\eta}\hat{\eta}^T)}{(1+\hat{\eta}^T\hat{\eta})^2}\left\|\tilde{\theta}_{Vi}\right\|^2+\frac{5\gamma_3\lambda_{\max}^2(R^{-1})\theta_{IMi}^2\sigma_{I,M}^4}{16Q_{\min}}\left\|\tilde{\theta}_{Ii}\right\|^2$$

$$+ \frac{5\gamma_3 \lambda_{\max}^2 (R^{-1}) \sigma_{IMi}^4}{16 Q_{\min}} \left\| \tilde{\theta}_{Ii} \right\|^4 + \frac{\gamma_3 \nabla_{\xi_i} \vartheta_{Mi}^2}{2} \left\| \tilde{\theta}_{Vi} \right\|^2 + \frac{5\lambda_3}{4 Q_{\min}} \left\| \varepsilon_{Mi} \right\|^2$$

$$- \left[\lambda_{\min}(K) - \frac{1}{2} \right] \|\Xi\| \|e_i\|^2 - \frac{\alpha_1 \theta_{VMi}^4 \lambda_{\max}^4 (R^{-1}) \nabla_{\xi_i} \vartheta_{Mi}^4 \sigma_{IMi}^4}{2} \|\Pi\| \left\| \tilde{\theta}_{Ii} \right\|^4$$

$$- \frac{\gamma_{Ii}}{2} \|\Xi\| \left\| \tilde{\theta}_{Ii} \right\|^2 - \gamma_1 \left(\lambda_{\min}(K) - \frac{3}{2} - \frac{\gamma_2}{4\gamma_1} \right) \|\Lambda\|^2 \|e_i\|^4 + \varepsilon_{WMi} + \|\Xi\| \varepsilon_{IMi} + \varepsilon_{cMi}$$

$$\leq - \frac{\gamma_3 Q_{\min}}{5} \left\| J_{\xi_i}(\xi_i) \right\|^2 + \frac{5\alpha_3 (\theta_{VMi}^2 \nabla_{\xi_i} \vartheta_{Mi}^2 + 1) \theta_{IMi}^2 \sigma_{IMi}^4 \lambda_{\max}^2 (R^{-1})}{16 Q_{\min}} \left\| \tilde{\theta}_{Ii} \right\|^2$$

$$+ \frac{5\lambda_{\max}^2 (R^{-1}) \sigma_{IMi}^4}{16 Q_{\min}} \left\| \tilde{\theta}_{Ii} \right\|^4 + \frac{\gamma_3 \nabla_{\xi_i} \vartheta_{Mi}^2}{2} \left\| \tilde{\theta}_{Vi} \right\|^2 - \frac{\gamma_1}{4} \|\Pi\| \frac{\lambda_{\min}(\hat{\eta}\hat{\eta}^T)}{(1 + \hat{\eta}^T \hat{\eta})^2} \left\| \tilde{\theta}_{Vi} \right\|^2 - \left[\lambda_{\min}(K) - \frac{1}{2} \right] \|\Xi\| \|e_i\|^2$$

$$- \frac{\gamma_1 \theta_{VMi}^4 \lambda_{\max}^4 (R^{-1}) \nabla_{\xi_i} \vartheta_{Mi}^4 \sigma_{IMi}^4}{2} \|\Pi\| \left\| \tilde{\theta}_{Ii} \right\|^4 - \frac{\lambda_{Ii}}{2} \|\Xi\| \left\| \tilde{\theta}_{Ii} \right\|^2$$

$$- \alpha_1 \left(\lambda_{\min}(K) - \frac{3}{2} - \frac{\lambda_2}{4\lambda_1} \right) \|\Lambda\|^2 \|e_i\|^4 + \varepsilon_{WMi} + \|\Xi\| \varepsilon_{IMi} + \varepsilon_{cMi} + \frac{5\lambda_3}{4 \overline{Q}_{\min}} \left\| \varepsilon_{Mi} \right\|^2$$

$$\leq - \frac{\gamma_3 \overline{Q}_{\min}}{5} \left\| J_{\xi_i}(\xi_i) \right\|^2 - \frac{5\alpha_3 (\theta_{VMi}^2 \nabla_{\xi_i} \vartheta_{Mi}^2 + 1) \theta_{IMi}^2 \sigma_{IMi}^4 \lambda_{\max}^2 (R^{-1})}{16 \overline{Q}_{\min}} \left\| \tilde{\theta}_{Ii} \right\|^2$$

$$- \frac{5\lambda_{\max}^2 (R^{-1}) \sigma_{IMi}^4}{16 \overline{Q}_{\min}} \left\| \tilde{\theta}_{Ii} \right\|^4 - \left[\lambda_{\min}(K) - \frac{1}{2} \right] \|\Xi\| \|e_i\|^2$$

$$- \frac{\gamma_1}{4} \|\Pi\| \frac{\lambda_{\min}(\hat{\eta}\hat{\eta}^T)}{(1 + \hat{\eta}^T \hat{\eta})^2} \left\| \tilde{\theta}_{Vi} \right\|^2 - \gamma_1 \left(\lambda_{\min}(K) - \frac{3}{2} - \frac{\lambda_2}{4\lambda_1} \right) \|\Lambda\|^2 \|e_i\|^4 + \varepsilon_{TCi}$$

$$\leq -\frac{\gamma_3 \bar{Q}_{\min}}{5}\left\|J_{\xi_i}(\xi_i)\right\|^2 - \frac{5\gamma_3(\theta_{VMi}^2 \nabla_{\xi_i} \vartheta_{Mi}^2 + 1)\theta_{IMi}^2 \sigma_{IMi}^4 \lambda_{\max}^2(R^{-1})}{16\bar{Q}_{\min}}\left\|\tilde{\theta}_{Ii}\right\|^2$$

$$-\frac{\gamma_1}{4}\|\Pi\|\frac{\lambda_{\min}(\hat{\eta}\hat{\eta}^T)}{(1+\hat{\eta}^T\hat{\eta})^2}\left\|\tilde{\theta}_{Vi}\right\|^2 - \left[\lambda_{\min}(K) - \frac{1}{2}\right]\|\Xi\|\|e_i\|^2 + \varepsilon_{TCi}$$

with $0 < \lambda_3 < \min\left\{\dfrac{5\lambda_{\min}(\hat{\eta}\hat{\eta}^T)}{32\nabla_{\xi_i}\vartheta_{Mi}^6 \bar{Q}_{\min}\theta_{VMi}^4 \lambda_{\max}^2(R^{-1})(1+\hat{\eta}^T\hat{\eta})^2}, 1\right\}$,

$$\Xi = \frac{5\gamma_3(\theta_{VMi}^2 \nabla_{\xi_i} \vartheta_{Mi}^2 + 1)\theta_{IMi}^2 \sigma_{IMi}^4 \lambda_{\max}^2(R^{-1})}{4\gamma_I Q_{\min}}\mathbf{I}, \Pi = \frac{5}{8Q_{\min}\lambda_1 \theta_{VMi}^4 \lambda_{\max}^2(R^{-1})\nabla_{\xi_i}\vartheta_{Mi}^4}\mathbf{I},$$ and

$$\varepsilon_{TCi} = \varepsilon_{WMi} + \|\Xi\|\varepsilon_{IMi} + \varepsilon_{cMi} + \frac{5\gamma_3}{4Q_{\min}}\|\varepsilon_{Mi}\|^2.$$

Hence, observe that $\dot{L} < 0$ provided

$$\left\|J_{\xi_i}(\xi_i)\right\| > \sqrt{\frac{5\varepsilon_{TCi}}{\gamma_3 \bar{Q}_{\min}}} \equiv b_{J_{\xi_i}} \text{ or } \left\|\tilde{\theta}_{Vi}\right\| > \sqrt{\frac{2\varepsilon_{TCi}}{\gamma_3 \nabla_{\xi_i}\vartheta_{Mi}^2}} \equiv b_{Wvi} \text{ or}\|e_i\| > \sqrt{\frac{\varepsilon_{TCi}}{\left[\lambda_{\min}(K) - \frac{1}{2}\right]\|\Xi\|}} \equiv b_{e_i} \text{ or}$$

$$\left\|\tilde{\theta}_{Ii}\right\| > \sqrt{\frac{16\bar{Q}_{\min}\varepsilon_{TCi}}{5\gamma_3(\theta_{VMi}^2 \nabla_{\xi_i} \vartheta_{Mi}^2 + 1)\theta_{IMi}^2 \sigma_{IMi}^4 \lambda_{\max}^2(R^{-1})}} \equiv b_{WIi}. \tag{A.5}$$

where $\bar{Q}_{\min}$ is defined similar to Lemma 1, $\nabla_{\zeta_i}\vartheta_{Mi}^2$ is the partial derivative of square of

terminal constraint error $\vartheta(\zeta_i, t_f - t)^2$ with respect to formation error ζ_i of ith robot.

Using the standard Lyapunov theory [28] and previous derivation (A.4-A.5),

within finite horizon, all the signals are bounded.

Proof of Theorem 2: Define the sum of Lyapunov functions given in (A.1) as

$$\bar{L} = \sum_{i=1}^{n} \gamma_3 J_{\xi_i}(\xi_i) + \frac{1}{2}\sum_{i=1}^{n} \gamma_3 tr\{\tilde{\theta}_{Vi}^T \Pi \tilde{\theta}_{Vi}\} + \frac{1}{2}\sum_{i=1}^{n} e_i^T \Xi e_i$$

$$+ \frac{1}{2}\sum_{i=1}^{n} tr\{\tilde{\theta}_{Ii}^T \Xi \tilde{\theta}_{Ii}\} + \frac{\lambda_1}{4}\sum_{i=1}^{n}(e_i^T \Lambda e_i)^2 + \frac{\lambda_2}{4}\sum_{i=1}^{n}(tr\{\tilde{\theta}_{Ii}^T \Lambda \tilde{\theta}_{Ii}\})^2 \tag{A.6}$$

Then, it is straightforward to realize from *Proof of Theorem* 1 that $\dot{\bar{L}} < 0$ provided

$$\|J_\Psi(\Psi)\| > \sum_{i=1}^{n}\sqrt{\frac{5\varepsilon_{TCi}}{\gamma_3\bar{Q}_{\min}}} \equiv \sum_{i=1}^{n} b_{J_{\xi_i}} \text{ or } \left\|\tilde{\bar{\theta}}_V\right\| > \sum_{i=1}^{n}\sqrt{\frac{2\varepsilon_{TCi}}{\gamma_3\nabla_{\xi_i}\vartheta_{Mi}^2}} \equiv \sum_{i=1}^{n} b_{Wvi} \text{ or }$$

$$\|\Theta\| > \sum_{i=1}^{n}\sqrt{\frac{\varepsilon_{TCi}}{\left[\lambda_{\min}(K)-\frac{1}{2}\right]\|\Xi\|}} \equiv \sum_{i=1}^{n} b_{e_i}$$

$$\left\|\tilde{\bar{\theta}}_I\right\| > \sum_{i=1}^{n}\sqrt{\frac{16\bar{Q}_{\min}\varepsilon_{TCi}}{5\gamma_3(\theta_{VMi}^2\nabla_{\xi_i}\vartheta_{Mi}^2+1)\theta_{IMi}^2\sigma_{IMi}^4\lambda_{\max}^2(R^{-1})}} \equiv \sum_{i=1}^{n} b_{WIi}. \tag{A.7}$$

where $\tilde{\bar{\theta}}_V = \begin{bmatrix} \tilde{\theta}_{V1}^T & \tilde{\theta}_{V2}^T & \cdots & \tilde{\theta}_{Vn}^T \end{bmatrix}^T$ $\tilde{\bar{\theta}}_I = \begin{bmatrix} \tilde{\theta}_{I1}^T & \tilde{\theta}_{I2}^T & \cdots & \tilde{\theta}_{In}^T \end{bmatrix}^T$ and, $\Theta = \begin{bmatrix} e_1^T & e_2^T & \cdots & e_n^T \end{bmatrix}^T$

$\Psi = \begin{bmatrix} \xi_1^T & \xi_2^T & \cdots & \xi_n^T \end{bmatrix}^T$. Note that since $b_{J_{\xi_i}}, b_{Wvi}, b_{e_i}$ and b_{WIi} are bound, and there is only

a finite number, n, of robots in the group, then $\sum_{i=1}^{n} b_{J_{\xi_i}}, \sum_{i=1}^{n} b_{Wvi}, \sum_{i=1}^{n} b_{e_i},$ and $\sum_{i=1}^{n} b_{WIi}$ are also

bounded. These bounds can be minimized by choosing proper design parameters, which

guarantees that all the formation errors are bounded (resulting in consensus on the

leaderless robot group's regulation errors), and the robots get their goal position with some

bounded regulation errors.

REFERENCES

[1]   Hong Y, Hu J, Gao L. Tracking control for multi agent consensus with an active leader and variable topology. *Automatic;*42(7):1177-1182,2006.

[2]   Qu Z. Cooperative control of dynamics systems. *New York:Springer- Veriag,*2009.

[3]   Ren W, Beard R. Distributed consensus in multi-vehicle cooperative control. *New York: Springer-Veriag,*2008.

[4]   Tian Y, Liu C. Consensus of multi agent systems with diverse input and communication delays. *IEEE Transactions on Systems, Man, and Cybernetics-*Part B,40(2):362-370,2010.

[5]   Cao Y, Li Y, Ren W, Chen Y. Distributed coordination of networked fractional-order systems. *IEEE Transaction on Systems, Man and Cybernetics.-*Part B; 40(2):362-370, 2010.

[6]   Olfati-Saber R, Murray R M. Consensus problems in networks of agents with switching topology and time-delays. *IEEE Transactions on Automatic Control* 2004; 49(9): 1520-1533.

[7]   Long X, Jiang J. Information consensus in partial synchronous network of multi-robot systems. *CIMCA* 2008*, IAWTIC* 2008*, and ISE* 2008.

[8]   Ren W, Beard R. Consensus seeking in multiagent systems under dynamically changing interaction topologies. *IEEE Transaction on Automatic Control,* 50(5); 655-661, 2005.

[9]   Bauso D, Giarre L, Pesenti R. Consensus for networks with unknown but bounded disturbances. *SIAM journal of Control and Optimization* 48 (3) (2009) 1756-1770; Doi:10.1137/060678786.

[10]   Feng S, Zhang H. Formation control for wheeled mobile robots based on consensus protocol. *Information and Automation (ICIA), 2011 IEEE International Conference on* , vol., no., pp.696-700, 6-8 June 2011.

[11]   Listmann K D, Masalawala M V, Adamy J. Consensus for formation control of nonholonomic mobile robots. *IEEE International Conference on Robotics and Automation, 2009. ICRA '09,* pp.3886-3891, 12-17 May 2009.

[12]   Sheng L, Pan Y J, and Gong X. Consensus formation control for a class of networked multiple mobile robot systems. *Journal of Control Science and Engineering,* 2012, Article ID 150250, 12 pages, 2012; doi:10.1155/2012/150250.

[13] Guzey H M, Jagannatan S. Adaptive neural network consensus based control of robot formations. *Proceedings of SPIE Vol. 8741, 87410M (2013) SPIE Digital Library.*

[14] Semsar-Kazerooni E, Khorasani K. Optimal consensus algorithms for cooperative team of agents subject to partial information. *Automatica*, vol. 44, no. 11, pp; 2766–2777, 2008.

[15] Heydari A, Balakrishan S N. Finite-horizon control-constrained nonlinear optimal control using single network adaptive critics. *IEEE Trans. on Neur. Net. and Learni. Syst.*, vol. 24, pp. 145–157, 2013.

[16] Vrabie D, Vamvoudakis K, Lewis F. Adaptive optimal controllers based on generalized policy iteration in a continuous-time framework. *Proc. of the IEEE Mediterranean Conf. on Control and Automation*, pp. 1402-1409, June 2009.

[17] Frihauf P, Krstic M, Basar T. Finite horizon LQ control for unknown discrete-time linear systems via extremum seeking. *Proc. of IEEE Contr. Decision Conf.*, pp. 5717-5722, 2012.

[18] Dierks T, Jagannathan S. Online optimal control of affine nonlinear discrete-time systems with unknown internal dynamics by using time-based policy update. *IEEE Trans. Neural Networks*, vol. 23, pp. 1118–1129, 2012.

[19] Beard R. Improving the closed-loop performance of nonlinear systems. *Ph.D. dissertation*, Rensselaer Polytechnic Institute, USA, 1995.

[20] Fierro R, Lewis F L. Control of a nonholonomic mobile robot: Backstepping Kinematics into dynamics. *Automation and Robotics Research Institute The University of Texas at Arlington,* 1996.

[21] Ghorbel F, Srinivasan B, Spong M W. On the positive definiteness and uniform boundedness of the inertia matrix of robot manipulators. *Proceedings of the 32nd IEEE Conference on Decision and Control, 1993,* pp.1103,1108 vol.2, 15-17 Dec 1993.

[22] Ren W, Beard R, Atkins E. Information consensus in multivehicle cooperative control. *IEEE Control and Systems Magazine* (2007).

[23] Li Z, Ren W, Liu X, Fu M. Consensus of Multi-Agent Systems With General Linear and Lipschitz Nonlinear Dynamics Using Distributed Adaptive Protocols. *IEEE Transactions on Automatic Control,* vol.58, no.7, pp.1786,1791, July 2013 doi: 10.1109/TAC.2012.2235715.

[24]   Dierks T, Brenner B, Jagannathan S. Neural Network-Based Optimal Control of Mobile Robot Formations with Reduced Information Exchange. *IEEE Transactions on Control Systems Technology,* vol.21, no.4, pp.1407, 1415, July 2013.

[25]   Lewis F L, Jagannathan S, Yesildirek A. *Neural Network Control of Robot Manipulators and Nonlinear Systems*, New York: Taylor & Francis, 1999.

[26]   Khalil H K. *Nonlinear System*, 3rd edtion, Prentice-Hall, Upper Saddle River, NJ, 2002.

[27]   Garulli A, Giannitrapani A. Analysis of consensus protocols with bounded measurement errors. *Systems & Control Letters*, Volume 60, Issue 1, January 2011, Pages 44-52, ISSN 0167-6911.

[28]   S. Jagannathan, *Neural network control of nonlinear discrete-time systems*, CRC Press, 2006.

II.   HYBRID CONSENSUS-BASED CONTROL OF NONHOLONOMIC MOBILE ROBOT FORMATION

ABSTRACT

This paper addresses the hybrid consensus-based formation keeping problem for nonholonomic mobile robots in the presence of a novel time-varying, composite, nonlinear velocity-tracking error system. First, continuous-time regulation and consensus-based formation controllers are developed for a group of wheeled mobile robots. These controllers are then used to create a hybrid automaton, which drives the robots to their goal positions while maintaining a specified formation. In order to avoid the hard switches between regulation and formation keeping controllers, a novel blended velocity tracking error approach is proposed in this work to create nonlinear, time-varying velocity error dynamics.   Therefore, the hybrid controller consists of two discrete modes, each with continuous dynamics, and the novel blended velocity tracking error approach provides a smooth transition between each mode. The controller in the regulation mode drives the robot to a goal position while the formation keeping controller ensures that the robots achieve a specified geometric formation *prior* to reaching their goal-position. Time-varying Lyapunov functions are used to rigorously demonstrate that the formation errors converge to a small bounded region around the origin and the size of the bound can be adjusted by using the switching conditions. Convergence to goal position while in formation is also demonstrated in the same Lyapunov analysis illustrating that the robots are converging to their goal positions while operating in both regulation and formation keeping mode. Simulation results verify the theoretical conjectures.

1. INTRODUCTION

Over the last few decades, the robot control research community has given significant attention to formation control of multiple vehicles since using multiple vehicles can be very beneficial for certain tasks since a single, heavily equipped vehicle may require much more power and lack the robustness needed to avoid failure. For example, in military missions, a group of autonomous vehicles are required to keep in a specified formation for area coverage and reconnaissance; hence, multiple vehicles can complete tasks requiring a large area coverage much faster than a single vehicle. Therefore, the coordination of multiple wheeled robots, unmanned air/ocean vehicles, satellites, aircraft and spacecraft [1]-[8] have been investigated as applications of vehicle formation control.

Mobile robot formation control is also the focus of researchers [9]-[12] and several different approaches such as behavior-based, generalized coordinates, virtual structure and leader-follower strategies, have been proposed. In the formation control of wheeled mobile robots [13], kinematics are considered and either perfect velocity tracking is assumed or only a nominal part of the nonlinear velocity tracking error dynamics are considered. A novel leader-follower-based formation control algorithm was developed in [3], which considers complete nonlinear dynamics of both the leader and the followers.

Consensus-based formation control [4]-[8] is considered to be more robust and reliable when compared to other formation control methods due to scalability [4], [7] and inherent properties that enable the formation to continue even if one of the robots experiences a failure. In consensus-based formation control, the robots share information regarding their position errors from their respective goal positions. The shared information

is then synthesized into a control law which seeks to achieve the same position error for all robots until each robot has reached its goal position. The desired formation is achieved and maintained by reaching and maintaining consensus on the position errors. Therefore, the main tasks in consensus-based formation control are described as: i) given an initial state, achieve a desired formation, and ii) maintain this formation while the robots move through the environment to reach their desired goal position. Completing task ii) is equivalent to solving the regulation problem for the formation.

For nonholonomic systems, the regulation problem is not straightforward due to nonholonomic constraints and Brockett's theorem. In [13], nonholonomic robot kinematics are transformed into polar coordinates to satisfy Brockett's theorem, and control velocities are developed to solve the regulation problem. However, the work in [13] assumed perfect velocity tracking and did not consider the robot dynamics. In addition, several others [4]-[8] have considered consensus-based formation control but failed to consider velocity tracking error dynamics in their controller design.

Motivated by the aforementioned limitations of existing consensus [4]-[8] and regulation controllers [13], this work develops a novel time-varying velocity tracking error system to solve the formation regulation control problem with guaranteed performance for nonholonomic wheeled mobile robots. A hybrid automaton is proposed to control the nonholonomic mobile robots with nonlinear dynamics in two discrete modes: a regulation mode and a formation keeping mode. The regulation mode drives each robot to a constant goal position while the formation-keeping mode ensures that the robots achieve and maintain a specified geometric formation *prior* to reaching their goal position to solve the formation regulation problem. In order to avoid hard switches between regulation and

formation keeping modes, a novel blended time-varying velocity tracking error approach is developed. The blended error approach ensures the robots' velocity tracking errors and control torques are continuous at the switching conditions. Time-varying Lyapunov functions are used in conjunction with multiple Lyapunov methods [15] to provide stability of the hybrid system. Unlike current approaches available in the literature [4]-[7], this work considers the kinematics and dynamics of each mobile robot as well as the formation.

The main contributions of the paper include the development of: a) a nonlinear consensus-based formation control technique which considers the nonlinear robot dynamics; b) a hybrid regulation-formation controller design for nonholonomic mobile robots; c) a novel blended velocity tracking error approach to avoid hard switches between different modes of the hybrid system; and d) analysis of the nonlinear hybrid system's stability using time-varying Lyapunov functions to prove the guaranteed performance of the approach.

The remainder of the paper is organized as follows. Section 2 presents a brief background on hybrid automata while Section 3 derives the continuous time regulation and formation controllers used by our hybrid controller. Section 4 discusses the main result and derives the hybrid regulation-formation controller of nonholonomic mobile robots. Before offering conclusions in Section 6, Section 5 provides simulation results to support the theoretical results.

2. BACKGROUND ON HYBRID AUTOMATA

In this section, the hybrid automata problem considered in this work is introduced first, followed by the necessity for a specialized method for analyzing hybrid controller designs.

The goal of the proposed control scheme is to keep the networked robots in a predefined formation while they move toward their desired positions. Therefore, two different discrete modes will be considered: regulation and formation modes. The general hybrid approach is depicted in Figure 2.1 where the regulation and formation modes are identified. The robots move to their respective goal locations in the regulation mode while monitoring the formation error. If the formation error threshold is exceeded, the robots transition to the formation mode wherein the robots are controlled to achieve their desired formation. Once the formation tracking is achieved, the robots return to the regulation mode. This cycle repeats until the each robot reaches its goal position.

The switching cycle creates a hybrid system with both continuous and discrete dynamics. Due to the hybrid nature of the system, traditional analysis techniques that consider purely discrete or purely continuous system dynamics may not be sufficient to analyze the system. The work in [15] illustrates through counter examples that two asymptotically stable systems may become unstable due to switching conditions when a hybrid system is formed.

Therefore, to prove the stability of hybrid systems such as the one modeled in Figure 2.1, the authors from [15] introduced an analysis method involving multiple Lyapunov

functions. In order to claim that the switched system is stable, the stability of each discrete state must be individually proven while considering restrictions on switching conditions.
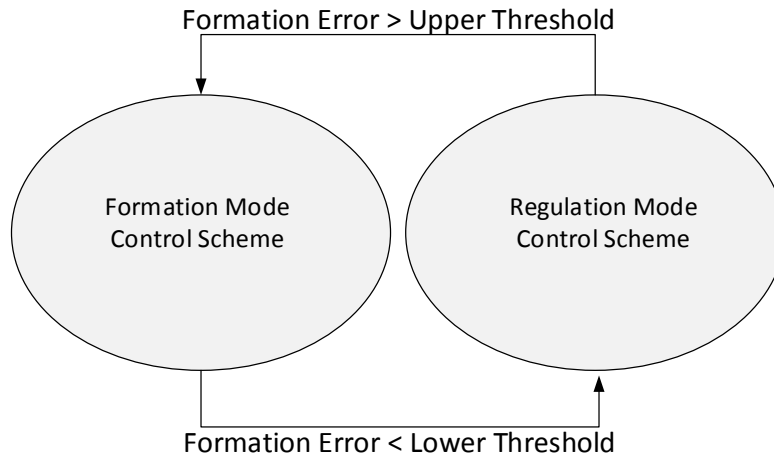
Figure 2.1 General hybrid scheme considered in this work.

Consider the switched hybrid system given by

$$\dot{X} = f_k(X) , \qquad\qquad (42)$$

where X is the state variable and each $f_k(X)$ describes continuous dynamics of the kth discrete mode. It is assumed that each f_k is globally Lipchitz continuous and that a finite number of switches occur among the discrete modes in a finite time. The following lemma presents the necessary and sufficient conditions needed to achieve the stability of a hybrid system.

Lemma 1 [15]: Given a hybrid system with m modes, let each mode contain continuous dynamics in the form of (42) with $k = 1, 2, \ldots, m$ and let each continuous system have an equilibrium point at the origin. Define m Lyapunov candidate functions corresponding to each of the m modes as $V_1, V_2, \ldots, V_m$ respectively. Let time t_{ck} denote the

time instant that mode k becomes active, and let time t_{ak} denote the time instant that mode

k was *previously* activated where $t_{ak} < t_{ck}$. Then, the hybrid system is stable if the following

criteria are satisfied for all modes, $k = 1, 2, \ldots, m$.

    1. V_k decreases when the dynamics f_k are active, and

    2. $V_k(t_{ck}) < V_k(t_{ak})$.

    Proof: See [15] for detailed proof.

    Graphically, the conditions for lemma can be illustrated by plotting the Lyapunov

functions as shown in Figure 3.1. The multiple Lyapunov function-based approach given

in *Lemma 1* will be utilized to prove the stability of the hybrid controller presented in

Section IV. Next, the regulation and formation controller design is given.

3. REGULATION AND CONSENSUS-BASED FORMATION CONTROL OF NONHOLONOMIC ROBOTS

In this section, first, a nonlinear continuous time regulation controller is designed for a single nonholonomic mobile robot. Then, the consensus-based formation control problem is considered for a group of nonholonomic mobile robots. For nonholonomic systems, additional considerations are required to solve both the regulation problem and the formation control problem due to the added complexities introduced by the nonholonomic constraint.
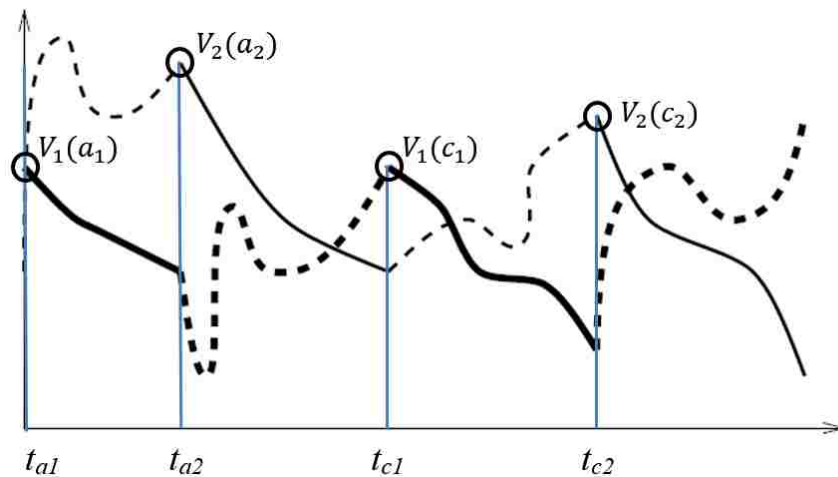
Figure 3.1 Multiple Lyapunov function values versus time (m = 2).

Solid lines indicate the system is active while dashed lines indicate that the system is inactive [15].

Consider the nonholonomic robot shown in Figure 3.2. The equations of motion about the center of mass, C, for the ith robot are written as [16]

$$\dot{q}_i = \begin{bmatrix} \dot{x}_{ci} \\ \dot{y}_{ci} \\ \dot{\theta}_i \end{bmatrix} = \begin{bmatrix} \cos\theta_i & -d_i\sin\theta_i \\ \sin\theta_i & d_i\cos\theta_i \\ 0 & 1 \end{bmatrix} \begin{bmatrix} v_i \\ \omega_i \end{bmatrix} = S_i(q_i)\bar{v}_i \quad, \tag{43}$$

where d_i is the distance from the rear axle to the robot's center of mass; $q_i = [x_{ci} \ y_{ci} \ \theta_i]^T$ denotes the Cartesian position of the center of mass and orientation of the ith robot; v_i, and ω_i represent linear and angular velocities, respectively, and $\bar{v}_i = [v_i \ \omega_i]^T$ for the ith robot.

Many robotic systems can be characterized as having an n-dimensional configuration space $\mathcal{C}$ with generalized coordinates $(q_1, ... q_n)$ subject to ℓ constraints [16]. Applying the transformation [16], the dynamics of the ith mobile robot are given by

$$\bar{M}_i \dot{\bar{v}}_i + \bar{V}_{mi}(q_i, \dot{q}_i)\bar{v}_i + \bar{F}_i(\bar{v}_i) + \bar{\tau}_{di} = \bar{\tau}_i \,, \tag{44}$$

where $\bar{M}_i \in \Re^{\rho x \rho}$ is a constant positive definite inertia matrix, $\bar{V}_{mi} \in \Re^{\rho x \rho}$ is the bounded centripetal and Coriolis matrix, $\bar{F}_i \in \Re^{\rho}$ is the friction vector, $\bar{\tau}_{di} \in \Re^{\rho}$ represents unknown bounded disturbances such that $\|\bar{\tau}_{di}\| \le d_M$ for a known constant, d_M, $\bar{B}_i \in \Re^{\rho x \rho}$ is a constant, nonsingular input transformation matrix, $\bar{\tau}_i = \bar{B}_i \tau_i \in \Re^{\rho}$ is the input vector, and $\tau_i \in \Re^{\rho}$ is the control torque vector. For complete details on (44) and the parameters that comprise it, see [16]. For this work $n = 3$, $\ell = 1$ and $\rho = 2$.

Next, a controller is designed to enable the ith nonholonomic robot to drive to its goal position during the regulation mode.

3.1   REGULATION CONTROL OF MOBILE ROBOTS

The kinematics of the ith mobile robot can be written as

$$
\begin{bmatrix} \dot{x}_i \\ \dot{y}_i \\ \dot{\theta}_i \end{bmatrix} = \begin{bmatrix} \cos(\theta_i) & 0 \\ \sin(\theta_i) & 0 \\ 0 & 1 \end{bmatrix} \begin{bmatrix} v_i \\ w_i \end{bmatrix},
\tag{45}
$$

where (x_i, y_i) is the point centered between the ith robot's driving wheels. The objective of the regulation controller design synthesis is to stabilize (45) about a desired posture, $q_{id} = [x_{id} \ \ y_{id} \ \ \theta_{id}]^T$. However, due to Brockett's theorem [18], smooth stabilizability of the driftless regular system (45) requires the number of inputs to equal to the number of states, a property not satisfied by (45). The above obstruction has a significant impact on controller design. In fact, to obtain a posture stabilizing controller, it is necessary to use discontinuous and/or time-varying control laws [13].

A technique which allows us to overcome the complication presented by the Brockett theorem is to apply a change of coordinates such that the input vector fields of the transformed equations are singular at the origin. This approach is carried out using a polar coordinate transformation, and the control law, once rewritten in terms of the original state variables, is discontinuous at the origin of the configuration space $\mathcal{C}$.

Consider again the robot shown in Figure 3.2. Let ρ_i be the distance of the point (x_i, y_i) of the robot to the goal point (x_{id}, y_{id}). Let α_i be the angle of the pointing vector to the goal with respect to the robot's main axis (labeled as X_R in Figure 3.2), and define β_i to be the angle of the same pointing vector with respect to the orientation error [13]. That is,

$$\rho_i = \sqrt{\Delta x_i^2 + \Delta y_i^2} \ , \ \alpha_i = -\theta_i + \text{atan2}\left(\Delta y_i, \Delta x_i\right) + \pi \ , \beta_i = \alpha_i + \theta_i - \theta_{id}, \tag{46}$$

where $\Delta x_i = x_{id} - x_i$ and $\Delta y_i = y_{id} - y_i$. Then, the polar coordinate kinematics of a mobile robot can be given as discussed in [13] and expressed as

$$\begin{bmatrix} \dot{\rho}_i \\ \dot{\alpha}_i \\ \dot{\beta}_i \end{bmatrix} = \begin{bmatrix} -\cos(\alpha_i) & 0 \\ \sin(\alpha_i)/\rho_i & -1 \\ \sin(\alpha_i)/\rho_i & 0 \end{bmatrix} \begin{bmatrix} v_i \\ \omega_i \end{bmatrix}. \tag{47}$$

From (47), it is observed that the input vector field associated with v_i is singular for $\rho_i = 0$, thus satisfying Brockett's Theorem. To drive mobile robots from any initial position to a goal position, a nonlinear control law is given as [13]

$$v_{id} = k_\rho \rho_i \cos\alpha_i \ , \ \omega_{id} = k_\alpha \alpha_i + k_\rho \left(\frac{\sin\alpha_i \cos\alpha_i}{\alpha_i} \right) \left(\alpha_i + k_\beta \beta_i \right), \tag{48}$$

where k_ρ, k_α, and k_β are positive design constants. As shown in [13], the controller (48) provides asymptotic converge to the constant desired posture. However, the results are obtained using the perfect velocity tracking assumption [16] (assuming that $v_{id} = v_i$ and $\omega_{id} = \omega_i$) which does not hold in practice.

To relax the perfect velocity tracking assumption, the backstepping technique will be employed next.

Define the velocity tracking error as

$$e_{iv}^R = \begin{bmatrix} e_{iv1}^R \\ e_{iv2}^R \end{bmatrix} = \bar{v}_{id} - \bar{v}_i, \tag{49}$$

where $\bar{v}_{id} = [v_{id} \ \omega_{id}]^T$. Rearranging (49) gives $\bar{v}_i = \bar{v}_{id} - e_{iv}^R$, and substituting this expression into the open loop system (47) while using (7) reveals

$$\begin{bmatrix} \dot{\rho}_i \\ \dot{\alpha}_i \\ \dot{\beta}_i \end{bmatrix} = \begin{bmatrix} -k_\rho \rho_i \cos^2 \alpha_i + e_{iv1}^R \cos \alpha_i \\ -k_\alpha \alpha_i - k_\rho \left(\frac{\sin \alpha_i \cos \alpha_i}{\alpha_i} \right) k_\beta \beta_i + e_{iv2}^R - \frac{\sin \alpha_i}{\rho_i} e_{iv1}^R \\ k_\rho \sin \alpha_i \cos \alpha_i - \frac{\sin \alpha_i}{\rho_i} e_{iv1}^R \end{bmatrix}. \tag{50}$$
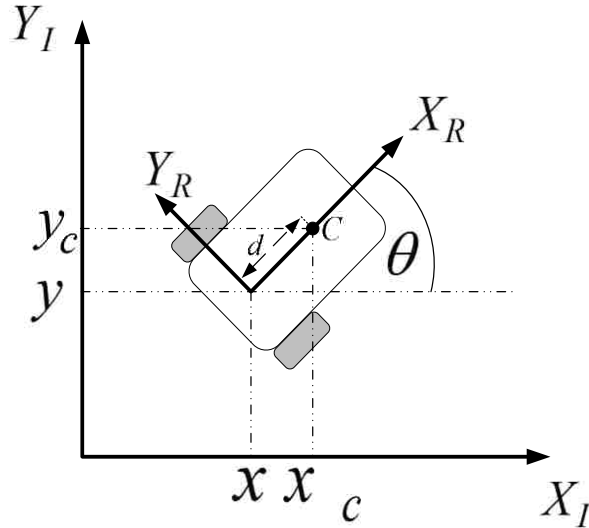
Figure 3.2 Nonholonomic mobile robot.

The closed loop kinematic system (50) explicitly considers the velocity tracking error (49). Therefore, the backstepping technique ensures the robot tracks the design velocities (48).

Differentiating (48) and using (44), the mobile robot velocity tracking error system as

$$\bar{M}_i \dot{e}_{iv}^R = -\bar{V}_{mi}(q_i, \dot{q}_i) e_{iv}^R - \bar{\tau}_i + f_i(z_i) + \bar{\tau}_{di}, \tag{51}$$

where $f(z_i) = \bar{M}_i \dot{\bar{v}}_{id} + \bar{V}_{mi}(q_i, \dot{q}_i)\bar{v}_{id} + \bar{F}_i(\bar{v}_i)$ and contains the mobile robot parameters such as masses, moments of inertia, friction coefficients, and so on. When the robot dynamics

are known, the control torque applied to the robot system (44), which ensures the desired velocity (48), is achieved and is written as

$$\bar{\tau}_i = K_v e_{iv}^R + f(z_i) + \lambda_i(\rho_i, \alpha_i, \beta_i), \tag{52}$$

where $\lambda_i(\rho_i, \alpha_i, \beta_i) = \begin{bmatrix} \cos\alpha_i\left(\rho_i + 0.5(\alpha_i^2 + k_\beta\beta_i^2)\right) - \sin\alpha_i\left(\alpha_i + k_\beta\beta_i\right) \\ \rho_i\alpha_i \end{bmatrix}$ is a function

of the polar coordinate error system (46) and is required for stability. Substituting (52) into (51) reveals the closed loop velocity tracking error dynamics

$$\bar{M}_i \dot{e}_{iv}^R = -K_v e_{iv}^R - \bar{V}_{mi}(q_i, \dot{q}_i)e_{iv}^R + \bar{\tau}_{di} - \lambda_i\left(\rho_i, \alpha_i, \beta_i\right). \tag{53}$$

The control torque (52) will be used in the development of the hybrid approach considered in Section 4 where stability is also considered. Next, the consensus-based formation controller is considered.

3.2   CONSENSUS-BASED FORMATION CONTROL

In [16], a controller was designed to ensure that all regulation errors for the linear systems achieved a common value. Due to the nonholonomic constraints considered in this paper, the formation consensus error is defined as the difference between the robot's own regulation error and the regulation error of its neighbor, referred to as robot j. As shown in [5], average consensus is achieved if the information exchange topology is both strongly connected and balanced. In the case that the information exchange topology has a spanning tree, the final consensus value is equal to the weighted average of initial conditions of those agents that have a directed path to all the other agents [5]. In this work, we will assume that the information exchange topology forms a spanning tree.

To begin, define the consensus error between the ith robot and robot j as

$\delta_{xi} = \Delta x_i - \Delta x_j$ $, \delta_{yi} = \Delta y_i - \Delta y_j$ and $\delta_{\theta i} = \Delta\theta_i - \Delta\theta_j$ for the x and y directions and the

bearing angle, respectively. In this work, it will be assumed that the desired heading angles, θ_{id}, are common for each robot in the formation so that each robot is oriented in the same direction when arriving at the goal points. Under this mild assumption, $\delta_{\theta i} = \theta_i - \theta_j$.

Next, the consensus formation error is transformed into the reference frame attached to the mobile robot as

$$e_{iF} = \begin{bmatrix} e_{i1} \\ e_{i2} \\ e_{i3} \end{bmatrix} = \begin{bmatrix} \cos\theta_i & \sin\theta_i & 0 \\ -\sin\theta_i & \cos\theta_i & 0 \\ 0 & 0 & 1 \end{bmatrix} \begin{bmatrix} \delta_{xi} \\ \delta_{yi} \\ \delta_{\theta i} \end{bmatrix}. \tag{54}$$

Taking the derivative of (54) reveals

$$\begin{bmatrix} \dot{e}_{i1} \\ \dot{e}_{i2} \\ \dot{e}_{i3} \end{bmatrix} = \begin{bmatrix} e_{i2}\omega_i + v_i - v_j\cos(\theta_i - \theta_j) \\ -e_{i1}\omega_i + v_j\sin(\theta_i - \theta_j) \\ \omega_i - \omega_j \end{bmatrix}, \tag{55}$$

which resembles the trajectory tracking error system from single robot control architectures that track a virtual reference cart [16]. In this work, instead of tracking a virtual cart, the robot attempts to reach consensus with its neighbor to achieve a desired formation, and each $e_{i(-)}$ represents the consensus error instead of the trajectory tracking error.

Under the perfect velocity tracking assumption, the consensus-based formation control velocity is given by

$$\bar{v}_{id}^F = \begin{bmatrix} v_{id}^F \\ \omega_{id}^F \end{bmatrix} = \begin{bmatrix} -k_1 e_{i1} + v_j\cos(\theta_i - \theta_j) \\ \omega_j - k_2 v_j e_{i2} - k_3\sin(\theta_i - \theta_j) \end{bmatrix}. \tag{56}$$

Next, the backstepping technique is once again employed. For convenience, we again denote the velocity tracking error using the definition in (49) with $\bar{v}_{id}$ replaced by $\bar{v}_{id}^F$ for formation control. Defining $e_{iv}^F = \begin{bmatrix} e_{iv1}^{FT} & e_{iv2}^{FT} \end{bmatrix}^T = \bar{v}_{id}^F - \bar{v}_i$ reveals, $\bar{v}_i = \bar{v}_{id}^F - e_{iv}^F$, and (55) becomes

$$\begin{bmatrix} \dot{e}_{i1} \\ \dot{e}_{i2} \\ \dot{e}_{i3} \end{bmatrix} = \begin{bmatrix} e_{i2}\omega_i - k_1 e_{i1} - e_{iv1}^F \\ -e_{i1}\omega_i + v_j \sin(\theta_i - \theta_j) \\ -k_2 v_j e_{i2} - k_3 \sin(\theta_i - \theta_j) - e_{iv2}^F \end{bmatrix}. \tag{57}$$

Finally, from the velocity tracking error in the form of dynamics (51), define the control torque which ensure the robot tracks the desired velocity (58) as

$$\bar{\tau}_i = K_v e_{iv}^F + f(z_i) + \gamma(e_{i1}, e_{i2}, e_{i3}), \tag{59}$$

where $\gamma(e_{i1}, e_{i2}, e_{i3}) = \begin{bmatrix} -e_{i1} & -\dfrac{1}{k_2}\sin e_{i3} \end{bmatrix}^T$ is a function of the consensus error states and is required for stability. Substituting (59) into (51) reveals the closed loop velocity tracking error dynamics

$$\bar{M}_i \dot{e}_{iv}^F = -K_v e_{iv}^F - \bar{V}_{mi}(q_i, \dot{q}_i)e_{iv}^F + \bar{\tau}_{di} - \gamma\left(e_{i1}, e_{i2}, e_{i3}\right). \tag{60}$$

The control torque (61) will be used in the development of the hybrid approach in Section 4, considered next, for the development of the hybrid consensus-based regulation/formation controller design.

4. HYBRID CONSENSUS-BASED FORMATION CONTROL OF NONHOLONOMIC ROBOTS

In this section, the regulation error based desired velocities (48) and the consensus based desired velocities are used to formally develop the hybrid regulation-formation controller for a group of nonholonomic mobile robots described by (44) and (45). The hybrid controller ensures that the nonholonomic systems reach their desired positions while keeping the formation on their way.

In our previous work [16], the linear and angular velocity tracking errors for point mass systems are switched between regulation and formation modes without consideration of discontinuities in the control input observed during a switching event. In practice, physical systems may not respond well to the high frequency signals introduced by the non-smooth controllers. Therefore, to avoid the discontinuous control inputs during a mode switch, novel blended velocity tracking errors are first introduced for both regulation and formation modes. Under the hybrid control approach, the regulation and formation mode controllers will be functions of the blended velocity tracking errors discussed next.

First, define the novel blended velocity tracking error for the regulation mode as

$$E_{vi}^{R}(t,t_0) = B_1(t,t_0)e_{iv}^{F}(t) + B_2(t,t_0)e_{iv}^{R}(t), \tag{62}$$

where $e_{iv}^{R}(t)$ is the regulation mode velocity tracking error from (8) using the desired regulation velocity (7), and e_{iv}^{F} is the formation mode velocity tracking error written in the form of (8) using the desired consensus-based velocity (56). The time-varying functions $B_1(t,t_0) = \exp(-k_d(t - t_0))$ and $B_2(t,t_0) = 1 - \exp(-k_d(t - t_0))$, are the blending functions with t_o being the time that the current mode (regulation or formation mode) was

initiated, and k_d is a design constant controlling the exponential convergence rate. Similarly, the blended velocity tracking error for the formation mode is written as

$$E_{vi}^{F}\left(t,t_{0}\right)=B_{1}\left(t,t_{0}\right)e_{iv}^{R}\left(t\right)+B_{2}\left(t,t_{0}\right)e_{iv}^{F}\left(t\right). \tag{63}$$

Remark: In both modes (regulation and formation), the velocity tracking errors e_{iv}^{R} and e_{iv}^{F} are both calculated to form the blended mode errors (62) and (63).

The blending functions are chosen to satisfy the desired continuity properties at the switching conditions. At $t = t_0$, $B_1(t, t_0) = 1$ and $B_1(t, t_0) \to 0$ as $t \to \infty$. Conversely, $B_2(t, t_0) = 0$ at $t = t_0$ and $B_2(t, t_0) \to 1$ as $t \to \infty$. Also, the blended regulation velocity tracking error, $E_{vi}^{R}\left(t,t_{0}\right)$, converges to the actual regulation velocity tracking error, $e_{iv}^{R}\left(t\right)$, as time goes to infinity and the blended formation velocity tracking error, $E_{vi}^{F}\left(t,t_{0}\right)$, converges to the actual formation velocity tracking error, $e_{iv}^{F}\left(t\right)$, as time goes to infinity as well.

Moving on, the blended velocity tracking error dynamics are formed by differentiating (62) and (63) and applying the results from Section 3. First, differentiating (62) and applying steps similar to those used to form (51) and (60) gives

$$\bar{M}\dot{E}_{vi}^{R}(t, t_0) = \bar{M}\left(\dot{B}_1(t, t_0)e_{iv}^{F}(t) + \dot{B}_2(t, t_0)e_{iv}^{R}(t)\right)$$

$$+\left(B_{1}(t, t_0)\left(-V_m e_{iv}^{F} + f_i(z_i^{F})\right) + B_2(t, t_0)\left(-V_m e_{iv}^{R} + f_i(z_i^{R})\right) - \bar{\tau}\right). \tag{64}$$

Next, differentiating (63), and applying steps similar to those used to form (51) and (60) reveals

$$\bar{M}\dot{E}_{vi}^{F}(t, t_0) = \bar{M}\left(\dot{B}_1(t, t_0)e_{iv}^{R}(t) + \dot{B}_2(t, t_0)e_{iv}^{F}(t)\right) + \left(B_1(t, t_0)\left(-V_m e_{iv}^{R} + \right.\right.$$

$$\left. f_i(z_i^{R})\right) + B_2(t, t_0)\left(-V_m e_{iv}^{F} + f_i(z_i^{F})\right) - \bar{\tau}\right). \tag{65}$$

To stabilize the blended regulation and formation velocity tracking error systems
(64) and (65), respectively, the novel torque control inputs are found to be

$$\bar{\tau}_i^{R} = K_4 E_{vi}^{R} + \bar{M}\left(\dot{B}_1\left(t, t_b\right)e_{iv}^{F}\left(t\right) + \dot{B}_2\left(t, t_b\right)e_{iv}^{R}\left(t\right)\right) - V_M E_{vi}^{R} + B_1\left(t, t_b\right)f_i\left(z_i^{F}\right) + B_2\left(t, t_c\right)f_i\left(z_i^{R}\right)$$

$$-B_1\left(t, t_b\right)\gamma\left(e_{i1}, e_{i2}, e_{i3}\right) + B_2\left(t, t_b\right)\lambda\left(\rho_i, \alpha_i, \beta_i\right) \tag{66}$$

and

$$\bar{\tau}_i^{F} = K_4 E_{vi}^{F} + \bar{M}\left(\dot{B}_2\left(t, t_c\right)e_{iv}^{F}\left(t\right) + \dot{B}_1\left(t, t_c\right)e_{iv}^{R}\left(t\right)\right)$$

$$-V_M E_{vi}^{F} + B_2\left(t, t_c\right)f_i\left(z_i^{F}\right) + B_1\left(t, t_c\right)f_i\left(z_i^{R}\right)$$

$$-B_2\left(t, t_c\right)\gamma\left(e_{i1}, e_{i2}, e_{i3}\right) + B_1\left(t, t_c\right)\lambda\left(\rho_i, \alpha_i, \beta_i\right) \tag{67}$$

where $K_4 \in R^{2\times2}$ is a positive definite matrix.

As discussed in [16], stability of the individual continuous controllers does not guarantee that the discrete dynamics and the hybrid switched system are also stable [15]. Therefore, the switching conditions between the modes must also be defined. The switching conditions considered in this work will be based on two criteria. First, the robots must consider the size of the formation errors to assess how well the formation is being maintained. Second, to enable smooth control inputs at the switching conditions, the robots must also measure the convergence of the blended velocity tracking errors (31) and (32) to their respective mode velocity tracking errors in the form of (8). First, the switching thresholds for assessing the formation keeping performance are defined. The upper and lower thresholds for switching between the formation and regulation modes are given as

$$\bar{\eta}_i(t) = \beta\left(e^{(t_0-t)} + \eta_{\min}\right) \tag{68}$$

$$\underline{\eta}_i(t) = \beta\left(e^{(t_0-t)} + \eta_{\min}\right)/\kappa, \tag{69}$$

respectively, where $\beta > 0$, $\kappa > 1$, $\eta_{\min} > 0$ are design constants, and t_0 is the initial time of all states. By construction of the time varying upper and lower bounds, a finite number of mode switches occurs in a finite time as required until *Lemma 1* is satisfied.

A robot switches from the regulation mode to the formation mode when the formation errors based Lyapunov function, $L_{iF1} = \left(e_{i1}^2 + e_{i2}^2\right)/2 + \left(1 - \cos e_{i3}\right)/k_2$ with k_2 being a design constant, exceeds the upper-threshold, $\bar{\eta}_i(t)$. In the formation keeping mode, the formation controller design in (70) brings the robots to a desired formation. Once the Lyapunov function converge to values below a lower-threshold of formation error, $\underline{\eta}_i(t)$, the robots transition back to the regulation mode. As long as the formation error Lyapunov, L_{iF1} remains below the upper-threshold, the regulation controller (66) is applied the systems and the nonholonomic robots arrive at their target positions in formation.

The second switching condition is based on the convergence of the blended velocity tracking errors. Under the hybrid approach, the regulation and formation mode controllers are functions of the blended velocity tracking errors, E_{vi}^R and E_{vi}^F, and it takes time for the blended errors to converge to the modal velocity tracking errors, e_{vi}^R and e_{vi}^F, respectively. It is observed, however, that the time durations that the robot controller operates in any single mode are unlikely to approach infinity. Therefore, the blended velocity tracking error for the formation mode is only approximately equal to the blended tracking error for

the regulation mode when switching from formation keeping to regulation and vice versa. The difference between the two blended errors is dependent upon the duration of the current operating mode and can be controlled through the switching conditions and the convergence rate, k_d.

Therefore, the additional switching conditions enforce the continuity condition and are written as

$$\| E_{vi}^R \left(t_c, t_b \right) - e_{iv}^R \left(t \right) \| < \delta_{ev} \;, \tag{71}$$

$$\| E_{vi}^F \left(t_b, t_a \right) - e_{iv}^F \left(t \right) \| < \delta_{ev} \;, \tag{72}$$

with δ_{ev} being a defined constant. The blended regulation velocity tracking error needs to satisfy (71) before the transitioning to the formation keeping mode while the blended formation velocity tracking error must satisfy (72) before switching back to the regulation mode.

The controller of each discrete state and the thresholds needed to move between each of the modes are demonstrated in Figure 4.1.

As illustrated in Figure 4.1, the ith robot is initiated in formation state at time t_a. Then, once the switching conditions are satisfied, the ith robot transitions to the regulation state at time t_b. The regulation state is active until the formation error exceeds the upper threshold at time t_c, and the formation state is activated once again and remains active until time t_d when the switching condition is satisfied.

Next, the following theorems are given to provide the stability of the blended velocity tracking error dynamics (64) and (65) under the control of the input torques (66) and (67), respectively. First, *Theorem* 3 presents the stability of the

$$\|e_{iF}\|_F^2 > \overline{\eta}_i(t), \| E_v^R(t_c, t_b) - e_{iv}^r(t) \| < \delta_{ev}$$

$$L_{iF1} \geq \eta_i(t) \qquad t_c \qquad\qquad\qquad\qquad L_{iF1} < \overline{\eta}_i(t)$$

$$t_a$$

Formation Mode

$$\overline{\tau}_i^F = K_4 E_{vi}^F + \overline{M}\left(\dot{B}_2(t,t_c)e_{iv}^F(t) + \dot{B}_1(t,t_c)e_{iv}^R(t)\right)$$
$$-V_M E_{vi}^F + B_2(t,t_c)f_i(z_i^F) + B_1(t,t_c)f_i(z_i^R)$$
$$-B_2(t,t_c)\gamma(e_{i1},e_{i2},e_{i3}) + B_1(t,t_c)\lambda(\rho_i,\alpha_i,\beta_i)$$

Regulation Mode

$$\overline{\tau}_i^R = K_4 E_{vi}^R + \overline{M}\left(\dot{B}_1(t,t_b)e_{iv}^F(t) + \dot{B}_2(t,t_b)e_{iv}^R(t)\right)$$
$$-V_M E_{vi}^R + B_1(t,t_b)f_i(z_i^F) + B_2(t,t_b)f_i(z_i^R)$$
$$-B_1(t,t_b)\gamma(e_{i1},e_{i2},e_{i3}) + B_2(t,t_b)\lambda(\rho_i,\alpha_i,\beta_i)$$

$$t_b \qquad\qquad\qquad\qquad\qquad t_b$$

$$\text{OR} \qquad\qquad \|e_{iF}\|_F^2 < \underline{\eta}_i(t), \| E_v^F(t_b, t_a) - e_{iv}^F(t) \| < \delta_{ev}\; t_d \qquad \text{OR}$$

$$\| E_v^F(t_b, t_a) - e_{iv}^F(t) \| \geq \delta_{ev} \qquad t_d > t_c > t_b > t_a \qquad \| E_v^R(t_c, t_b) - e_{iv}^r(t) \| \geq \delta_{ev}$$
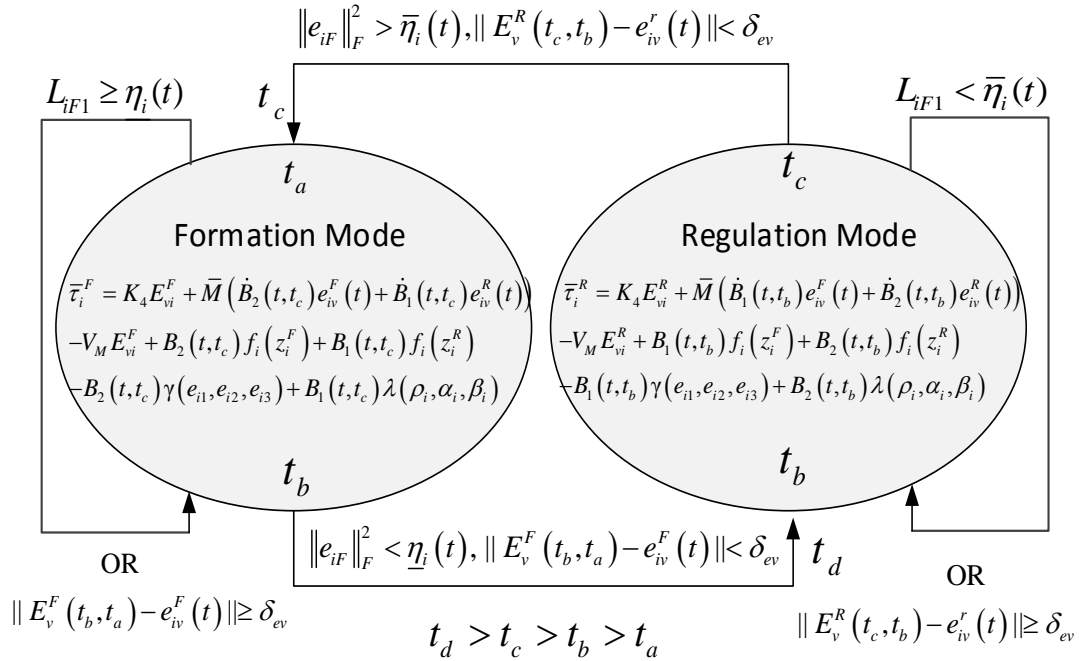
Figure 4.1 Formation and regulation modes for nonholonomic systems.

blended velocity tracking error for regulation followed by the stability of the blended velocity tracking error for formation keeping in *Theorem* 4. *Theorem* 5 presents the stability of the hybrid controller.

Theorem 1: Given the ith mobile robot system described by (44) and (45), let the blended velocity tracking error and its dynamics for driving the nonholonomic system to the goal configuration, q_{id}, be given by (62) and (64), respectively, and let the control torque vector be defined by (66). Then, in the absence of disturbances ($\overline{\tau}_{di} = 0$), the

velocity tracking error system (64) and kinematic system (47) converge to the origin asymptotically, and the ith robot tracks its desired velocity and converges to its desired posture. That is, $E_{vi}^{R}\left(t,t_{0}\right)\to 0$ and $q_{i}\to q_{id}$.

Proof: See appendix.

Theorem 2: Given the consensus error dynamics (55) for the ith robot in the network, let the blended velocity tracking error and the error dynamics, (63) and (65) be defined for the ith robot, respectively, and let the control torque be given by (67). Then, in the absence of disturbances $(\bar{\tau}_{di}=0)$, the velocity tracking error system (65) and consensus error system (57) converge to the origin asymptotically, and the ith robot tracks its desired velocity to achieve consensus with its neighbor robot j. That is, $E_{vi}^{F}\left(t,t_{0}\right)\to 0$ and $\Delta x_{i}\to \Delta x_{j}, \Delta y_{i}\to \Delta y_{j}$, and $\Delta\theta_{i}\to\Delta\theta_{j}$. Further, if the information exchange topology has a directed spanning tree, the final consensus errors are equal to the weighted average of initial consensus errors.

Proof: See appendix.

Remark: *Theorems 1* and *2* provide stability of each discrete mode by using different time-varying Lyapunov functions. However, a hybrid system can become unstable by using improper switching conditions among modes [15]. In our case, the formation errors may become unbounded during regulation modes or the distance error may eventually go to infinity during formation modes. Therefore, the stability of the switched system is provided next.

Theorem 3: Given the error dynamics of *N* networked nonholonomic robots in the form of (47), let the regulation velocity controller and torque control provided by *Theorem*

1 be applied to the ith robot when the Lyapunov function, L_{iF1} is less than the ith upper-threshold (68) and the blended velocity tracking error satisfies (71). Let the formation velocity controller and torque controller from *Theorem 2* be applied to the ith robot when L_{iF1} exceeds the ith upper threshold until L_{iF1} converges to a value below the ith lower-threshold (69), and the blended velocity tracking error satisfies (72). Then, the nonholonomic system (44) and (45)will become stable converges to its desired posture while in formation.

Proof: See appendix.

Next, simulation results are given to verify the theoretical conjectures.

5. SIMULATION RESULTS

To illustrate the effectiveness of the proposed hybrid controller, a group of four nonholonomic mobile robots in the form of (44) is considered. The robots are initiated from an arbitrary position and move to a desired position around origin in the shape of a square. Using the hybrid approach, the robots establish the square shape prior to moving to the goal position. The desired and initial positions, initial bearing angles and the initial velocities of the nonholonomic mobile robots are given by

$$x_1(t_0) = 156, x_2(t_0) = 132, x_3(t_0) = 96, x_4(t_0) = 120,$$

$$y_1(t_0) = -108, y_2(t_0) = -156, y_3(t_0) = -168, y_4(t_0) = -120$$

$$, x_1^d = 5, x_2^d = 5, x_3^d = -5, x_4^d = -5, y_1^d = 5, y_2^d = -5,$$

$$y_3^d = 5, y_4^d = -5, \theta_1(t_0) = 2\pi, \theta_2(t_0) = 2\pi, \theta_3(t_0) = 2\pi,$$

$$\theta_4(t_0) = 2\pi, \theta_1^d = 2\pi, \theta_2^d = 2\pi, \theta_3^d = 2\pi, \theta_4^d = 2\pi.$$

These desired positions inherently provide a square shape when the robots reach their desired locations. The connectivity graph among the robots is selected as given in Figure 5.1. It is observed that the graph is connected and satisfies the required assumption stated in [8]. Each robot receives one of its neighbor robot's regulation errors, and the overall formation is established since the graph is connected. The parameters for the robot dynamics (44) are selected as

$$\bar{M}_i = \begin{bmatrix} m_i + \dfrac{2Iyy}{r_i^2} & 0 \\ 0 & \dfrac{m_i d_i^2 + IT + 2Iyyb_i^2}{r_i^2 - 4mW_i d_i^2} \end{bmatrix}, \quad \bar{V}_{mi} = \begin{bmatrix} 0 & -d_i w_i(m_i - 2mW_i) \\ dw_i(m_i - 2mW) & 0 \end{bmatrix},$$

$$\bar{F_i} = \begin{bmatrix} Fvv_i + Fdsign(v_i) \\ Fvw_i + Fdsign(w_i) \end{bmatrix}, \bar{B_i} = \begin{bmatrix} 1/r_i & 1/r_i \\ b_i/r_i & -b_i/r_i \end{bmatrix}, \bar{\tau}_{di} = \begin{bmatrix} 0 \\ 0 \end{bmatrix}$$

with $m_i = 10, mW_i = 2, r_i = 0.05, b_i = 0.4, d_i = 0.1,$ $Iyy = 1, IT = 5, Fv = 0.5, Fd = 0.8$ being

the total mass of the ith robot, mass of one wheel of the ith robot , wheel radius of the ith

robot, half of the width of the ith robot, the distance of the rear axle of the ith robot from

its center of mass, wheel moment of inertia, total moment of inertia of the robot platform,

coefficient of the Viscous friction and the coefficient of the Coulomb friction, respectively.
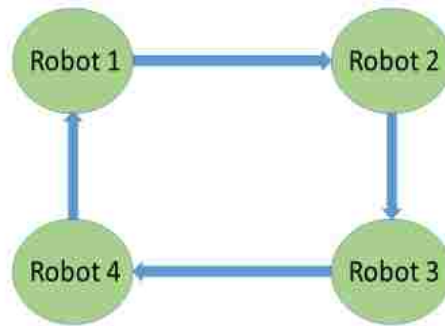
Figure 5.1 Connectivity Graph of four nonholonomic mobile robots.

The controller gains are then selected with $K_4 = 30$, $k_1 = 2, k_2 = 1, k_3 = 0.5$

$k_\rho = 0.5, k_\beta = 0.25/k_\rho, k_\alpha = k_\beta$. The decay rate of the blended velocity tracking errors in

(62) and (63) are shown as $k_d = 2$, the switching parameters for the upper (68) and lower

(69) thresholds are selected as $\beta = \eta_{min} = 1$ and $\kappa = 1.34$, respectively, and the blended

velocity tracking error convergence threshold is selected as $\delta_{ev} = 0.1$.

The performance of the controller analyzed in *Theorem 3* (the hybrid blended

approach) is presented next. The four mobile robots described above are considered along

with the controller torques (66) and (67). Figure 5.2 shows the movements of the four nonholonomic mobile robots. The desired set points are selected in such a way that the robots form a square shape around origin when they arrive to their desired set points. The initial positions of each robot is pointed via text arrows in Figure 5.2.

The robots move to reach consensus with their respective neighbors and subsequently achieve the square shape prior to reaching their goal positions. When comparing Figure 5.2 and the robot movements in [16], the effect of nonholonomic constraints can be realized easily. In [16], the omnidirectional robots travel directly to the temporary set point to form a square shape; however, in Figure 5.2, the nonholonomic mobile robots' motions are subject to nonholonomic constraints requiring different paths to form the square shape.

Figure 5.3 presents the time-evolution of polar coordinate distance errors, ρ_i, $i = 1, 2, 3, 4$, defined in (5) for each robot. Initially, the formation error Lyapunov function, L_{F1}, exceeds the defined threshold and the robots begin in formation keeping mode. The robots travel from their initial positions and achieve their desired formations, and the robots remain in the formation mode until the distance errors reach consensus. Once in formation, the Lyapunov function, L_{F1}, becomes less than the defined threshold, and the robots transition to the regulation mode. Subsequently, the distance errors converge to zero all together as the robots travel to the goal positions simultaneously.

The smooth blended regulation and formation velocity tracking errors, (62) and (63), of the robots are presented in Figure 5.4 and Figure 5.5, respectively. Since the robots are initiated in formation mode, the formation velocity tracking error converges to zero

after the first couple of seconds as can be seen in Figure 5.5. The time at which the robots transition from the formation mode to the regulation mode lasts 3.7 seconds for robot 1, and 2.3, 4.3, and 3.5 seconds for robots 2, 3, and 4, respectively.

The composite blended velocity tracking error, which combines Figure 5.4 during the formation mode and Figure 5.5 for the regulation mode is shown in Figure 5.6. Figure 5.6 also provides a zoomed in time span for the time period that contains the switch from the formation mode to the regulation mode. After examining Figure 5.6, we see that the switch from the formation mode to the regulation mode is smooth and does not produce large peaks in the velocity tracking error as a result of the blended velocity tracking error approach.

As the value of decay rate of the blending function, k_d, is increased, the blended approach converges to hard switching conditions where smoothness is not considered. The experiment was repeated for $k_d = 50$. The formation trajectory for this scenario is similar to the trajectories shown in Figure 5.2. However, the composite blended velocity tracking errors shown in Figure 5.7 illustrate that large peaks in the velocity tracking errors are present at both the beginning of the simulation and when each robot transitions from the formation state to the regulation state at 11.95 seconds. It is interesting to observe that the switching time where $k_d = 50$ is actually larger than the case where $k_d = 2$. The later switching time is attributed to the formation errors taking longer to converge to below the switching threshold as a result of the large initial transient response when $k_d = 50$.
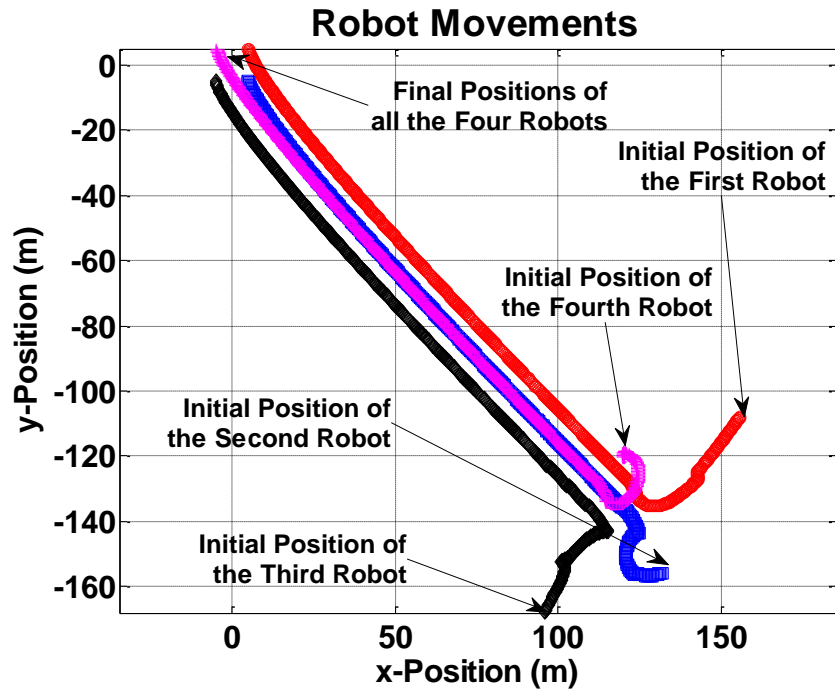
Figure 5.2 Movements of four nonholonomic mobile robots.
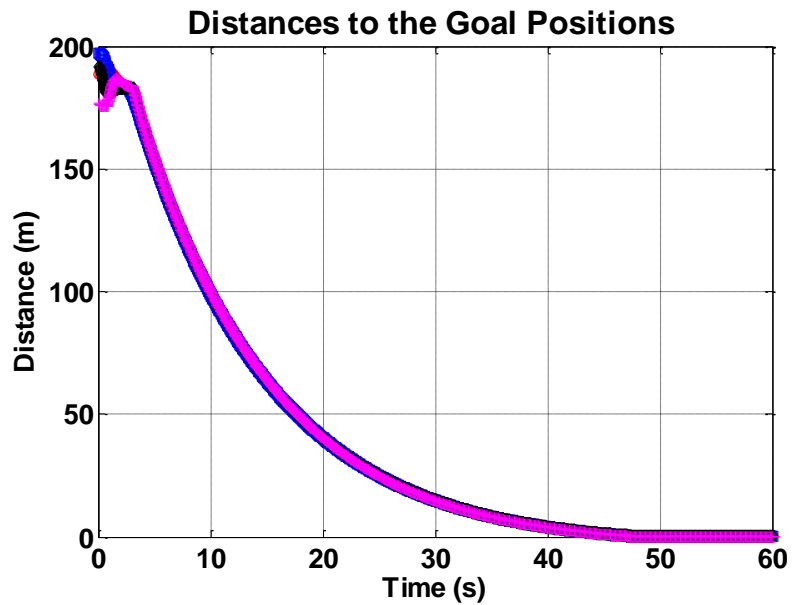
Figure 5.3 Distances of each robot to their goal positions.

Comparing the transient behaviors in Figure 5.6 and Figure 5.7, it is observed that the choice of k_d is a tradeoff between the magnitude of errors and the duration of their transient responses. Selecting smaller values of k_d produces small, smooth crests in the velocity tracking error at the penalty of a longer transient period before the velocity tracking errors converge back to zero. In contrast, larger values of k_d allow the velocity tracking errors to converge to zero quickly while transitioning from one state to another at the cost of large, abrupt spikes in the error signals. In practice, large and abrupt spikes in signals used by the control laws are undesirable.
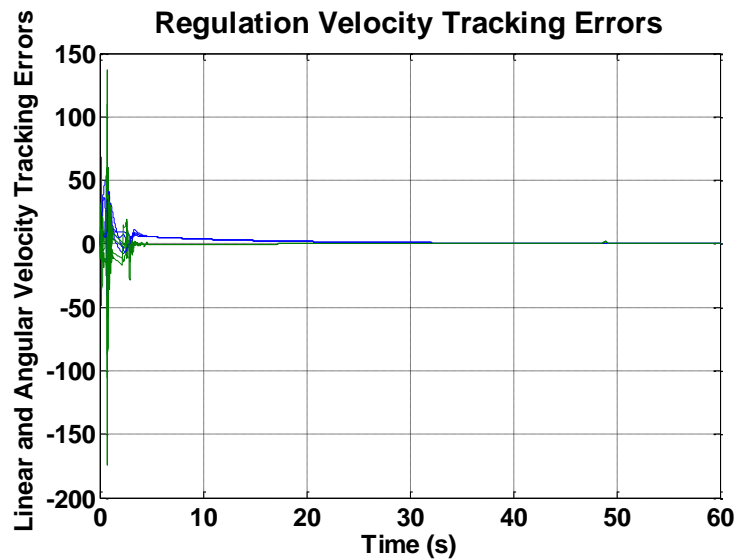
Figure 5.4 Blended formation velocity tracking errors (linear (m/s) and angular (rad/sec)).
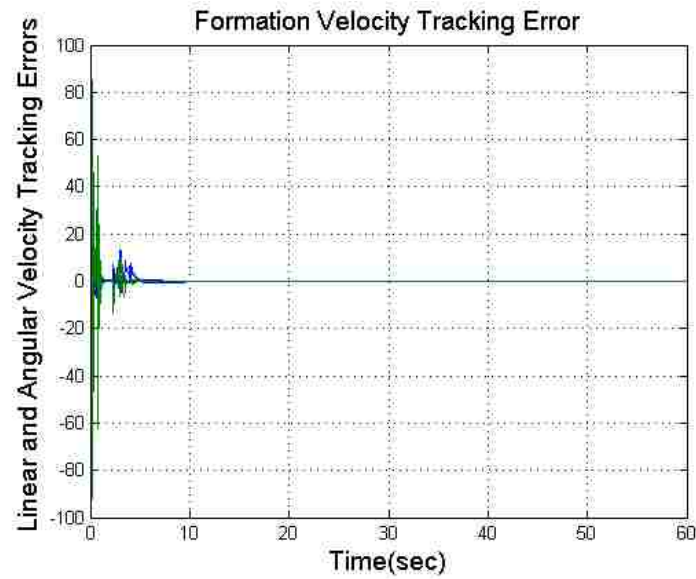
Figure 5.5 Blended regulation velocity tracking errors (linear (m/s) and angular (rad/sec)).
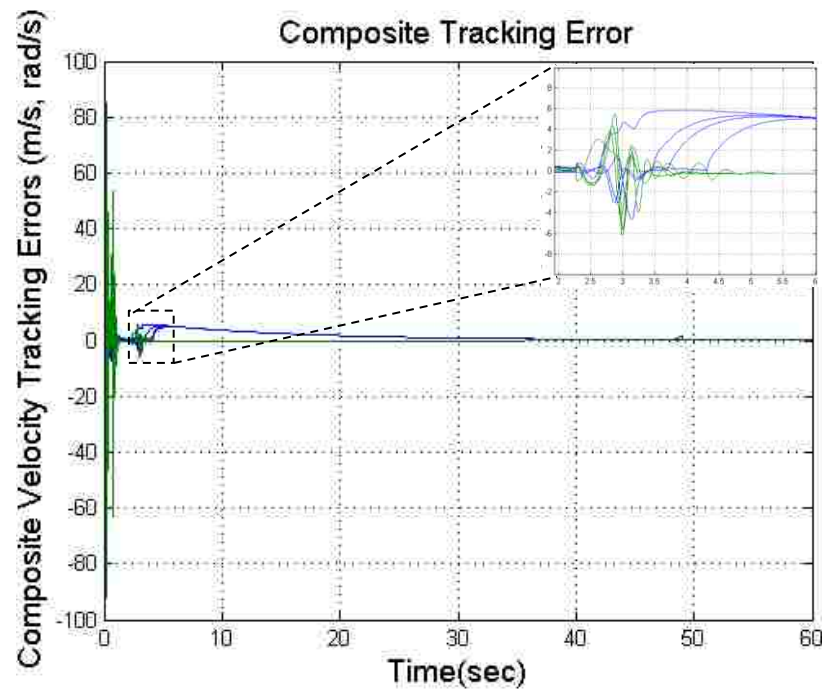
Figure 5.6 Composite blended formation velocity tracking errors (linear (m/s) and angular (rad/sec)), kd=2.
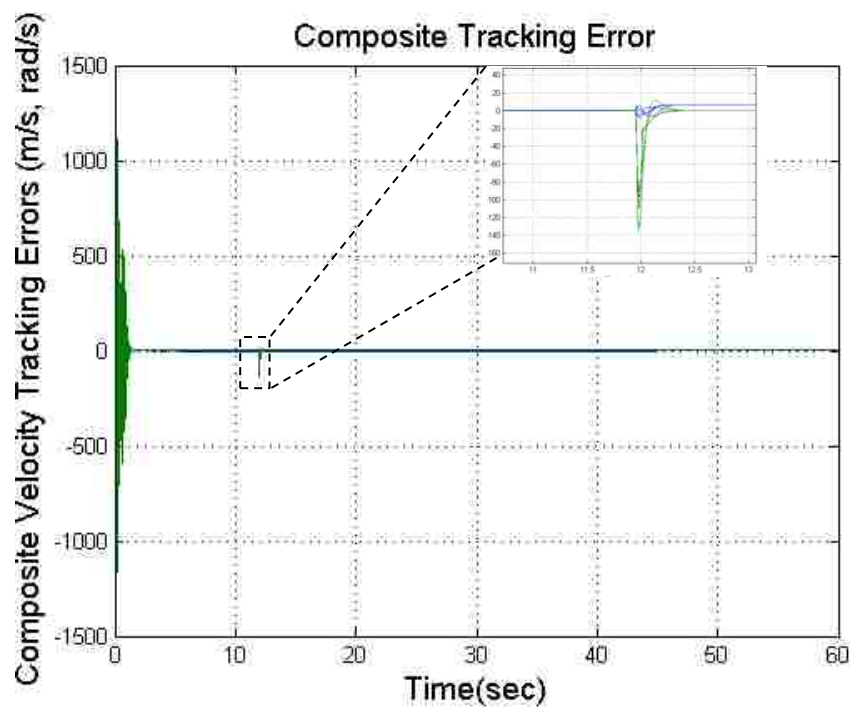
Figure 5.7 Composite blended formation velocity tracking errors (linear (m/s) and angular (rad/sec)), kd=50.

6. CONCLUSION AND FUTURE WORK

The results of the paper provide controllers to the user to regulate a single robot to a desired posture and for a group of nonholonomic robots to reach consensus on their regulation errors to achieve a desired posture in a desired shape. This was accomplished through the development of two novel continuous time regulation and formation controllers for nonholonomic mobile robots. Then, a novel hybrid regulation-formation controller was developed by using a novel blended velocity tracking error approach. Time-varying Lyapunov functions were used to prove the stability of the hybrid approach, and simulation results verified the performance improvements of the proposed approach over traditional hard switched hybrid control architectures. The blended velocity tracking error approach reduced the size of the discontinuity at the switching conditions which led to smaller peak velocity tracking errors and smaller peak required torques at the switching conditions. The blended hybrid controller is beneficial when multiple tasks need to be accomplished at the same time. Future work will investigate extending the approach to include other discrete modes, such as obstacle avoidance.

APPENDIX

Proof of Theorem 1: Define the blended regulation Lyapunov candidate function for each robot as

$$L_{Ri} = B_1^2\left(t,t_b\right)\left(\left(e_{i1}^2 + e_{i2}^2\right)\big/2 + \left(1 - \cos e_{i3}\right)\big/k_2\right) + B_2^2(t,t_b)\frac{1}{2}\left(\rho_i^2 + \rho_i\left(\alpha_i^2 + k_\beta \beta_i^2\right)\right) +$$

$$\frac{1}{2}E_{vi}^{R^T}\bar{M}_i E_{vi}^R \tag{A1}$$

Then, the derivative of (A1) is calculated to be

$$\dot{L}_{Ri} = 2B_1\left(t,t_b\right)\dot{B}_1\left(t,t_b\right)\left(\left(e_{i1}^2 + e_{i2}^2\right)\big/2 + \left(1 - \cos e_{i3}\right)\big/k_2\right)$$

$$+2B_2\left(t,t_b\right)\dot{B}_2\left(t,t_b\right)\frac{1}{2}\left(\rho_i^2 + \rho_i\left(\alpha_i^2 + k_\beta \beta_i^2\right)\right)$$

$$+B_1^2\left(t,t_b\right)\left(-k_1 e_{i1}^2 - k_3 \sin^2 e_{i3}\big/k_2 - e_{i1}e_{iv1}^F - \sin e_{i3}e_{iv2}^F\big/k_2\right)$$

$$+B_2^2\left(t,t_b\right)\begin{pmatrix} -k_\rho \rho_i^2 \cos^2 \alpha_i - k_\alpha \rho_i \alpha_i^2 - \dfrac{k_\rho}{2}\rho_i \cos^2 \alpha_i\left(\alpha_i^2 + k_\beta \beta_i^2\right) \\[2mm] +e_{iv1}^R\left(\cos\alpha_i\left(\rho_i + \dfrac{1}{2}\left(\alpha_i^2 + k_\beta \beta_i^2\right)\right) - \sin\alpha_i\left(\alpha_i + k_\beta \beta_i\right)\right) \\[2mm] +\rho_i \alpha_i e_{iv2}^R \qquad\qquad\qquad\qquad (\end{pmatrix} + E_{vi}^{R^T}\bar{M}_i \dot{E}_{vi}^R. \tag{A2}$$

Next, applying the definitions of $\lambda(\rho_i, \alpha_i, \beta_i)$ and $\gamma(e_{i1}, e_{i2}, e_{i3})$ defined in (13) and (22), respectively, gives

$$\dot{L}_{Ri} = 2B_1\left(t,t_b\right)\dot{B}_1\left(t,t_b\right)\left(\left(e_{i1}^2 + e_{i2}^2\right)\big/2 + \left(1 - \cos e_{i3}\right)\big/k_2\right)$$

$$+2B_2\left(t,t_b\right)\dot{B}_2\left(t,t_b\right)\frac{1}{2}\left(\rho_i^2 + \rho_i\left(\alpha_i^2 + k_\beta \beta_i^2\right)\right)$$

$$+B_1^2\left(t,t_b\right)\left(-k_1 e_{i1}^2 - k_3 \sin^2 e_{i3}\big/k_2 - e_{iv}^{FT}\gamma\left(e_{i1},e_{i2},e_{i3}\right)\right)$$

$$+B_2^2\left(t,t_b\right)\begin{pmatrix}-k_\rho\rho_i^2\cos^2\alpha_i-k_\alpha\rho_i\alpha_i^2\\-k_\rho\rho_i\cos^2\alpha_i\left(\alpha_i^2+k_\beta\beta_i^2\right)/2+e_{iv}^{RT}\lambda\left(\rho_i,\alpha_i,\beta_i\right)\end{pmatrix}+E_{vi}^{R^T}\bar{M}_i\dot{E}_{vi}^R .\qquad\text{(A3)}$$

Now, substituting the blended regulation tracking error dynamics (64) into (A3),

$\dot{L}_{Ri}$ becomes

$$\dot{L}_{Ri}=2B_1\left(t,t_b\right)\dot{B}_1\left(t,t_b\right)\left(\left(e_{i1}^2+e_{i2}^2\right)/2+\left(1-\cos e_{i3}\right)/k_2\right)$$

$$+2B_2\left(t,t_b\right)\dot{B}_2\left(t,t_b\right)\frac{1}{2}\left(\rho_i^2+\rho_i\left(\alpha_i^2+k_\beta\beta_i^2\right)\right)$$

$$+B_1^2\left(t,t_b\right)\left(-k_1e_{i1}^2-k_3\sin^2 e_{i3}/k_2\right)+B_2^2\left(t,t_b\right)\begin{pmatrix}-k_\rho\rho_i^2\cos^2\alpha_i-k_\alpha\rho_i\alpha_i^2\\-k_\rho\rho_i\cos^2\alpha_i\left(\alpha_i^2+k_\beta\beta_i^2\right)/2\end{pmatrix}$$

$$+E_v^{R^T}\begin{pmatrix}\bar{M}\left(\dot{B}_1\left(t,t_b\right)e_{iv}^F\left(t\right)+\dot{B}_2\left(t,t_b\right)e_{iv}^R\left(t\right)\right)+B_1\left(t,t_0\right)\left(-V_me_{iv}^F+f_i\left(z_i^F\right)\right)\\+B_2\left(t,t_0\right)\left(-V_me_{iv}^R+f_i\left(z_i^R\right)\right)-\bar{\tau}\end{pmatrix}$$

$$-B_1^2(t,t_b)e_{iv}^{FT}\gamma(e_{i1},e_{i2},e_{i3})+B_2^2\left(t,t_b\right)e_{iv}^{RT}\lambda\left(\rho_i,\alpha_i,\beta_i\right).\qquad\text{(A4)}$$

Moving on, adding and subtracting

$B_1(t,t_b)B_2(t,t_b)e_{iv}^{R^T}\gamma(e_{i1},e_{i2},e_{i3})$ and $B_1(t,t_b)B_2(t,t_b)e_{iv}^{F^T}\lambda(\rho_i,\alpha_i,\beta_i)$ to (A4) and

collecting like terms yields

$$\dot{L}_{Ri}=2B_1\left(t,t_b\right)\dot{B}_1\left(t,t_b\right)\left(\left(e_{i1}^2+e_{i2}^2\right)/2+\left(1-\cos e_{i3}\right)/k_2\right)$$

$$+2B_2\left(t,t_b\right)\dot{B}_2\left(t,t_b\right)\frac{1}{2}\left(\rho_i^2+\rho_i\left(\alpha_i^2+k_\beta\beta_i^2\right)\right)+B_1^2\left(t,t_b\right)\left(-k_1e_{i1}^2-k_3\sin^2 e_{i3}/k_2\right)$$

$$+B_2^2\left(t,t_b\right)\left(-k_\rho\rho_i^2\cos^2\alpha_i-k_\alpha\rho_i\alpha_i^2\right)-B_2^2\left(t,t_b\right)k_\rho\rho_i\cos^2\alpha_i\left(\alpha_i^2+k_\beta\beta_i^2\right)/2$$

$$+E_{vi}^{R^T}\left(\bar{M}\left(\dot{B}_1(t,t_b)e_{iv}^F(t)+\dot{B}_2(t,t_b)e_{iv}^R(t)\right)+B_1(t,t_b)\left(-V_me_{iv}^F+f_i(z_i^F)\right)+\right.$$

$$B_2(t,t_b)\left(-V_me_{iv}^R+f_i(z_i^R)\right)-\bar{\tau}\bigg)-B_1(t,t_b)(B_1(t,t_b)e_{iv}^{F^T}+$$

$$B_2(t,t_b)e_{iv}^{R^T})\gamma(e_{i1},e_{i2},e_{i3})$$

$$+B_2(t,t_b)(B_2(t,t_b)e_{iv}^{R^T}+B_1(t,t_b)e_{iv}^{F^T})\lambda(\rho_i,\alpha_i,\beta_i)$$

$$+ B_1(t,t_b)B_2(t,t_b)e_{iv}^{R^T}\gamma(e_{i1},e_{i2},e_{i3})-B_2(t,t_b)B_1(t,t_b)e_{iv}^{F^T}\lambda(\rho_i,\alpha_i,\beta_i). \tag{A5}$$

Then, apply the definition of E_{vi}^R to factor the bottom rows of (A5) into terms pre-multiplied by $E_{vi}^{R^T}$, and the rows containing V_m are factored into $E_{vi}^{R^T}V_M E_{vi}^R$ to give

$$\dot{L}_{Ri}=2B_1(t,t_b)\dot{B}_1(t,t_b)\left(\left(e_{i1}^2+e_{i2}^2\right)/2+(1-\cos e_{i3})/k_2\right)$$

$$+2B_2(t,t_b)\dot{B}_2(t,t_b)\frac{1}{2}\left(\rho_i^2+\rho_i\left(\alpha_i^2+k_\beta\beta_i^2\right)\right)+B_1^2(t,t_b)\left(-k_1 e_{i1}^2-k_3\sin^2 e_{i3}/k_2\right)$$

$$+B_2^2(t,t_b)\left(-k_\rho\rho_i^2\cos^2\alpha_i-k_\alpha\rho_i\alpha_i^2\right)-B_2^2(t,t_b)\frac{k_\rho}{2}\rho_i\cos^2\alpha_i\left(\alpha_i^2+k_\beta\beta_i^2\right)$$

$$+B_2^2(t,t_b)\left(-k_\rho\rho_i^2\cos^2\alpha_i-k_\alpha\rho_i\alpha_i^2\right)-B_2^2(t,t_b)k_\rho\rho_i\cos^2\alpha_i\left(\alpha_i^2+k_\beta\beta_i^2\right)/2$$

$$+E_{vi}^{R^T}\left(\overline{M}\left(\dot{B}_1(t,t_b)e_{iv}^F(t)+\dot{B}_2(t,t_b)e_{iv}^R(t)\right)-V_M E_{vi}^R+B_1(t,t_b)f_i(z_i^F)+\right.$$

$$B_2(t,t_b)f_i(z_i^R)-\overline{\tau}-B_1(t,t_b)\gamma(e_{i1},e_{i2},e_{i3})+B_2(t,t_b)\lambda(\rho_i,\alpha_i,\beta_i)\Big)+$$

$$B_1(t,t_b)B_2(t,t_b)e_{iv}^{R^T}\gamma(e_{i1},e_{i2},e_{i3})-B_2(t,t_b)B_1(t,t_b)e_{iv}^{F^T}\lambda(\rho_i,\alpha_i,\beta_i)\ . \tag{A6}$$

Finally, use the torque equation (66) in (A6) and write the derivatives $\dot{B}_1$ and $\dot{B}_2$ in terms of B_1 and substitute in (A.6)

$$\dot{L}_{Ri}=-2k_d B_1^2(t,t_b)\left(\left(e_{i1}^2+e_{i2}^2\right)/2+(1-\cos e_{i3})/k_2\right)$$

$$+k_d B_2(t,t_b)B_1(t,t_b)\left(\rho_i^2+\rho_i\left(\alpha_i^2+k_\beta\beta_i^2\right)\right)$$

$$+B_1^2(t,t_b)\left(-k_1 e_{i1}^2-k_3\sin^2 e_{i3}/k_2\right)+B_2^2(t,t_b)\left(-k_\rho\rho_i^2\cos^2\alpha_i-k_\alpha\rho_i\alpha_i^2\right)$$

$$-B_2^2\left(t,t_b\right)k_\rho\rho_i\cos^2\alpha_i\left(\alpha_i^2+k_\beta\beta_i^2\right)\big/2\ -E_{vi}^{R^T}K_4E_{vi}^R+B_1(t,t_b)B_2(t,t_b)e_{iv}^{R^T}\gamma(e_{i1},e_{i2},e_{i3})\ -$$

$$B_2(t,t_b)B_1(t,t_b)e_{iv}^{F^T}\lambda(\rho_i,\alpha_i,\beta_i). \tag{A7}$$

The first and last lines in (A7) also go to zero as $t\rightarrow\infty$ exponentially fast (controlled

through $B_1(\cdot)$ and the control gain , k_d).

Again examining the behavior of (A7) as $t\rightarrow\infty$,

$$\dot{L}_{Ri}\rightarrow-k_\rho\rho_i^2\cos^2\alpha_i-k_\alpha\rho_i\alpha_i^2-\frac{k_\rho}{2}\rho_i\cos^2\alpha_i\left(\alpha_i^2+k_\beta\beta_i^2\right)-e_{iv}^{R^T}K_4e_{iv}^R. \tag{A8}$$

since $B_1(\cdot)\rightarrow0, B_2(\cdot)\rightarrow1$, and $E_{vi}^R(t,t_b)\rightarrow e_{iv}^R(t)$.

It is observed that $\dot{L}_{Ri}$ is only negative semi-definite since at $\alpha_i=\pm\pi/2$, $\dot{L}_i$ is no

longer a function of β_i. Thus, the velocity tracking error and kinematic error states are

bounded. To achieve asymptotic convergence, Barbalat's Lemma is invoked [25]. First,

taking the derivative of (A.8) reveals that $\ddot{L}_i$ is bounded since all of the system states are

bounded. Therefore, since $\ddot{L}_i$ is bounded, $\dot{L}$ is uniformly continuous and converges to zero.

Thus, ρ_i, $\dot{\rho}_i$, $|e_{iv}^R|$ and $||\dot{e}_{iv}||$ are also guaranteed to converge to zero.

Then, using $\lambda_i\left(\rho_i,\alpha_i,\ \beta_i\right)$ and (A.1), it can be concluded that α_i and β_i also

converge to zero revealing that the velocity tracking error system (64) and kinematic

system (47) converge to the origin asymptotically, and the ith robot tracks its desired

velocity and converges to its desired posture. That is, $e_{iv}^R\rightarrow0$ and $q_i\rightarrow q_{id}$.

Proof of Theorem 2: Define the blended formation Lyapunov candidate function

for each robot as

$$L_{Fi}=B_2^2\left(t,t_c\right)\left(\left(e_{i1}^2+e_{i2}^2\right)\big/2+(1-\cos e_{i3})\big/k_2\right)+B_1^2(t,t_c)\frac{1}{2}\left(\rho_i^2+\rho_i\left(\alpha_i^2+k_\beta\beta_i^2\right)\right)+$$

$$\frac{1}{2}E_{vi}^{F^T}\bar{M}_iE_{vi}^F\ . \tag{A9}$$

Remark: The Lyapunov function, (A9) is slightly different than the Lyapunov function, (A1) defined in *Theorem 1*. The difference between (A1) and (A9) is the blended function squares are switched in (A9) which causes the regulation term vanish while the formation terms vanishes in (A1) as $t \to \infty$. Since the proof of *Theorem 2* has similarities with the proof of *Theorem 1*, some intermediate steps are combined in the proof of *Theorem 2*.

Now, taking derivative of (A9) , using the definitions of $\gamma(e_{i1}, e_{i2}, e_{i3})$ and $\lambda(\rho_i, \alpha_i, \beta_i)$, and inserting the blended formation tracking error dynamics (65), adding and subtracting $B_1(t, t_c)B_2(t, t_c){e_{iv}^{R}}^T \gamma(e_{i1}, e_{i2}, e_{i3})$ and $B_1(t, t_c)B_2(t, t_c){e_{iv}^{F}}^T \lambda(\rho_i, \alpha_i, \beta_i)$ into (A9) and collecting like terms yields

$$\dot{L}_{Fi} = 2B_2\left(t, t_c\right)\dot{B}_2\left(t, t_c\right)\left(\left(e_{i1}^2 + e_{i2}^2\right)\big/2 + \left(1 - \cos e_{i3}\right)\big/k_2\right)$$

$$+2B_1\left(t, t_c\right)\dot{B}_1\left(t, t_c\right)\frac{1}{2}\left(\rho_i^2 + \rho_i\left(\alpha_i^2 + k_\beta\beta_i^2\right)\right) \ + B_1^2\left(t, t_b\right)\left(-k_1 e_{i1}^2 - k_3 \sin^2 e_{i3}\big/k_2\right)$$

$$+B_1^2\left(t, t_c\right)\left(-k_\rho\rho_i^2\cos^2\alpha_i - k_\alpha\rho_i\alpha_i^2\right) \ -B_1^2\left(t, t_c\right)\frac{k_\rho}{2}\rho_i\cos^2\alpha_i\left(\alpha_i^2 + k_\beta\beta_i^2\right)$$

$$+{E_{vi}^{F}}^T\left(\overline{M}\left(\dot{B}_2(t, t_c)e_{iv}^F(t) + \dot{B}_1(t, t_c)e_{iv}^R(t)\right) + B_2(t, t_c)\left(-V_m e_{iv}^F + f_i(z_i^F)\right) +$$

$$B_1(t, t_c)\left(-V_m e_{iv}^R + f_i(z_i^R)\right) - \bar{\tau}\right) - B_2(t, t_c)(B_2(t, t_c){e_{iv}^{F}}^T +$$

$$B_1(t, t_c){e_{iv}^{R}}^T)\gamma(e_{i1}, e_{i2}, e_{i3})$$

$$+B_1(t, t_c)(B_1(t, t_c){e_{iv}^{R}}^T + B_2(t, t_c){e_{iv}^{F}}^T)\lambda(\rho_i, \alpha_i, \beta_i)$$

$$+ B_1(t, t_c)B_2(t, t_c){e_{iv}^{R}}^T \gamma(e_{i1}, e_{i2}, e_{i3}) - B_2(t, t_c)B_1(t, t_c){e_{iv}^{F}}^T \lambda(\rho_i, \alpha_i, \beta_i). \tag{A11}$$

Then, substitute the torque equation (67), apply the definition of E_{vi}^F to factor the bottom rows of (A11) into terms pre-multiplied by $E_{vi}^{F^T}$, and factor the rows containing V_m into the form of $E_{vi}^{F^T} V_M E_{vi}^F$ to give

$$\dot{L}_{Fi} = 2k_d B_2\left(t, t_c\right) B_1\left(t, t_c\right)\left(\left(e_{i1}^2 + e_{i2}^2\right)/2 + \left(1 - \cos e_{i3}\right)/k_2\right)$$

$$-2k_d B_1^2\left(t, t_c\right)\left(\rho_i^2 + \rho_i\left(\alpha_i^2 + k_\beta \beta_i^2\right)\right) + B_2^2(t, t_c)\left(-k_1 e_{i1}^2 - \frac{k_3}{k_2}\sin^2 e_{i3}\right) +$$

$$B_1^2(t, t_c)\left(-k_\rho \rho_i^2 \cos^2 \alpha_i - k_\alpha \rho_i \alpha_i^2 - \frac{k_\rho}{2}\rho_i \cos^2 \alpha_i\left(\alpha_i^2 + k_\beta \beta_i^2\right)\right) - E_v^{R^T} K_4 E_{vi}^R$$

$$+ B_1(t, t_c)B_2(t, t_c)e_{iv}^{R^T}\gamma(e_{i1}, e_{i2}, e_{i3}) - B_2(t, t_c)B_1(t, t_c)e_{iv}^{F^T}\lambda(\rho_i, \alpha_i, \beta_i). \qquad (A12)$$

The lines contains $B_1\left(t, t_c\right)$ of (A12) goes to zero as $t \to \infty$ exponentially fast (controlled through control gain, k_d). Using the identities of blended functions used in the proof of *Theorem 1* to simplify (A12) reveals

$$\dot{L}_{Fi} \to -k_1 e_{i1}^2 - \frac{k_3}{k_2}\sin^2 e_{i3} - e_{iv}^{F^T} K_4 e_{iv}^F \qquad (A13)$$

as $t \to \infty$.

Since (A.13) is not a function of e_{i2}, $\dot{L}_{if}$ is negative semi-definite, and the consensus errors and velocity tracking error are bounded. However, Barbalat's Lemma [15] can be used to show asymptotic convergence.

First, take the derivative of (A.13) while using (55) and (60) while observing the boundedness of all signals to reveal that $\ddot{L}_{iF}$ is also bounded. Therefore, $\dot{L}_{iF}$ converges to zero and thus e_{i1}, $\dot{e}_{i1}$, e_{i3}, $\dot{e}_{i3}$, $||e_{iv}^F||$, and $||\dot{e}_{iv}^F||$ all converge to zero as well. Finally, examining the definition of $\dot{e}_{i3}$ in (60) while noting that $\dot{e}_{i3} \to 0$ reveals that e_{i2} must also converge to zero. Therefore, the velocity tracking error system (60) and consensus error

system (57) converge to the origin asymptotically, and the ith robot tracks its desired velocity and reaches consensus with its neighbor robot j.

Proof of Theorem 3: Recall both the regulation and formation Lyapunov functions, (A1) and (A9) defined in *Theorem 1* and *Theorem 2, respectively. Theorems 1* and *2* illustrated the asymptotic convergence of the blended regulation and formation controllers, respectively, independently of one another. *Theorem 3* proves that the switched system is also stable.

Consider the following combined Lyapunov functions of all the mobile robots in the networked group as $L_R = L_{R1} + L_{R2}$, $L_F = L_{F1} + L_{F2}$ with

$$L_{R1} = \sum_{i=1}^{N} B_1^2\left(t,t_b\right)\left(\left(e_{i1}^2 + e_{i2}^2\right)/2 + \left(1 - \cos e_{i3}\right)/k_2\right) + \sum_{i=1}^{N} B_2^2\left(t,t_b\right)\frac{1}{2}\left(\rho_i^2 + \rho_i\left(\alpha_i^2 + k_\beta \beta_i^2\right)\right),$$

$$L_{F1} = \sum_{i=1}^{N} B_2^2\left(t,t_c\right)\left(\left(e_{i1}^2 + e_{i2}^2\right)/2 + \left(1 - \cos e_{i3}\right)/k_2\right) + \sum_{i=1}^{N} B_1^2\left(t,t_c\right)\frac{1}{2}\left(\rho_i^2 + \rho_i\left(\alpha_i^2 + k_\beta \beta_i^2\right)\right),$$

$$L_{R2} = \sum_{i=1}^{N} \frac{1}{2} E_{vi}^{R^T} \bar{M}_i E_{vi}^R, \quad L_{F2} = \sum_{i=1}^{N} \frac{1}{2} E_{vi}^{F^T} \bar{M}_i E_{vi}^F.$$

The proof will be completed in two steps: a) showing that L_{R2} and L_{F2} satisfy

Lemma 1; and b) Showing that L_{R1} and L_{F1} satisfy *Lemma 1*. That is, we will show that $L_F(t_a) > L_F(t_c)$ and $L_R(t_b) > L_R(t_d)$ where $t_a < t_b < t_c < t_d$ are the switching times defined in Figure 4.1.

a) First, consider L_{R2} and L_{F2} are functions of the blended velocity tracking errors. At the switching time from the formation mode to the regulation mode, t_b, the blended velocity tracking error is required to satisfy the switching condition defined in (69).

To satisfy *Lemma 1*, we require $\left\|E_{vi}^R(t_b, t_b) - E_{vi}^F(t_b, t_a)\right\| < \bar{\delta}_{ev}$ (for a computable

constant, $\bar{\delta}_{ev}$). The blended regulation velocity tracking error (62) can be given at the switching time, t_b, as

$$E_{vi}^R(t_b, t_b) = B_1(t_b, t_b)e_{iv}^F(t_b) + B_2(t_b, t_b)e_{iv}^R(t_b) = e_{iv}^F(t_b) \quad \text{since} \quad B_1(t_b, t_b) = 1 \quad \text{and}$$

$$B_2(t_b, t_b) = 0.$$

Now assume $E_{vi}^F(t_b, t_a) = e_{iv}^F(t) + \delta_{ev}$ at time t_b (from switching condition, (69) where $\|\delta_{ev}\| < \bar{\delta}_{ev}$), then it can be shown that

$$\left\|E_{vi}^R(t_b, t_b) - E_{vi}^F(t_b, t_a)\right\| = \left\|e_{iv}^F(t_b) - e_{iv}^F(t_b) - \delta_{ev}\right\| = \|\delta_{ev}\| < \bar{\delta}_{ev}.$$

As $t \to \infty$, recall that $E_{vi}^R(t, t_b) \to e_{iv}^R(t)$. At the switching time from the regulation mode to the formation mode, t_c, the blended regulation velocity tracking error must satisfy the switching condition (68).

As before, we require $\left\|E_{vi}^F(t_c, t_c) - E_{vi}^R(t_c, t_b)\right\| < \bar{\delta}_{ev}$ to ensure the *Lemma 1* is satisfied. The blended formation velocity tracking error can be given at the switching time, t_c, as

$$E_{vi}^F(t_c, t_c) = B_1(t_c, t_c)e_{iv}^R(t_c) + B_2(t_c, t_c)e_{iv}^F(t_c) = e_{iv}^R(t_c). \quad \text{Assume} \quad E_{vi}^R(t_c, t_b) =$$

$e_{iv}^R(t) + \delta_{ev}$ at time t_c (through satisfaction of the switching condition, (33)). Then,

$\left\|E_{vi}^F(t_c, t_c) - E_{vi}^R(t_c, t_b)\right\| = \|e_{iv}^R(t_c) - e_{iv}^R(t_c) - \delta_{ev}\| < \bar{\delta}_{ev}$. As $t \to \infty$, $E_{vi}^F(t, t_c) \to$

$e_{iv}^F(t)$.

At the switching conditions, we can therefore ensure the requirements of *Lemma 1* hold for the blended velocity tracking errors $E_{vi}^F(t, t_0)$ and $E_{vi}^R(t, t_0)$. Since the mass matrix, M_i , is constant, the Lyapunov functions L_{R2} and L_{F2} satisfy the *Lemma 1*.

b) Next, we will show that the first parts of the Lyapunov functions, L_{R1} and L_{F1}, satisfy

Lemma   1.   To   accomplish   this,   we   will   illustrate   that
$L_{R1}(t_b) > L_{R1}(t_d)$ and $L_{F1}(t_a) > L_{F1}(t_c)$ for switching times $t_a < t_b < t_c < t_d$.

To   proceed,   use   the   property   of   the   blended   function,
$B_1(t_0,t_0) = 1, B_2(t_0,t_0) = 0$, $\forall t_0$ at the switching time and consider the Lyapunov functions

at the switching times

$$L_{R1}(t_b) = \sum_{i=1}^{N} \frac{1}{2}\left(e_{i1}^2(t_b) + e_{i2}^2(t_b)\right) + \frac{1}{k_2}\left(1 - \cos e_{i3}(t_b)\right)$$

$$L_{R1}(t_d) = \sum_{i=1}^{N} \frac{1}{2}\left(e_{i1}^2(t_d) + e_{i2}^2(t_d)\right) + \frac{1}{k_2}\left(1 - \cos e_{i3}(t_d)\right)$$

,

$$L_{F1}(t_a) = \sum_{i=1}^{N} \frac{1}{2}\left(\rho_i^2(t_a) + \rho_i(t_a)\left(\alpha_i^2(t_a) + k_\beta \beta_i^2(t_a)\right)\right), \text{and}$$

$$L_{F1}(t_c) = \sum_{i=1}^{N} \frac{1}{2}\left(\rho_i^2(t_c) + \rho_i(t_c)\left(\alpha_i^2(t_c) + k_\beta \beta_i^2(t_c)\right)\right).$$

.

From the switching conditions, it is automatically satisfied that $L_{R1}(t_b) > L_{R1}(t_d)$.

However, it is not trivial to show that $L_{F1}(t_a) > L_{F1}(t_c)$. To prove the inequality, we will

show that the function $L_{F1}(T)$, for $T = t_a, t_b, t_c, ...$, is a decrescent function that is upper

and lower bounded by Lyapunov functions $\bar{L}_{F1}(T)$ and $\underline{L}_{F1}(T)$, respectively, with

$\bar{L}_{F1}(T) \to 0$ asymptotically and $\underline{L}_{F1}(T) \to 0$ asymptotically as $T \to \infty$ and independently

of the mode of operation. That is, it will be shown that the upper and lower bounds decrease

during both the regulation and formation modes.

First, define the upper bound of $L_{F1}(T)$ as

$$\bar{L}_{F1}(T) = \sum_{i=1}^{N} \frac{1}{2}\left(\rho_i^2(T) + \rho_i(T)\Gamma\right) \tag{A.14}$$

where Γ is a computable constant. Since $\alpha(t), \beta(t)$ are both in the range of $[-\pi, \pi)$, one can easily compute Γ which satisfies the inequality.

The value of the upper bound (A.14) at the switching times t_a and t_c is a function of regulation error, ρ. To show ρ is always decreasing, rewrite the regulation error, ρ, at the beginning and end of formation mode as

$$\rho_i(t_a) = \rho_{av}(t_a) + \sigma_{\rho i}(t_a) \tag{A.15}$$

$$\rho_i(t_b) = \rho_{av}(t_a) + \sigma_{\rho i}(t_b) \tag{A.16}$$

where $\rho_{av}(t_a) = \dfrac{1}{N} \sum\limits_{i=1}^{N} \rho_i(t_a)$ is the average regulation error at the beginning of the formation mode, and $\sigma_{\rho i}(t), i = 1, 2 \ldots N$ are the deviations of the regulation errors. It is observed that and $\sum\limits_{i=1}^{N} \sigma_{\rho i}(t_a) = 0$, $\sum\limits_{i=1}^{N} \sigma_{\rho i}(t_b) = 0$ by definition of $\rho_{av}(t)$.

Next, substitute (A.15) into (A.14) to rewrite the upper bound at time t_a, $\bar{L}_{F1}(t_a)$, as

$$\bar{L}_{F1}(t_a) = \sum\limits_{i=1}^{N} \frac{1}{2} \left(\left(\rho_{av} + \sigma_{\rho i}(t_a) \right)^2 + \left(\rho_{av} + \sigma_{\rho i}(t_a) \right) \Gamma \right)$$

$$= \frac{N}{2} \rho_{av}^2 + \frac{1}{2} \sum\limits_{i=1}^{N} 2\sigma_{\rho i}(t_a) \rho_{av} + \frac{1}{2} \sum\limits_{i=1}^{N} \sigma_{\rho i}(t_a)^2 + \frac{N\Gamma}{2} \rho_{av} + \frac{\Gamma}{2} \sum\limits_{i=1}^{N} \sigma_{\rho i}(t_a)$$

The second and the last terms evaluate to zero since $\sum\limits_{i=1}^{N} \sigma_{\rho i}(t_a) = 0$. Then,

$$\bar{L}_{F1}(t_a) = \frac{N}{2} \rho_{av}^2 + \frac{1}{2} \sum\limits_{i=1}^{N} \sigma_{\rho i}(t_a)^2 + \frac{N\Gamma}{2} \rho_{av}$$

Then, substitute (A.16) into (A.14) to rewrite the upper bound at time t_b, $\bar{L}_{F1}(t_b)$, as

$$\bar{L}_{F1}(t_b) = \sum_{i=1}^{N} \frac{1}{2} \left(\rho_i^2(t_b) + \rho_i(t_b) \Gamma \right) = \frac{N}{2} \rho_{av}^2 + \frac{1}{2} \sum_{i=1}^{N} \sigma_{\rho i}(t_b)^2 + \frac{N\Gamma}{2} \rho_{av}$$

Now, compute the difference between $\bar{L}_{F1}(t_a)$ and $\bar{L}_{F1}(t_b)$ to give

$$\Delta L_{F1} = \frac{1}{2} \sum_{i=1}^{N} \left(\sigma_{\rho i}(t_b)^2 - \sigma_{\rho i}(t_a)^2 \right).$$

In order to claim that $\Delta L_{F1} < 0$ (i.e., $\bar{L}_{F1}(t_a) > \bar{L}_{F1}(t_b)$), we will show that $\left| \sigma_{\rho i}(t_a) \right| \geq \left| \sigma_{\rho i}(t_b) \right|$. First, recall that the formation controller of *Theorem 2* achieves consensus on the Cartesian coordinate regulation errors, Δx and Δy as defined in (74).

Therefore, define $\Delta x_i(t_a) = \Delta x_{av}(t_a) + \sigma_{\Delta xi}(t_a), \Delta y_i(t_a) = \Delta y_{av}(t_a) + \sigma_{\Delta yi}(t_a)$

$\Delta x_i(t_b) = \Delta x_{av}(t_a) + \sigma_{\Delta xi}(t_b), \Delta y_i(t_b) = \Delta y_{av}(t_a) + \sigma_{\Delta yi}(t_b)$ where $\Delta x_{av}(t) = \frac{1}{N} \sum_{i=1}^{N} \Delta x_i(t)$,

$\Delta y_{av}(t) = \frac{1}{N} \sum_{i=1}^{N} \Delta y_i(t)$ are the average Cartesian coordinate distance errors on x and y

directions respectively, $\sigma_{\Delta yi}(t), i = 1,2 \dots V$ are the deviations of the regulation error in

the y- component of the Cartesian coordinate system, $\sigma_{\Delta xi}(t), i = 1,2 \dots V$ are the

deviations of the regulation error in the x- component of the Cartesian coordinate system,

and $\sum_{i=1}^{N} \sigma_{\Delta xi}(t_a) = \sum_{i=1}^{N} \sigma_{\Delta xi}(t_b) = \sum_{i=1}^{N} \sigma_{\Delta yi}(t_a) = \sum_{i=1}^{N} \sigma_{\Delta yi}(t_b) = 0$.

Since the robots reach consensus on their Cartesian coordinate regulation errors

during their formation mode, deviations among the robots' regulation errors decrease

during the formation mode, i.e. $\left| \sigma_{\Delta xi}(t_a) \right| > \left| \sigma_{\Delta xi}(t_b) \right|, \left| \sigma_{\Delta yi}(t_a) \right| > \left| \sigma_{\Delta yi}(t_b) \right|$. Now, consider

the polar coordinate transformation (46)

$$\sum_{i=1}^{N}\rho_i^2 = \sum_{i=1}^{N}\Delta x_i^2 + \Delta y_i^2 \quad \text{or}$$

$$N\rho_{av}^2 + \frac{1}{2}\sum_{i=1}^{N}\sigma_{\rho i}\left(t_a\right)^2 = N\left(\Delta x_{av}^2 + \Delta y_{av}^2\right) + \frac{1}{2}\sum_{i=1}^{N}\left(\sigma_{\Delta xi}\left(t_a\right)^2 + \sigma_{\Delta yi}\left(t_a\right)^2\right) \tag{A.17}$$

From the definition of ρ_i , $N\rho_{av}^2 = N\left(\Delta x_{av}^2 + \Delta y_{av}^2\right)$ and (A.17) can be rewritten as

$$\frac{1}{2}\sum_{i=1}^{N}\sigma_{\rho i}\left(t_a\right)^2 = \frac{1}{2}\sum_{i=1}^{N}\left(\sigma_{\Delta xi}\left(t_a\right)^2 + \sigma_{\Delta yi}\left(t_a\right)^2\right) \tag{A.18}$$

Since $\left|\sigma_{\Delta xi}\left(t_a\right)\right| > \left|\sigma_{\Delta xi}\left(t_b\right)\right|, \left|\sigma_{\Delta yi}\left(t_a\right)\right| > \left|\sigma_{\Delta yi}\left(t_b\right)\right|$, it follows from (A.18) that

$$\left|\sigma_{\rho i}\left(t_a\right)\right| > \left|\sigma_{\rho i}\left(t_b\right)\right| \ .$$

Then, the bounding function $\bar{L}_{F1}\left(t_a\right)$ in (A.14) decreases during the formation keeping mode. In the *Theorem 1*, it is proven that the regulation errors based Lyapunov function decreases over the regulation mode time period, $[t_b, t_c)$ such that $\bar{L}_{F1}(t_b) > \bar{L}_{F1}(t_c)$. Therefore, the regulation errors are decreasing during both the regulation mode and the formation keeping mode revealing that $\bar{L}_{F1}\left(t_a\right) > \bar{L}_{F1}\left(t_c\right)$.

Since $\bar{L}_{F1}(t_a) > \bar{L}_{F1}(t_b) > \bar{L}_{F1}(t_c) > \bar{L}_{F1}(t_d)$ *for all* switching times $t_a < t_b < t_c < t_d$, it follows that $\bar{L}_{F1}(t) \rightarrow 0$ as $t \rightarrow \infty$.

Next, define the lower bounding function of $L_{F1}(T)$ as $\underline{L}_{F1}(T) = \frac{1}{2}\sum_{1}^{N}\rho_i^2(T)$ such that $\underline{L}_{F1}(T) < L_{F1}(T)$ for all $T = t_a, t_b, t_c, \dots$ Using the same techniques as above, it is straight forward to show that $\underline{L}_{F1}(t_a) > \underline{L}_{F1}(t_b) > \underline{L}_{F1}(t_c) > \underline{L}_{F1}(t_d)$ and $\underline{L}_{F1}(T) \rightarrow 0$ as $T \rightarrow \infty$.

Therefore, $L_{F1}(T)$ is upper and lower bounded by positive definite functions that each converge to zero asymptotically as $T \to \infty$. That is, $L_{F1}(T)$ is an asymptotically stable decrescent Lyapunov function [18] illustrating that $L_{F1}(t_a) > L_{F1}(t_c)$.

Thus, it follows that $L_F(t_a) > L_F(t_c)$ and $L_R(t_b) > L_R(t_d)$ where $t_a < t_b < t_c < t_d$ satisfying *Lemma 1* and completing the proof.

REFERENCES

[1]   R.R. Nair, L. Behera, V. Kumar, M. Jamshidi, "Multisatellite Formation Control for Remote Sensing Applications Using Artificial Potential Field and Adaptive Fuzzy Sliding Mode Control," *IEEE Sys. Jour.*, vol.9, no.2, pp.508-518, June 2015.

[2]   Y. Wang, W. Yan, J. Li, "Passivity-based formation control of autonomous underwater vehicles," *IET Control Theory & Applications*, vol.6, no.4, pp.518-525, March 2012.

[3]   T. Dierks and S. Jagannathan, "Neural Network Control of Mobile Robot Formations Using RISE Feedback," *IEEE Trans. on Systems, Man, and Cybernetics, Part B: Cybernetics*, vol.39, pp.332-347, Apr. 2009.

[4]   W. Ren and E. Atkins, "Distributed multi-vehicle coordinated control via local information exchange," *International Journal of Robust and Nonlinear Control*, vol. 17, no. 10-11, pp. 1002–1033, 2007.

[5]   R. Olfati-Saber and R. M. Murray, 'Consensus problems in networks of robot switching topology and time-delays', *IEEE Trans. on Automatic Control*, vol. 49, no. 9,pp. 1520–1533, Sep. 2004.

[6]   C. Kecai, J. Bin, Y. Dong, "Distributed consensus of multiple nonholonomic mobile robots," *IEEE/CAA Journal of Automatica Sinica,* vol.1, no.2, pp.162-170, April 2014.

[7]   D. Di Paola, D. Naso, B. Turchiano, "Consensus-based robust decentralized task assignment for heterogeneous robot networks," *American Control Conference (ACC), 2011*, June 2011, pp.4711-4716.

[8]   X. Geng, "Consensus-reaching of Multiple Robots with Fewer Interactions," *2009 WRI World Congress on Computer Science and Information Engineering,* , March 2009, pp.249-253.

[9]   S. Mastellone, D. Stipanoviˊc, C. Graunke, K. Intlekofer, and M. Spong, "Formation control and collision avoidance for multi-   agent nonholonomic systems: Theory and experiments," *Int. J. Rob. Res.*,vol. 27, no. 1, pp. 107–126, Jan. 2008.

[10]   M. Breivik, M. Subbotin, and T. Fossen, "Guided formation control for wheeled mobile robots," in *Proc. IEEE Int. Conf. Robot.Autom .,*Dec. 2006, pp. 1–7.

[11]   Y. Liang and H. Lee, "Decentralized formation control and obstacle avoidance for multiple robots with nonholonomic constraints," in *Proc. IEEE Am. Control Conf.*, Jun. 2006, pp. 5596–5601.

[12]   S. S. Ge and C. H. Fua, "Queues and artificial potential trenches for multirobot formations," *IEEE Trans. Robot.*, vol. 21, no. 4, pp.   646–656,Aug. 2005.

[13]   S. Feng and H. Zhang, "Formation control for wheeled mobile robots based on consensus protocol," *IEEE International Conference on Information and Automation (ICIA),* June 2011, pp.696-700.

[14]   A. D. Luca, G. Oriolo, and M. Vendittelli, "Control of wheeled mobile robots: An experimental overview," in RAMSETE—Articulated and Mobile Robotics for Services and Technologies, S. Nicosia, B. Siciliano, A. Bicchi, and P. Valigi, Eds. New York: Springer-Verlag, vol. 270, pp. 181–223, 2001.

[15]   M. S. Branicky, "Multiple Lyapunov functions and other analysis tools for switched and hybrid systems," *IEEE Trans. on Automatic Control*, vol.43, no.4, pp.475-482, Apr. 1998.

[16]   H. M. Guzey, T. Dierks and S. Jagannathan, "Hybrid consensus-based formation control of agents with second order dynamics," in *American Control Conference (ACC), 2015* , July 2015, pp.4386-4391.

[17]   R. Fierro and F. L. Lewis, "Control of a nonholonomic mobile robot using neural networks," *IEEE Trans. on Neural Networks*, vol. 8, pp. 589-600, Jul. 1998.

[18]   S. Miah, H. Chaoui, and P. Sicard, "Linear time-varying control law for stabilization of hopping robot during flight phase," *2014 IEEE 23rd Int. Symp on Industrial Electronics (ISIE),* Jun. 2014 , pp.1550-1554.

[19]   F. L. Lewis, S. Jagannathan, and A. Yesildirek. *Neural Network Control of Robot Manipulators and Nonlinear Systems*, New York: Taylor & Francis, 1999.

III. DISTRIBUTED CONSENSUS-BASED EVENT-TRIGGERED APPROXIMATE CONTROL OF NONHOLONOMIC MOBILE ROBOT FORMATIONS

ABSTRACT

In this paper, the distributed consensus-based formation control of networked nonholonomic mobile robots using neural networks (NN) in the presence of uncertain robot dynamics with event-based communication is presented. The robots communicate their location and velocity information with their neighbors, at event-based sampling instants, to drive themselves to a pre-defined desired formation by using a distributed control technique. For relaxing the perfect velocity tracking assumption, control torque is designed to reduce the velocity tracking error, by explicitly taking into account each robot dynamics and the formation dynamics of the network of robots via NN approximation. The approximated dynamics are employed to generate the control torque with event-sampled measurement updates and communication. With a distributed formation control approach, the Lyapunov stability method is utilized to develop a decentralized event-sampling condition and to demonstrate the consensus of network of mobile robot formation. Finally, simulation results are presented to verify theoretical claims and to demonstrate the reduction in computations and communication cost.

1. INTRODUCTION

In the literature, there are several approaches which accomplish the formation control objective - leader-follower control [1],[2], virtual structure [3] or behavior-based approaches [4], to name a few. Of all these approaches, consensus-based formation control[5]-[10] is considered to be more robust and reliable due to scalability and its inherent properties that enable the robots to maintain their formation even if one of the robots experiences a failure.

In earlier works[5],[8]-[12], consensus-based schemes have been studied for generalized linear systems with known system dynamics and applied to systems with time-varying communication graphs [5], bounded disturbances [8], and communication delays during state information sharing [9]. In these works [4][5][7][12][13], the individual robot and the formation dynamics are neglected which can affect the formation keeping as shown here. In addition, due to periodic sampling in these controllers, they are computationally inefficient.

In contrast, in this paper, an adaptive event-based distributed formation control of networked robots is introduced wherein the dynamics of the individual robot and the formation are explicitly taken into account. Neural-network (NN) are utilized as function approximators to learn the dynamics of each mobile robot and the formation.

To mitigate computational complexity of control techniques, in the recent years, event-based sampling has become more popular [14]-[18] wherein the execution time of the control inputs is based on the real-time operation of the system. Thus, event sampling of feedback information reduces computations for adaptive formation control when the

dynamics are uncertain. Moreover, since the mobile robots need location and velocity information from their neighbors to reach consensus, they share their information among each other through a resource limited communication network. Therefore, utilizing the communication network in an event sampled context lead to minimizing network congestion and undesired performance of the controller.

In the event-sampled framework [14]-[18], the measured state vector is sampled using certain state dependent criteria referred to as the event-triggering condition and the controller is executed at these aperiodic sampling instants. The event-triggering condition is designed by taking into account the stability and the closed-loop performance, and hence, it is proven to be advantageous over its periodic counterpart.

Initially, the event-triggered techniques from the literature [14][17][18] were designed for ensuring stable operations of the closed-loop system by assuming that a stabilizing controller exists for the system under consideration. Developing an event-triggering condition and establishing the existence of positive minimum inter-event time was the main focus in these works [14][17][18].

Similarly, when the robot and formation dynamics become uncertain, a suitable adaptive sampling condition is needed for formation control which ensures formation stability and also the NN adaptation. However, event-based sampling can make the stablility analysis involved. The formation errors are obtained at these sampling instants and are utilized to obtain the desired velocities for each robot in order to drive the robots to a predefined formation. Then the control torque is designed to ensure that the velocities of each robot track the desired velocities.

First, to determine the formation error, a unique virtual reference cart is defined using the regulation errors of the neighborhood robots in the network. However, due to the uncertain dynamics of each robot, there will be a persistent velocity tracking error. Using the NN-based representation of the mobile robot dynamics, the control inputs are obtained to minimize this velocity tracking error with event-sampled feedback.

It is worth mentioning that the velocity tracking errors of each robot acts as a virtual subsystem for the formation error dynamics. Thus by using the distributed backstepping controller design, it will be shown that by reducing the velocity tracking errors, the formation error reduces and the robots reach a desired formation. It should be noted that, in contrast to the existing consensus based formation control approaches [5]-[9],[12], the uncertain dynamics of the mobile robots are explicitly taken into account, relaxing the perfect velocity tracking assumption. The overall control scheme will be distributed since the controllers at each robot are designed using the consensus based formation error, which is a function of the position and velocities of all the neighborhood robots.

Since the unknown NN weights are tuned only at the event-sampled instants, the computations are reduced when compared to traditional and adaptive NN control schemes, but it introduces aperiodic weight tuning. A novel event-sampling condition is derived in such a way that the robots use locally available and previously transmitted information from others to determine the feedback instants. This reduces the communication costs and ensures stability and performance of the overall formation. In other words, the adaptive event-sampling mechanism enables asynchronous broadcast of position and velocity information of each robot, reducing the network congestion. Finally, the extension of the

Lyapunov direct method is used to prove the local uniform ultimate boundedness (UUB) of the tracking and the parameter estimation errors with event-sampled feedback.

The contributions of this paper include the development of - a) a novel distributed adaptive consensus-based formation control of networked robots by taking into account both the uncertain dynamics of each robot and its formation; b) a novel adaptive event-sampling condition using both current information of the robot under consideration and previous information for neighborhood robots to determine the feedback instants which in turn results in asynchronous communication; and c) the demonstration of overall stability of the robot formation using the Lyapunov stability theory.

In this paper, $\Re^n$ is used to denote n dimensional Euclidean space. Euclidean-norm is used for vectors and for matrices, Frobenius norm is used.

2. BACKGROUND AND PRELIMINARIES

In this section, a brief background on the event-sampled control implementation is provided. Later, the dynamics of the mobile robots are introduced.

2.1 EVENT-SAMPLED CONTROL

In contrast to periodic/continuous feedback based control techniques, the event sampled controller implementation is relatively new and involves many challenges. Here, the event-based control problem is introduced by highlighting the challenges involved in the design with respect to controller adaptation and system stability.

In an event sampled framework, the system state vector is sensed continuously but available to the controller only at the event-sampled instants. To denote the sampling instants we define an increasing sequence of time instants $\{t_k\}_{k=0}^{\infty}$, referred to as the event sampled instants satisfying $t_{k+1} > t_k$, $\forall k = 0, 1, \cdots, n$. Let $t_0 = 0$ be the initial sampling instant. At the instant t_k, the sampled state $x(t_k)$, is available to the controller, and the last sampled state at the controller denoted by $\breve{x}(t)$ is updated.

The error, $e_{ET}(t)$, introduced due to the event sampled state can be written as

$$e_{ET}(t) = x(t) - \breve{x}(t), \quad t_k < t \leq t_{k+1}, \forall k = 0, 1, \cdots, n, \tag{75}$$

where $e_{ET}(t)$ is referred to as event sampling error. Thus, the event sampling error becomes zero at every sampling instant and update of the state, that is, $e_{ET}(t_k) = 0$, $\forall k = 0, 1, \cdots, n$.

For the event-triggered controllers, as mentioned before, an event-sampling mechanism/condition is required to determine the sampling instants, without jeopardizing the system stability. Also, if the controller parameters are adaptive and updated from the

feedback information, the parameter adaptation process is also dependent on the event-based sampling instants. Therefore, the event-sampling mechanism should be carefully designed so that event-based feedback does not impede with the adaptation process of the controller. Next, the dynamics of the mobile robots will be presented.

2.2   MOBILE ROBOT DYNAMICS

Consider the non-holonomic robot shown in Figure 2.1, where x_r, y_r denote Cartesian positions with respect to the robot frame, d is the distance between the rear-axis and the center of mass of the robot, r, R are the radius of the rear wheels, and half of the robot width, respectively.

The equations of motion about the center of mass, C, for the ith robot in a networked robot formation are written as

$$\dot{q}_i = \begin{bmatrix} \dot{x}_{ci} \\ \dot{y}_{ci} \\ \dot{\theta}_i \end{bmatrix} = \begin{bmatrix} \cos\theta_i & -d_i\sin\theta_i \\ \sin\theta_i & d_i\cos\theta_i \\ 0 & 1 \end{bmatrix} \begin{bmatrix} v_i \\ \omega_i \end{bmatrix} = S_i(q_i)\bar{v}_i, \tag{76}$$

where $q_i = [x_{ci} \ y_{ci} \ \theta_i]^T$ denotes the Cartesian position of the center of mass and orientation of the ith robot; v_i, and ω_i represent linear and angular velocities, respectively, and $\bar{v}_i = [v_i \ \omega_i]^T$ for the ith robot. Mobile robotic systems, in general, can be characterized as underactuated systems with constraints [1].

At higher velocities, $\bar{v}_i$, the dynamics of the robots become significant [1] and have to be explicitly considered. The dynamics of the ith mobile robot are given by

$$\bar{M}_i\dot{\bar{v}}_i + \bar{V}_{mi}(q_i, \dot{q}_i)\bar{v}_i + \bar{F}_i(\bar{v}_i) + \bar{\tau}_{di} = \bar{\tau}_i, \tag{77}$$

where $\bar{M}_i \in \Re^{\rho \times \rho}$ is a constant positive definite inertia matrix, $\bar{V}_{mi} \in \Re^{\rho \times \rho}$ is the bounded

centripetal and Coriolis matrix, $\bar{F}_i \in \Re^\rho$ is the friction vector, $\bar{\tau}_{di} \in \Re^\rho$ represents unknown

bounded disturbances such that $\left\|\bar{\tau}_{di}\right\| \le d_M$ for a known constant, d_M, $\bar{B}_i \in \Re^{\rho \times \rho}$ is a

constant, nonsingular input transformation matrix, $\bar{\tau}_i = \bar{B}_i \tau_i \in \Re^\rho$ is the input vector, and

$\tau_i \in \Re^\rho$ is the control torque vector. For complete details on (44) and the parameters, refer

to [1].

Assumption 1: The robotic system (44) satisfies the following properties: $\bar{M}_i$ is a

known positive definite matrix and it is bounded by B_{iM} and $0 < \bar{M}_i^{-1} < B_{im}$, the norm of $\bar{V}_{mi}$,

and $\left\|\bar{\tau}_{di}\right\| \le d_M$ are all bounded. The matrix $\dot{\bar{M}}_i - 2\bar{V}_{mi}$ is the skew-symmetric [1]. The

cartesian position and the velocity are assumed to be measurable.

Next, the consensus based formation control problem will be introduced.

2.3   CONSENSUS BASED FORMATION CONTROL

Consensus in a group decision making process is a scenario in which the group

members reach an agreement in the best interest of the whole group [10]. In consensus

based control of networked systems, the controller forces the states of each system in the

network to the same value, which is called the consensus point [13]. Further, in formation

control of mobile robots, reaching consensus on positions and orientations of each robot

will bring the network of robots to the same location which will cause collision. Therefore,

consensus on regulation errors is required [5] to avoid collision.

Hence, we first define the regulation errors for each robot in the network, in terms of their

positions and orientations as $\Delta x_i = x_i - x_i^r$, $\Delta y_i = y_i - y_i^r$, $\Delta \theta_i = \theta_i - \theta_i^r$ with x_i^r, y_i^r, θ_i^r

being the reference position and bearing angles. The time invariant desired positions ,

x_i^r, y_i^r, and the orientations, θ_i^r, will provide the desired formation for the networked system.

Now, the consensus errors are defined for each robot as a function of the regulation error of the robot and its neighbors as

$$\delta_{xi} = \frac{1}{\varsigma_i} \sum_{k \in N_i} (\Delta x_i - \Delta x_k) = \Delta x_i - \frac{1}{\varsigma_i} \sum_{k \in N_i} \Delta x_k \, , \quad \delta_{yi} = \frac{1}{\varsigma_i} \sum_{k \in N_i} (\Delta y_i - \Delta y_k) = \Delta y_i - \frac{1}{\varsigma_i} \sum_{k \in N_i} \Delta y_k \, , \quad \text{and}$$

$$\delta_{\theta i} = \frac{1}{\varsigma_i} \sum_{k \in N_i} (\Delta \theta_i - \Delta \theta_k) = \Delta \theta_i - \frac{1}{\varsigma_i} \sum_{k \in N_i} \Delta \theta_k \, , \tag{78}$$

along x and y directions and the bearing angle, respectively with N_i, ς_i being the set of robots and number of robots in the neighborhood of the ith robot. The main purpose of the consensus based controller will be to force formation errors (78) go to zero so that the network of robots is in consensus.

Achieving a formation by a network of robots depends on the reference coordinates of each robot provided the robots in the network share the position and velocity information with at least one of its neighbors. Therefore, the following assumption is needed.

Assumption 2: The robots determine their formation errors, (78), based on the information exchange topology of the communication network. The information exchange topology is connected similar to [5].

Remark 1: Driving the formation errors (78) close to zero will not result in the desired formation unless Assumption 2 is satisfied [5]. The minimal communication that is required for four robots to satisfy the connectedness is given in Figure 2.1. Connectedness of the network ensures that there is no isolated agent/robot in the network.

In other words, each agent receives information from one agent and transmits information to at least one other agent which requires $\varsigma_i \geq 1, \forall i = 1, 2, \ldots, N$.
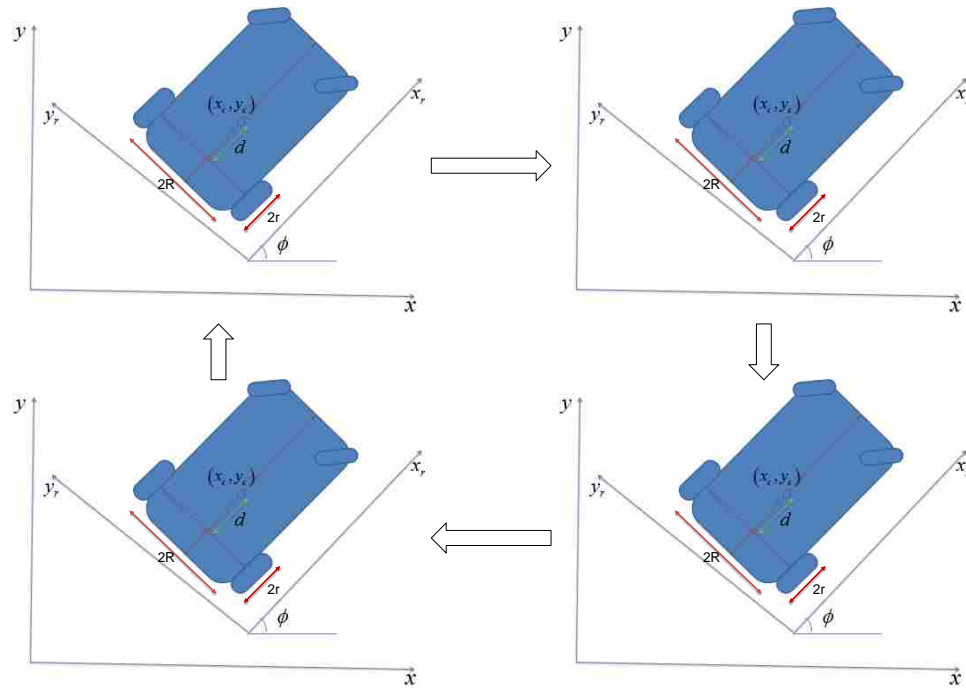
Figure 2.1 Differentially driven mobile robots.

Remark 2: In [5], a controller was designed to ensure that all regulation errors for the linear systems achieved a common value. The benefit of such consensus based formation controller is that the ith robot will be able to reach consensus with its neighbor when the communication is not available with the jth robot anymore. As shown in [5] average consensus is achieved if the information exchange topology is both strongly connected and balanced.

3. PERIODICALLY DRIVEN DISTRIBUTED CONTROLLER DESIGN

The main focus of this section is to formulate the back-stepping formation control of mobile robots by minimizing the consensus-based formation error. For this to happen, this formation error is obtained from the robot kinematics and utilized to derive the velocities at which the robots should move. The perfect velocity tracking assumption [1] becomes undesirable due to the robot dynamics. Therefore, by explicitly taking into account the dynamics of each robot, controllers are designed to minimize the velocity tracking error. The velocity tracking error acts as a virtual control input to the formation error dynamics and makes the robots reach consensus.

First, define the states for the virtual nonholonomic mobile robot as

$$x_j = \frac{1}{\varsigma_i}\sum_{k\in N_i}x_k, \mathrm{y}_j = \frac{1}{\varsigma_i}\sum_{k\in N_i}y_k, \theta_j = \frac{1}{\varsigma_i}\sum_{k\in N_i}\theta_k, \quad \mathrm{v}_j = \frac{1}{\varsigma_i}\sum_{k\in N_i}v_k, \omega_j = \frac{1}{\varsigma_i}\sum_{k\in N_i}\omega_k.$$ This definition

of the virtual cart is unique in the sense that the average values of the neighbor states are utilized to generate consensus errors for the formation. Then, the formation errors can be rewritten as $\delta_{xi} = \Delta x_i - \Delta x_j$, $\delta_{yi} = \Delta y_i - \Delta y_j$, $\delta_{\theta i} = \Delta\theta_i - \Delta\theta_j$. If the reference bearing angles of each robot in the network are different, then the robots move in different direction, which is undesirable for maintaining a formation. Therefore, the following assumption is needed.

Assumption 3: The desired heading angles, θ_{id}, are same for each robot in the formation so that each robot is oriented in the same direction [5], which yields $\delta_{\theta i} = \theta_i - \theta_j$. Next, the consensus-based formation errors (78) are transformed into the reference frame attached to the mobile robot using the transformation [1] given by

$$e_{iF} = \begin{bmatrix} e_{i1} \\ e_{i2} \\ e_{i3} \end{bmatrix} = \begin{bmatrix} \cos\theta_i & \sin\theta_i & 0 \\ -\sin\theta_i & \cos\theta_i & 0 \\ 0 & 0 & 1 \end{bmatrix} \begin{bmatrix} \delta_{xi} \\ \delta_{yi} \\ \delta_{\theta i} \end{bmatrix}. \tag{79}$$

Taking the derivative of (54) reveals

$$\dot{e}_{iF} = \begin{bmatrix} -\sin\theta_i \omega_i \delta_{xi} + \cos\theta_i \dot{\delta}_{xi} + \cos\theta_i \omega_i \delta_{yi} + \sin\theta_i \dot{\delta}_{yi} \\ -\cos\theta_i \omega_i \delta_{xi} - \sin\theta_i \dot{\delta}_{xi} - \sin\theta_i \omega_i \delta_{yi} + \cos\theta_i \dot{\delta}_{yi} \\ \dot{\delta}_{\theta i} \end{bmatrix}. \tag{80}$$

Using the expression (76) in (80) gives

$$\dot{e}_{1F} = \begin{bmatrix} \dot{\delta}_{xi} & \dot{\delta}_{yi} & \dot{\delta}_{\theta i} \end{bmatrix}^T \tag{81}$$

with $\dot{\delta}_{xi} = \begin{pmatrix} -\sin\theta_i \omega_i \delta_{xi} + \cos\theta_i \begin{pmatrix} \cos\theta_i v_i - d_i \sin\theta_i \omega_i \\ -\cos\theta_j v_j + d_j \sin\theta_j \omega_j \end{pmatrix} \\ +\cos\theta_i \omega_i \delta_{yi} + \sin\theta_i \begin{pmatrix} \sin\theta_i v_i + d_i \cos\theta_i \omega_i \\ -\sin\theta_j v_j - d_j \cos\theta_j \omega_j \end{pmatrix} \end{pmatrix}$, and

$$\dot{\delta}_{yi} = \begin{pmatrix} -\cos\theta_i \omega_i \delta_{xi} - \sin\theta_i \begin{pmatrix} \cos\theta_i v_i - d_i \sin\theta_i \omega_i \\ -\cos\theta_j v_j + d_j \sin\theta_j \omega_j \end{pmatrix} \\ -\sin\theta_i \omega_i \delta_{yi} + \cos\theta_i \begin{pmatrix} \sin\theta_i v_i + d_i \cos\theta_i \omega_i \\ -\sin\theta_j v_j - d_j \cos\theta_j \omega_j \end{pmatrix} \end{pmatrix}.$$

On simplification, using the trigonometric identities and (54), the formation error dynamics are obtained as

$$\begin{bmatrix} \dot{e}_{i1} \\ \dot{e}_{i2} \\ \dot{e}_{i3} \end{bmatrix} = \begin{bmatrix} e_{i2}\omega_i + v_i - v_j \cos e_{i3} \\ -e_{i1}\omega_i + v_j \sin e_{i3} \\ \omega_i - \omega_j \end{bmatrix}. \tag{82}$$

Remark 3: It can be observed that (55) resembles the error system for a single robot tracking a virtual reference cart [1]. In this work, instead of tracking a virtual cart, the mobile robots attempt to reach consensus with their neighbors, and each $e_{i(-)}$ represents the consensus error instead of the trajectory tracking error. In order to stabilize the open-

loop formation error dynamics (55), linear and angular velocities are designed as virtual control inputs.

Under the perfect velocity tracking assumption, the consensus-based formation control velocity is proposed as

$$\bar{v}_{id}^F = \begin{bmatrix} v_{id}^F \\ \omega_{id}^F \end{bmatrix} = \begin{bmatrix} -k_1 e_{i1} + v_j \cos e_{i3} \\ \omega_j - k_2 v_j e_{i2} - k_3 \sin e_{i3} \end{bmatrix}. \tag{83}$$

with $k_1, k_2, k_3 > 0$, being the design constants. If each robot perfectly tracks its desired velocities (56), the group of robots will reach the desired formation. Since the perfect velocity tracking assumption is undesirable [1],[19], there will be an error in tracking velocities defined for each robot as $e_{iv}^F = [e_{iv1}^F \ e_{iv2}^F]^T = \bar{v}_i - \bar{v}_{id}^F$, which reveals, $\bar{v}_i = \bar{v}_{id}^F + e_{iv}^F$.

Remark: The desired velocities (56) will make the formation errors of robots less than a pre-defined lower threshold, $\left(l_1 e_1^2 + l_2 e_2^2 + l_3 e_3^2\right) \leq \underline{\eta}$. Once the norm of the formation errors becomes less than the threshold, the regulation or tracking controller can be applied similar to our work in [16].

The consensus error system (55) becomes

$$\begin{bmatrix} \dot{e}_{i1} \\ \dot{e}_{i2} \\ \dot{e}_{i3} \end{bmatrix} = \begin{bmatrix} e_{i2}\omega_i + \begin{pmatrix} e_{iv1}^F - k_1 e_{i1} \\ + v_j \cos\left(\theta_i - \theta_j\right) \end{pmatrix} - v_j \cos\left(\theta_i - \theta_j\right) \\ v_j \sin\left(\theta_i - \theta_j\right) - e_{i1}\omega_i \\ \left(e_{iv2}^F + \varnothing_j - k_2 v_j e_{i2} - k_3 \sin\left(\theta_i - \theta_j\right)\right) - \varnothing_j \end{bmatrix}. \tag{84}$$

Simplifying the expression in (84) leads to the consensus based formation error dynamics similar to [1] as

$$\begin{bmatrix} \dot{e}_{i1} \\ \dot{e}_{i2} \\ \dot{e}_{i3} \end{bmatrix} = \begin{bmatrix} e_{i2}\omega_i - k_1 e_{i1} - e_{iv1}^F \\ -e_{i1}\omega_i + v_j \sin(\theta_i - \theta_j) \\ -k_2 v_j e_{i2} - k_3 \sin(\theta_i - \theta_j) - e_{iv2}^F \end{bmatrix} \tag{85}$$

Using (44), the velocity tracking error dynamics of the individual robot are obtained as

$$\bar{M}_i \dot{e}_{iv}^F = -\bar{M}_i \dot{\bar{v}}_{id}^F - \bar{V}_{mi}(q_i, \dot{q}_i)\left(\bar{v}_{id}^F + e_{iv}^F\right) - \bar{F}_i(\bar{v}_i) - \bar{\tau}_{di} + \bar{\tau}_i . \tag{86}$$

Since the nonlinear dynamics of each robot are uncertain, defining $f\left(\bar{z}_i\right) = \bar{M}_i \dot{\bar{v}}_{id}^F + \bar{V}_{mi}(q_i, \dot{q}_i)\bar{v}_{id}^F + \bar{F}_i(\bar{v}_i)$, yields

$$\bar{M}_i \dot{e}_{iv}^F = -\bar{V}_{mi}(q_i, \dot{q}_i)e_{iv}^F - f\left(\bar{z}_i\right) - \bar{\tau}_{di} + \bar{\tau}_i \tag{87}$$

where $\bar{z}_i = \left[1, \bar{v}_i^T, \bar{v}_{id}^{FT}, \dot{\bar{v}}_{id}^{FT}, \theta_i, \theta_j, e_{iF}^T, \dot{e}_{iF}^T\right]$ is the set of inputs required to construct the

uncertain function $f(\bar{z}_i)$ which brings the dynamics of the neighbor robots through the

velocity tracking error. The uncertain dynamics in [1] is a function of the dynamics of the

leader, whereas, in the consensus based scenario, it can be from any neighbor or neighbors

of ith robot and hence the formation. Note that $\bar{z}_i$ is a function of individual robot and

formation dynamics, therefore all the position and velocity information need to be

communicated among the robots.

The uncertain nonlinear dynamics (87) are represented as

$$f(\bar{z}_i) = \Theta_i^T \psi_i\left(H^T \bar{z}_i\right) + \chi_i \tag{88}$$

where $\Theta_i \in \mathfrak{R}^{2 \times h_i}$ is the desired NN weights with h_i being the number of hidden layer

neurons, $\psi_i\left(H^T \bar{z}_i\right)$ is the basis function with $H^T \in \mathfrak{R}^{h_i \times ni}$ is the mapping between the inputs

and the hidden-layer neurons , ni is the number of inputs to the NN, χ_i is the bounded NN

reconstruction error satisfying $\|\chi_i\| \le \chi_M$, with χ_M being a positive constant. The unknown

NN weights can be estimated as $\hat{\Theta}_i$ and estimated uncertain dynamics can be given by

$$\hat{f}(z_i) = \hat{\Theta}_i^T \psi_i(z_i) . \tag{89}$$

Now, the NN weight estimation error is defined as $\tilde{\Theta}_i = \Theta_i - \hat{\Theta}_i$ and the estimation error dynamics can be obtained as $\dot{\tilde{\Theta}}_i = -\dot{\hat{\Theta}}_i$. The control torque, using (87), is obtained as

$$\overline{\tau}_i = -K_v e_{iv}^F + \hat{f}(z_i) - \gamma(e_{i1}, e_{i2}, e_{i3}) \tag{90}$$

where γ is the stabilizing term required due to the formation error system. Substituting (90) into (87) reveals the closed-loop velocity tracking error dynamics with

$$\tilde{f}(\breve{z}_i) = \tilde{\Theta}_i \psi_i(z_i) + \chi_i, \text{ as } \overline{M}_i \dot{e}_{iv}^F = -K_v e_{iv}^F + \overline{\tau}_{di} - \gamma(e_{iF}) + \tilde{f}(\breve{z}_i) - \overline{V}_{mi}(q_i, \dot{q}_i) e_{iv}^F \tag{91}$$

Next, the following standard assumption is needed.

Assumption 4: The target NN weights are bounded by positive values, for all the robots in the network $i = 1, 2, \ldots, N,$ such that $\|\Theta_i\| \leq \Theta_M$ with Θ_M being a positive bounded constant.

Remark 4: Calculation of the term, $\hat{f}(\breve{z}_i)$, requires computation of $\dot{v}_{id}^F$, which is a function of the dynamics of robot j, and $\dot{\breve{v}}_j$. Therefore, the proposed control law not only compensates the dynamics of the ith robot, but also the dynamics of the formation. To calculate $\dot{\breve{v}}_{id}^F$, it is assumed the neighbor robots communicate their state information to the ith robot, which includes x_j, y_j, θ_j and the linear, angular velocities, through a lossless wireless network.

Next, the formation stability results for the group of mobile robots in the presence of uncertain robot dynamics with continuous or periodically driven feedback are presented.

Theorem 1: Given the consensus error dynamics (55) for the ith robot in the network, let the consensus-based formation controller (56) be applied to the ith robot under minimal communication scenario. Consider the Assumptions 1,2, and 3 holds. Let the control torque be defined by (90) with

$$\gamma(e_{i1}, e_{i2}, e_{i3}) = \begin{bmatrix} -e_{i1} \\ -\frac{1}{k_2}\sin e_{i3} \end{bmatrix}. \tag{92}$$

Further, tune the unknown NN weights by using

$$\dot{\hat{\Theta}}_i = \Lambda_1 \psi_i(z_i) e_{iv}^{F^T} - \Lambda_1 \kappa_i \hat{\Theta}_i \tag{93}$$

where $\Lambda_1 > 0, \kappa_i > 0$ are small positive design parameters. Then, the velocity tracking error (91) and consensus error (57) and the NN weight estimation errors remain bounded. In addition, a) i^{th} robot tracks its desired velocity and b) the network of mobile robots reach a desired formation under the minimum communication topology, when the gains are chosen such that $k_1 > 0, \ \dfrac{k_3}{k_2} > 0, \ K_v > 0, \kappa_i > 0$.

Proof: See Appendix.

In the next section, the event-based sampling instants will be determined and then the event sampled controller design for the formation control of mobile robots will be introduced unlike the periodic sampling given in this section.

4. EVENT-TRIGGERED CONTROLLER DESIGN

In this section, the NN controller design with event-sampled feedback, for the network of nonholonomic mobile robots will be presented and the aperiodic NN weight adaptation law will be derived from the Lyapunov stability analysis. The event-sampling mechanism is designed using stability analysis such that the event-sampling error (75) satisfies a state-dependent threshold for every inter-event period for each robot, which is of the form

$$\left\| \overline{\mathrm{E}}_{iET} \right\| \le \sigma_i \mu_{ik} \left\| \breve{\mathrm{E}}_i \right\|, \qquad t_k \le t < t_{k+1}, \ k = 1, 2, 3.. \tag{94}$$

with $0 < \sigma_i < 1$, and μ_{ik} is a positive design parameter and $E_{iET}, \breve{E}_i$ are functions of event-sampling error and the formation, and velocity tracking errors respectively. By using the event-sampled feedback, the objective is to reduce the computations from periodic parameter adaptation without compromising the stability while ensuring acceptable tracking performance.

Remark 5: Once an event is triggered for the ith robot, it broadcasts its position and velocity information to its neighbors and also updates its own control torque with its current sensor measurement, resetting the measurement error to zero in the sensor measurement.

Remark 6: The event-sampling mechanism is designed at each robot with the event-sampling error satisfying (94). This makes the event-based broadcast instants asynchronous, which ensures that the communication link shared by the network of robots is not accessed by all the robots at the same time, reducing the conjestion in the network.

Since the formation and the velocity tracking errors of each robot are functions of both its own as well as its neighbor robots states, the event triggering errors will have two

parts due to: a) its own state vector; and that of b) its neighbors. Realize that the first part of the event trigger error is continuously available for each robot whereas the second part of the event triggering error is not available except at event sampled instants. Therefore, a novel decentralized sampling scheme is developed to determine the event sampling instants of each robot by using last sampled information of neighborhood robots. The following definitions are needed.

Definition 1: Define first, $\forall i = 1, 2, \ldots, N$, $t_k \leq t < t_{k+1}$

$$\breve{x}_i(t) = x_i\left(t_k^i\right),\ \breve{y}_i(t) = y_i\left(t_k^i\right),\ \breve{\theta}_i(t) = \theta_i\left(t_k^i\right),\breve{v}_i(t) = \breve{v}_i\left(t_k^i\right),\breve{\omega}_i(t) = \omega_i\left(t_k^i\right),$$

$$\varepsilon_{xi} = \breve{x}_i(t) - x_i(t),\ \varepsilon_{yi} = \breve{y}_i(t) - y_i(t),\varepsilon_{\theta i} = \breve{\theta}_i(t) - \theta_i(t),$$

$$\varepsilon_{vi} = \breve{v}_i(t) - v_i(t),\varepsilon_{\omega i} = \breve{\omega}_i(t) - \omega_i(t)$$

$$\Delta\breve{x}_i(t) = \Delta x_i\left(t_k^i\right),\ \Delta\breve{y}_i(t) = \Delta y_i\left(t_k^i\right),\ \Delta\breve{\theta}_i(t) = \Delta\theta_i\left(t_k^i\right),$$

$$\breve{e}_{i1}(t) = e_{i1}\left(t_k^i\right),\ \breve{e}_{i2}(t) = e_{i2}\left(t_k^i\right),\ \breve{e}_{i3}(t) = e_{i3}\left(t_k^i\right)\ . \tag{95}$$

The superscript in the sampling instants will be dropped from hereon for notational simplicity. By using (95), the event triggered consensus errors are defined as $\breve{\delta}_{xi} = \Delta\breve{x}_i - \Delta\breve{x}_j$, $\breve{\delta}_{yi} = \Delta\breve{y}_i - \Delta\breve{y}_j$ and $\breve{\delta}_{\theta i} = \Delta\breve{\theta}_i - \Delta\breve{\theta}_j$, along x and y directions and the bearing angle, respectively. The event triggered formation errors can be represented in terms of the continuous-time formation and the measurement errors as

$$\begin{bmatrix} \breve{\delta}_{xi} \\ \breve{\delta}_{yi} \\ \breve{\delta}_{\theta i} \end{bmatrix} = \begin{bmatrix} \Delta\breve{x}_i - \Delta\breve{x}_j \\ \Delta\breve{y}_i - \Delta\breve{y}_j \\ \Delta\breve{\theta}_i - \Delta\breve{\theta}_j \end{bmatrix} = \begin{bmatrix} \breve{x}_i - x_i^r - \left(\breve{x}_j - x_j^r\right) \\ \breve{y}_i - y_i^r - \left(\breve{y}_j - y_j^r\right) \\ \breve{\theta}_i - \theta_i^r - \left(\breve{\theta}_j - \theta_j^r\right) \end{bmatrix}$$

$$= \begin{bmatrix} x_i + \varepsilon_{xi} - x_i^r - \left(x_j + \varepsilon_{xj} - x_j^r \right) \\ y_i + \varepsilon_{yi} - y_i^r - \left(y_j + \varepsilon_{yj} - y_j^r \right) \\ \theta_i + \varepsilon_{\theta i} - \theta_i^r - \left(\theta_j + \varepsilon_{\theta j} - \theta_j^r \right) \end{bmatrix} = \begin{bmatrix} \delta_{xi} \\ \delta_{yi} \\ \delta_{\theta i} \end{bmatrix} + \begin{bmatrix} \varepsilon_{xi} \\ \varepsilon_{yi} \\ \varepsilon_{\theta i} \end{bmatrix} - \begin{bmatrix} \varepsilon_{xj} \\ \varepsilon_{yj} \\ \varepsilon_{\theta j} \end{bmatrix}. \tag{96}$$

Define the event triggering errors by using (96) as

$$\varepsilon_i = \begin{bmatrix} \varepsilon_{i1} \\ \varepsilon_{i2} \\ \varepsilon_{i3} \end{bmatrix} = \begin{bmatrix} \breve{e}_{i1} \\ \breve{e}_{i2} \\ \breve{e}_{i3} \end{bmatrix} - \begin{bmatrix} e_{i1} \\ e_{i2} \\ e_{i3} \end{bmatrix} = \begin{bmatrix} \breve{e}_{i1} \\ \breve{e}_{i2} \\ \breve{e}_{i3} \end{bmatrix} - \begin{bmatrix} \cos\theta_i & \sin\theta_i & 0 \\ -\sin\theta_i & \cos\theta_i & 0 \\ 0 & 0 & 1 \end{bmatrix} \left(\begin{bmatrix} \breve{\delta}_{xi} \\ \breve{\delta}_{yi} \\ \breve{\delta}_{\theta i} \end{bmatrix} - \left(\begin{bmatrix} \varepsilon_{xi} \\ \varepsilon_{yi} \\ \varepsilon_{\theta i} \end{bmatrix} - \begin{bmatrix} \varepsilon_{xj} \\ \varepsilon_{yj} \\ \varepsilon_{\theta j} \end{bmatrix} \right) \right). \tag{97}$$

Also define

$$\varepsilon_i^i = \begin{bmatrix} \varepsilon_{i1}^i \\ \varepsilon_{i2}^i \\ \varepsilon_{i3}^i \end{bmatrix} = \begin{bmatrix} \breve{e}_{i1} \\ \breve{e}_{i2} \\ \breve{e}_{i3} \end{bmatrix} - \begin{bmatrix} \cos\theta_i & \sin\theta_i & 0 \\ -\sin\theta_i & \cos\theta_i & 0 \\ 0 & 0 & 1 \end{bmatrix} \left(\begin{bmatrix} \breve{\delta}_{xi} \\ \breve{\delta}_{yi} \\ \breve{\delta}_{\theta i} \end{bmatrix} - \begin{bmatrix} \varepsilon_{xi} \\ \varepsilon_{yi} \\ \varepsilon_{\theta i} \end{bmatrix} \right),$$

$$\varepsilon_i^j = \begin{bmatrix} \varepsilon_{i1}^j \\ \varepsilon_{i2}^j \\ \varepsilon_{i3}^j \end{bmatrix} = \begin{bmatrix} \cos\theta_i & \sin\theta_i & 0 \\ -\sin\theta_i & \cos\theta_i & 0 \\ 0 & 0 & 1 \end{bmatrix} \begin{bmatrix} \varepsilon_{xj} \\ \varepsilon_{yj} \\ \varepsilon_{\theta j} \end{bmatrix}, \text{ then the event trigger errors (97) can be written as}$$

$$\varepsilon_i = \varepsilon_i^i + \varepsilon_i^j. \tag{98}$$

Remark 7: The event trigger error given by (98) has two parts as mentioned before with the second part ε_i^j is not available continuously because the state information of the jth robot is not updated at the ith robot. A novel event-sampling condition is derived in Theorem 3, using the Lyapunov stability theory, in such a way that only locally available information from the ith robot along with the past position and velocity information for the jth robot are utilized.

Now, to define the formation error dynamics with event-sampled measurement error, consider (56), during the kth inter-event period, the desired virtual control equations

are obtained as

$$\breve{\bar{v}}_{id}^F = \begin{bmatrix} \breve{v}_{id}^F \\ \breve{\omega}_{id}^F \end{bmatrix} = \begin{bmatrix} -k_1\breve{e}_{i1} + \breve{v}_j\cos\breve{e}_{i3} \\ \breve{\omega}_j - k_2\breve{v}_j\breve{e}_{i2} - k_3\sin\breve{e}_{i3} \end{bmatrix}, \qquad t_k \le t < t_{k+1}, \tag{99}$$

where $\breve{\omega}_j = \omega_j(t_k), \breve{v}_j = v_j(t_k)$ are event-sampled angular and linear velocities of the jth robot, respectively. After defining the event-sampled signals, (99) can be rewritten with the measurement errors as

$$\breve{\bar{v}}_{id}^F = \begin{bmatrix} \breve{v}_{id}^F \\ \breve{\omega}_{id}^F \end{bmatrix} = \begin{bmatrix} -k_1e_{i1} + v_j\cos e_{i3} + v_{i\varepsilon} \\ \omega_j - k_2v_j\bar{e}_{i1} - k_3\sin e_{i3} + \omega_{i\varepsilon} \end{bmatrix}, t_k \le t < t_{k+1}, \tag{100}$$

where $v_{i\varepsilon}, \omega_{i\varepsilon}$ are given by $v_{i\varepsilon} = -v_j[\cos e_{i3} - \cos\breve{e}_{i3}] + \varepsilon_{vj}\cos\breve{e}_{i3} - k_1\varepsilon_{i1}$ and

$$\omega_{i\varepsilon} = k_3[\sin e_{i2} - \sin\breve{e}_{i3}] + \varepsilon_{\omega j} - k_2v_j\varepsilon_{i2} - k_2\varepsilon_{vj}e_{i2} - k_2\varepsilon_{vj}\varepsilon_{i2}.$$

To get the closed-loop formation error dynamics in the presence of measurement error, use (100) in (55), which reveals the event-sampled formation error dynamics as

$$\begin{bmatrix} \dot{e}_{i1} \\ \dot{e}_{i2} \\ \dot{e}_{i3} \end{bmatrix} = \begin{bmatrix} e_{i2}\omega_i - k_1e_{i1} + v_{i\varepsilon} - e_{iv1}^F \\ -e_{i1}\omega_i + v_j\sin e_{i3} \\ -k_2v_je_{i2} - k_3\sin e_{i3} + \omega_{i\varepsilon} - e_{iv2}^F \end{bmatrix} \tag{101}$$

The closed loop formation error dynamics in the presence of event trigger errors are obtained in (101). Similarly, the velocity tracking errors in the event sampled framework is derived next.

The unknown NN weights can be estimated as $\hat{\Theta}_i$ and estimate of the unknown dynamics with event sampled feedback can be obtained as

$$\hat{f}(z_i) = \hat{\Theta}_i^T\psi_i(\breve{z}_i), \quad t_k \le t < t_{k+1}. \tag{102}$$

with $\breve{z}_i = z_i + e_{iz}$, being the event-sampled signals at the ith mobile robot. The unknown NN

weight estimation error is defined as $\tilde{\Theta}_i = \Theta_i - \hat{\Theta}_i$ and the estimation error dynamics can

be given as $\dot{\tilde{\Theta}}_i = -\dot{\hat{\Theta}}_i$. The event-sampled control torque, using (102), is obtained as

$$\bar{\tau}_i = -K_v \breve{e}_{iv}^F + \hat{f}\left(\breve{z}_i\right) - \breve{\gamma}\left(\breve{e}_{i1}, \breve{e}_{i2}, \breve{e}_{i3}\right), \qquad t_k \leq t < t_{k+1}, \tag{103}$$

with

$$\breve{e}_{iv}^F = e_{iv}^F + e_{iET} \tag{104}$$

where the event triggered velocity tracking error $\breve{e}_{iv}^F(t) = e_{iv}^F(t_k)$ is defined similar to the

event triggered formation errors and $\breve{\gamma}$ is the stabilizing term with measurement error due

to event-sampled mechanism.

Note the velocity tracking error, e_{iv}^F, is not available continuously as it is a function

of the states of the neighbor robots; the event trigger error, e_{iET} in (104) is also not

available continuously at the ith robot in the network. Therefore, consider

$$e_{iET} = \breve{e}_{iv}^F - e_{iv}^F = \bar{v}_i\left(t_k\right) - \bar{v}_i\left(t\right) - \bar{v}_i^d\left(t_k\right) + \bar{v}_i^d\left(t\right) = [\varepsilon_{vi} \quad \varepsilon_{\omega i}]^T - [v_{i\varepsilon} \quad \omega_{i\varepsilon}]^T$$

$$= \begin{bmatrix} \varepsilon_{vi} - \breve{v}_j \cos \breve{e}_{i3} + v_j \cos e_{i3} + k_1 \varepsilon_{i1} \\ \varepsilon_{\omega i} - k_3[\sin e_{i2} - \sin \breve{e}_{i3}] - \varepsilon_{\omega j} + k_2 \breve{v}_j \varepsilon_{i2} + k_2 \varepsilon_{vj} e_{i2} \end{bmatrix}.$$ Using this, we define the components

of the measurement error due to the ith and the jth robots as

$$e_{iET}^i = \begin{bmatrix} \varepsilon_{vi} - \breve{v}_j \cos \breve{e}_{i3} + k_1 \varepsilon_{i1} \\ \varepsilon_{\omega i} - k_3[\sin e_{i2} - \sin \breve{e}_{i3}] + k_2 \breve{v}_j \varepsilon_{i2} \end{bmatrix}, e_{iET}^j = [v_j \cos e_{i3} \quad -\varepsilon_{\omega j} + k_2 \varepsilon_{vj} e_{i2}]^T. \tag{105}$$

Substituting (103) into (87) reveals the closed-loop velocity tracking error dynamics

$$\bar{M}_i \dot{e}_{iv}^F = -K_v e_{iv}^F + \bar{\tau}_{di} - \breve{\gamma}\left(\breve{e}_{i1}, \breve{e}_{i2}, \breve{e}_{i3}\right) + \tilde{f}\left(\breve{z}_i\right) - K_v e_{iET}$$

$$+[f\left(z_i\right) - f\left(\breve{z}_i\right)] - \bar{V}_{mi}(q_i, \dot{q}_i)e_{iv}^F, \qquad t_k \leq t < t_{k+1} \tag{106}$$

where $\tilde{f}\left(\breve{z}_i\right)=\tilde{\Theta}_i\psi_i\left(\breve{z}_i\right)+\chi_i$. With the formation error dynamics (101) and the velocity

tracking error dynamics (60) driven by the event-sampling errors, the stability results for

the network of mobile robots are presented. Next the definition for UUB is introduced.

Definition 2 [1]*:* An equilibrium point x_e is said to be uniformly ultimately bounded

(UUB) if there exists a compact set $S\subset\mathfrak{R}^n$ so that for all $x_0\in S$ there exists a bound B

and a time $T\left(B,x_0\right)$ such that $\left\|x(t)-x_e\right\|\le B$ for all $t\ge t_0+T$.

The following theorems provide the stability analysis for the control law that does

not require the perfect velocity tracking assumption. As noted before, the controller is

updated only at the event-sampling instants.

Theorem *2* (Input-to-state stability)**:** Given the consensus error dynamics (101)

and the velocity tracking error dynamics (60) for the ith robot in the network, let the

consensus-based formation controller (103) be applied to the ith robot. Define the control

torque by (103) with

$$\breve{\gamma}\left(\breve{e}_{i1},\breve{e}_{i2},\breve{e}_{i3}\right)=[-\breve{e}_{i1} \quad -\frac{1}{k_2}\sin\breve{e}_{i3}]^T. \qquad (107)$$

further, tune the unknown NN weights using the adaptation rule (93) with the measurement

error satisfying the inequality $\left\|e_{iET}\right\|\le\bar{B}_{iETM}$, with $\bar{B}_{iETM}$ being a positive constant. Consider

Assumptions 1,2 and 3 hold. The velocity tracking (60) and consensus errors (57) are UUB

and a) the ith robot tracks its desired velocity; b) the networked mobile robots reach any

desired formation under minimum communication scenario, in the presence of bounded

measurement error when the gains are chosen such that

$$k_1 > k_2^2/2 + 3/2, \ k_3/k_2 > 0.5, \ K_v > 3/2, k_2 > 0$$

and c) the closed-loop system is input-to-state stable (ISS), with the input being a function of the measurement error e_{iET}.

Proof: See Appendix.

Remark 8: If the nonlinear dynamics of each robot satisfy Lipschitz continuity, then by using *Theorem* 2, it can be shown that the event-sampling mechanism does not exhibit zeno-behavior [14].

Remark 9: The result in *Theorem* 2 shows that the closed-loop system in the presence of a bounded measurement error is locally ISS. That is, the continuous closed-loop system admits an ISS Lyapunov function. However, for the event-sampled implementation of the controller, the boundedness of the event-sampled measurement error is required to be proven. Next, the closed-loop signals are indeed shown to be bounded using which the measurement error and the existence of $0 < \bar{\mu}_{ik} < 1$, satisfying the event trigger condition (94) will be demonstrated.

In the following *theorem*, the event-sampling mechanism is designed and stability of the robot formation is analyzed by using the Lyapunov stability theory in the presence of disturbance torque input and NN reconstruction error.

Theorem 3: Given the consensus error dynamics (60) for the ith robot in the network with the disturbance torque and the NN approximation error $\bar{\tau}_d \neq 0, \chi_i \neq 0$, respectively. Consider the Assumptions 1,2 and 3 hold. Let the consensus-based formation control input, (103) with (107), be applied to the ith mobile robot at the event-based sampling instants and the event-sampling condition be defined by (94). Further, consider the unknown NN

weights are tuned at the event sampling instants using the aperiodic tuning rule (93). Then the velocity tracking error (60) and consensus error systems (57) are UUB and a) the ith robot tracks its desired velocity; and b) the networked mobile robots reach any desired formation under minimum communication, when the gains are selected such that

$$k_1 > k_2^2/2 + 3/2, \; k_3/k_2 > 3/2, \; K_v > 5/2, k_2 > 0.$$

Proof: See Appendix.

Remark 10: The event-sampling condition satisfying (94) is designed in *Theorem* 3 such that E_i is a function of formation and velocity tracking errors calculated at the ith robot and $\bar{E}_{iET} = [E_{iET}^i \quad E_{jET}^i]^T$ is the event-sampling error available continuously at the ith robot. The terms $\underline{E}_{jET}^i = [\varepsilon_{xyi} \; \varepsilon_{xyi} \; \varepsilon_{xyi}^2 \; \varepsilon_{xyi}^2 \; \varepsilon_{vi}^4 \; \varepsilon_{\omega i}^2 \; \varepsilon_{vi}^2]^T$ and $E_{iET}^i = [\|e_{iET}^i\|^2 \; \|\varepsilon_{i1}^i\|^2$ $\|\varepsilon_{i2}^i\|^2 \; \|\varepsilon_{i1}^i\|^4 \; \|\varepsilon_{i2}^i\|^4]^T$ are function of the measurement errors defined in (97) and (105), with $\varepsilon_{xyi} = 2(\|\varepsilon_{xi}\|^2 + \|\varepsilon_{yi}\|^2)$, $\varepsilon_{xyi}^2 = 8(\|\varepsilon_{xi}\|^4 + \|\varepsilon_{yi}\|^4)$. The design terms $\mu_{ik} = 1\backslash \bar{K}_{iET}^i$, is a function of the control gains k_1, k_2, k_3, K_v.

Remark 11: It can be observed from *Theorem* 3 that the event-sampling condition is dependent on the locally available position and velocity information. This ensures that the communication among the mobile robots in the network is required only when there are events. This considerably reduces that communication cost in contrast to the consensus based controllers in [5]-[13].

Remark 12: From the results in *Theorem*s 2 and 3, it can be seen that the measurement error is bounded for all the inter-event period due to the event-sampling condition (94) with the value of μ_{ik} obtained from (94). By using the states of the closed-

loop system and defining $Z = [e_i \; e_{vi}^F \; \tilde{\Theta}]^T$, the ISS characterization can be obtained. Thus the existence of a positive minimum inter event-time can be established [14] .

Remark 13: The event-sampling condition obtained from (94) requires the information regarding the last updated information of the jth robot to determine the event-based sampling instants. Also, for the event-sampling condition, the formation errors for the ith robot can be calculated with the previously obtained information from the jth robot.

Remark 14: From the results in *Theorem* 2, it can be seen that the measurement error is bounded for all the inter-event period due to the event-sampling condition (94) with the value of μ_{ik} obtained from [15]. By choosing the gains as required in the Lyapunov conditions in [15], we obtain $0 < \mu_{ik} < 1, \; \forall k.$

Remark 15: Once the velocity tracking and the formation errors converge to a small value, a dead-zone operator can be used to prevent further events [15]. This way the feedback information is not utilized frequently and computations, communication can be reduced further.

Remark 16: It can also be observed that the event-sampling mechanism is not a function of the NN weights as in [15]. This eliminates the need for a mirror estimator as in the adaptive event-sampling mechanism designed in [15].

5. RESULTS AND DISCUSSIONS

To illustrate the effectiveness of the proposed event-based NN controller, a group of four non-holonomic mobile robots is considered. The robots are initiated from an arbitrary position and move to a desired shape of a square. Using the proposed approach, the robots establish the square shape while ensuring the velocity tracking error converges to a small value. The main simulation results are given in the first part by using the minimum communication information depicted in Figure 2.1, wherein each robot will have information from one other robot. Even with minimum communication, acceptable results are observed. In the second part of the simulation section, each robot is assumed to have communication with all the other robots in the network. The results in the second part is compared with the minimum communication case and discussed in the second part.

5.1 MINIMUM COMMUNICATION CASE

The desired and initial positions, initial bearing angles and the initial velocities of the non-holonomic mobile robots are given by

$$x_1^r = 25, x_2^r = 25, x_3^r = -25, x_4^r = -25, y_1^r = 25, y_2^r = -25,$$

$$x_1(t_0) = 192, x_2(t_0) = 132, x_3(t_0) = 96, x_4(t_0) = 120,$$

$$y_3^r = -25, y_4^r = 25, y_1(t_0) = -108, y_2(t_0) = -156,$$

$$y_3(t_0) = -168, y_4(t_0) = -120, \theta_1(t_0) = 0, \theta_2(t_0) = 0,$$

$$\theta_3(t_0) = 0, \theta_4(t_0) = 0, \theta_1^d = \pi, \theta_2^d = \pi, \theta_3^d = \pi, \theta_4^d = \pi.$$

The controller gains are selected as $K_v = 30$ $k_1 = 0.065, k_2 = 0.065, k_3 = 0.08$ and the steady state desired linear velocity is selected as $v_i^r = 0.9$ m/s . The parameters for the

robot dynamics are selected as $m = 5$ kg, $I = 3\text{kg}^2$, $R = 0.15\,\text{m}, \text{r}=0.08\,\text{m}, \text{ d}=0.4\,\text{m}$ for each robot. Figure 5.1 depicts the motion of 4 independent non-holonomic mobile robots.
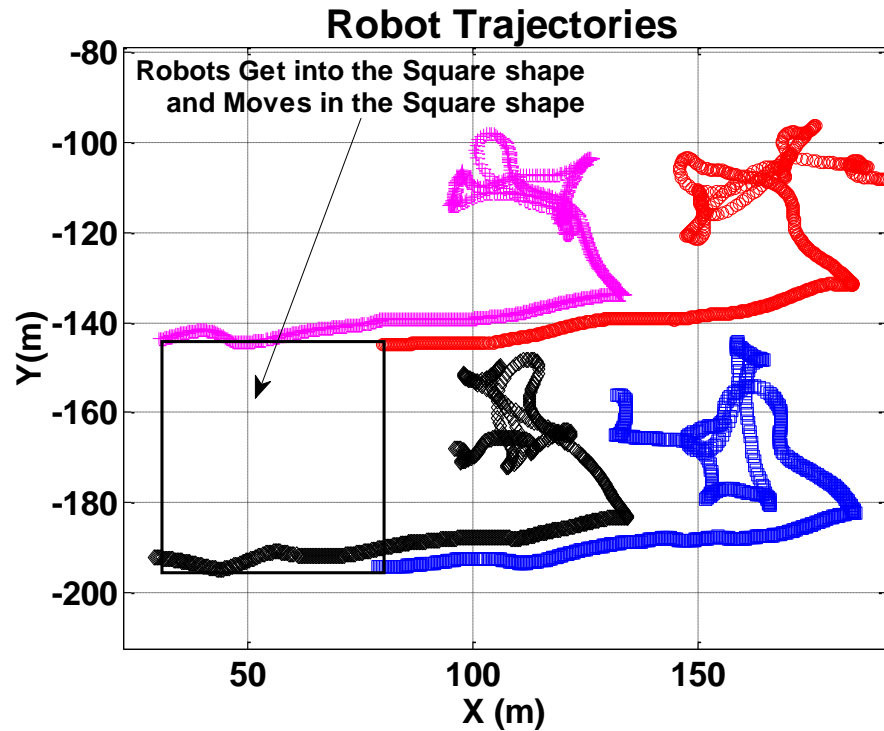
Figure 5.1 Mobile robots moving to their desired formation.

They are initiated in a non-square shape which can be seen In Figure 5.1. Given their desired locations, they form a square shape by minimizing consensus error along x, y, θ. The nonlinear robot dynamics are considered uncertain as described in the problem formulation.

The initial movements of the robots are oscillatory as the consensus error varies over time. Since the robots have nonholonomic constraints, due to the consensus error resulting from minimal communication, oscillations are observed but eventually this gets

settled. The adaptation parameters for the NN weights estimation is selected as $F_i = 1, \kappa_i = 0.5$. Once the unknown weights are tuned, the robots reach consensus along x, y directions.

The robots reach consensus at about 500th second as observed in Figure 5.2 and Figure 5.3. The difference between the desired and the actual linear and angular velocities are plotted in Figure 5.3. The NN weight estimates of each robot converge into a steady state bound as shown in Figure 5.4. Since the robots may move in different terrain, the friction terms can change over time, and the total mass of each robot may change as well as other dynamics parameters. Therefore, learning the robot dynamics online is valuable and is achieved.
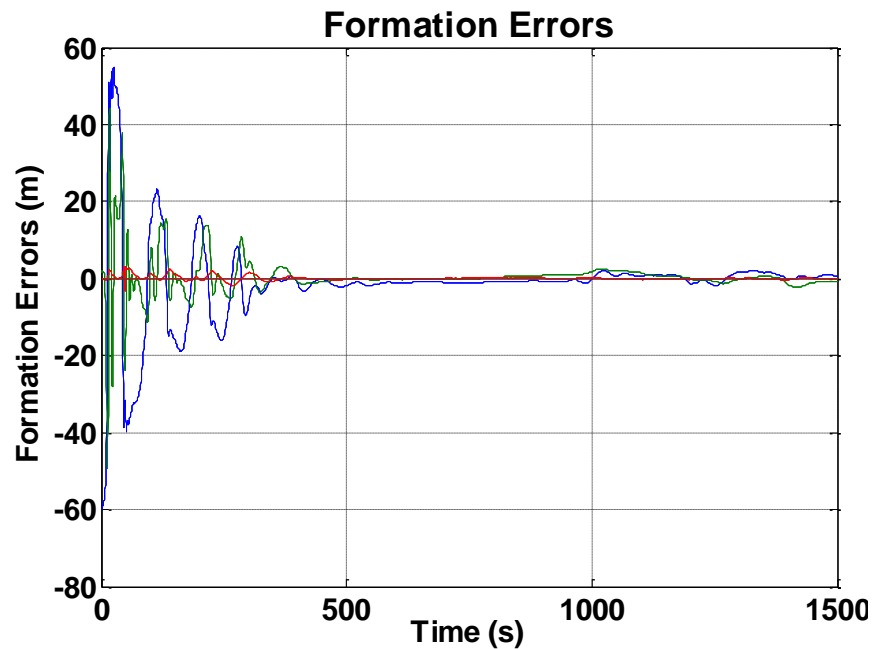
Figure 5.2 Formation errors.
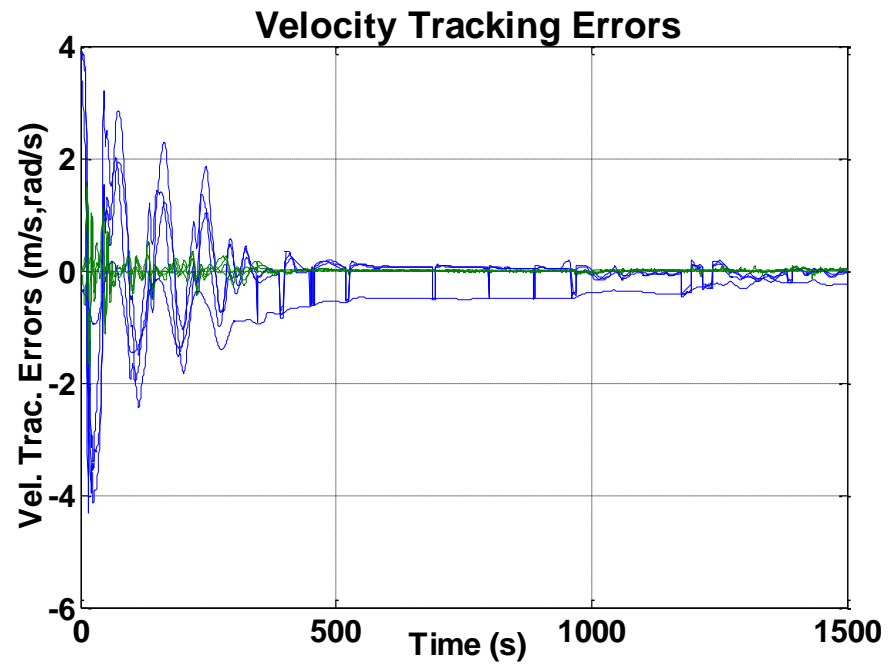
Figure 5.3 Velocity tracking errors.
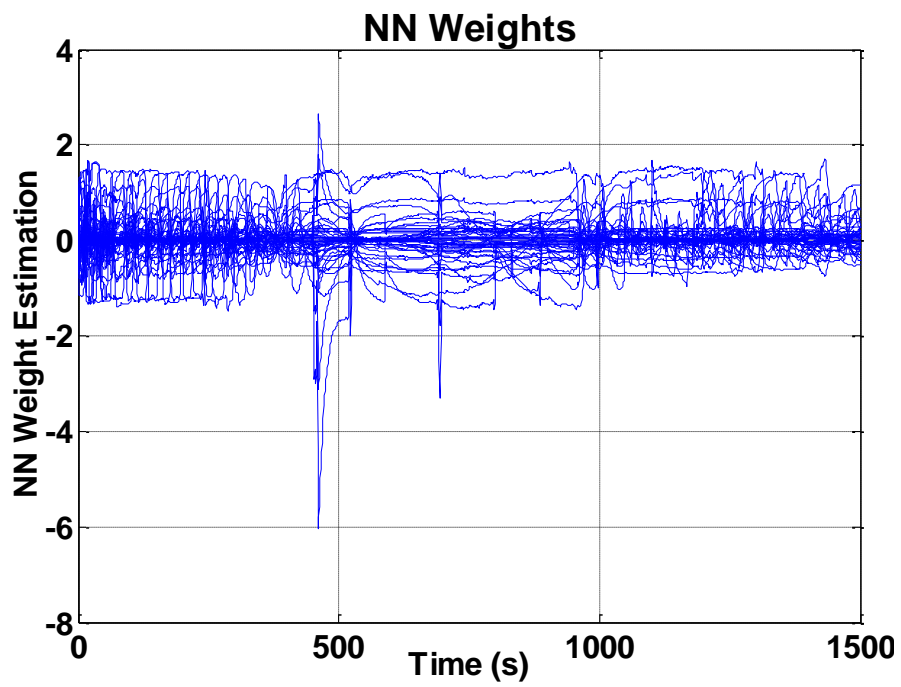
Figure 5.4 NN weights (continuous).
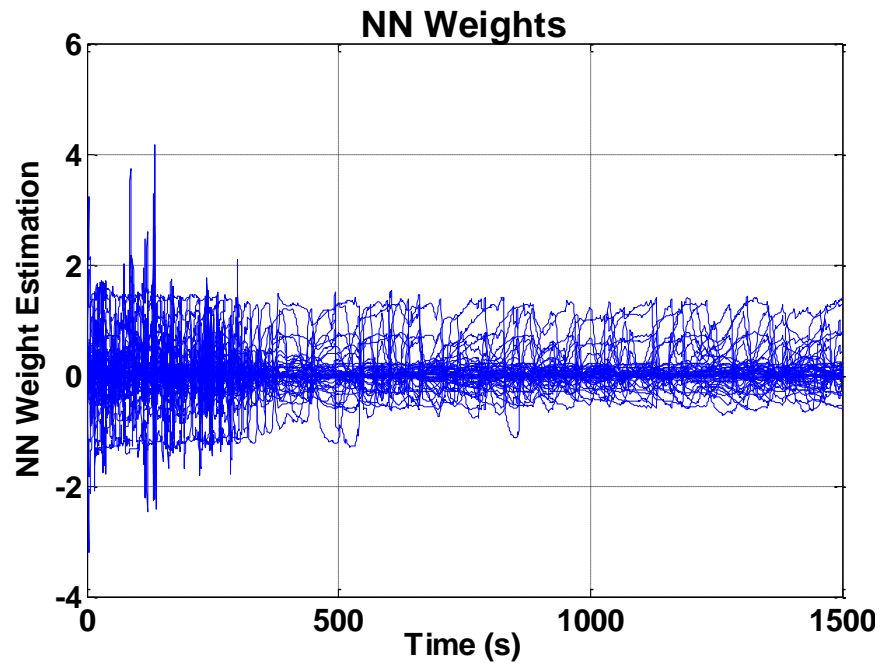
Figure 5.5 NN weights (event triggered).
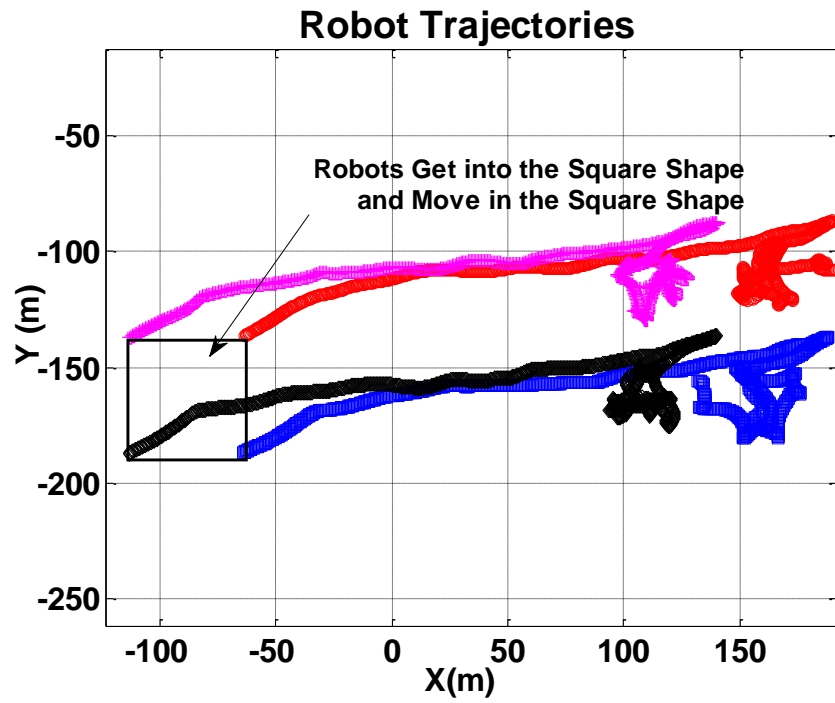
Figure 5.6 Robot Trajectories with event trigger controllers.
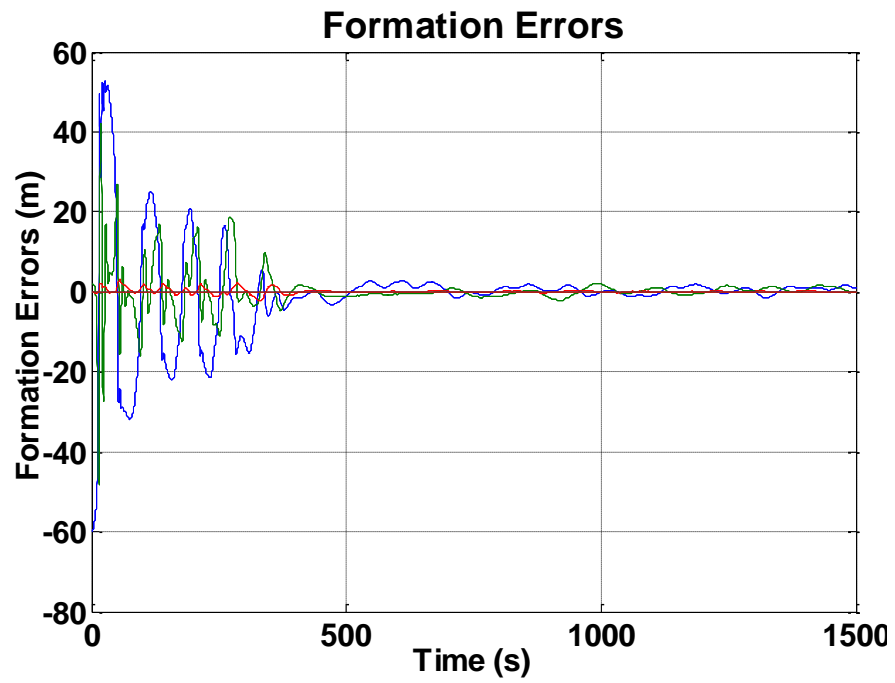
Figure 5.7 Formation errors.
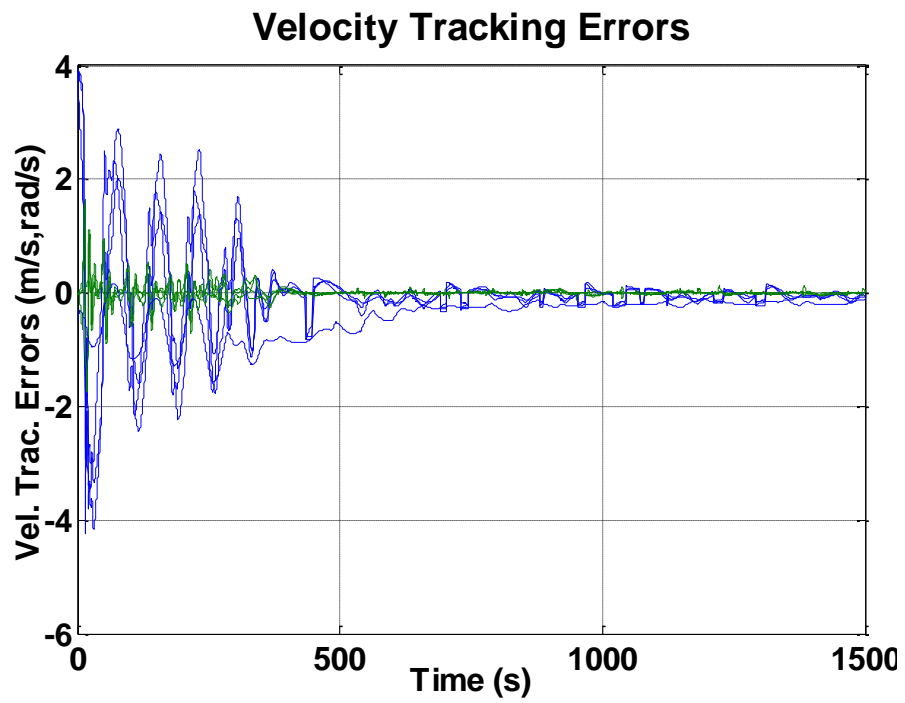
Figure 5.8 Velocity tracking errors.

The event-sampling mechanism was designed with k_1, k_2, k_3, k_v as selected in the controller with $\sigma = 0.99$. To compare the controller with continuous feedback, all the controller gains and initial values of the parameters and the initial conditions of the robots were unchanged. With the proposed event-sampled feedback, the mobile robots were able to reach the desired consensus as seen in Figure 5.6.

The formation errors remain bounded in Figure 5.7 and the velocity tracking error remains bounded as in Figure 5.8. However, due to the aperiodic feedback, these bounds are slightly large when compared to the continuous counterpart.
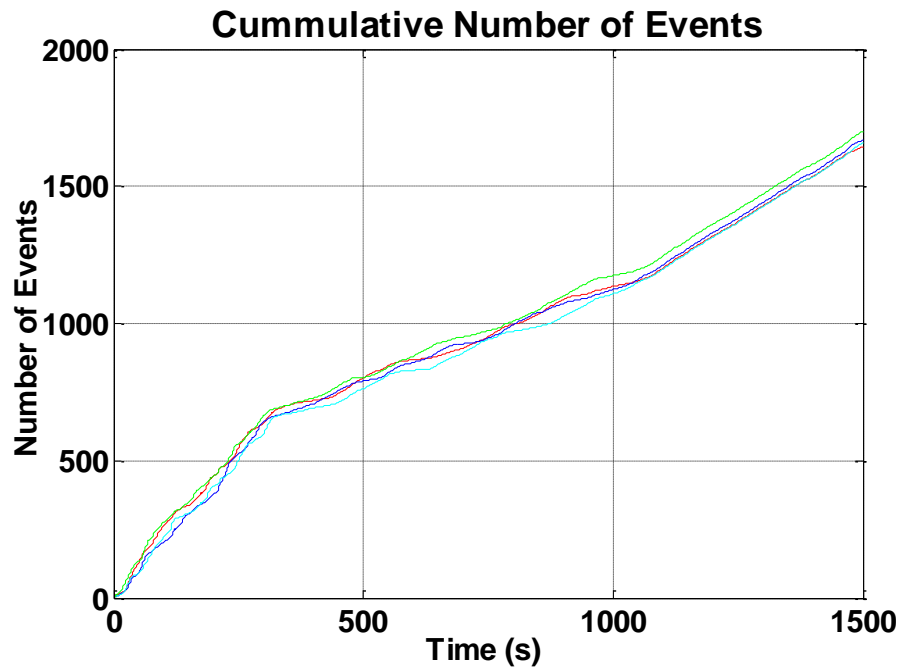
Figure 5.9 Cumulative number of events of each robot.

The NN adaptation with aperiodic event-based updates resulted in a bounded parameter estimation error as depicted in Figure 5.5. Clearly, the bounds on these errors

were higher compared to the continuously updated case. Due to the designed event-sampling mechanism at each robot, the total number of NN weight updates and the communication instants are considerably reduced as seen in Figure 5.9.

5.2   FULL COMMUNICATION CASE

In this case, the initial conditions, controller gains and all the parameters are chosen same as in case A. Only full communication is considered. The simulation is run for sixteen seconds and event triggered controller results are given. Comparing Figure 5.10 with Figure 5.1 and Figure 5.6, it is obvious that the oscillations are reduced significantly when the number of communication links are increased.
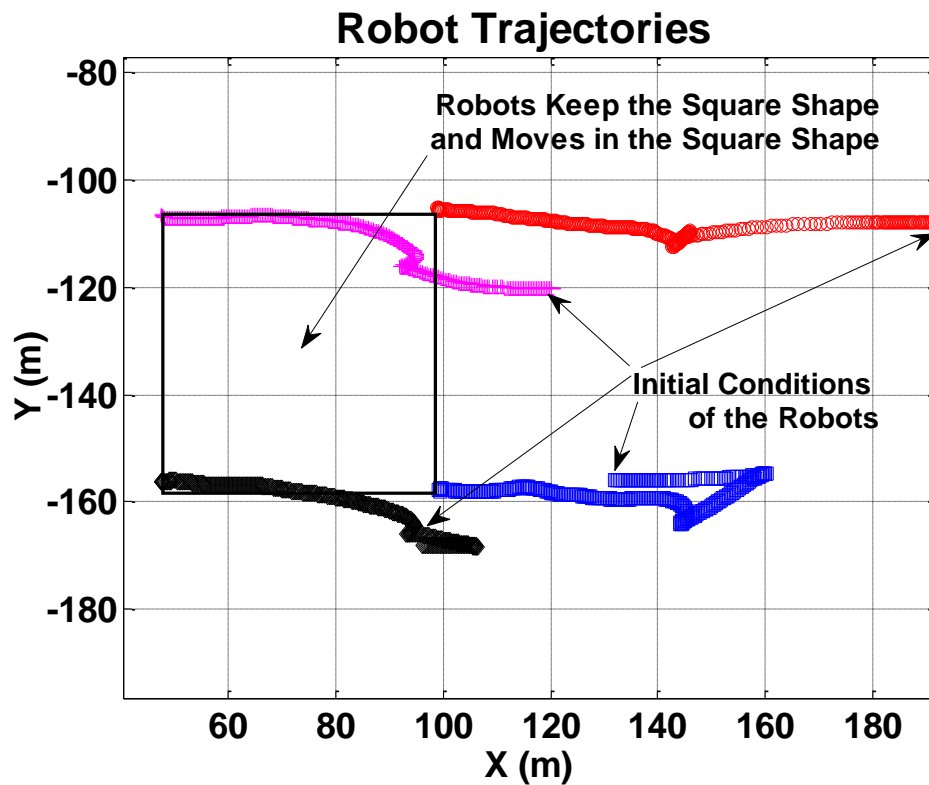
Figure 5.10 Robot trajectories.

Each robot considers the positions and velocities of all other robots in it's formation error definition and uses their control torque to approximate the uncertain formation dynamics. Though the network of robots reach consensus with minimal communication in the previous case, oscillations are observed which can be eliminated with additional communication from neighbors.

Increasing the communication links among robots not only reduces the oscillations but also reduces the time of consensus. Figure 5.11 and Figure 5.12 plots the formation and the velocity tracking errors of all four robots, respectively.
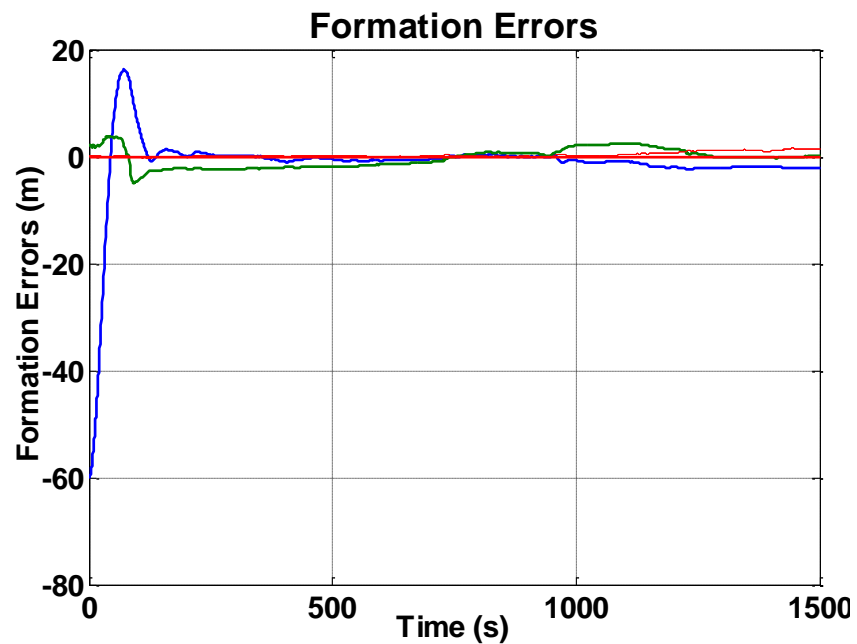
Figure 5.11 Formation errors.
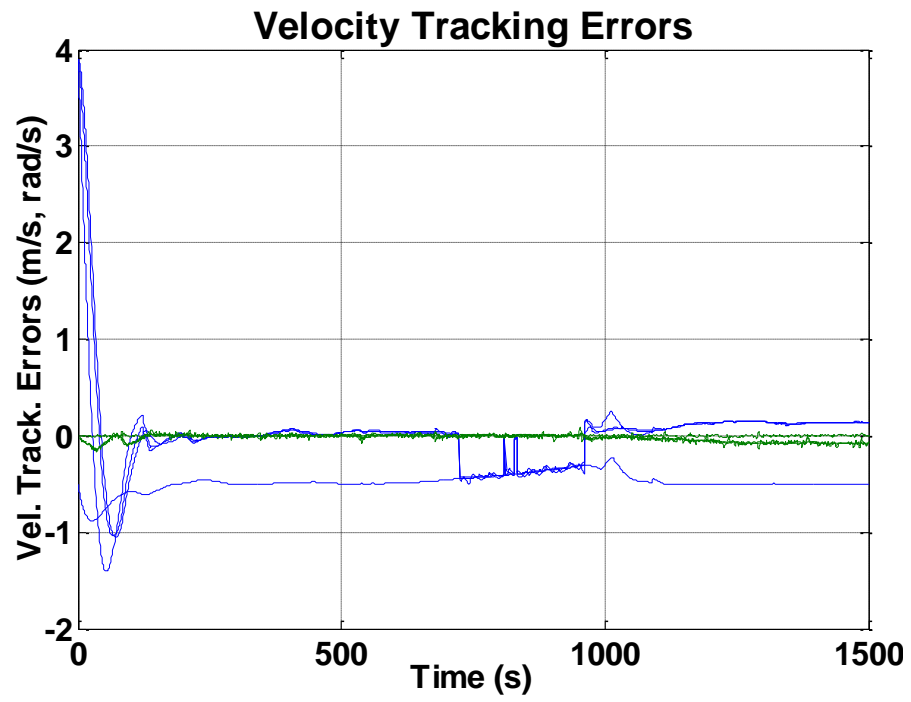
Figure 5.12 Velocity tracking errors.

6. CONCLUSIONS

In this paper, an event-based formation control scheme for a network of mobile robots was presented. The NN based event-sampled torque control of mobile robots was able to bring the robots to consensus by stabilizing the formation as well as velocity tracking errors in the presence of event sampled measurement errors, NN reconstruction errors and bounded disturbance. The event-sampling mechanism was able to generate additional events so that the formation error remains bounded and due to asynchronous mode, communication overhead is minimized.

In the case of minimal communication, oscillatory behavior is observed initially though this becomes better over time while full communication with other robots enhance the formation control. The event-sampling condition at each robot and the NN adaptation rules were derived using the Lyapunov stability analysis. The analytical results were verified using the simulation examples and the efficiency of the event-sampled controller execution was demonstrated in the presence of minimal communication information and with full communication overhead. It was observed that the robots reached consensus even in the presence of minimal communication. However, the consensus was reached much faster and the robots moved with much less oscillations when the full communication was available for all the robots.

APPENDIX

Proof of Theorem 1: Consider the following combined Lyapunov candidate

$$L = \sum_{i=1}^{N} L_{iF} ,$$ (108)

where the Lyapunov functions for each robot is given by

$$L_{iF} = \frac{1}{2}(e_{i1}^2 + e_{i2}^2 + e_{iv}^{F^T} \bar{M}_i e_{iv}^F + tr\tilde{\Theta}_i^T \Lambda \tilde{\Theta}_i) + \frac{1}{k_2}(1 - \cos e_{i3})$$ (109)

with $\Lambda = \Lambda_1^{-1}$. Taking the derivative of (109) and substituting the consensus error system (55) and velocity tracking error dynamics (91) reveal

$$\dot{L}_{iF} = -k_1 e_{i1}^2 - (k_3/k_2)\sin^2 e_{i3} - e_{i1}e_{iv1} - (1/k_2)\sin e_{i3}e_{iv2} - e_{iv}^{F^T} K_v e_{iv}^F - e_{iv}^{F^T} \gamma(e_{i1}, e_{i2}, e_{i3})$$

$$+ e_{iv}^{F^T}(\tilde{\Theta}_i \psi_i(z_i) + \chi_i + \bar{\tau}_{di}) + 0.5(e_{iv}^{F^T}(\dot{\bar{M}}_i - 2\bar{V}_{mi}(q_i \dot{q}_i))\dot{e}_{iv}^F + tr\{\tilde{\Theta}_i^T \Lambda \dot{\tilde{\Theta}}_i\})$$

Next, applying skew symmetric property [1] and recalling the definition of $\gamma(e_{i1}, e_{i2}, e_{i3})$ in (92) results in

$$\dot{L}_{iF} = -k_1 e_{i1}^2 - (k_3/k_2)\sin^2 e_{i3} - e_{iv}^{F^T} K_v e_{iv}^F + e_{iv}^{F^T}(\tilde{\Theta}_i \psi_i(z_i) + \chi_i + \bar{\tau}_{di}) + 0.5 tr\{\tilde{\Theta}_i^T \Lambda \dot{\tilde{\Theta}}_i\}$$ (110)

Using the upper bound on the disturbance and the NN approximation error along with the Young's inequality yields

$$\dot{L}_{iF} \le -k_1 e_{i1}^2 - (k_3/k_2)\sin^2 e_{i3} - K_v \|e_{iv}^F\|^2 + 0.5\|e_{iv}^F\|^2$$

$$+ 0.5((\chi_M + d_M)^2 + tr\{e_{iv}^{F^T}\tilde{\Theta}_i \psi_i(z_i) + \tilde{\Theta}_i^T \Lambda \dot{\tilde{\Theta}}_i\})$$ (111)

Use the adaptation rule (93) and the rotation property of trace operator, combine similar terms to get

$$\dot{L}_{iF} \leq -k_1 e_{i1}^2 - \frac{k_3}{k_2}\sin^2 e_{i3} - (K_v - \frac{1}{2})\|e_{iv}^F\|^2 - \frac{\kappa_i}{2}tr\,\tilde{\Theta}_i^T\tilde{\Theta}_i + \eta_{Bi}$$

with $\eta_{Bi} = 0.5\|d_M + \chi_M\|^2$. Then the derivative of the combined Lyapunov function (108) is given as

$$\dot{L} \leq \sum_{i=1}^{N}(-k_1 e_{i1}^2 - (k_3/k_2)\sin^2 e_{i3} - (K_v - 0.5)\|e_{iv}^F\|^2 - 0.5\kappa_i\,tr\{\tilde{\Theta}_i^T\tilde{\Theta}_i\} + \eta_B) \tag{112}$$

where $\eta_B = N\eta_{Bi}$. It can be observed from (112) that the Lyapunov derivative is less than zero as long as $K_v > 0.5, (k_3/k_2) > 0,\ \kappa_i > 0,$ provided

$$e_{i1} > \sqrt{\frac{\eta_B}{k_1}},\ or,\ \sin e_{i3} > \sqrt{\frac{k_2\eta_B}{k_3}}, or,\ \|e_{iv}^F\| > \sqrt{\frac{\eta_B}{K_v}},\ or,\ \|\tilde{\Theta}_i\| > \sqrt{\frac{\eta_B}{\kappa_i}}.$$

Therefore, a) all the formation errors, velocity tracking errors and NN weight approximation errors are bounded; b) Since the Lyapunov function (108) contains all the individual Lyapunov functions and it is proven that each robot reach consensus on regulation errors, it will provide the desired formation shape for the networked mobile robot group.

Proof of Theorem 2: Consider the Lyapunov candidate (108) and taking the derivative of (109), we have

$$\dot{L}_i = e_{i1}\dot{e}_{i1} + e_{i2}\dot{e}_{i2} + (\dot{e}_{i3}\sin e_{i3}/k_2) + e_{iv}^{F\,T}\bar{M}_i\dot{e}_{iv}^F + \frac{1}{2}e_{iv}^{F\,T}\dot{\bar{M}}_i e_{iv}^F + tr\{\tilde{\Theta}_i^T\Lambda\dot{\tilde{\Theta}}_i\}. \tag{113}$$

Utilizing the consensus error dynamics and the velocity tracking error dynamics with measurement error from (101) and (60), to get

$$\dot{L}_i = e_{i1}\left(e_{i2}\omega_i - k_1 e_{i1} + v_{i\varepsilon} - e_{iv1}^F\right) + e_{i2}\left(-e_{i1}\omega_i + v_j\sin(e_{i3})\right)$$

$$+\frac{\sin e_{i3}}{k_2}\left(-k_2 v_j e_{i2} - k_3\sin(e_{i3}) + \omega_{i\varepsilon} - e_{iv2}^F\right)$$

$$-e_{iv}^{F^T}(K_v e_{iv}^F - \breve{\gamma}(e_i) + 0.5 e_{iv}^{F^T}(\dot{\bar{M}}_i - 2\bar{V}_{mi}(q_i \dot{q}_i))e_{iv}^F + \bar{\tau}_{di} + \tilde{f}(\breve{z}_i) + K_v e_{iET})$$

$$+[f(z_i) - f(\breve{z}_i)]) + tr\{\tilde{\Theta}_i^T \Lambda \dot{\tilde{\Theta}}_i\}. \tag{114}$$

Using the definition of e_{i3} and skew symmetry property and expanding the expression, we obtain

$$\dot{L}_i = e_{i1} e_{i2} \omega_i - k_1 e_{i1}^2 + e_{i1} v_{i\varepsilon} - e_{i1} e_{i2} \omega_i + v_j e_{i2} \sin e_{i3} - v_j e_{i2} \sin e_{i3} - \frac{k_3}{k_2}\sin^2(e_{i3})$$

$$+(\frac{\omega_{i\varepsilon}}{k_2} - \frac{e_{iv2}^F}{k_2})\sin e_{i3} - e_{i1}e_{iv1}^F - e_{iv}^{F^T} K_v e_{iv}^F - e_{iv}^{F^T}\breve{\gamma}(e_i) + e_{iv}^{F^T}\tilde{f}(\breve{z}_i) + e_{iv}^{F^T} K_v e_{iET}$$

$$+e_{iv}^{F^T}[f(z_i) - f(\breve{z}_i)] + tr\{\tilde{\Theta}_i^T \Lambda \dot{\tilde{\Theta}}_i\}.$$

$$\dot{L}_i = -k_1 e_{i1}^2 + e_{i1} v_{i\varepsilon} - \frac{k_3}{k_2}\sin^2(e_{i3}) + \frac{1}{k_2}\omega_{i\varepsilon}\sin e_{i3} - K_v\left\|e_{iv}^F\right\|^2 - \sin e_{i3} e_{iv2}^F/k_2 - e_{i1}e_{iv1}^F - e_{iv}^{F^T}\breve{\gamma}(e_{iF})$$

$$+e_{iv}^{F^T}(\tilde{\Theta}_i^T \psi(\breve{z}_i) + \bar{\tau}_{di} + \chi_i) + e_{iv}^{F^T} K_v e_{iET} + e_{iv}^{F^T}[f(z_i) - f(\breve{z}_i)] + tr\{\tilde{\Theta}_i^T \Lambda \dot{\tilde{\Theta}}_i\}. \tag{115}$$

Using (107) in (115) and defining the bound $\left\|\psi_i(z_i)\right\| \le \psi_M \ \forall i = 1, 2, \ldots, N$, we obtain

$$\dot{L}_i \le -k_1 e_{i1}^2 - (k_3/k_2)\sin^2(e_{i3}) - (K_v - 0.5)\left\|e_{iv}^F\right\|^2 + e_{i1} v_{i\varepsilon} + (\omega_{i\varepsilon}/k_2)\sin e_{i3} + (e_{iv2}^F/k_2)\sin e_{i3}$$

$$-(e_{iv2}^F/k_2)[\sin e_{i3} - \sin\breve{e}_{i3}] + e_{iv1}^F e_{i1} + e_{iv}^{F^T}\tilde{\Theta}_i^T \psi(\breve{z}_i) + e_{iv}^{F^T} K_v e_{iET} + 2\psi_M^2\left\|\Theta_i\right\|^2 + e_{iv}^{F^T}(\bar{\tau}_{di} + \chi_i)$$

$$+e_{iv1}^F \varepsilon_{i1} - (e_{iv2}^F/k_2)\sin e_{i3} - e_{i1}e_{iv1}^F + tr\{\tilde{\Theta}_i^T \Lambda \dot{\tilde{\Theta}}_i\}.$$

Utilizing the definition of the formation errors in the presence of measurement errors as well as $\breve{v}_j$, we get

$$\dot{L}_i \le -k_1 e_{i1}^2 - (k_3/k_2)\sin^2(e_{i3}) - (K_v - 0.5)\left\|e_{iv}^F\right\|^2 + \sin e_{i3}/k_2 - e_{iv2}^F[\sin e_{i3} - \sin\breve{e}_{i3}]/k_2$$

$$-e_{i1}k_2(\breve{v}_j+\varepsilon_{vj})\varepsilon_{i2}-e_{i1}k_2\varepsilon_{vj}e_{i2}+e_{iv}^{F^T}\tilde{\Theta}_i^T\psi(\breve{z}_i)+e_{iv}^{F^T}K_ve_{iET}+e_{iv1}^F\varepsilon_{i1}+2\psi_M^2\|\Theta_i\|^2$$

$$+e_{i1}k_3[\sin e_{i3}-\sin\breve{e}_{i3}]-(1/k_2)\sin e_{i3}(\breve{v}_j+\varepsilon_{vj})[\cos e_{i3}-\cos\breve{e}_{i3}]$$

$$+e_{i1}\varepsilon_{\omega j}-e_{i1}k_2\varepsilon_{vj}\varepsilon_{i2}+(1/k_2)\sin e_{i3}\varepsilon_{vj}\cos\breve{e}_{i3}-(1/k_2)\sin e_{i3}k_1\varepsilon_{i1}$$

$$+L_v\varepsilon_i+e_{iv}^{F^T}(\bar{\tau}_{di}+\chi_i)+tr\{\tilde{\Theta}_i^T\Lambda\dot{\tilde{\Theta}}_i\}. \tag{116}$$

Apply the norm operator, utilize the boundedness of the trigonometric terms and the bounds on the disturbance torque and reconstruction error, to obtain

$$\dot{L}_i\le-k_1e_{i1}^2-(k_3/k_2)\sin^2(e_{i3})-(K_v-0.5)\|e_{iv}^F\|^2+(1/k_2)\|e_{iv1}^F\|$$

$$+e_{i1}k_2(\varepsilon_{i2}\breve{v}_j+\varepsilon_{i2}\varepsilon_{vj}-\breve{e}_{i2}\varepsilon_{vj})+\|e_{i1}\|(k_3+\|\varepsilon_{\omega j}\|)$$

$$+e_{iv}^{F^T}\tilde{\Theta}_i^T\psi(\breve{z}_i)+\|e_{iv}^{F^T}\|(\|K_ve_{iET}\|+2\psi_M^2\|\Theta_i\|^2+\|\varepsilon_{i1}\|+d_B+\chi_M)$$

$$+tr\{\tilde{\Theta}_i^T\Lambda\dot{\tilde{\Theta}}_i\}+(1/k_2)(\|(\breve{v}_j+\varepsilon_{vj})\|+\|\varepsilon_{vj}\|+k_1\|\varepsilon_{i1}\|+1)\|\sin e_{i3}\|. \tag{117}$$

Use Young's and the triangular inequalities, and the trace operator in (117) to get

$$\dot{L}_i\le-k_1e_{i1}^2-(k_3/k_2)\sin^2(e_{i3})-(K_v-0.5)\|e_{iv}^F\|^2$$

$$+\left(\|e_{iv}^F\|^2/2\right)+0.5(\|\varepsilon_{i2}\|\|\breve{v}_j\|+\|\varepsilon_{i2}\|\|\varepsilon_{vj}\|+\|\breve{e}_{i2}\|\|\varepsilon_{vj}\|)^2+tr\{e_{iv}^{F^T}\tilde{\Theta}_i^T\psi(\breve{z}_i)\}$$

$$+0.5\left(e_{i1}^2k_2^2+\|e_{iv}^{F^T}\|^2+(d_B+\chi_M)^2+\|K_v\|^2\|e_{iET}\|^2\right)+\|\varepsilon_{i1}\|^2 2\psi_M^2\|\Theta_i\|^2$$

$$+\|e_{i1}\|^2/2+4k_3^2+\|\varepsilon_{\omega j}\|^2/2+2\|\breve{v}_j\|^2/k_2^2+0.5k_2^2$$

$$+5\|\varepsilon_{vj}\|^2/2k_2^2+k_1^2\|\varepsilon_{i1}\|^2/2k_2^2+2\|\sin e_{i3}\|+tr\{\tilde{\Theta}_i^T\Lambda\dot{\tilde{\Theta}}_i\}.$$

Utilizing the parameter adaptation rule defined in (93) and the definition of the NN weights estimation error, we have

$$\dot{L}_i \le -k_1 e_{i1}^2 - \left(k_3/k_2\right)\sin^2(e_{i3}) - \left(K_v - 0.5\right)\left\|e_{iv}^F\right\|^2$$

$$+0.5((\left\|\varepsilon_{i2}\right\|\left\|\breve{v}_j\right\| + \left\|\varepsilon_{i2}\right\|\left\|\varepsilon_{vj}\right\| + \left\|\breve{e}_{i2}\right\|\left\|\varepsilon_{vj}\right\|)^2 + e_{i1}^2 k_2^2 + \left\|e_{iv}^{F^T}\right\|^2)$$

$$+\left(\left\|e_{iv}^F\right\|^2/2\right) + \frac{1}{2}(d_B + \chi_M)^2 + \frac{1}{2}\left\|K_v\right\|^2 \left\|e_{iET}\right\|^2 + \left\|\varepsilon_{i1}\right\|^2 + 2\psi_M^2 \left\|\Theta_i\right\|^2 + \frac{\left\|e_{i1}\right\|^2}{2} + 4k_3^2$$

$$+\frac{\left\|\varepsilon_{\omega j}\right\|^2}{2} + \frac{2\left\|\breve{v}_j\right\|^2}{k_2^2} + \frac{5\left\|\varepsilon_{vj}\right\|^2}{2k_2^2}$$

$$+\frac{k_1^2\left\|\varepsilon_{i1}\right\|^2}{2k_2^2} + \frac{1}{2k_2^2} + 2\left\|\sin e_{i3}\right\| - tr\left\{\tilde{\Theta}_i^T\left(\psi_i\left(\breve{z}_i\right)\breve{e}_{iv}^{F^T} - \kappa_i\hat{\Theta}_i\right) - e_{iv}^{F^T}\tilde{\Theta}_i^T\psi\left(\breve{z}_i\right)\right\}. \tag{118}$$

Combining the similar terms and using the Young's inequality once again yields

$$\dot{L}_i \le -k_1 e_{i1}^2 - k_3/k_2 \sin^2(e_{i3}) - \left(K_v - 0.5\right)\left\|e_{iv}^F\right\|^2 + \left\|e_{iv}^F\right\|^2/2$$

$$+0.5((\left\|\varepsilon_{i2}\right\|\left\|\breve{v}_j\right\| + \left\|\varepsilon_{i2}\right\|\left\|\varepsilon_{vj}\right\| + \left\|\breve{e}_{i2}\right\|\left\|\varepsilon_{vj}\right\|)^2 + e_{i1}^2 k_2^2 + \left\|e_{iv}^{F^T}\right\|^2)$$

$$+0.5((d_B + \chi_M)^2 + \left\|K_v\right\|^2 \left\|e_{iET}\right\|^2) + \left\|\varepsilon_{i1}\right\|^2 + 2\psi_M^2 \left\|\Theta_i\right\|^2 + 4k_3^2 + 0.5(\left\|e_{i1}\right\|^2 + \left\|\varepsilon_{\omega j}\right\|^2)$$

$$+(\left\|\bar{v}_j^d\right\|^2 + \left\|\varepsilon_{vj}\right\|^2 + \left\|e_{jv}^F\right\|^2 + 2.5\left\|\varepsilon_{vj}\right\|^2)/k_2^2 + k_1^2\left\|\varepsilon_{i1}\right\|^2/2k_2^2 + 1/2k_2^2 + 2\left\|\sin e_{i3}\right\| - \kappa_i\left\|\tilde{\Theta}_i\right\|^2.$$

Combining similar terms reveals

$$\dot{L}_i \le -K_i \Xi_i + \underline{B}_i + 2\left\|e_{jv}^F\right\|^2/k_2^2. \tag{119}$$

Where

$$\underline{B}_i = 0.5k_3^2 + 1/2k_2^2 + 2\left(\left\|\bar{v}_j^d\right\|^2 + \left\|\varepsilon_{vj}\right\|^2\right)/k_2^2 + (d_B + \chi_M)^2/2 + 2\psi_M^2 \left\|\Theta_i\right\|^2 + 0.5\left\|K_v\right\|^2 \left\|e_{iET}\right\|^2$$

$$+(0.5 + k_1/k_2)\left\|\varepsilon_{i1}\right\|^2 + 1/k_2^2 + \frac{1}{2}\left\|e_{i1}\varepsilon_{i2}\right\|^2 + \frac{1}{2}\left\|\varepsilon_{\omega j}\right\|^2 + (\frac{k_2^2}{2} + \frac{\left\|\breve{e}_{i2}\right\|^2}{2} + \frac{5}{k_2})\left\|\varepsilon_{vj}\right\|^2 + \frac{1}{2}\left\|\varepsilon_i\right\|^2,$$

and $\quad \overline{k}_1 = (k_1 - (k_2^2 + 3)/2),\ \Xi_i = [e_{i1}^2\ \sin^2(e_{i3})\ \|e_{iv}^F\|^2\ \|\tilde{\Theta}_i\|^2],\ K_i = [\overline{k}_1\ \ \overline{k}_2\ \ \overline{k}_3\ \ \kappa_i],$

$\overline{k}_2 = (k_3/k_2 - 0.5),\ \overline{k}_3 = (K_v - 3/2).$ The derivative of the Lyapunov (108) can be found

by combining individual Lyapunovs terms (119). In the combined Lyapunov function of

the network of robots, the jth terms can be switched between i^{th} and j^{th} robot as

$2\|e_{iv}^F\|^2 \leftrightarrow 2\|e_{jv}^F\|^2$. Then, after combining velocity tracking error terms of the ith robot

yields the Lyapunov function

$$\dot{L} \leq \sum_{i=1}^{N}\left(-K_i\Xi_i + \underline{B}_i\right). \tag{120}$$

with the updated gains of velocity tracking error term $\overline{k}_3 = (K_v - 3/2 + 2/k_2^2)$. From (120)

: a) it can be seen that the formation, velocity tracking and the NN weights estimation errors

are bounded in the presence of the bounded measurement errors as long as

$k_1 > k_2^2/2 + 3/2,\ k_3/k_2 > 0.5,\ K_v > 3/2 - 2/k_2^2, \kappa_i > 0$; b) each robot reach consensus on

regulation errors, it will provides the desired formation shape for the networked mobile

robot group.

Proof of Theorem 3:

Case 1: With the event-sampled measurement error, $e_{iET} = 0,\ \forall i = 1,2,\ldots,N$. Since

it is already shown in the proof of the first theorem, the proof of the first case is omitted.

Case 2: During the inter-event period $e_{iET} \neq 0,\ \forall t \in [t_k.t_{k+1}), \dot{\hat{\Theta}} = 0,$ therefore, using

the Lyapunov candidate function (108) and the first derivative is obtained as (113).

Utilizing the consensus error dynamics and the velocity tracking error dynamics with

event-sampled measurement error from (101) and (60), get

$$\dot{L}_i = e_{i1}\left(e_{i2}\omega_i - k_1 e_{i1} + v_{i\varepsilon} - e_{iv1}^F\right) + e_{i2}\left(-e_{i1}\omega_i + v_j \sin(e_{i3})\right)$$

$$+\frac{\sin e_{i3}}{k_2}\left(-k_2 v_j e_{i2} - k_3 \sin(e_{i3}) + \omega_{i\varepsilon} - e_{iv2}^F\right)$$

$$-e_{iv}^{F^T}(K_v e_{iv}^F - \breve{\gamma}(e_i) + \overline{\tau}_{di} + \tilde{f}(\breve{z}_i) + K_v e_{iET}) + [f(z_i) - f(\breve{z}_i)]). \tag{121}$$

Using the definition of e_{i3}, we obtain

$$\dot{L}_i = e_{i1}e_{i2}\omega_i - k_1 e_{i1}^2 + e_{i1}v_{i\varepsilon} - e_{i1}e_{i2}\omega_i + v_j e_{i2}\sin e_{i3} - v_j e_{i2}\sin e_{i3} - \frac{k_3}{k_2}\sin^2(e_{i3})$$

$$+(\frac{\omega_{i\varepsilon}}{k_2} - \frac{e_{iv2}^F}{k_2})\sin e_{i3} - e_{i1}e_{iv1}^F - e_{iv}^{F^T}K_v e_{iv}^F - e_{iv}^{F^T}\breve{\gamma}(e_i) + e_{iv}^{F^T}\tilde{f}(\breve{z}_i)$$

$$+e_{iv}^{F^T}K_v e_{iET} + e_{iv}^{F^T}[f(z_i) - f(\breve{z}_i)].$$

$$\dot{L}_i = -k_1 e_{i1}^2 + e_{i1}v_{i\varepsilon} - \frac{k_3}{k_2}\sin^2(e_{i3}) + \frac{1}{k_2}\omega_{i\varepsilon}\sin e_{i3} - K_v\left\|e_{iv}^F\right\|^2 - \frac{1}{k_2}\sin e_{i3}e_{iv2}^F - e_{i1}e_{iv1}^F$$

$$-e_{iv}^{F^T}\breve{\gamma}(e_{i1}, e_{i2}, e_{i3}) + e_{iv}^{F^T}(\tilde{\Theta}_i^T \psi(\breve{z}_i) + \overline{\tau}_{di} + \chi_i) + e_{iv}^{F^T}K_v e_{iET} + e_{iv}^{F^T}[f(z_i) - f(\breve{z}_i)]. \tag{122}$$

Using (107) in (122) and do the similar steps done in *Theorem* 1 yields

$$\dot{L}_i \le -k_1 e_{i1}^2 - k_3/k_2 \sin^2(e_{i3}) - (K_v - 0.5)\left\|e_{iv}^F\right\|^2 + e_{i1}v_{i\varepsilon} + \omega_{i\varepsilon}\sin e_{i3}/k_2 + e_{iv2}^F \sin e_{i3}/k_2$$

$$-e_{iv2}^F\left(\sin e_{i3} - \sin \breve{e}_{i3}\right)/k_2 + e_{iv1}^F e_{i1} + e_{iv}^{F^T}\tilde{\Theta}_i^T \psi(\breve{z}_i) + e_{iv}^{F^T}K_v e_{iET} + 0.5\left\|\Theta_i^T \psi_M\right\|^2$$

$$+e_{iv}^{F^T}(\overline{\tau}_{di} + \chi_i) + e_{iv1}^F \varepsilon_{i1} - e_{iv2}^F/k_2 \sin e_{i3} - e_{i1}e_{iv1}^F.$$

Utilize the definition of the event-sampled formation errors as well as the definition of $\breve{v}_j$

to get

$$\dot{L}_i \le -k_1 e_{i1}^2 - \frac{k_3}{k_2}\sin^2(e_{i3}) - (K_v - 0.5)\left\|e_{iv}^F\right\|^2 + \sin e_{i3}/k_2 + e_{iv1}^F \varepsilon_{i1} - \frac{e_{iv2}^F}{k_2}[\sin e_{i3} - \sin \breve{e}_{i3}]$$

$$-e_{i1}k_2(\breve{v}_j + \varepsilon_{vj})\varepsilon_{i2} - e_{i1}k_2\varepsilon_{vj}e_{i2} + e_{iv}^{F^T}K_v e_{iET} + e_{iv}^{F^T}\tilde{\Theta}_i^T\psi(\breve{z}_i) + 0.5\left\|\Theta_i^T\psi_M\right\|^2$$

$$+e_{i1}k_3[\sin e_{i3} - \sin \breve{e}_{i3}] - e_{i1}k_2\varepsilon_{vj}\varepsilon_{i2} \quad -\frac{1}{k_2}\sin e_{i3}(\breve{v}_j + \varepsilon_{vj})[\cos e_{i3} - \cos \breve{e}_{i3}] + \frac{1}{k_2}\sin e_{i3}\varepsilon_{vj}\cos \breve{e}_{i3}$$

$$-\frac{1}{k_2}\sin e_{i3}k_1\varepsilon_{i1} + L_v\varepsilon_i + e_{iv}^{F^T}\left(\bar{\tau}_{di} + \chi_i\right) + e_{i1}\varepsilon_{\omega j}. \tag{123}$$

Applying the norm operator, we obtain the inequality as

$$\dot{L}_i \leq -k_1 e_{i1}^2 - (k_3/k_2)\sin^2(e_{i3}) - (K_v - 0.5)\left\|e_{iv}^F\right\|^2 + \left(\|\sin e_{i3}\|/k_2\right) + e_{iv1}^F\varepsilon_{i1}$$

$$+\frac{1}{k_2}e_{iv2}^F\left\|[\sin e_{i3} - \sin \breve{e}_{i3}]\right\| + e_{i1}k_2\varepsilon_{i2}\breve{v}_j$$

$$-e_{i1}k_2 e_{i2}\varepsilon_{vj} + \left\|e_{iv}^{F^T}\right\|\left\|K_v e_{iET}\right\| + \left\|e_{iv}^{F^T}\right\|\left\|\tilde{\Theta}_i^T\psi(\breve{z}_i)\right\| + 0.5\left\|\Theta_i^T\psi_M\right\|^2 + \left\|e_{iv}^{F^T}\right\|\left\|\bar{\tau}_{di} + \chi_i\right\|$$

$$+e_{i1}\left\|k_3[\sin e_{i3} - \sin \breve{e}_{i3}]\right\| + \left\|e_{i1}\right\|\left\|\varepsilon_{\omega j}\right\|$$

$$+\left(\|\sin e_{i3}\|\left\|\varepsilon_{vj}\cos \breve{e}_{i3}\right\|/k_2\right) + (k_1/k_2)\|\varepsilon_{i1}\|\|\sin e_{i3}\| + \|\sin e_{i3}\|\|(\breve{v}_j + \varepsilon_{vj})\|\|[\cos e_{i3} - \cos \breve{e}_{i3}]\|/k_2.$$

By utilizing the boundedness of the trigonometric terms and the bounds on the disturbance torque and reconstruction error, we get

$$\dot{L}_i \leq -k_1 e_{i1}^2 - (k_3/k_2)\sin^2(e_{i3}) - (K_v - 0.5)\left\|e_{iv}^F\right\|^2 + e_{i1}k_2\varepsilon_{i2}\breve{v}_j + \|e_{i1}\|\left(k_3 + \|\varepsilon_{\omega j}\|\right)$$

$$+\left\|e_{iv1}^F\right\|\left(1/k_2 + \left\|\tilde{\Theta}_i^T\psi(\breve{z}_i)\right\|\right)$$

$$+e_{i1}k_2\varepsilon_{i2}\varepsilon_{vj} - e_{i1}k_2\breve{e}_{i2}\varepsilon_{vj} + \left\|e_{iv}^{F^T}\right\|\left(\|K_v e_{iET}\| + 0.5\left\|\Theta_i^T\psi_M\right\|^2 + \|\varepsilon_{i1}\| + d_B + \chi_M\right)$$

$$+(1/k_2)\left(\|(\breve{v}_j + \varepsilon_{vj})\| + \|\varepsilon_{vj}\| + k_1\|\varepsilon_{i1}\| + 1\right)\|\sin e_{i3}\|. \tag{124}$$

Use Young's inequality and the triangular inequality in (124) to get

$$\dot{L}_i \leq -k_1 e_{i1}^2 - \frac{k_3}{k_2}\sin^2(e_{i3}) - \left(K_v - \frac{1}{2}\right)\|e_{iv}^F\|^2 + \frac{\|e_{iv}^F\|^2}{2} + 2\|\sin e_{i3}\|$$

$$+ (\|\varepsilon_{i2}\|\|\breve{v}_j\| + \|\varepsilon_{i2}\|\|\varepsilon_{vj}\| + \|\breve{e}_{i2}\|\|\varepsilon_{vj}\|)^2)$$

$$+0.5((\frac{1}{k_2} + \|\tilde{\Theta}_i^T \psi(\breve{z}_i)\|)^2 + 0.5(e_{i1}^2 k_2^2 + \|e_{iv}^{F^T}\|^2 + (d_B + \chi_M)^2 + \|K_v\|^2 \|e_{iET}\|^2) + \|\varepsilon_{i1}\|^2 + \frac{1}{2k_2^2}$$

$$+\frac{1}{2}\|\Theta_i^T \psi_M\|^2 + \frac{\|e_{i1}\|^2}{2} + 4k_3^2 + \frac{\|\varepsilon_{\omega j}\|^2}{2} + \frac{2\|\breve{v}_j\|^2}{k_2^2} + \frac{5\|\varepsilon_{vj}\|^2}{2k_2^2} + \frac{k_1^2\|\varepsilon_{i1}\|^2}{2k_2^2} \text{ .Combining similar terms}$$

reveals

$$\dot{L}_i \leq -(k_1 - \frac{k_2^2}{2}k_2^2/2 - 3/2)e_{i1}^2 - (k_3/k_2 - 0.5)\sin^2(e_{i3}) - (K_v - 3/2)\|e_{iv}^F\|^2$$

$$+0.5\|K_v\|^2\|e_{iET}\|^2 + (0.5 + k_1/k_2)\|\varepsilon_{i1}\|^2$$

$$+0.5k_2^2\breve{v}_j^2\|\varepsilon_{i2}\|^2 + 0.5\|e_{i1}\varepsilon_{i2}\|^2 + 0.5\|\varepsilon_{\omega j}\|^2 + (0.5k_2^2 + 0.5\|\breve{e}_{i2}\|^2 + 5/k_2)\|\varepsilon_{vj}\|^2 + 0.5\|\varepsilon_i\|^2 + \bar{B}_i.$$

with the bounding term $\bar{B}_i = 1/k_2^2 + 0.5k_3^2 + 0.5\|\tilde{\Theta}_i^T \psi(\breve{z}_i)\|^2 + 1/2k_2^2 + \|2\breve{v}_j\|^2/k_2$

$+0.5((d_B + \chi_M)^2 + \|\Theta_i^T \psi_M\|^2)$. It should be noted that $\breve{v}_j$ represents the last updated velocity

information from the jth robot and it is held constant until the next event at the jth robot

and realize that $\tilde{\Theta}_i$ is bounded between two event sampled time instants as well as the

desired NN weights Θ_i. For simplicity, defining

$\bar{k}_1 = (k_1 - k_2^2/2 - 3/2), \ \bar{k}_2 = (k_3/k_2 - 0.5), \ \bar{k}_3 = (K_v - 3/2), \ K_i = [\bar{k}_1 \ \bar{k}_2 \ \bar{k}_3],$

$E_i = [e_{i1}^2 \ \sin^2(e_{i3}) \ \|e_{iv}^F\|^2]^T, \ E_{iET} = [\|e_{iET}\|^2 \ \|\varepsilon_{i1}\|^2 \ \|\varepsilon_{i2}\|^2 \ \|\varepsilon_{i1}\varepsilon_{i2}\|^2]^T,$

$k_{i1e} = 0.5\|K_v\|^2, k_{i2e} = (1 + k_1/k_2), k_{i3e} = 0.5(k_2^2\breve{v}_j^2 + 1 + \|\breve{e}_{i1}\|^2),$

$$k_{i4e} = 0.5, K_{iET} = \begin{bmatrix} k_{i1e} & k_{i2e} & k_{i3e} & k_{i4e} \end{bmatrix}, \text{ yields}$$

$$\dot{L}_i \leq -K_i E_i + K_{iET} E_{iET} + 0.5 \left\| \varepsilon_{\omega j} \right\|^2 + (0.5 + 0.5k_2^2 + 0.5 \left\| \breve{e}_{i2} \right\|^2 + 5/k_2) \left\| \varepsilon_{vj} \right\|^2 + \bar{B}_i. \tag{125}$$

Use the definitions of the event-trigger errors to get

$$K_{iET} E_{iET} = k_{i1e} \left\| e_{iET}^i + e_{iET}^j \right\|^2 + k_{i2e} \left\| \varepsilon_{i1}^i + \varepsilon_{i1}^j \right\|^2 + k_{i3e} \left\| \varepsilon_{i2}^i + \varepsilon_{i2}^j \right\|^2 + k_{i4e} \left\| \left(\varepsilon_{i1}^i + \varepsilon_{i1}^j \right) \left(\varepsilon_{i2}^i + \varepsilon_{i2}^j \right) \right\|^2,$$

and use the triangular inequality to obtain

$$K_{iET} E_{iET} \leq 2k_{i1e} \left\| e_{iET}^i \right\|^2 + 2k_{i1e} \left\| e_{iET}^j \right\|^2 + 2k_{i2e} \left\| \varepsilon_{i1}^i \right\|^2 + 2k_{i2e} \left\| \varepsilon_{i1}^j \right\|^2$$

$$+ 2k_{i3e} \left\| \varepsilon_{i2}^i \right\|^2 + 2k_{i3e} \left\| \varepsilon_{i2}^j \right\|^2 + \left\| \varepsilon_{i1}^i \right\|^4 + \left\| \varepsilon_{i1}^j \right\|^4 + \left\| \varepsilon_{i2}^i \right\|^4 + \left\| \varepsilon_{i2}^j \right\|^4 \tag{126}$$

Consider the second element, $\left\| e_{iET}^j \right\|^2$, and recall $e_{iET}^j = [v_j \cos e_{i3} \quad -\varepsilon_{\omega j} + k_2 \varepsilon_{vj} e_{i2}]^T$, then,

$$\left\| e_{iET}^j \right\|^2 = \left\| \begin{bmatrix} v_j \cos e_{i3} \\ -\varepsilon_{\omega j} + k_2 \varepsilon_{vj} e_{i2} \end{bmatrix} \right\|^2 = v_j^2 \cos^2 e_{i3} + \left(-\varepsilon_{\omega j} + k_2 \varepsilon_{vj} e_{i2} \right)^2 \leq v_j^2 + 2\varepsilon_{\omega j}^2 + 2k_2^2 \varepsilon_{vj}^2 e_{i2}^2$$

$$\leq v_j^2 + 2\varepsilon_{\omega j}^2 + 4k_2^2 \varepsilon_{vj}^2 \breve{e}_{i2}^2 + 8k_2^2 \varepsilon_{vj}^4 + 4k_2^2 \varepsilon_{i2}^{i\,4} + 4k_2^2 \varepsilon_{i2}^{j\,4}. \tag{127}$$

Then, using (127) in (126) yields

$$K_{iET} E_{iET} \leq 2k_{i1e} \left\| e_{iET}^i \right\|^2 + 2k_{i2e} \left\| \varepsilon_{i1}^i \right\|^2 + 2k_{i2e} \left\| \varepsilon_{i1}^j \right\|^2$$

$$+ 2k_{i1e} \left(v_j^2 + 2\varepsilon_{\omega j}^2 + 4k_2^2 \varepsilon_{vj}^2 \breve{e}_{i2}^2 + 8k_2^2 \varepsilon_{vj}^4 + 4k_2^2 \varepsilon_{i2}^{i\,4} + 4k_2^2 \varepsilon_{i2}^{j\,4} \right)$$

$$+ 2k_{i3e} \left\| \varepsilon_{i2}^i \right\|^2 + 2k_{i3e} \left\| \varepsilon_{i2}^j \right\|^2 + \left\| \varepsilon_{i1}^i \right\|^4 + \left\| \varepsilon_{i1}^j \right\|^4 + \left\| \varepsilon_{i2}^i \right\|^4 + \left\| \varepsilon_{i2}^j \right\|^4 \tag{128}$$

Define

$$K_{iET}^i = [2k_{i1e} \ 2k_{i2e} \ 2k_{i3e} \ 1 \ 1 + 8k_{i1e}k_2^2],$$

$$K_{iET}^j = [2k_{i2e} \ 2k_{i3e} \ 1 \ 1 \ 16k_{i1e}k_2^2 \ 4k_{i1e} + 0.5 \ 8k_{i1e}k_2^2 \breve{e}_{i2}^2 + k_{vj}]$$

$$E_{iET}^i = [\left\| e_{iET}^i \right\|^2 \ \left\| \varepsilon_{i1}^i \right\|^2 \ \left\| \varepsilon_{i2}^i \right\|^2 \ \left\| \varepsilon_{i1}^i \right\|^4 \ \left\| \varepsilon_{i2}^i \right\|^4], E_{iET}^j = [\left\| \varepsilon_{i1}^j \right\|^2 \ \left\| \varepsilon_{i2}^j \right\|^2 \ \left\| \varepsilon_{i1}^j \right\|^4 \ \left\| \varepsilon_{i2}^j \right\|^4 \ \varepsilon_{vj}^4 \ \varepsilon_{\omega j}^2 \ \varepsilon_{vj}^2]$$

to get

$$K_{iET}E_{iET} \leq K^i_{iET}E^i_{iET} + K^j_{iET}E^j_{iET}. \tag{129}$$

Use the inequality (129) in(125), then obtain

$$\dot{L}_i \leq -K_i E_i + K^i_{iET}E^i_{iET} + K^j_{iET}E^j_{iET} + \bar{B}_i. \tag{130}$$

For the system of N robots in the robot network, we have the Lyapunov function derivative as the sum of all the Lyapunov derivatives of the form, which yields

$$\dot{L}_i \leq -K_i E_i + K^i_{iET}E^i_{iET} + K^i_{iET}E^j_{iET} + \bar{B}_i \tag{131}$$

Recall that E^i_{iET} is available for the ith robot however E^j_{iET} is not. In the combined Lyapunov function of the network of robots, the unknown parts can be switched between i^{th} and j^{th} robot as $E^j_{iET} + v^2_j \leftrightarrow E^i_{jET} + v^2_i$. Then, the Lyapunov function can be written as

$$\dot{L} \leq \sum_{i=1}^{N} -K_i E_i + K^i_{iET}E^i_{iET} + K^i_{jET}E^i_{jET} + \bar{B}_i + 2v^{d2}_i + 2e^{F\,2}_{iv1} \tag{132}$$

Take the bounded term $2v^{d2}_i$ into the bounded terms and redefine $\bar{B}_i = \bar{B}_i + 2v^{d2}_i$, update the last term of K_i as

$\bar{k}_3 = (K_v - 7/2)$. Note that $v^d_i(t) = v^d_i(t_k)$, $\forall t \in [t_k, t_{k+1})$. The switched part,

$E^i_{jET} = \begin{bmatrix} \left\|\varepsilon^i_{j1}\right\|^2 & \left\|\varepsilon^i_{j2}\right\|^2 & \left\|\varepsilon^i_{j1}\right\|^4 & \left\|\varepsilon^i_{j2}\right\|^4 & \varepsilon^4_{vi} & \varepsilon^2_{\omega i} & \varepsilon^2_{vi} \end{bmatrix}$, is still not completely computable

continuously since the first four term needs bearing angle of the jth robot. Therefore, an upper bound is found for the first four terms in the following step. Consider

$$\begin{bmatrix} \varepsilon^i_{j1} \\ \varepsilon^i_{j2} \end{bmatrix} = \begin{bmatrix} \cos\theta_j & \sin\theta_j \\ -\sin\theta_j & \cos\theta_j \end{bmatrix} \begin{bmatrix} \varepsilon_{xi} \\ \varepsilon_{yi} \end{bmatrix}, \left\|\varepsilon^i_{j1}\right\|^2 = \left\|\cos\theta_j \varepsilon_{xi} + \sin\theta_j \varepsilon_{yi}\right\|^2$$

$$\left\|\varepsilon^i_{j2}\right\|^2 = \left\|-\sin\theta_j \varepsilon_{xi} + \cos\theta_j \varepsilon_{yi}\right\|^2. \tag{133}$$

Since the bearing angle of the jth robot is not available, (133)should be simplified by using triangular inequality, Young's inequality and the upper bound on sinusoidal function as

$$\left\| \varepsilon_{j1}^i \right\|^2 \leq 2\left\| \varepsilon_{xi} \right\|^2 + 2\left\| \varepsilon_{yi} \right\|^2, \left\| \varepsilon_{j2}^i \right\|^2 \leq 2\left\| \varepsilon_{xi} \right\|^2 + 2\left\| \varepsilon_{yi} \right\|^2. \tag{134}$$

Further,

$$\left\| \varepsilon_{j1}^i \right\|^4 \leq 8\left\| \varepsilon_{xi} \right\|^4 + 8\left\| \varepsilon_{yi} \right\|^4, \left\| \varepsilon_{j2}^i \right\|^4 \leq 8\left\| \varepsilon_{xi} \right\|^4 + 8\left\| \varepsilon_{yi} \right\|^4. \tag{135}$$

Now, by considering the inequalities (134) and(135), do the update

$$\mathrm{E}_{jET}^i = \begin{bmatrix} \varepsilon_{xyi} & \varepsilon_{xyi} & \varepsilon_{xyi}^2 & \varepsilon_{xyi}^2 & \varepsilon_{vi}^4 & \varepsilon_{\omega i}^2 & \varepsilon_{vi}^2 \end{bmatrix} \text{ with } \varepsilon_{xyi} = 2(\left\| \varepsilon_{xi} \right\|^2 + \left\| \varepsilon_{yi} \right\|^2), \varepsilon_{xyi}^2 = 8(\left\| \varepsilon_{xi} \right\|^4 + \left\| \varepsilon_{yi} \right\|^4).$$

Now combine the two terms as $\bar{K}_{iET}^i = \begin{bmatrix} K_{iET}^i & K_{jET}^i \end{bmatrix}$, $\bar{E}_{iET}^i = \begin{bmatrix} E_{iET}^i & E_{jET}^i \end{bmatrix}$ and get the derivative of the Lyapunov as

$$\dot{L} \leq \sum_{i=1}^{N} -\mathrm{K}_i \mathrm{E}_i + \bar{K}_{iET}^i \bar{E}_{iET}^i + \bar{B}_i. \tag{136}$$

Separate the error vector as

$$-K_i \mathrm{E}_i = -(\bar{\mathrm{k}}_1 \left(\hat{e}_{i1} + \varepsilon_{i1}^j \right)^2 + \bar{\mathrm{k}}_2 \sin^2(\hat{e}_{i3} + \varepsilon_{i3}^j) + \bar{\mathrm{k}}_3 \left\| \hat{e}_{iv}^F + e_{iET}^j \right\|^2)$$

$$\leq - \begin{pmatrix} \left(\bar{\mathrm{k}}_1 - 2\bar{\mathrm{k}}_1^2 \right) \hat{e}_{i1}^2 + \left(\bar{\mathrm{k}}_1 - 0.5 \right) \left(\varepsilon_{i1}^j \right)^2 \\ + \left(\bar{\mathrm{k}}_3 - 2\bar{\mathrm{k}}_3^2 \right) \left(\hat{e}_{iv}^F \right)^2 + \left(\bar{\mathrm{k}}_3 - 0.5 \right) \left(e_{iET}^j \right)^2 \end{pmatrix}$$

where $\hat{e}_{i1} = \breve{e}_{i1} + \varepsilon_{i1}^i, \hat{e}_{i1} = \breve{e}_{i3} + \varepsilon_{i3}^i, \hat{e}_{iv}^F = \breve{e}_{iv}^F + e_{iET}^i$. Define $\breve{K}_i = \begin{bmatrix} \left(\bar{\mathrm{k}}_1 - 2\bar{\mathrm{k}}_1^2 \right) & \left(\bar{\mathrm{k}}_3 - 2\bar{\mathrm{k}}_3^2 \right) \end{bmatrix}$,

$\breve{\mathrm{E}}_i = \begin{bmatrix} \hat{e}_{i1}^2 & \left\| \breve{e}_{iv}^F \right\|^2 \end{bmatrix}$, $\varepsilon_{iL}^j = \begin{bmatrix} \left(\bar{\mathrm{k}}_1 - 0.5 \right) \left(\varepsilon_{i1}^j \right)^2 & \left(\bar{\mathrm{k}}_3 - 0.5 \right) \left\| e_{iET}^j \right\|^2 \end{bmatrix}$, similar to the steps between equations (131) and (132), the unknown event triggering errors, $\varepsilon_{iL}^j \leftrightarrow \varepsilon_{jL}^i$, can be switched among the robots in the combined Lyapunov function and the event triggering

errors, and coefficients can be re-defined as $\underline{K}^i_{iET} = \begin{bmatrix} \bar{K}^i_{iET} & \begin{bmatrix} 1 & 1 \end{bmatrix} \end{bmatrix}$, $\underline{E}^i_{iET} = \begin{bmatrix} \bar{E}^i_{iET} & \varepsilon^i_{jL} \end{bmatrix}$.

Then, the inequality (136) is obtained as

$$\dot{L} \leq \sum_{i=1}^{N} \left(-\breve{K}_i \breve{E}_i + \underline{K}^i_{iET} \underline{E}^i_{iET} + \bar{B}_i \right). \tag{137}$$

Using the event-sampling condition (94) in(137), we get $\dot{L} \leq \sum_{i=1}^{N} (-\breve{K}_i \breve{E}_i + \underline{K}^i_{iET} \mu_i \breve{E}_i + \bar{B}_i)$.

Choosing $\mu_{ik} = 1/\underline{K}^i_{iET}$, the Lyapunov derivative is further simplified such that

$\dot{L} \leq \sum_{i=1}^{N} -\left(\breve{K}_i - 1 \right) \breve{E}_i + \bar{B}_i.$ It can be seen that the formation and velocity tracking errors are

bounded during the inter-event period as long as $k_1 > k_2^2/2 + 3/2, k_3/k_2 > 0.5, K_v > 5/2,$

$\bar{k}_1 > 2\bar{k}_1^2, \bar{k}_3 > 2\bar{k}_3^2$ and since the unknown NN weights are not updated, they remain

constant during the inter-event period. Therefore, from Case (i) and Case (ii), it can be

concluded that: a) the velocity tracking errors, formation errors and the NN weights

estimation errors remain bounded during the inter-event period; b) Since the Lyapunov

function (108) contains all the individual Lyapunov functions and each robot reach

consensus on regulation errors. Due to the event-sampling condition, the measurement

error introduced by the event-sampled feedback is also bounded.

REFERENCES

[1]   T. Dierks and S. Jagannathan, "Neural network output feedback control of robot formations," in *IEEE Transactions on Systems, Man, and Cybernetics, Part B (Cybernetics)*, vol. 40, no. 2, pp. 383- 399, April 2010.

[2]   Y. Hong, J. Hu, and L. Gao, 'Tracking control for multi-agent consensus with an active leader and variable topology,' *Automatica*, 42(7), pp.1177-1182, 2006.

[3]   C. B. Low, 'A dynamic virtual structure formation control for fixed-wing UAVs,' *9th International Conference on Control and Automation (ICCA),* December, pp. 627-632, 2011.

[4]   T. Balch, and R. C. Arkin, 'Behavior-based formation control for multi-robot teams,' *IEEE Transactions on Robotics and Automation*, 14(6), pp.926-939, 1998.

[5]   W. Ren, and R. W. Beard, 'Consensus seeking in multi-agent systems under dynamically changing interaction topologies,' *IEEE Transactions on Automatic Control*, , 50(5), pp.655-661, 2005.

[6]   H. K. Min, F. Sun, S. Wang, and H. Li, 'Distributed adaptive consensus algorithm for networked Euler-Lagrange systems,' *IET Control Theory & Applications*, 5(1), pp.145-154,2011.

[7]   E. Semsar-Kazerooni, and K. Khorasani, 'Analysis of actuator faults in a cooperative team consensus of unmanned systems,' *IEEE ACC'09 American Control Conference*, June, pp. 2618-2623, 2009.

[8]   D. Bauso, L. Giarré and R. Pesenti, 'Consensus for networks with unknown but bounded disturbances,' *SIAM Journal on Control and Optimization*, 48(3), pp.1756-1770, 2009.

[9]   Y. P. Tian, and C. L. Liu, 'Consensus of multi-agent systems with diverse input and communication delays,' *IEEE Transactions on Automatic Control*, 53(9), pp.2122-2128, 2008.

[10]   R. Olfati-Saber, and R. M. Murray, 'Consensus problems in networks of agents with switching topology and time-delays,' *IEEE Transactions on Automatic Control*, 49(9), pp.1520-1533, 2004.

[11]   Z. Qu, 'Cooperative control of dynamical systems: applications to autonomous vehicles,' *Springer Science & Business Media*, 2009.

[12]   L. Sheng, Y. J. Pan, and X. Gong, 'Consensus formation control for a class of networked multiple mobile robot systems,' *Journal of Control Science and Engineering*, pp.1-12, 2012.

[13]   E. Semsar-Kazerooni, and K. Khorasani, 'Optimal consensus algorithms for cooperative team of agents subject to partial information,' *Automatica*, 44(11), pp.2766-2777, 2008.

[14]   P. Tabuada, 'Event-triggered real-time scheduling of stabilizing control tasks,' *IEEE Transactions on Automatic Control,* 52(9), pp.1680-1685, 2007.

[15]   A. Sahoo, H. Xu, and S. Jagannathan, 'Near optimal event-triggered control of nonlinear discrete time systems using neuro-dynamic programming,' *IEEE Transactions on Neural Networks and Learning systems*, (In press), 2015.

[16]   X. Zhong, Z. Ni, H. He, X. Xu and D. Zhao, 'Event-triggered reinforcement learning approach for unknown nonlinear continuous-time system,' *IEEE International Joint Conference on Neural Networks (IJCNN)*, July, pp. 3677-3684, 2014.

[17]   M. Guinaldo, D. Lehmann, J. Sanchez, S. Dormido and K. H. Johansson 'Distributed event-triggered control with network delays and packet losses,' *IEEE 51st Annual Conference on Decision and Control (CDC),* December, pp. 1-6, 2012.

[18]   X. Wang, and M. D. Lemmon, 'Event-triggering in distributed networked control systems,' *IEEE Transactions on Automatic Control*, 56(3), pp.586-601, 2011.

[19]   R. Fierro, and F. L. Lewis, 'Control of a non-holonomic mobile robot using neural networks,' *IEEE Transactions on Neural Networks,* 9(4), pp.589-600, 1998.

IV. MODIFIED CONSENSUS-BASED OUTPUT FEEDBACK CONTROL OF QUADROTOR UAV FORMATIONS USING NEURAL NETWORKS

ABSTRACT

In this paper, a novel nonlinear output feedback neural network (NN)-based consensus controller is developed for a group of quadrotor unmanned aerial vehicles (UAVs). One UAV in the group tracks a desired trajectory while the rest of the group uses consensus-based formation controllers without knowledge of the desired trajectory. Each UAV estimates its own and its neighbor's velocities through a novel nonlinear NN-based observer by using position and orientation information. Neighboring UAV positions and orientation information is assumed to be available via wireless communication or obtained through local sensors. Since quadrotor UAVs have six degree of freedom with only four control inputs, the UAV's pitch and roll angles are utilized as virtual control inputs to bring all UAVs to consensus points along x and y directions. The Lyapunov stability theorem is utilized to demonstrate that all the position errors, orientation errors, velocity tracking errors, observer estimation errors, and NN weight estimation errors are semi-globally uniformly ultimately bounded (SGUUB) in the presence of bounded disturbances. The effectiveness of our consensus-based output feedback formation control of quadrotor UAVs is demonstrated in simulation validating our theoretical claims.

1. INTRODUCTION

Improvements on low-cost wireless communication has led to research on networked autonomous systems in the past 20 years. Inspired by nature, these networked unmanned systems are capable of accomplishing a given task without requiring external supervision.

Quadrotor UAVs are easier to build and maintain when compared to conventional helicopters [1]. However, the dynamics of quadrotor UAVs are not only nonlinear, but also coupled and under-actuated. They have six degree of freedom and can be modeled as having four independent control inputs; one for elevation adjustments and three for rotational control inputs. Many controller schemes are proposed in the literature for trajectory tracking problems of quadrotors [2]-[3] where the control objective is to track the Cartesian position and a yaw angle. Much research has also been dedicated to controlling groups of quadrotor UAVs [1]–[13].

Quadrotor UAV leader-follower formation controller design is introduced in [4] while considering the fourth order linearized dynamics of quadrotors. A relative distance approach is utilized for adaptive leader-follower formation keeping when the GPS signal is lost in [8]. However, the nonlinear quadrotor dynamics are assumed to be exactly known in both [4],[8] which is not realistic in practical applications

An NN-based adaptive formation controller is developed for quadrotor UAVs in [1]. The availability of position, orientation and velocities of the follower as well as the leader for the leader-follower based formation controller design in [1] is quite a strong

assumption, and it may not be practical. Further, there are several limitations of leader-follower-based formation control over the consensus based approach.

First in leader-follower approaches, the controller algorithms need to be uniquely defined for each follower in the network based on its own leader's state information. Therefore, the scalability of traditional leader-follower approaches can be quite difficult whereas the consensus-based formation controller algorithm is scalable since the assignment of relative leaders is not required. In other words, the same algorithm can be duplicated and used for each agent in the network in the consensus scenario to enable scalability. Secondly, for leader-follower approaches, communication disruptions between a leader and its followers results in the follower and the agents behind the follower to lose the desired formation. Consensus-based approaches are not susceptible to these degradations as explained next.

Robustness and reliability are two key benefits of the consensus-based formation control [4]–[8]. In addition, scalability of the consensus-based formation controller enables the formation to continue even if one of the agents in the network experiences a failure. The quadrotor UAVs share information regarding their position errors from their respective reference locations in consensus-based formation control. The shared information is then synthesized into a control law which seeks to achieve the same position error for all quadrotors until each of them has the same position error. The desired formation is achieved and maintained by reaching and maintaining consensus on the position errors. The desired shape of the formation is selected by choosing the reference points of each UAV accordingly.

There are several consensus-based formation control techniques for quadrotor UAVs in the literature [5],[6],[10],[11]. In [5], a consensus based formation control of multiple quadrotor UAVs is developed in the presence of an unknown mass matrix while the rest of the nonlinear dynamics are assumed to be bounded. Additionally, it is assumed that each UAV can access its own states as well as the states of its neighbors. Consensus control of quadrotor formation in the presence of switching topologies is considered in [6], while time delays and switching topologies are considered for the consensus-based controller design in [11]. In both works [6],[11], linearized quadrotor UAV dynamics are considered.

Consensus-based formation control of quadrotor UAV formation is delivered in the presence of second order nonlinear UAV dynamics and switching topologies in [10] wherein the full state availability of the follower UAV, state measurements of the leader UAV and knowledge of the nonlinear UAV dynamics are needed. However, assuming the dynamics are completely known is not practical [1]. Highly nonlinear dynamics of quadrotor UAVs such as aerodynamics friction dynamics have either been simplified or ignored in all previous consensus-based control techniques, which can be seen in [5],[6],[10],[11].

In [12], the nonlinear dynamics-like aerodynamics friction became significant at high speeds. In [13], the authors developed output feedback tracking control of a single UAV in the presence of uncertain nonlinear quadrotor dynamics, and its stability analysis is demonstrated. Nevertheless, developing consensus-based output feedback formation control of quadrotor UAVs in the presence of uncertain dynamics is still an open problem.

In this paper, a novel consensus-based output feedback formation controller is developed for a group of quadrotor UAVs in the presence of uncertain quadrotor dynamics. A modified consensus-based formation controller is considered where a designated formation leader tracks its own trajectory independently from the other UAVs in the formation [20]. The other UAVs in the formation have no knowledge about the leader's desired trajectory.

Each UAV is assumed to share its position and velocity states with neighboring UAVs via wireless communication. Alternatively, each UAV may obtain the required states through local sensors when the shared communication is not available. A novel NN-based extended observer is developed for each follower UAV to estimate its own velocities as well as its neighbors. To support UAVs joining or leaving a formation or neighborhood, a novel size reduction matrix is defined to remove the zero elements in the observer design corresponding to the states of a UAV that has left the formation. The size reduction matrix provides a method to ensure that an invertible observer matrix is always available.

Each UAV determines its consensus-based formation errors by using the position, orientation, reference location and estimated velocities of neighbors. Since the underactuated quadrotor UAVs have no direct control over the position errors along x and y directions, novel desired pitch and roll angles are utilized as virtual controllers to reach consensus for those directions. An elevation controller is also developed by considering the formation error along z direction.

The contribution of the NN-based consensus-based output feedback control of the quadrotor UAV formation includes the following: 1) the design of a novel NN based nonlinear extended observer which explicitly considers the time varying topology of the

network to estimate the velocity of the UAV under consideration and its neighbors which enables the quadrotors to maintain any desired formation shape—even without communication among each other; 2) the development of a novel 'size reduction matrix' scheme to avoid invertibility issues in the observer design of the group of UAVs in the presence of time varying network topology; 3) the development of a nonlinear consensus-based output feedback-adaptive formation control technique for a group of quadrotor UAVs; and 4) demonstration of formation keeping using any number of quadrotors in the presence of changing communication topologies through Lyapunov analysis.

The remainder of the paper is organized as follows. Section 2 presents a brief background on quadrotor UAV dynamics, NNs, and random graphs. Section 3 provides the observer and controller design of the leader UAV. Section 4 discusses the main results and derives the consensus-based output feedback formation controller design. Before offering conclusions in Section 6, Section 5 provides simulation results to support the theoretical conjectures.

2. BACKGROUND AND PRELIMINARIES

This section presents a brief background on NNs, random graphs, quadrotor UAV dynamics, and the modified consensus formation control approach considered in this work. Notice that an agent is interchangeably used throughout this paper for a UAV.

2.1 NEURAL NETWORKS

Two layer NNs are considered in this work which consist of one layer of tunable hidden weights, $W \in \mathbb{R}^{L \times b}$, and another randomly assigned constant weights layer, $\bar{N} \in \mathbb{R}^{a \times L}$, where a denotes the number of inputs, b is the number of outputs and L being the number of neurons on the hidden layer NN. Any smooth function $f(x)$ can be approximated [19] through a two-layer NN as $f(x) = W^T \sigma(\bar{N}^T x) + \varepsilon$, where ε is the bounded NN approximation error such that $\|\varepsilon\| < \varepsilon_M$, and $\sigma(\bullet): \mathbb{R}^a \to \mathbb{R}^L$ is the hidden layer activation function. The approximation property holds for any input x since the input layer weights $\bar{N}$ are randomly selected; therefore, the activation function, $\sigma(x) = \sigma(\bar{V}^T x)$, forms a stochastic basis in the compact set, S [19]. In this work, a sigmoid activation function is utilized. Further, the target weights are assumed to be bounded by a known positive value W_M such that $\|W\|_F < W_M$ on any compact subset of $\mathbb{R}^n$ [19]. Throughout this work, $\|\bullet\|$ and $\|\bullet\|_F$ will be used as the vector and Frobenius norm, respectively [19]. For complete details of NN, refer to [19]. The definition of semi-globally uniformly ultimately bounded (SGUUB) is introduced next.

Definition 1: The equilibrium point x_e is said to be SGUUB if there exists a ball centered around the origin with an arbitrary radius r $S(0,r) = S_r \subset \mathbb{R}^n$ so that for all $x_0 \in \mathbb{R}^n$, there exists a bound $B > 0$ and a time $T(B, x_0)$ such that $\|x(t) - x_e\| \leq B$ for all $t > t_0 + T$. Further, the stability result becomes globally uniformly ultimately bounded (GUUB) if $S_r = \mathbb{R}^n$ [13].

Next, some background information is provided on the Random graph.

2.2   RANDOM GRAPH

A graph is a symbolical presentation of network connectivity, which can be considered as a virtual set of connected nodes. A random graph is a graph that is obtained by randomly sampling from a collection of graphs. In [10], the set of edges and the vertices of a graph $\Gamma = (\vee, E)$ are denoted by $\vee$ and E, respectively. In this work, for a random graph on N vertices, the existence of an edge between a pair of vertices in the set $\overline{C} = \{1, 2, \ldots, N\}$ is determined at random and independent of other edges. Define the sample space of the random graph as P and let $p(t)$ be a topology indicator such that $\mathrm{p} : R^+ \to M$. Also, let t_k's be the switching times of the edges in a dynamical graph, $\Gamma(t)$, with $t_k \in R^+, k = 1, 2, \ldots$ Note that the indicator, $p(t)$, is a piecewise left continuous function which remains constant during the time interval $t \in [t_k, t_{k+1})$ and changes to another topology in P at t_{k+1}. In a realistic communication scenario, collisions, channel fading or noises may cause packet exchanging problems among nodes.

Assumption 1 [4]: Even though the connectivity graph can change at random in a certain time instant, t_k's , the graph is assumed to remain connected at any given time.

Connectedness physically means, networked agents, that there is no isolated agent in the network. In other words, each agent (or UAV) receives at least one other UAV's information and transmits its information to at least one other UAV.

For the dynamical network $\Gamma(t)$ with N vertices, the adjacency matrix is defined as

$$H(t) = \{h_{ij}(t)\}_{N \times N} \tag{138}$$

with $h_{ij}(t) = 1$ if information flows from agent j to agent i at time t; otherwise, $h_{ij}(t) = 0$.

The corresponding time varying Laplacian matrix is defined as $L(p(t)) = [l_{ij}(p(t))]_{N \times N}$

where $l_{ij}(t) = -h_{ij}(t)$ if $i \neq j$, $l_{ij}(t) = \sum_{k=1}^{N} h_{ik}(t)$ if $i = j$.

Let the connectivity of the ith agent be fixed during the time period, which is known as a dwell time in the literature, $\left[t_{si}^k, t_{fi}^k\right]$ where t_{si}^k and t_{fi}^k begin with k^{th} starting and final time of the ith agent's communication network topology, respectively. Assume that $0 < \inf_k \{t_{fi}^k - t_{si}^k\} \leq \sup_k \{t_{fi}^k - t_{si}^k\} < +\infty$ [10].

2.3   QUADRATOR UAV DYNAMICS

Consider a quadrotor UAV with six degree of freedom in the inertial coordinate frame, E^a , as $\left[\rho_i^T \quad \Theta_i^T\right] \in E^a$ where $\rho_i^T = \begin{bmatrix} x_i & y_i & z_i \end{bmatrix}^T \in E^a$ are the Cartesian positions of ith UAV and $\Theta_i^T = \begin{bmatrix} \phi_i & \theta_i & \psi_i \end{bmatrix}^T \in E^a$ describes the orientation of the ith UAV referred

to as roll, pitch, and yaw angles, respectively. The translational and angular velocities of ith UAV are given in the body-fixed frame attached to the center of the UAV E^b. The dynamics of the UAV in the body fixed frame are given by [13]

$$M_i \begin{bmatrix} \dot{v}_i \\ \dot{w}_i \end{bmatrix} = \bar{S}_i(w_i) \begin{bmatrix} v_i \\ w_i \end{bmatrix} + \begin{bmatrix} N_1(v_i) \\ N_2(w_i) \end{bmatrix} + \begin{bmatrix} G_i(R) \\ 0_{3\times 1} \end{bmatrix} + U_i + \tau_{di} \tag{139}$$

where $U = \begin{bmatrix} 0 & 0 & u_{i1} & u_{i2}^T \end{bmatrix}^T \in \mathbb{R}^6$, $M_i = diag\{m_i I_3, J_i\} \in \mathbb{R}^{6\times 6}$, m_i is the total mass of the ith UAV, $J_i \in \mathbb{R}^{3\times 3}$ $v_i = \begin{bmatrix} v_{xi} & v_{yi} & v_{zi} \end{bmatrix}^T \in \mathbb{R}^3$, and $w_i = \begin{bmatrix} w_{xi} & w_{yi} & w_{zi} \end{bmatrix}^T \in \mathbb{R}^3$, $N_i(\bullet) \in \mathbb{R}^{3\times 1}, i = 1,2$ represents the positive definite inertia matrix, the translational velocities, the angular velocity and the nonlinear aerodynamic effects, respectively, u_{i1} provides the thrust along the z direction while $u_{2i} \in \mathbb{R}^3$ provides the rotational torques, $\tau_{di} = \begin{bmatrix} \tau_{d1i}^T & \underline{\tau}_{d2i}^T \end{bmatrix} \in \mathbb{R}^6, \tau_{d1i}^T \in \mathbb{R}^3, \tau_{d2i}^T \in \mathbb{R}^3$ represents the unknown, but bounded disturbances such that $\|\tau_{di}\| < \tau_M$ for all time t, with τ_M being and unknown positive constant, $I_{n\times n} \in \mathbb{R}^{n\times n}$ is an $n\times n$ identity matrix, and $0_{m\times l} \in \mathbb{R}^{m\times l}$ is an $m\times l$ matrix of all zeros. Further, $G_i(R) \in \mathbb{R}^3$ is the gravity vector, $\bar{S}_i(w_i) = diag\{-m_i S_i(w_i), S_i(J_i w_i)\} \in \mathbb{R}^{6\times 6}$ with $S(\bullet) \in \mathbb{R}^{3\times 3}$ representing the general form of a skew symmetric matrix as defined in [13].

The matrix, $R_i \in \mathbb{R}^{3\times 3}$ is the translational rotation matrix, which is used to rotate a vector in the body fixed frame to the inertial coordinate frame given as a solution similar to [13] as

$$R_i(\Theta_i) = R_i = \begin{bmatrix} c_\theta c_\psi & s_\phi s_\theta c_\psi - c_\phi s_\psi & c_\phi s_\theta c_\psi + s_\phi s_\psi \\ c_\theta s_\psi & s_\phi s_\theta c_\psi + c_\phi s_\psi & c_\phi s_\theta c_\psi - s_\phi s_\psi \\ -s_\theta & s_\phi c_\theta & c_\phi c_\theta \end{bmatrix},$$

where the abbreviations $s_{(\bullet)}$ and $c_{(\bullet)}$ have been used for $\sin(\bullet)$ and $\cos(\bullet)$, respectively. It

is important to note that $\|R_i\|_F = R_{max}$ for a known constant, R_{max}, $R_i^{-1} = R_i^T$, $\dot{R}_i = R_i S_i(w_i)$

, and $\dot{R}_i^T = -S_i(w_i) R_i^T$. It is also necessary to define a rotational transformation matrix

from the fixed body to the inertial coordinate frame as in [13]

$$T_i(\Theta_i) = T_i = \begin{bmatrix} 1 & s_\phi t_\theta & c_\phi t_\theta \\ 0 & c_\phi & -s_\phi \\ 0 & s_\phi/c_\theta & c_\phi/c_\theta \end{bmatrix}, \quad T_i^{-1} = \begin{bmatrix} 1 & 0 & -s_\theta \\ 0 & c_\phi & s_\phi/c_\theta \\ 0 & -s_\phi & c_\phi/c_\theta \end{bmatrix} \text{ where abbreviation } t_{(\bullet)} \text{ has}$$

been used for $\tan(\bullet)$. The transformation matrix T_i is bounded as long as

$-(\pi/2) < \phi_i < (\pi/2)$, $-(\pi/2) < \theta_i < (\pi/2)$, and $-\pi \le \psi_i \le \pi$. These regions will be

referred to as the stable operation regions of the UAV, and under these mild conditions, it

is observed that $\|T_i\|_F < T_{max}$.

Using the notations defined above, the kinematics of the ith UAV can be written

as

$$\dot{\rho}_i = R_i v_i$$

$$\dot{\Theta}_i = T_i w_i. \tag{140}$$

Next, the modified consensus-base formation control approach considered in this

work is introduced.

2.4   MODIFIED CONSENSUS-BASED FORMATION CONTROL

In this paper, a novel consensus-based NN output feedback formation controller is developed for a group of N UAVs. The leader UAV and N follower UAVs are assumed to have the dynamics in the form of (139). In the modified-consensus based approach, the leader tracks its own trajectory without considering the formation [20]. The remaining UAVs in the formation, the followers, implement consensus-based controllers which allow all UAVs within the formation to track the same trajectory as the formation leader even though the leader's desired trajectory is not explicitly known by the formation.

To achieve this objective, a time-invariant reference point is assigned to each follower UAV as well as the leader UAV in three dimensional space as illustrated in Figure 2.1. The consensus based formation controllers of follower UAVs provide consensus on the distance of each UAV from its reference point, while each UAV also tracks an independent desired yaw angle, ψ_i^d. In other words, the shape of the formation is provided by choosing the reference points accordingly. In order to get the desired formation, consensus on regulation errors on the x, y and z directions is provided through the controllers. In [20], a modified-consensus based approach is utilized for linear systems with known system dynamics through state feedback controller. However, our approach deals with uncertain nonlinear quadrotor dynamics and doesn't require all states of the neighbor UAVs.
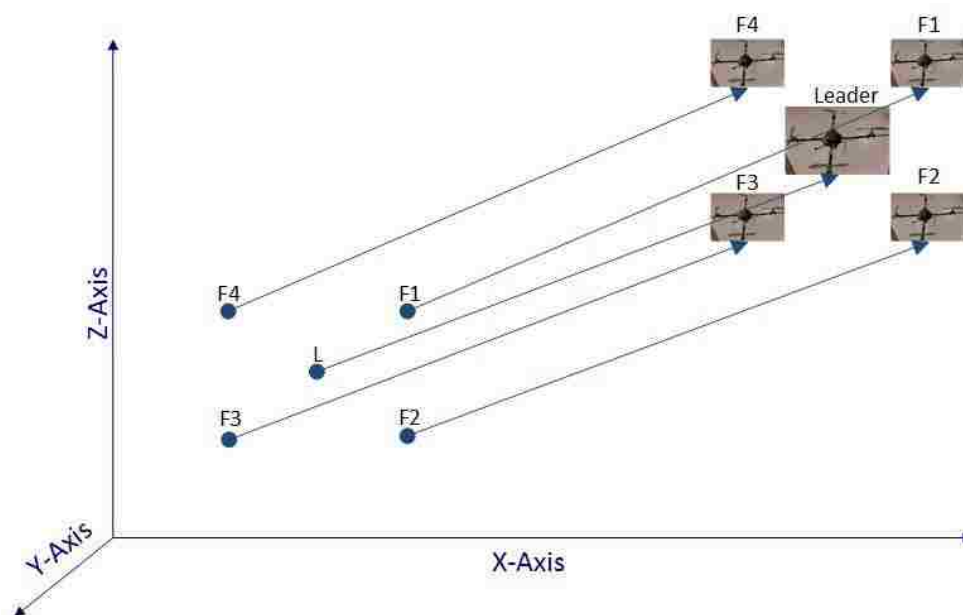
Figure 2.1 Consensus based flight formation of a group of quadrotor UAVs.

3. SINGLE UAV CONTROL

In this work, a modified consensus-based formation controller is considered where designated formation leader tracks its own trajectory without considering the formation [20]. Therefore, this section presents a trajectory tracking controller for the single quadrotor UAV, or agent, which will serve as the formation leader. First the NN-based observer design is presented followed by the NN-based output feedback backstepping controller similar to [1].

3.1 FORMATION LEADER NN OBSERVER DESIGN

To estimate the translational and angular velocities of UAVs, an NN based observer is designed in [13] without explicit knowledge of the UAV dynamics in (139). To begin, define the augmented vectors as $X = \begin{bmatrix} \rho^T & \Theta^T \end{bmatrix}^T$ and $\bar{V} = \begin{bmatrix} v^T & w^T \end{bmatrix}^T$ which have dynamics defined in (140) and (139), respectively. They can also be rewritten as [13]

$$\dot{X} = A(t)\bar{V} + \zeta_1$$

$$\dot{\bar{V}} = f_o(x_o) + \bar{G} + M^{-1}U + \bar{\tau}_d \qquad (141)$$

with ζ_1 being bounded sensor measurement noise such that $\|\zeta_1\| < \zeta_{1M}$ for a known constant ζ_M, $f_o(x_o) = M^{-1}\left(\bar{S}(w)\bar{V} + \begin{bmatrix} N_1(v) & N_2(w) \end{bmatrix}^T\right)$ with $x_0 = \bar{V}$,

$\bar{G} = M^{-1}G(R) \in \mathbb{R}^6$, $\bar{\tau}_d = \begin{bmatrix} \bar{\tau}_{d1}^T & \bar{\tau}_{d2}^T \end{bmatrix}^T = \begin{bmatrix} \tau_{d1}^T/m & J^{-1}\tau_{d2}^T \end{bmatrix}^T \in \mathbb{R}^6$ and

$$A(t) = A = \begin{bmatrix} R & 0_{3\times3} \\ 0_{3\times3} & T \end{bmatrix}. \qquad (142)$$

Next, define a change of variable as $Z = \bar{V}$ whose time derivative is given as (141)

[13]. Then, define the NN observer estimation of X and Z as $\hat{X}$, $\hat{Z}$, respectively, as well

as the observer estimation errors $\tilde{X} = X - \hat{X}$. The observer is now proposed as [13]

$$\dot{\hat{X}} = A\hat{Z} + K_{o1}\tilde{X}$$

$$\dot{\hat{Z}} = \hat{f}_{o1} + \bar{G} + K_{o2}A^{-1}\tilde{X} + M^{-1}U \tag{143}$$

where K_{o1} and K_{o2} are positive design constants. The observer velocity estimation is

written as [13]

$$\hat{V} = \begin{bmatrix} \hat{v}^T & \hat{w}^T \end{bmatrix}^T = \hat{Z} + K_{o3}A^{-1}\tilde{X} \tag{144}$$

with K_{o3} being a positive design constant. The uncertain nonlinear function in (143) is

estimated through a two layer NN as $\hat{f}_{o1} = \hat{W}_o^T \sigma\left(V_o^T \hat{x}_o\right) = \hat{W}_o^T \hat{\sigma}_o$ where $\hat{W}_o^T$ is the estimate

of W_o^T , and $\hat{x}_o$ is the NN input written in terms of the observer velocity estimates as

$\hat{x}_o = \begin{bmatrix} 1 & \hat{X}^T & \hat{V}^T & \tilde{X}^T \end{bmatrix}^T$. Define the estimation error of the velocity vector as $\tilde{V} = \bar{V} - \hat{V}$,

then the following lemma holds.

Lemma 1 [13]: Let the NN observer be defined by (143) and (144), and let the NN

observer weights be tuned by

$$\dot{\hat{W}}_o = F_o \hat{\sigma}_o \tilde{X}^T - \kappa_{o1} F_o \hat{W}_o \tag{145}$$

where $F_o = F_o^T > 0$ and $\kappa_{o1} > 0$ are design parameters. Then, there exists positive constant

design parameters K_{o1}, K_{o2} and K_{o3} where $K_{o1} > K_{o3} + \left(2N_o\right)/\kappa_{o1}$, $K_{o3} > \left(2N_0\right)/\kappa_{o1}$, and

$K_{o2} = K_{o3}\left(K_{o1} - K_{o3}\right)$ with N_0 the number of neurons in the hidden layer NN, such that

observer estimation errors $\tilde{X}$, $\tilde{V}$ and the NN observer weight estimation errors

$\tilde{W}_o = W_o - \hat{W}_o$ are SGUUB.

Proof: See [13].

Next, the controller of the leader UAV is given.

3.2 LEADER UAV CONTROLLER DESIGN

In this section, the desired linear and angular velocities are defined by considering

the velocity tracking error. Since the velocity tracking errors on x and y directions are

not directly actuated [13], desired pitch and roll angles are designed to bring the UAV to

the desired x and y location. The velocity tracking error on z axis is controlled through

u_1 while the angular velocity tracking errors are controlled through u_2. To begin, consider

the position error

$$\bar{e}_\rho = \rho^r - \rho \in E^a \tag{146}$$

with $\rho^r, \dot{\rho}^r$ being the given reference position and velocity state vectors to track in three

dimensional space. Differentiating (146) and using (140) yields

$$\dot{\bar{e}}_\rho = \dot{\rho}^r - Rv \ . \tag{147}$$

The desired translational velocity is selected to stabilize the position error dynamics

(147) as

$$v^d = \begin{bmatrix} v_x^d & v_y^d & v_z^d \end{bmatrix}^T = R^T \left(\dot{\rho}^r + K_\rho \bar{e}_\rho \right) \tag{148}$$

where $K_\rho = diag\{k_{\rho x}, k_{\rho y}, k_{\rho z}\} \in \mathbb{R}^{3\times 3}$ is a diagonal positive definite matrix. Substituting

(148) into (147) and considering the velocity tracking error $\bar{e}_c = v^d - v = \begin{bmatrix} e_{vx} & e_{vy} & e_{vz} \end{bmatrix}^T$

yields the closed loop translational tracking error

$$\dot{\bar{e}}_\rho = -K_\rho \bar{e}_\rho + R\bar{e}_c \quad . \tag{149}$$

Then, the translational velocity tracking error dynamics are obtained as

$$\dot{e}_c = \dot{v}_d - \dot{v} = -\frac{1}{m} N_1(v) - S(w)e_c - \frac{1}{m}G(R) - \frac{1}{m}u_1 E_z + R^T \left(\ddot{\rho}^r + K_\rho \dot{\rho} - K_\rho Rv \right) - \bar{\tau}_{d1} \tag{150}$$

with $E_z = \begin{bmatrix} 0 & 0 & 1 \end{bmatrix}^T$. Realize that velocity tracking errors in (150) along x and y directions

are not directly controllable through u_1. Therefore, x and y components of the velocity

tracking errors are controlled through desired pitch and roll angles defined as

$$\theta_d = a\tan\left(\frac{c_{\psi d}\bar{x} + s_{\psi d}\bar{y} + k_{v1}\hat{e}_{vx}}{\bar{z} - g} \right) ,$$

$$\phi_d = a\tan\left(\frac{c_{\psi d}\bar{y} + s_{\psi d}\bar{x} + k_{v2}\hat{e}_{vy}}{gc_{\theta d} - c_{\theta d}\bar{z} - s_{\theta d}c_{\psi d}\bar{y} - s_{\theta d}c_{\psi d}\bar{x}} \right) \tag{151}$$

with $\bar{x} = \ddot{x}_d + k_{\rho x}\dot{x}_d - \hat{v}_{R1} + \hat{f}_{c11}$, $\bar{y} = y_d + k_{\rho y}\dot{y}_d - \hat{v}_{R2} + \hat{f}_{c12}$ $\bar{z} = \ddot{z}_d + {}_\rho k_z \hat{z}_{-3} \dot{y}_{+1}$,

x_d, y_d, z_d are the desired locations, $\hat{f}_{1c} = \begin{bmatrix} \hat{f}_{11c} & \hat{f}_{12c} & \hat{f}_{13c} \end{bmatrix}^T$ is the NN estimation of the

unknown part of the translational velocity tracking error dynamics (150). Recall that the

actual velocities are assumed to be unavailable in this work; therefore, the velocity tracking

errors are written using observer estimated velocities defined as $\begin{bmatrix} \hat{e}_{vx} & \hat{e}_{vy} & \hat{e}_{vz} \end{bmatrix}^T = v^d - \hat{v}$.

Moving on, the thrust control input and the rotational control inputs are given as

$$u_1 = mk_{v3}\hat{e}_{vz} + m\left(c_{\phi d}s_{\theta d}c_{\psi d} + s_{\phi d}s_{\psi d} \right)\bar{x} + m\left(c_{\phi d}s_{\theta d}c_{\psi d} - s_{\phi d}s_{\psi d} \right)\bar{y} + mc_{\phi d}c_{\theta d}\left(\bar{y} - g \right), \tag{152}$$

$$u_2 = \hat{f}_{c2} + K_\omega \hat{e}_\omega \ , \tag{153}$$

respectively, where $\hat{f}_{2c}$ is the NN estimation of the unknown part of angular velocity tracking error dynamics, K_ω is a constant design matrix, and $\hat{e}_\omega$ is the estimated velocity tracking error. The details of the single UAV controller design (151),(152),(153) can be seen in [1].

Next, an NN consensus-based output feedback formation controller design of quadrotor UAV formation is provided.

4. CONSENSUS-BASED FORMATION CONTROL

In this section, a novel consensus-based NN output feedback formation controller is developed for the follower UAVs. The proposed consensus based approach has two fundamental benefits over traditional leader-follower based controllers [1]. First, output feedback formation control enables to keep desired formation with limited communication or using only local sensors without communication among the UAVs. Second, relative leaders for each UAV needs to be assigned in [1], and the follower UAVs will lose formation when the communication with its local leader. In this work, relative or local leaders are not required. Instead, each UAV utilizes its neighbors' states for the formation controller, and the neighbors can be updated over time as UAVs join and leave the formation.

To being the controller development, the desired translational velocities are developed as a virtual kinematic controller. Then, the dynamic controller is developed to stabilize the velocity tracking error dynamics. Desired pitch and roll angles are obtained to make sure the translational velocities on x and y directions achieve the desired velocities. Each UAV tracks an independent desired yaw angle, ψ_i^d; therefore, once the desired pitch roll and yaw angles are on hand, the desired angular velocity is developed to keep desired angles. Both the angular and translational velocities are assumed unmeasurable and NN-based observers are utilized to recover the unknown states.

4.1 EXTENDED OBSERVER DESIGN

Assume that each UAV is communicating with ξ_i number of other UAVs in its neighborhood set, N_i. Unlike traditional observers designed to estimate only local states, such as velocities [13], the extended observer presented in this section estimates the ith UAV's velocities as well as its neighbor UAVs' velocities.

The extended observer design considers the communication topology among the UAVs explicitly through the adjacency matrix commonly used in graph theory. Therefore, consider the ith row of the adjacency matrix (138) of the ith UAV and define it as $H_i(t)$. By using $H_i(t)$, a novel matrix is defined for size reduction and row shifting of matrices as $Q_i(t) = \{q_{kj}(t)\} \in \mathbb{R}^{\xi_i \times N}$ where $q_{kj}(t) = 1$ if and only if there is information flows from the jth UAV to the ith UAV and the jth UAV is the kth non-zero element in $H_i(t)$ at time t; otherwise, $q_{kj} = 0$.

Combine all the states of UAV's in the network (neighboring set) and define the augmented vectors as

$$X = \begin{bmatrix} X_1^T & \cdots & X_{Ni}^T \end{bmatrix}^T \in \mathbb{R}^{6N \times 1} \quad \bar{V} = \begin{bmatrix} \bar{V}_i^T & \cdots & \bar{V}_{Ni}^T \end{bmatrix}^T \in \mathbb{R}^{6N \times 1}.$$

Define the augmented states for each UAV as

$$X_{\xi i} = \begin{bmatrix} X_i^T & \left((Q_i \otimes I_{6 \times 6}) X \right)^T \end{bmatrix}^T$$

$$\bar{V}_{\xi i} = \begin{bmatrix} \bar{V}_i^T & \left((Q_i \otimes I_{6 \times 6}) \bar{V} \right)^T \end{bmatrix}^T. \tag{154}$$

The dynamics of the new augmented states (154) are given as

$$\dot{X}_{\xi i} = A_{\xi i}(t)\bar{V}_{\xi i} + \zeta_{1\xi i}$$

$$\dot{\bar{V}}_{\xi i} = f_{o\xi i}(x_{o\xi i}) + \bar{G}_{\xi i} + M_{\xi i}^{-1}U_{\xi i} + \bar{\tau}_{d\xi i} \tag{155}$$

where $\zeta_{1\xi i} \in \mathbb{R}^{12(p+1)}$ represents bounded sensor measurement noises of each UAV such

that $\|\zeta_{1\xi i}\| \leq \zeta_{1Mi}, N_i, \quad U_{\xi i} = \begin{bmatrix} U_i^T & U_{ni}^T \end{bmatrix}^T \in \mathbb{R}^{6(\xi_i+1)}$ with $U_{ni} = \{U_j^T\} \in \mathbb{R}^{6\xi_i}, j \in N_i$, and

$\bar{\tau}_{dNi} \in \mathbb{R}^{12(p+1)}$ are being the controller inputs and the bounded disturbances of the neighbor

UAVs'. The terms $A_{\xi i} = diag\{A_i \quad A_{ni}\} \in \mathbb{R}^{6(\xi_i+1)\times 6(\xi_i+1)}, \bar{G}_{\xi i} = diag\{\bar{G}_i \quad \bar{G}_{ni}\} \in \mathbb{R}^{6(\xi_i+1)\times 6(\xi_i+1)}$

$M_{\xi i} = diag\{M_i \quad M_{ni}\} \in \mathbb{R}^{6(\xi_i+1)\times 6(\xi_i+1)}$ with

$$A_{ni} = (Q_i \otimes I_{6\times 6})diag\{A_j\}(Q_i \otimes I_{6\times 6})^T \in \mathbb{R}^{12\xi_i \times 12\xi_i}, j \in N$$

$$\bar{G}_{ni} = (Q_i \otimes I_{6\times 6})diag\{\bar{G}_j\}(Q_i \otimes I_{6\times 6})^T \in \mathbb{R}^{12\xi_i \times 12\xi_i}, j \in N$$

$$M_{ni} = (Q_i \otimes I_{6\times 6})diag\{M_j\}(Q_i \otimes I_{6\times 6})^T \in \mathbb{R}^{12\xi_i \times 12\xi_i}, j \in N \text{ are square diagonal matrices,}$$

and

$$f_{o\xi i}(x_{o\xi i}) = \begin{bmatrix} f_{oi}^T(x_{oi}) & f_{oni}^T(x_{oni}) \end{bmatrix}^T \in \mathbb{R}^{6(\xi_i+1)} \text{ where } f_{oni}^T(x_{oni}) = \{f_{oi}^T(x_{oi})\} \in \mathbb{R}^{6\xi_i}, \forall j \in N_i$$

are the uncertain nonlinear dynamics vector of all neighbor UAV with $x_{oni} \in \mathbb{R}^{6\xi_i \times 1}$ being

the vector which contains all the linear and angular velocities of the neighbor UAVs.

Further, there exists a positive constant upper bound such that $\|A_{\xi i}^{-1}\|_F \leq A_{Mi}^I$.

Define a change of variables as $Z_{\xi i} = \bar{V}_{\xi i}$, and denote the NN observer estimation

of $X_{\xi i}$ and $\bar{V}_{\xi i}$ as $\hat{X}_{\xi i}$ and $\hat{V}_{\xi i}$, respectively, with observer estimation errors written as

$\tilde{X}_{\xi i} = X_{\xi i} - \hat{X}_{\xi i}$ and $\tilde{V}_{\xi i} = \bar{V}_{\xi i} - \hat{V}_{\xi i}$, respectively. Then, our proposed observer takes the form of

$$\dot{\hat{X}}_{\xi i} = A_{\xi i}\hat{Z}_{\xi i} + K_{o1}\tilde{X}_{\xi i}$$

$$\dot{\hat{Z}}_{\xi i} = \hat{f}_{o1\xi i} + \bar{G}_{\xi i} + K_{o2}A_{\xi i}^{-1}\tilde{X}_{\xi i} + M_{\xi i}^{-1}U_{\xi i} \ . \tag{156}$$

The reduction matrix is fixed during the dwell time, the time between two communication graphs switching, of ith UAV as assumed before. Observe that $A_{\xi i}^{-1}, M_{\xi i}^{-1}$ are needed in (156), and each can be calculated by using the matrices $R_i, T_i, R_j, T_j, M_j \ \forall j \in N_i$ since they are invertible individually and the zero terms are removed using the transformation matrix, Q_i. Additionally, the inverse is upper bounded $\left\| A_{\xi i}^{-1} \right\| \le A_{Mi}$ with A_{Mi} being a positive constant, [13]. Then, the velocity estimation of ith UAV and its neighbor UAVs are proposed as

$$\hat{V}_{\xi i} = \begin{bmatrix} \hat{v}_i^T & \hat{w}_i^T & \hat{v}_{Ni}^T & \hat{w}_{Ni}^T \end{bmatrix}^T = \hat{Z}_{\xi i} + K_{o3}A_{\xi i}^{-1}\tilde{X}_{\xi i} \tag{157}$$

with $\hat{v}_{Ni} \in \mathbb{R}^{3p}, \hat{w}_{Ni} \in \mathbb{R}^{3p}$ being the linear and angular velocity estimates of neighbor UAVs, respectively.

Noting $\hat{Z}_{\xi i} = \hat{V}_{\xi i} - K_{o3}A_{\xi i}^{-1}\tilde{X}_{\xi i}$ from (157) and the definition of $\dot{\hat{Z}}_{\xi i}$ above, adding and subtracting $\left(A_{\xi i}^T - K_{o3}\dot{A}_{\xi i}^{-1} \right)\tilde{X}_{\xi i}$ to the error dynamics of the observer estimation error gives

$$\dot{\tilde{X}}_{\xi i} = A_{\xi i}\tilde{V}_{\xi i} - \left(K_{o1} - K_{o3} \right)\tilde{X}_{\xi i} + \zeta_{1\xi i}$$

$$\dot{\tilde{Z}}_{\xi i} = \left(f_{o\xi i} + \left(A_{\xi i}^T - K_{o3}\dot{A}_{\xi i}^{-1} \right)\tilde{X}_{\xi i} \right) - \hat{f}_{o1\xi i} - K_{o2}A_{\xi i}^{-1}\tilde{X}_{\xi i} - \left(A_{\xi i}^T - K_{o3}\dot{A}_{\xi i}^{-1} \right)\tilde{X}_{\xi i} + \bar{\tau}_{d\xi i} . \tag{158}$$

The uncertain function $f_{o1\xi i}$ in (156) is written $f_{o1\xi i} = W_{o\xi i}^T \sigma\left(V_{o\xi i}^T x_{o\xi i}\right) + \varepsilon_o$ with the constant ideal bounded weights subject to $\left\|W_{o\xi i}\right\|_F \leq W_{oMi}$ for a known constant W_{oMi}. The term ε_o represents the bounded NN approximation error such that $\left\|\varepsilon_{oi}\right\| \leq \varepsilon_{oMi}$ for a constant ε_{oMi}. The NN estimate is given as $\hat{f}_{o1\xi i} = \hat{W}_{o\xi i}^T \sigma\left(V_{o\xi i}^T \hat{x}_{o\xi i}\right) = \hat{W}_{o\xi i}^T \hat{\sigma}_{\xi i}$ with $\hat{W}_{o\xi i} = diag\left\{\hat{W}_{oi} \quad \hat{W}_{oni}\right\}$ where $\hat{W}_{oni} = \left(Q_i \otimes I_{6\times 6}\right) diag\left\{\hat{W}_{oj}\right\}\left(Q_i \otimes I_{6\times 6}\right)^T$, $j \in N$ and the NN weight estimation error is written as $\tilde{W}_{o\xi i} = W_{o\xi i} - \hat{W}_{o\xi i}$ with $W_{o\xi i}$ being the ideal NN weights and $\hat{x}_{o\xi i} = \left[1, \hat{X}_i^T, \hat{V}_i^T, \tilde{X}_i^T, \hat{X}_j^T, \hat{V}_j^T, \tilde{X}_j^T\right]$, $\forall j \in N_i$ is the NN input vector.

Moving on and adding and subtracting $W_{o\xi i}^T \sigma\left(V_{o\xi i}^T \hat{x}_{o\xi i}\right)$, and using (158), the observer estimation error dynamics becomes

$$\dot{\tilde{V}}_{\xi i} = -K_{o3}\tilde{V}_{\xi i} + \tilde{f}_{o1\xi i} - A_{\xi i}^{-1}\left(K_{o2} - K_{o3}\left(K_{o1} - K_{o3}\right)\right)\tilde{X}_{\xi i} - A_{\xi i}^T \tilde{X}_{\xi i} + \zeta_{2\xi i} \tag{159}$$

where $\tilde{f}_{o\xi i} = \tilde{W}_{o\xi i}^T \hat{\sigma}_{\xi i}$, $\tilde{W}_{o\xi i} = W_{o\xi i} - \hat{W}_{o\xi i}$, $\zeta_{2\xi i} = \varepsilon_o + \bar{\tau}_{d\xi i} - K_{o3}A_{\xi i}^{-1}\zeta_{1\xi i} + W_{o\xi i}\tilde{\sigma}_{\xi i} \in \mathbb{R}^6$, and $\tilde{\sigma}_{\xi i} = \sigma_{\xi i} - \hat{\sigma}_{\xi i}$. Realize that $\left\|\zeta_{2\xi i}\right\| \leq \zeta_{2Mi}$ with ζ_{2Mi} being a positive computable design constant defined as $\zeta_{2Mi} = \varepsilon_{Moi} + M_{Mi}\tau_{Mi} + K_{o3}A_{Mi}^I\zeta_{1Mi} + 2W_{0Mi}\sqrt{N_{oi}}$ where $M_{Mi} = \left\|M_i^{-1}\right\|_F$. The known constant N_{oi} is the number of neurons in the hidden layer NN of ith UAV which allows the upper bound of the activation function vector to be written as $\left\|\sigma_{oi}\right\| \leq \sqrt{N_{oi}}$.

Next, the theorem statement is given to provide stability of the extended observer design.

Theorem 1: Let the NN-based observer be defined by (156) and (157) for the UAVs and let the NN weights be tuned according to

$$\dot{\hat{W}}_{o\xi i} = F_{o\xi i} \hat{\sigma}_{o\xi i} \tilde{X}_{\xi i}^T - \kappa_{o1} F_{o\xi i} \hat{W}_{o\xi i} \,. \tag{160}$$

Then, there exists computable positive design parameters K_{o1}, K_{o2} and K_{o3} where $K_{o1} > K_{o3} + (2N_{oi})/\kappa_{o1}$, $K_{o3} > (2N_{0i})/\kappa_{o1}$, and $K_{o2} = K_{o3}(K_{o1} - K_{o3})$ such that the observer estimation errors, $\tilde{X}_{\xi i}$ and $\tilde{V}_{\xi i}$, and the NN observer weight estimation errors, $\tilde{W}_{o\xi i}$, are all SGUUB.

Proof: Consider the following Lyapunov function

$$L_{oi} = \frac{1}{2} \left(\tilde{X}_{\xi i}^T \tilde{X}_{\xi i} + \tilde{V}_{\xi i}^T \tilde{V}_{\xi i} + tr\left\{ \tilde{W}_{o\xi i}^T F_{o\xi i}^{-1} \tilde{W}_{o\xi i} \right\} \right)$$

$$= \frac{1}{2} \begin{pmatrix} \left[\tilde{X}_i^T \quad \left((Q_i \otimes I_{6\times 6}) \tilde{X} \right)^T \right] \left[\tilde{X}_i^T \quad \left((Q_i \otimes I_{6\times 6}) \tilde{X} \right)^T \right]^T \\ + \left[\tilde{V}_i^T \quad \left((Q_i \otimes I_{6\times 6}) \tilde{V} \right)^T \right] \left[\tilde{V}_i^T \quad \left((Q_i \otimes I_{6\times 6}) \tilde{V} \right)^T \right]^T \\ + tr\left\{ \tilde{W}_{o\xi i}^T F_{o\xi i}^{-1} \tilde{W}_{o\xi i} \right\} \end{pmatrix} \tag{161}$$

with $F_{o\xi i} = diag\left\{ F_{oi} \quad (Q_i \otimes I_{6\times 6}) diag\left\{ F_{oj} \right\} (Q_i \otimes I_{6\times 6})^T \right\}, j \in N$. The derivative of (161) is given as

$$\dot{L}_{oi} = \tilde{X}_i^T \dot{\tilde{X}}_i + \tilde{V}_{\xi i}^T \dot{\tilde{V}}_{\xi i} + tr\left\{ \tilde{W}_{oi}^T F_{oi}^{-1} \dot{\tilde{W}}_{oi} \right\} + \left((Q_i \otimes I_{6\times 6}) \tilde{X} \right)^T \left((Q_i \otimes I_{6\times 6}) \dot{\tilde{X}} \right)$$

$$+ \left((Q_i \otimes I_{6\times 6}) \tilde{V} \right)^T \left((Q_i \otimes I_{6\times 6}) \dot{\tilde{V}} \right) + tr\left\{ \bar{Q}_i^T diag\left\{ \tilde{W}_{oj} \right\}^T \bar{Q}_i F_{oni}^{-1} \bar{Q}_i diag\left\{ \dot{\tilde{W}}_{oj} \right\} \bar{Q}_i^T \right\} \tag{162}$$

with $\bar{Q}_i = (Q_i \otimes I_{6\times 6}), j \in N$. Using the property of the Kronecker product and the reduction matrix $\bar{Q}_i$ in (162) yields

$$\dot{L}_{oi} = \tilde{X}_i^T \dot{\tilde{X}}_i + \tilde{V}_{\xi i}^T \dot{\tilde{V}}_{\xi i} + tr\left\{ \tilde{W}_{oi}^T F_{oi}^{-1} \dot{\tilde{W}}_{oi} \right\} + \sum_{j \in N_i} \left(\tilde{X}_j^T \dot{\tilde{X}}_{jj} \right) + \sum_{j \in N_i} \left(\tilde{V}_j^T \dot{\tilde{V}}_j \right) + \sum_{j \in N_i} \left(\tilde{W}_{oj}^T \dot{\tilde{W}}_{oj} \right). \tag{163}$$

Combine the similar terms in (163) to get

$$\dot{L}_{oi} = \tilde{X}_i^T \dot{\tilde{X}}_i + \tilde{V}_{\xi i}^T \dot{\tilde{V}}_{\xi i} + tr\left\{\tilde{W}_{oi}^T F_{oi}^{-1} \dot{\tilde{W}}_{oi}\right\} + \sum_{j \in N_i}\left(\tilde{X}_j^T \dot{\tilde{X}}_j + \tilde{V}_j^T \dot{\tilde{V}}_j + \tilde{W}_{oj}^T \dot{\tilde{W}}_{oj}\right). \tag{164}$$

Using the error dynamics (158),(159), and the NN weight update law (160) in (164), we have

$$\dot{L}_{oi} = -\tilde{X}_i^T \left(K_{o1} - K_{o3}\right)\tilde{X}_i + \tilde{X}_i^T \zeta_{1i} - \tilde{V}_i^T K_{o3}\tilde{V}_i + \tilde{V}_i^T \zeta_{2i} - tr\left\{\tilde{W}_{oi}^T\left(\hat{\sigma}_{oi}\tilde{X}_i^T - \hat{\sigma}_{oi}\tilde{V}_i^T - \kappa_{o1}\hat{W}_{oi}\right)\right\}$$

$$-\sum_{j \in N_i}\left(tr\left\{\tilde{W}_{oj}^T\left(\hat{\sigma}_{oj}\tilde{X}_j^T - \hat{\sigma}_{oj}\tilde{V}_j^T - \kappa_{o1}\hat{W}_{oj}\right)\right\}\right)$$

$$+\sum_{j \in N_i}\left(-\tilde{X}_j^T\left(K_{o1} - K_{o3}\right)\tilde{X}_j + \tilde{X}_j^T \zeta_{1j} - \tilde{V}_j^T K_{o3}\tilde{V}_j + \tilde{V}_j^T \zeta_{2j}\right) \quad . \tag{165}$$

Now, after completing the squares with respect to $\left\|\tilde{X}_i\right\|, \left\|\tilde{V}_i\right\|, \left\|\tilde{W}_{oi}\right\|, \left\|\tilde{X}_j\right\|, \left\|\tilde{V}_j\right\|, \left\|\tilde{W}_{oj}\right\|$

and utilizing the similar inequalities used in [1] yields

$$\dot{L}_{oi} \leq -\left(\left(\kappa_{o1}\left(K_{o1} - K_{o3}\right) - 2N_o\right)/2\kappa_{o1}\right)\left\|\tilde{X}_i\right\|^2 - \left(\left(\kappa_{o1}K_{o3} - 2N_o\right)/2\kappa_{o1}\right)\left\|\tilde{V}_i\right\|^2$$

$$-\left(\kappa_{o1}/4\right)\left\|\tilde{W}_{oi}\right\|_F^2 + \eta_{oi} - \sum_{j \in N_i}\left(\left(\left(\kappa_{o1}\left(K_{o1} - K_{o3}\right) - 2N_o\right)/2\kappa_{o1}\right)\left\|\tilde{X}_j\right\|^2\right)$$

$$-\sum_{j \in N_i}\left(\left(\left(\kappa_{o1}K_{o3} - 2N_o\right)/2\kappa_{o1}\right)\left\|\tilde{V}_i\right\|^2 + \left(\kappa_{o1}/4\right)\left\|\tilde{W}_{oi}\right\|_F^2 + \eta_{oj}\right) \tag{166}$$

with $\eta_{oi} = \kappa_{o1}W_{oMi} + \zeta_{1i}^2 / \left(2\left(K_{o1} - K_{o3}\right)\right) + \zeta_{2i}^2 / \left(2K_{o3}\right)$.

Next, rewrite the inequality (166) in terms of augmented error sates as

$$\dot{L}_{oi} \leq -\left(\left(\kappa_{o1}\left(K_{o1} - K_{o3}\right) - 2N_o\right)/2\kappa_{o1}\right)\left\|\tilde{X}_{\xi i}\right\|^2$$

$$-\left(\left(\kappa_{o1}K_{o3} - 2N_o\right)/2\kappa_{o1}\right)\left\|\tilde{V}_{\xi i}\right\|^2 - \left(\kappa_{o1}/4\right)\left\|\tilde{W}_{o\xi i}\right\|_F^2 + \eta_{o\xi i} \tag{167}$$

where $\eta_{o\xi i} = \eta_{oi} + \sum_{j \in N_i} (\eta_{oj})$ .Finally, we can claim that (167) is negative provided

$K_{o1} > K_{o3} + (2N_o)/\kappa_{o1}$, $K_{o3} > (2N_o)/\kappa_{o1}$ and the following inequalities hold:

$$\left\| \tilde{X}_{\xi i} \right\| > \sqrt{\eta_{o\xi i} / \left(\left(\kappa_{o1} (K_{o1} - K_{o3}) - 2N_o \right) / 2\kappa_{o1} \right)} \qquad \text{or}$$

$\left\| \tilde{V}_{\xi i} \right\| > \sqrt{\eta_{o\xi i} / \left(\left(\kappa_{o1} K_{o3} - 2N_o \right) / 2\kappa_{o1} \right)}$ or $\left\| \tilde{W}_{o\xi i} \right\| > \sqrt{4\eta_{o\xi i} / \kappa_{o1}}$.

The initial compact set can be made arbitrarily large by selecting proper gains; therefore, the system is SGUUB [1].

Next, the consensus-based output feedback formation controller is derived in the presence of estimated velocities and uncertain dynamics.

4.2   CONSENSUS CONTROLLER DESIGN

The objective of the consensus-based control law is to maintain a specified formation shape, and the shape of the formation is provided by choosing the reference points accordingly. Therefore, consider a time-invariant reference point in three dimensional space for the ith UAV as

$$\rho_i^d = \begin{bmatrix} x_i^d & y_i^d & z_i^d \end{bmatrix}, \qquad (168)$$

and define the position error as $e_{\rho i} = \begin{bmatrix} e_{xi} & e_{yi} & e_{zi} \end{bmatrix}^T = \rho_i^d - \rho_i \in E^a$. Then, define the consensus errors on x, y and z directions as

$$\delta_{xi} = \sum_{j \in N_i} (e_{xi} - e_{xj}) , \delta_{yi} = \sum_{j \in N_i} (e_{yi} - e_{yj}) , \delta_{zi} = \sum_{j \in N_i} (e_{zi} - e_{zj}) ,$$

and the vector form of the consensus error for i^{th} UAV is

$$\delta_i = \begin{bmatrix} \delta_{xi} & \delta_{yi} & \delta_{zi} \end{bmatrix}^T = \sum_{j \in N_i} (e_{\rho j} - e_{\rho i}). \qquad (169)$$

Taking derivative of (169) and using (140) yields

$$\dot{\delta}_i = -\xi_i R_i v_i + \sum_{j \in N_i} R_j v_j \ . \tag{170}$$

Choose the desired translational velocity as

$$v_i^d = \begin{bmatrix} v_{xi}^d & v_{yi}^d & v_{zi}^d \end{bmatrix}^T = \frac{R_i^T}{\xi_i} \left(K_\delta \delta_i + \sum_{j \in N_i} R_j v_j \right) \in E^b \ . \tag{171}$$

Using the desired translational velocity (171) in (170) as a virtual control input and considering the consensus velocity tracking error $e_{ci} = v_i^d - v_i$ yields the closed loop consensus error dynamics as

$$\dot{\delta}_i = -\xi_i R_i \left(v_i^d - e_{ci} \right) + \sum_{j \in N_i} R_j v_j$$

$$= -\xi_i R_i \left(\frac{R_i^T}{\xi_i} \left(K_\delta \delta_i + \sum_{j \in N_i} R_j v_j \right) - e_{ci} \right) + \sum_{j \in N_i} R_j v_j$$

$$= -K_\delta \delta - \sum_{j \in N_i} R_j v_j + \xi_i R_i e_{ci} + \sum_{j \in N_i} R_j v_j$$

$$= -K_\delta \delta_i + \xi_i R_i e_{ci} \ . \tag{172}$$

Then, the dynamics of the consensus velocity tracking error can be given as

$$\dot{e}_{ci} = \dot{v}_i^d - \dot{v}_i$$

$$= -S_i(w_i) v_i^d + \frac{R_i^T}{\xi_i} \left(K_\delta \left(-\xi_i R_i v_i + \sum_{j \in N_i} R_j v_j \right) - \sum_{j \in N_i} \left(S_j(w_j) v_j - R_j \dot{v}_j \right) \right)$$

$$+ S_i(w_i) v_i - \frac{1}{m_i} N_1(v_i) - \frac{1}{m_i} G_i(R_i) - \frac{1}{m_i} u_{1i} E_z - \tau_{d1i} \ . \tag{173}$$

Using the definition of consensus velocity tacking error $e_{ci} = v_i^d - v_i$ in (173) yields

$$\dot{e}_{ci} = -S_i(w_i)e_{ci} + \frac{R_i^T}{\xi_i}\left(K_\delta\left(-\xi_i R_i v_i + \sum_{j\in N_i} R_j v_j\right) - \sum_{j\in N_i}\left(S_j(w_j)v_j - R_j \dot{v}_j\right)\right)$$

$$-\frac{1}{m_i}N_1(v_i) - \frac{1}{m_i}G_i(R_i) - \frac{1}{m_i}u_{1i}E_z - \tau_{d1i} \ . \tag{174}$$

In the velocity tracking error dynamics, the control input u_{i1} only influences the z direction error; therefore, the pitch and roll angles, θ_i^d and ϕ_i^d, respectively, are used as virtual control inputs to the x and y directions.

Now, define the desired angles vector $\Theta_i^d = \begin{bmatrix} \phi_i^d & \theta_i^d & \psi_i^d \end{bmatrix}^T$ and $R_i^d = R(\Theta_i^d)$.

Then, add and subtract $\dfrac{1}{m_i}G_i(R_i^d)$ into (174) to give

$$\dot{e}_{ci} = -S_i(w_i)e_{ci} - \frac{1}{m_i}G_i(R_i) + \frac{1}{m_i}G_i(R_i^d) - \frac{1}{m_i}G_i(R_i^d)$$

$$+\frac{R_i^T}{\xi_i}\left[\begin{array}{c} K_\delta\left(-\xi_i R_i v_i + \sum_{j\in N_i} R_j v_j\right) \\ -\sum_{j\in N_i}\left(S_j(w_j)v_j - R_j \dot{v}_j\right) - R_i \frac{1}{m_i}N_1(v_i) \end{array}\right] - \frac{1}{m_i}u_{1i}E_z - \tau_{d1i} \ . \tag{175}$$

Rearranging the above relation to move $-\dfrac{1}{m_i}G_i(R_i) + \dfrac{1}{m_i}G_i(R_i^d)$ into the parenthesis and leave $-\dfrac{1}{m_i}G_i(R_i^d)$ out of the parenthesis in (175) yields

$$\dot{e}_{ci} = -S_i(w_i)e_{ci} - \frac{1}{m_i}G_i(R_i^d)$$

$$-\frac{1}{m_i}u_{1i}E_z - \tau_{d1i} + \frac{R_i^T}{\xi_i}\begin{pmatrix} K_\delta\left(-\xi_i R_i v_i + \sum_{j\in N_i} R_j v_j\right) - \sum_{j\in N_i}\left(S_j(w_j)v_j - R_j\dot{v}_j\right) \\ -R_i\left(\frac{1}{m_i}N_1(v_i) + \frac{1}{m_i}G_i(R_i) - \frac{1}{m_i}G_i(R_i^d)\right) \end{pmatrix}. \tag{176}$$

Then, adding and subtracting

$$\frac{R_i^{dT}}{\xi_i}\left(-K_\delta\xi_i R_i\hat{v} + K_\delta\sum_{j\in N_i} R_j\hat{v}_j - \sum_{j\in N_i}\left(S_j(\hat{w}_j)\hat{v}_j\right)\right) \text{ to (176) yields}$$

$$\dot{e}_{ci} = -S_i(w_i)e_{ci} - \frac{1}{m_i}G_i(R_i^d) + \frac{R_i^{dT}}{\xi_i}\left(-K_\delta\xi_i R_i\hat{v} + K_\delta\sum_{j\in N_i} R_j\hat{v}_j - \sum_{j\in N_i}\left(S_j(\hat{w}_j)\hat{v}_j\right)\right)$$

$$+\frac{R_i^T}{\xi_i}\begin{pmatrix} -K_\delta\xi_i R_i v_i + K_\delta\sum_{j\in N_i} R_j v_j \\ -\sum_{j\in N_i}\left(S_j(w_j)v_j\right) + \sum_{j\in N_i}\left(R_j\dot{v}_j\right) \\ -R_i\left(\frac{1}{m_i}N_1(v_i) + \frac{1}{m_i}\left(G_i(R_i) - G_i(R_i^d)\right)\right) \end{pmatrix}$$

$$-\frac{R_i^{dT}}{\xi_i}\left(-K_\delta\xi_i R_i\hat{v}_i + K_\delta\sum_{j\in N_i} R_j\hat{v}_j - \sum_{j\in N_i}\left(S_j(\hat{w}_j)v_j\right)\right) - \frac{1}{m_i}u_{1i}E_z - \tau_{d1i} \quad . \tag{177}$$

Now, combine the uncertain terms in (177) and define

$$\bar{f}_{ci1} = \frac{R_i^T}{\xi_i}\begin{pmatrix} -K_\delta\xi_i R_i v_i + K_\delta\sum_{j\in N_i} R_j v_j \\ -\sum_{j\in N_i} S_j(w_j)v_j + \sum_{j\in N_i} R_j\dot{v}_j \\ -R_i\left(\frac{1}{m_i}N_1(v_i) + \frac{1}{m_i}\left(G_i(R_i) - G_i(R_i^d)\right)\right) \end{pmatrix},$$

$$-\frac{R_i^{dT}}{\xi_i}\left(-K_\delta\xi_i R_i\hat{v}_i + K_\delta\sum_{j\in N_i} R_j\hat{v}_j - \sum_{j\in N_i}\left(S_j(\hat{w}_j)\hat{v}_j\right)\right)$$

then, rewrite (177) as

$$\dot{e}_{ci} = -S_i\left(w_i\right)e_{ci} - \frac{1}{m_i}G_i\left(R_i^d\right) + \frac{R_i^{dT}}{\xi_i}\left(-K_\delta\xi_iR_i\hat{v}_i + f_{ci1}\left(x_{ci1}\right) + \sum_{j\in N_i}\left(K_\delta R_j\hat{v}_j - \left(S_j\left(\hat{w}_j\right)\hat{v}_j\right)\right)\right)$$

$$-\frac{1}{m_i}u_{1i}E_z - \tau_{d1i} \qquad\qquad\qquad (178)$$

with, $f_{ci1}\left(x_{ci1}\right) = \begin{bmatrix} f_{ci11} & f_{ci12} & f_{ci13}\end{bmatrix}^T \in \mathbb{R}^3 = R_i^d\xi_i\bar{f}_{ci1}$ being an unknown function.

The neural network expression of the uncertain function is written as

$f_{ci1} = \begin{bmatrix} f_{ci11} & f_{ci12} & f_{ci13}\end{bmatrix}^T = W_{ci1}^T\sigma_i\left(V_{ci1}^Tx_{ci1}\right) + \varepsilon_{ci1}$ where W_{ci1}, V_{ci1} are the bounded target

weights such that $\|W_{ci1}\| \le W_{Mci1}, \|V_{ci1}\| \le V_{Mci1}$ with W_{Mci1}, V_{Mci1} being constants, and ε_{ci1} is

the NN approximation error, which satisfies $\|\varepsilon_{ci1}\| \le \varepsilon_{Mci1}$ for a constant ε_{Mci1}.

The NN estimate of the uncertain function f_{ci1} can then be written as

$$\hat{f}_{ci1} = \begin{bmatrix} \hat{f}_{ci11} & \hat{f}_{ci12} & \hat{f}_{ci13}\end{bmatrix}^T = \hat{W}_{ci1}^T\sigma_i\left(V_{ci1}^T\hat{x}_{ci1}\right) = \hat{W}_{ci1}^T\hat{\sigma}_{c1i} \ ,$$

where $\hat{W}_{ci1}$ is the NN estimate of W_{ci1}, and $\hat{x}_{ci1}$ is the NN input given as

$$\hat{x}_{ci1} = \begin{bmatrix} 1, \hat{V}_i^T, \Theta_i^T, \tilde{X}_i^T, \dot{\rho}_l^{dT}, \ddot{\rho}_l^{dT}, \hat{V}_j^T, \Theta_j^T, \tilde{X}_j^T\end{bmatrix} \ \ \forall j \in N_i.$$

Next, expand the consensus velocity tracking error dynamics (178) in terms of

its *x, y,* and *z* components as

$$\begin{bmatrix} \dot{e}_{cix} \\ \dot{e}_{ciy} \\ \dot{e}_{ciz} \end{bmatrix} = -S_i(w_i)e_{ci} - g \begin{bmatrix} -s_{\theta d} \\ c_{\theta d}s_{\phi d} \\ c_{\theta d}c_{\phi d} \end{bmatrix}$$

$$+ \frac{1}{\xi_i} \begin{bmatrix} c_{\theta d}c_{\psi d} & c_{\theta d}s_{\psi d} & -s_{\theta d} \\ s_{\phi d}s_{\theta d}c_{\psi d} - c_{\phi d}s_{\psi d} & s_{\phi d}s_{\theta d}s_{\psi d} + c_{\phi d}c_{\psi d} & s_{\phi d}c_{\theta d} \\ c_{\phi d}s_{\theta d}c_{\psi d} + s_{\phi d}s_{\psi d} & c_{\phi d}s_{\theta d}s_{\psi d} - s_{\phi d}c_{\psi d} & c_{\phi d}c_{\theta d} \end{bmatrix} \bullet \begin{bmatrix} -k_{\delta x}\xi_i\hat{v}_{xiR} + \hat{f}_{ci11} + \sum_{j \in N_i}\left(k_{\delta x}\hat{v}_{xjR} - \hat{v}_{xjS}\right) \\ -k_{\delta y}\xi_i\hat{v}_{yiR} + \hat{f}_{ci12} + \sum_{j \in N_i}\left(k_{\delta y}\hat{v}_{yjR} - \hat{v}_{yjS}\right) \\ -k_{\delta z}\xi_i\hat{v}_{ziR} + \hat{f}_{ci13} + \sum_{j \in N_i}\left(k_{\delta z}\hat{v}_{zjR} - \hat{v}_{zjS}\right) \end{bmatrix}$$

$$-\frac{1}{m_i} \begin{bmatrix} 0 \\ 0 \\ u_{1i} \end{bmatrix} - \tau_{d1i} \tag{179}$$

while observing

$$\hat{v}_{iR} = \begin{bmatrix} \hat{v}_{xiR} & \hat{v}_{yiR} & \hat{v}_{ziR} \end{bmatrix}^T = R_i\hat{v}_i \in \mathbb{R}^3$$

$$\hat{v}_{jS} = \begin{bmatrix} \hat{v}_{xjS} & \hat{v}_{yjS} & \hat{v}_{zjS} \end{bmatrix}^T = S_j(\hat{w}_j)\hat{v}_j \in \mathbb{R}^3, \forall i, j = 1, 2, \ldots, N$$

Realize that the error states $\dot{e}_{cix}, \dot{e}_{ciy}$ are not controllable through the thrust controller u_{1i}. Therefore, the pith and roll angles are utilized as the virtual controller to these two error states. First, define the desired consensus velocity tracking error dynamics on x and y direction as

$$\dot{e}_{ci} = -\left(K_\delta \begin{bmatrix} k_{v1} & 0 \\ 0 & k_{v2} \end{bmatrix} + \begin{bmatrix} 1 & 0 & 0 \\ 0 & 1 & 0 \end{bmatrix} S_i(w_i) \begin{bmatrix} 1 & 0 \\ 0 & 1 \\ 0 & 0 \end{bmatrix} \right) e_{ci}. \tag{180}$$

The form of (180) was chosen due to its stability properties. Equating the difference between (180) and the first two rows of (179) to zero yields

$$-g\begin{bmatrix} -s_{\theta d} \\ c_{\theta d}s_{\phi d} \end{bmatrix} + \frac{1}{\xi_i}\begin{bmatrix} c_{\theta d}c_{\psi d} & c_{\theta d}s_{\psi d} & -s_{\theta d} \\ s_{\phi d}s_{\theta d}c_{\psi d} - c_{\phi d}s_{\psi d} & s_{\phi d}s_{\theta d}s_{\psi d} + c_{\phi d}c_{\psi d} & s_{\phi d}c_{\theta d} \end{bmatrix} \cdot \begin{bmatrix} \Delta_{xi} \\ \Delta_{yi} \\ \Delta_{zi} \end{bmatrix} + \begin{bmatrix} K_\delta k_{v1}e_{cxi}c_{\theta d} \\ K_\delta k_{v2}e_{cyi}c_{\phi d} \end{bmatrix} = \begin{bmatrix} 0 \\ 0 \end{bmatrix}$$

$$(181)$$

with

$$\Delta_{xi} = -k_{\delta x}\xi_i\hat{v}_{xiR} + \hat{f}_{ci11} + \sum_{j\in N_i}\left(k_{\delta x}\hat{v}_{xjR} - \hat{v}_{xjS}\right), \quad \Delta_{yi} = -k_{\delta y}\xi_i\hat{v}_{yiR} + \hat{f}_{ci12} + \sum_{j\in N_i}\left(k_{\delta y}\hat{v}_{yjR} - \hat{v}_{yjS}\right),$$

$$\Delta_{zi} = -k_{\delta z}\xi_i\hat{v}_{ziR} + \hat{f}_{ci13} + \sum_{j\in N_i}\left(k_{\delta z}\hat{v}_{zjR} - \hat{v}_{zjS}\right) - g \quad, c_{\theta d} = \cos\left(\theta_i^d\right), s_{\theta d} = \sin\left(\theta_i^d\right),$$

$$c_{\phi d} = \cos\left(\phi_i^d\right), s_{\phi d} = \sin\left(\phi_i^d\right), \quad c_{\psi d} = \cos\left(\psi_i^d\right), s_{\psi d} = \sin\left(\psi_i^d\right).$$

Note that the trigonometric functions of the desired pitch and roll angles, $c_{\theta d}, c_{\phi d}$ are used in (181) instead of c_θ, c_ϕ because the equality only holds when the UAV reaches the desired pitch and roll angles which is developed and utilized as virtual controller.

Then, by applying some basic math operations, (181) yields

$$s_{\theta d}\Delta_{zi} = c_{\theta d}\left(c_{\psi d}\Delta_{xi} + s_{\psi d}\Delta_{yi} + k_{v1}e_{vxi}\right) \tag{182}$$

and

$$c_{\phi d}\left(c_{\psi d}\Delta_{yi} - s_{\psi d}\Delta_{xi} + k_{v2}e_{vyi}\right) = s_{\phi d}\left(gc_{\theta d} - s_{\phi d}c_{\theta d}\right)\Delta_{zi} - s_{\theta d}s_{\psi d}\Delta_{yi} - s_{\theta d}c_{\psi d}\Delta_{xi}. \tag{183}$$

Define the estimated velocity tracking errors as

$$\hat{e}_{ci} = \begin{bmatrix} \hat{e}_{cxi} & \hat{e}_{czi} & \hat{e}_{czi} \end{bmatrix}^T = v_i^d - \hat{v}_i = v_i^d - \left(v_i - \hat{v}_i\right) = e_{ci} + \tilde{v}_i ,$$

where $\tilde{v}_i$ is the translational velocity observer estimation error. Then, the desired pitch and roll angles are defined to satisfy (182) and (183). First, consider (182) as

$$\frac{s_{\theta d}}{c_{\theta d}} = \frac{c_{\psi d}\Delta_{xi} + s_{\psi d}\Delta_{yi} + k_{v1}e_{vxi}}{\Delta_{zi}} \quad \text{and obtain}$$

$$\theta_i^d = a\tan\left(\frac{c_{\psi d}\Delta_{xi} + s_{\psi d}\Delta_{yi} + k_{v1}\hat{e}_{cxi}}{\Delta_{zi}}\right). \tag{184}$$

Then consider (183) as

$$\frac{s_{\phi d}}{c_{\phi d}} = \frac{c_{\psi d}\Delta_{yi} + s_{\psi d}\Delta_{xi} + k_{v2}\hat{e}_{cyi}}{gc_{\theta d} - c_{\theta d}\Delta_{zi} - s_{\theta d}c_{\psi d}\Delta_{yi} - s_{\theta d}c_{\psi d}\Delta_{xi}} \quad \text{and use the inverse trigonometric function to get}$$

$$\phi_i^d = a\tan\left(\frac{c_{\psi d}\Delta_{yi} + s_{\psi d}\Delta_{xi} + k_{v2}\hat{e}_{cyi}}{gc_{\theta d} - c_{\theta d}\Delta_{zi} - s_{\theta d}c_{\psi d}\Delta_{yi} - s_{\theta d}c_{\psi d}\Delta_{xi}}\right). \tag{185}$$

The desired roll (184) and pitch (185) angles serve as the virtual control inputs that stabilize the under-actuated portion of the velocity error dynamics (174). Subsequently, the desired angular velocities and rotational torques will be considered to ensure the desired angles are tracked.

Remark 1: In this work, it is assumed that one of the UAVs in the group, named as leader UAV or l^{th} UAV, tracks a time varying desired trajectory and the rest of the group reaches consensus on their regulation errors, $e_{\rho i}$, with their neighbor UAVs.. Note that the desired trajectory of the leader, ρ^r in (146), is time invariant and differs from the time in-variant reference point of the leader UAV, ρ_l^d defined as (168). Through the consensus-based controller, the followers will eventually have the same regulation error as the leader UAV, i.e., $e_{\rho i} \rightarrow e_{\rho l} \ \forall i = 1, 2, \ldots, N$.

Remark 2: In this work, the main purpose of the controller is to make the formation errors (169) go to zero. Making the formation errors (169) go to zero does not guarantee that the desired formation is achieved all the time. *Assumption 1* is needed for the UAV

formation to be able to reach a consensus on their $e_{\rho i}'$s.

Lemma 2: The formation error (169) can be obtained through communication among the UAVs or by using local sensors built in each UAV.

Proof: The formation error $\delta_i = \sum_{j \in N_i} \left(e_{\rho j} - e_{\rho i} \right)$ is function of ith UAVs own regulation error $e_{\rho i}$, which is available, and the regulation errors of it's neighbors, $e_{\rho j}$. Recall that $e_{\rho j} = \rho_j^d - \rho_j$ and observe that it is function of the neighbors' current positions and the reference point. Therefore, the current position, ρ_j can be obtained by using relative distance plus the current position of the ith UAV, ρ_i. Then, the formation errors (169) are available under the mild assumption that the time invariant reference positions, ρ_j^d, of all neighbors are available for the ith UAV *a priori*.

Remark 3: We propose two different scenarios to obtain the consensus-based formation errors (169): a) Each UAV broadcasts its own error states, $e_{\rho i}$, and its neighbors use this information; and b) Each UAV obtains the current states, $\rho_j \ \forall j \in N_i$, and identity its neighbors by using local sensors and determining $e_{\rho j} \ \forall j \in N_i$. The first Scenario is applicable when the UAVs are farther to each other, and the second scenario is preferable when the UAVs are closer and broadcasting the state information is insecure.

Since the desired yaw angle ψ_i^d is specified initially for each UAV and desired roll and pitch angles are determined, the desired orientation vector, Θ_i^d is now fully defined. Therefore, the desired angular velocity w_i^d needs to be defined to make sure $\Theta_i \rightarrow \Theta_i^d$ as $t \rightarrow \infty$. First, define the attitude tracking error

$$e_{\Theta i} = \Theta_i^d - \Theta_i \in E^a \tag{186}$$

and the dynamics of (186) as

$$\dot{e}_{\Theta i} = \dot{\Theta}_i^d - T_i w_i \ . \tag{187}$$

The desired angular velocity is selected as

$$w_i^d = T_i^{-1}\left(\dot{\Theta}_i^d + K_\Theta e_\Theta\right) \tag{188}$$

where $K_\Theta = diag\left\{k_{\Theta 1}, k_{\Theta 2}, k_{\Theta 3}\right\}$ is a diagonal positive-definite design matrix with each

$k_{\Theta i} > 0, i = 1, 2, 3$. Define the angular velocity tracking error as

$$e_{wi} = w_i^d - w_i , \tag{189}$$

and by considering that $w_i = w_i^d - e_{wi}$, the closed loop orientation tracking error dynamics

is given as

$$\dot{e}_{wi} = -K_\Theta e_{\Theta i} + T_i e_{wi} \ . \tag{190}$$

Since the desired angular velocity (188) requires $\dot{\Theta}_i^d$ which subsequently requires $\dot{\hat{v}}_i, \dot{\hat{f}}_{c1i}$,

$\dot{w}_i^d$ will also be required for the development of u_{2i} which needs the information of $\ddot{\hat{v}}_i, \ddot{\hat{f}}_{c1i}$

which is not a practical assumption [13]. Therefore, an NN-based virtual control input is

proposed as in [13]; hence,

$$\dot{\hat{\Theta}}_i^d = T_i \hat{\Omega}_i^d + K_{\Omega 1} \tilde{\Theta}_i^d$$

$$\dot{\hat{\Omega}}_i^d = \hat{f}_{\Omega 1} + K_{\Omega 2} T_i^{-1} \tilde{\Theta}_i^d \tag{191}$$

with $K_{\Omega 1}, K_{\Omega 2}$ being positive constants, $\Omega_i^d = w_i^d - T_i^{-1} K_\Theta e_{\Theta i}, \hat{\Theta}_i^d, \hat{\Omega}_i^d$ are the estimates of

Θ_i^d, Ω_i^d respectively, $\tilde{\Theta}_i^d = \Theta_i^d - \hat{\Theta}_i^d$. Then, the estimate of the desired angular velocity is

proposed as

$$\hat{w}_i^d = \hat{\Omega}_i^d + T_i^{-1} K_\Theta e_{\Theta i} + K_{\Omega 3} T_i^{-1} \tilde{\Theta}_i^d \tag{192}$$

where $K_{\Omega 3}$ is another design constant.

In (191), the uncertain function $f_{\Omega 1}(x_{\Omega i})$ is estimated through an NN similar to

[13]. However, the NN input is different than [13] in our case since $f_{\Omega 1}(x_{\Omega i})$ is a function

of neighbor UAV states as well as the *ith* UAV states. The NN expression is given as

$f_{\Omega 1 i}(x_{\Omega i}) = W_{\Omega i}^T \sigma(V_{\Omega i}^T x_{\Omega i}) + \varepsilon_{\Omega i}$ by target weights $W_{\Omega i}, V_{\Omega i}$ such that $\|W_{\Omega i}\| \le W_{M \Omega i}$ for a

constant $W_{M \Omega i}$ and $\varepsilon_{\Omega i}$ is the NN approximation error wherein $\|\varepsilon_{\Omega i}\| \le \varepsilon_{M \Omega}$ for a constant

$\varepsilon_{M \Omega i}$. The NN estimate of $f_{\Omega 1 i}$ is given as $\hat{f}_{\Omega 1 i}(\hat{x}_{\Omega i}) = \hat{W}_{\Omega i}^T \sigma(V_{\Omega i}^T \hat{x}_{\Omega i}) + \varepsilon_{\Omega i}$ where $\hat{W}_{\Omega i}^T$ is

the NN estimate of $W_{\Omega i}^T$, $\hat{x}_{\Omega i}$ is the NN inputs written in terms of the virtual control input

estimates, and NN observer velocity estimates of the ith UAV as well as the neighborhood

UAVs. The NN input is selected as

$$\hat{x}_{\Omega i} = \begin{bmatrix} 1, \Theta_i^{dT}, \hat{\Omega}_i^{dT}, \hat{V}_i^T \tilde{\Theta}_i^{dT}, \dot{\rho}_l^d, \ddot{\rho}_l^d \\ , \ddot{\rho}_l^d, \Theta_j^{dT}, \hat{\Omega}_j^{dT}, \hat{V}_j^T, \tilde{\Theta}_j^{dT} \end{bmatrix}^T.$$

Lemma 3 [13]: Let the NN virtual controller be defined by (191) and (192),

respectively, with the NN update law

$$\dot{\hat{W}}_{\Omega i} = F_\Omega \tilde{\Theta}_i^{dT} - \kappa_{\Omega 1} F_\Omega \hat{W}_{\Omega i} \tag{193}$$

where $F_\Omega = F_\Omega^T > 0, \kappa_{\Omega 1} > 0$ are design parameters. Then, there exists positive design constants $K_{\Omega 1} > K_{\Omega 3} + N_\Omega / \kappa_{\Omega 1}$, $K_{\Omega 2} = K_{\Omega 3} (K_{\Omega 1} - K_{\Omega 3})$, and $K_{\Omega 3} > 2 N_\Omega / \kappa_{\Omega 1}$ where N_Ω is the number of hidden layer neurons, such that the virtual controller estimation errors $\tilde{\Theta}_i^d$ and $\tilde{w}_i^d$, and the virtual control NN weight estimation errors $\tilde{W}_{\Omega i}$ are SGUUB.

Proof: Define the Lyapunov function as

$$L_{\Omega i} = \frac{1}{2} \tilde{\Theta}_i^{dT} \tilde{\Theta}_i^d + \frac{1}{2} \tilde{w}_i^{dT} \tilde{w}_i^d + tr\left\{ \tilde{W}_{\Omega i}^T F_\Omega^{-1} \tilde{W}_{\Omega i} \right\}. \tag{194}$$

Then, the upper bound is given for $\dot{L}_{\Omega i}$ and is given in [13] as

$$\dot{L}_{\Omega i} \le -\left(K_{\Omega 1} - K_{\Omega 3} - \frac{N_\Omega}{\kappa_{\Omega 1}} \right) \left\| \tilde{\Theta}_i^d \right\|^2 - \left(\frac{K_{\Omega 3}}{2} - \frac{N_\Omega}{\kappa_{\Omega 1}} \right) \left\| \tilde{w}_i^d \right\|^2 - \frac{\kappa_{\Omega 1}}{4} \left\| \tilde{W}_{\Omega i} \right\|_F^2 + \eta_{\Omega i}. \tag{195}$$

See [13] for proof details.

Next, the translational and rotational controllers, u_{1i}, u_{2i} , are developed, respectively, to reach consensus.

4.3 CONTROLLER DESIGN

In the previous sections, the velocities were estimated through the extended observers (157) and kinematic controllers were given by (171) and (188). The desired roll and pitch were provide by (184) and (185), respectively, and a virtual control for generating the target angular rates was given in (191). Now, the actual thrust and rotation controllers, u_{1i}, u_{2i} , can be produced.

The thrust controller is addressed first. Consider the velocity tracking error dynamics (179). The dynamic controller is calculated to stabilize the last row of (179) as

$$u_{1i} = m_i k_{v3i} \hat{e}_{czi} + m_i \left(c_{\phi d} s_{\theta d} c_{\psi d} + s_{\phi d} s_{\psi d} \right) \Delta_{xi} + m_i \left(c_{\phi d} s_{\theta d} s_{\psi d} - s_{\phi d} c_{\psi d} \right) \Delta_{yi} + m_i c_{\phi d} c_{\theta d} \Delta_{zi}. \tag{196}$$

Using the virtual controllers (184) and (185), the thrust controller in (196), and adding and subtracting $R_i^{dT}W_{cli}^T\hat{\sigma}_{cli}^T$ yields the closed loop translational consensus velocity tracking error dynamics (179)

$$\dot{e}_{ci} = -S_i(w_i)e_{ci} - K_v\hat{e}_{ci} + R_i^{dT}\tilde{W}_{cli}^T\hat{\sigma}_{cli}^T + \varsigma_{cli}$$

$$= -\left(S_i(w_i) + K_v\right)e_{ci} - K_v\tilde{v}_i + R_i^{dT}\tilde{W}_{cli}^T\hat{\sigma}_{cli}^T + \varsigma_{cli} \tag{197}$$

with $\varsigma_{cli} = R_i^{dT}W_{cli}^T\tilde{\sigma}_{cli}^T + R_i^{dT}\varepsilon_{cli} - \tau_{d1i}$, $\tilde{W}_{cli} = W_{cli} - \hat{W}_{cli}$ and $\tilde{\sigma}_{cli} = \sigma_{cli} - \hat{\sigma}_{cli}$. Further $\left\|R_i^d\right\|_F = R_{iMax}^d$ for a known constant R_{iMax}^d, and $\left\|\varsigma_{cli}\right\| \leq \varsigma_{Mc1i}$ for a computable constant

$\varsigma_{Mc1i} = R_{iMax}^d\varepsilon_{Mc1i} + 2R_{iMax}^dW_{Mc1i}\sqrt{N_{c1}} + M_{Mi}\tau_{Mi}$ where M_{Mi} is defined in previous sections, with N_{c1} being the number of hidden layer neurons.

The rotational torques controller, u_{2i}, is addressed next. Take the first derivative of (189), multiply with J_i, substitute the UAV dynamics (139), and add and subtract $T_i^T e_{\Theta i}$ to get

$$J_i\dot{e}_{wi} = J_i\dot{w}_i^d - J_i\dot{w}_i$$

$$= \left(J_i\dot{w}_i^d - S_i(J_iw_i)w_i - N_{2i}(w_i) + T_i^T e_{\Theta i}\right) - u_{2i} - \tau_{d2i} - T_i^T e_{\Theta i}$$

$$= f_{c2i}(x_{c2i}) - u_{2i} - -\tau_{d2i} - T_i^T e_{\Theta i} \tag{198}$$

where $f_{c2i}(x_{c2i}) = f_{c2i} = J_i\dot{w}_i^d - S_i(J_iw_i)w_i - N_{2i}(w_i) + T_i^T e_{\Theta i} \in \mathbb{R}^3$ is an uncertain function and approximated through a NN as $f_{c2i}(x_{c2i}) = W_{c2i}^T\sigma(V_{c2i}^Tx_{c2i}) + \varepsilon_{c2i}$ by target weights W_{c2i}^T, V_{c2i}^T such that $\left\|W_{c2i}\right\|_F \leq W_{Mc2i}$ for a known constant W_{Mc2i} and ε_{c2i} is the function approximation error such that $\left\|\varepsilon_{c2i}\right\| \leq \varepsilon_{Mc2i}$ for a known constant ε_{Mc2i}. The estimated

function is given with the estimated NN weights as $\hat{f}_{c2i}\left(x_{c2i}\right)=\hat{W}_{c2i}^{T}\sigma\left(V_{c2i}^{T}\hat{x}_{c2i}\right)=\hat{W}_{c2i}^{T}\hat{\sigma}_{c2i}$

where $\hat{W}_{c2i}$ is the NN estimate of W_{c2i} and

$$\hat{x}_{c2i}=\left[1,\hat{w}_{i}^{T},\dot{\hat{\Omega}}_{i}^{dT},\tilde{\Theta}_{i}^{dT},e_{\Theta i}^{T},\hat{w}_{j}^{T},\dot{\hat{\Omega}}_{j}^{dT},\tilde{\Theta}_{j}^{dT},e_{\Theta j}^{T}\right]^{T}\forall j\in N_{i}$$ is the NN input in terms of observer

states of ith UAV and the neighbor UAVs and virtual controller estimates. Since the actual

and the desired angular velocities are not measurable and estimated, the estimated velocity

tracking error is given as

$$\hat{e}_{wi}=\hat{w}_{i}^{d}-\hat{w}_{i}=e_{wi}-\tilde{w}_{i}^{d}+\tilde{w}_{i}\ . \tag{199}$$

The rotation torque control input can be given as

$$u_{2i}=\hat{f}_{c2i}+K_{w}\hat{e}_{wi}\ . \tag{200}$$

The closed loop angular velocity tracking error dynamics (198)comes along with

the controller (200) and adding and subtracting $W_{c2i}^{T}\hat{\sigma}_{c2i}$

$$J_{i}\dot{e}_{wi}=\tilde{W}_{c2i}^{T}\hat{\sigma}_{c2i}-K_{w}e_{wi}+K_{w}\tilde{w}_{i}^{d}-K_{w}\tilde{w}_{i}-T_{i}^{T}e_{\Theta i}+\varsigma_{c2i} \tag{201}$$

where $\tilde{W}_{c2i}^{T}=W_{c2i}^{T}-\hat{W}_{c2i}^{T}$, $\varsigma_{c2i}=\varepsilon_{c2i}+W_{c2i}^{T}\tilde{\sigma}_{c2i}-\tau_{d2i}$ and $\tilde{\sigma}_{c2i}=\sigma_{c2i}-\hat{\sigma}_{c2i}$. Further,

$\left\|\varsigma_{c2i}\right\|\leq\varsigma_{Mc2i}$ for a computable constant $\varsigma_{Mc2i}=\varepsilon_{Mc2i}+2W_{Mc2i}\sqrt{N_{c2i}}+\tau_{dMi}$ where N_{c2i} is the

number of hidden layer neurons.

Combine both translational and rotational velocity tracking errors as

$e_{Si}=\left[e_{ci}^{T}\quad e_{wi}^{T}\right]^{T}$ whose closed loop dynamics are (197) and (201), respectively. Then, the

overall velocity tracking error dynamics are given as

$$\overline{J}_{i}\dot{e}_{Si}=A_{di}^{T}\tilde{f}_{ci}-\left(K_{S}+S_{Si}\left(w_{i}\right)\right)e_{Si}-K_{S}\tilde{V}_{i}-\overline{T}_{i}^{T}\overline{e}_{\Theta i}+K_{S}\tilde{\tilde{w}}_{i}^{d}+\varsigma_{i} \tag{202}$$

where $\bar{J}_i = \begin{bmatrix} I_{3\times3} & 0_{3\times3} \ ; & 0_{3\times3} & J_i \end{bmatrix} \in \mathbb{R}^{6\times6}$ is a constant,

$K_S = \begin{bmatrix} K_v & 0_{3\times3} \ ; & 0_{3\times3} & K_w \end{bmatrix} > 0 \in \mathbb{R}^{6\times6}, S_{Si}(w_i) = \begin{bmatrix} S_i(w_i) & 0_{3\times3} \ ; & 0_{3\times3} & 0_{3\times3} \end{bmatrix} \in \mathbb{R}^{6\times6},$

$e_{Si}^T S_{Si}(w_i) e_{Si} = 0 , \bar{T}_i = \begin{bmatrix} 0_{3\times6} \ ; & 0_{3\times3} & T_i \end{bmatrix}, \bar{e}_{\Theta i} = \begin{bmatrix} 0_{1\times3} & e_{\Theta i}^T \end{bmatrix}^T , \ \tilde{\bar{w}}_i^d = \begin{bmatrix} 0_{1\times3} & \tilde{w}_i^{dT} \end{bmatrix}^T ,$

$\varsigma_{ci} = \begin{bmatrix} \varsigma_{c1i}^T & \varsigma_{c2i}^T \end{bmatrix}^T \in \mathbb{R}^6$, and $\|\varsigma_{ci}\| \le \varsigma_{Mci}$ for a positive computable constant

$\varsigma_{Mci} = \sqrt{\varsigma_{Mci}^2 + \varsigma_{Mci}^2}$.

Next, *Theorem* 2 is provided to show the stability.

Theorem 2: Given the dynamics of ith quadrotor UAV (139) in a group of UAVs, let the NN observer be defined by (156) and (157) with the NN update law for the observer provided by (160). Given a time-invariant reference points for each UAV in the network, let the desired consensus velocity for the UAV to track be defined by (171) with the desired pitch and roll angles defined by (184) and (185), respectively. Let the NN virtual controller be given by (191) and (192) with the NN update law given by (193). Let the dynamic NN controller for thrust and rotational torques be defined by (196) and (200), respectively, with the NN update law

$$\dot{\hat{W}}_{ci} = F_c \hat{\sigma}_{ci} (A_{di} \dot{e}_{Si}) - \kappa_{c1} F_c \hat{W}_{ci} \tag{203}$$

where $F_c = F_c^T > 0$ and $\kappa_{c1} > 0$ are constant design parameters. Then, there exists positive design constants $K_{o1}, K_{o2}, K_{o3}, K_{\Omega1}, K_{\Omega2}$ and $K_{\Omega3}$, and positive definite design matrices K_v, K_w, K_ρ and K_Θ such that the UAVs reach consensus on their regulation errors on x, y and z directions. That is, the observer estimation error $\tilde{X}_{\xi i}$ and $\tilde{V}_{\xi i}$, the NN observer weight estimation errors $\tilde{W}_{oi}$, the virtual control estimation errors $\tilde{\Theta}_i^d, \tilde{w}_i^d$, the virtual

control NN weight estimation errors $\tilde{W}_{\Omega i}$, the consensus and orientation errors, and velocity tracking errors $\delta_i, e_{\Theta i}$ and e_{Si}, respectively, and the dynamic controller NN weight estimation errors $\tilde{W}_{ci}$ are all SGUUB.

Proof: Define the combined formation Lyapunov function

$$L_{UAV} = \sum_{i=1}^{N} L_{UAVi} \tag{204}$$

with

$$L_{UAVi} = K_{SM}^2 L_{oi} + K_{SM}^2 L_{\Omega i} + L_{ci} \tag{205}$$

where $L_{oi}, L_{\Omega i}$ are given in (161) and (194), respectively, K_{SM} is the maximum singular value of K_S, and

$$L_{ci} = \frac{1}{2}\left(\delta_i^T \delta_i + e_{\Theta i}^T e_{\Theta i} + e_{Si}^T e_{Si} + tr\left\{ \tilde{W}_{ci}^T F_c^{-1} \tilde{W}_{ci} \right\} \right).$$

Now, observe the Lyapunov derivative $\dot{L}_{ci} = \delta_i^T \dot{\delta}_i + e_{\Theta i}^T \dot{e}_{\Theta i} + e_{Si}^T \dot{e}_{Si} + tr\left\{ \tilde{W}_{ci}^T F_c^{-1} \dot{\tilde{W}}_{ci} \right\}$

and substitute the closed loop error dynamics (172), (190), and (202) to get

$$\dot{L}_{ci} = -\delta_i^T K_\rho \delta_i + \delta_i^T R_i e_{ci} - e_{\Theta i}^T K_\Theta e_{\Theta i} - e_{Si}^T K_S e_{Si} - e_{Si}^T K_S \tilde{V}_i$$

$$+ e_{Si}^T K_S \tilde{\bar{w}}_i^d + e_{Si}^T \varsigma_{ci} + tr\left\{ \tilde{W}_{ci}^T \left(F_c^{-1} \dot{\tilde{W}}_{ci} + \hat{\sigma}_{ci} \left(A_d e_{Si} \right)^T \right) \right\} \tag{206}$$

after some simplifications. Define $e_{Ki} = \begin{bmatrix} \delta_i^T & e_{\Theta i}^T \end{bmatrix}^T$, $\Pi_i = diag\left\{ R_i, 0_{3 \times 3} \right\}$,

$K_K = diag\left\{ K_\rho, K_\Theta \right\}$ and substitute the NN weight update law (203) in (206) to get

$$\dot{L}_{ci} = -e_{Ki}^T K_K e_{Ki} - e_{Si}^T K_S e_{Si} + e_{Ki}^T \Pi_i e_{Si} - e_{Si}^T K_S \tilde{V}_i$$

$$+ e_{Si}^T K_S \tilde{\bar{w}}_i^d + e_{Si}^T \varsigma_{ci} + tr\left\{ \tilde{W}_{ci}^T \left(F_c^{-1} \dot{\tilde{W}}_{ci} + \hat{\sigma}_{ci} \left(A_d e_{Si} \right)^T \right) \right\}.$$

Observe that $tr\left\{\tilde{W}_{ci}^T\left(W_{ci}-\tilde{W}_{ci}\right)\right\}\leq\left\|\tilde{W}_{ci}\right\|_F W_{\Omega i}-\left\|\tilde{W}_{ci}\right\|_F^2,\left\|\tilde{\tilde{w}}_i^d\right\|=\left\|\tilde{w}_i^d\right\|$, and constants

Π_M,W_{Mc} exist such that $\left\|\Pi_i\right\|<\Pi_M$ and $\left\|W_{ci}\right\|\leq W_{Mi}$. Then, complete the squares with

respect to $\left\|e_{Ki}\right\|,\left\|\tilde{W}_{ci}\right\|_F$ and $\left\|e_{Si}\right\|$ to get an upper bound for $\dot{L}_{ci}$ as

$$\dot{L}_{ci}\leq-\frac{K_{Km}}{2}\left\|e_{Ki}\right\|^2-\frac{1}{2}\left(K_{Sm}-\frac{\Pi_M^2}{K_{Km}}-2\right)\left\|e_{Si}\right\|^2-\frac{\kappa_{c1}}{6}\left\|\tilde{W}_{ci}\right\|_F^2+\frac{1}{2}\left(K_{SM}^2+3\frac{\left(A_{dM}\sqrt{N_{ci}}\right)^2}{\kappa_{c1}}\right)\left\|\tilde{V}_i\right\|^2$$

$$+\frac{1}{2}\left(K_{SM}^2+3\frac{\left(A_{dM}\sqrt{N_{ci}}\right)^2}{\kappa_{c1}}\right)\left\|\tilde{w}_i^d\right\|^2+\eta_{ci}\tag{207}$$

where K_{Sm},K_{Km} are the minimum singular values of K_S and K_K respectively, K_{KM} is

the maximum singular value of K_K. $\eta_{ci}=\kappa_{c1}W_{Mci}^2/2+\varsigma_{cMi}/\left(2K_{Sm}\right)$, and $\left\|A_d\right\|_F\leq A_{dM}$ for

a known constant A_{dM}.

Now, the derivative of the Lyapunov function (205) which deals with the observer

estimation errors as well will be given. Define the velocity estimation errors of neighbor

UAVs' of the ith UAV as $\tilde{V}_{n\xi i}$ by excluding its own velocity estimation error, $\tilde{V}_i$ from $\tilde{V}_{\xi i}$

. Realize that the triangular inequality can be utilized to show that $\left\|\tilde{V}_{\xi i}\right\|\leq\left\|\tilde{V}_{n\xi i}\right\|+\left\|\tilde{V}_i\right\|$. The

upper bounds (167), (195), (207) for all Lyapunov functions is combined as

$$\dot{L}_{UAVi}\leq-K_{SM}^2\left(\left(\kappa_{o1}\left(K_{o1}-K_{o3}\right)-2N_{oi}\right)/2\kappa_{o1}\right)\left\|\tilde{X}_{\xi i}\right\|^2$$

$$-\frac{K_{SM}^2}{2}\left(K_{o3}-\frac{2N_{oi}}{\kappa_{o1}}-3\frac{\left(A_{dM}\sqrt{N_{ci}}\right)^2}{\kappa_{c1}K_{SM}^2}\right)\left\|\tilde{V}_i\right\|^2$$

$$-\frac{K_{SM}^2}{2}\left(K_{o3}-\frac{2N_o}{\kappa_{o1}}\right)\left\|\tilde{V}_{n\xi i}\right\|^2 -\frac{K_{SM}^2}{4}\kappa_{o1}\left\|\tilde{W}_{o\xi i}\right\|_F^2 -K_{SM}^2\left(K_{\Omega1}-K_{\Omega3}-\frac{N_{\Omega i}}{\kappa_{\Omega1}}\right)\left\|\tilde{\Theta}_i^d\right\|^2$$

$$-\frac{K_{SM}^2}{2}\left(K_{\Omega3}-\frac{2N_{\Omega i}}{\kappa_{\Omega1}}-1-3\frac{\left(A_{dM}\sqrt{N_{ci}}\right)^2}{\kappa_{c1}K_{SM}^2}\right)\left\|\tilde{w}_i^d\right\|^2$$

$$-\frac{K_{Km}}{2}\left\|e_{Ki}\right\|^2 -\frac{1}{2}\left(K_{Sm}-\frac{\Pi_M^2}{K_{Km}}-2\right)\left\|e_{Si}\right\|^2 -\frac{\kappa_{c1}}{6}\left\|\tilde{W}_{ci}\right\|_F^2$$

$$-\frac{\kappa_{o1}K_{SM}^2}{4}\left\|\tilde{W}_{o\xi i}\right\|_F^2 -\frac{\kappa_{\Omega1}K_{SM}^2}{4}\left\|\tilde{W}_{\Omega i}\right\|_F^2 +\eta_{UAVi} \tag{208}$$

with $\eta_{UAVi}=K_{SM}^2\left(\eta_{o\xi i}+\eta_{\Omega i}\right)+\eta_{ci}$. Then, $\dot{L}_{UAVi}<0$ by choosing the controller gain such that

$$K_{o1}>K_{o3}+2N_{oi}/\kappa_{o1},\, K_{o3}>2N_{oi}/\kappa_{o1}+1+3\frac{\left(A_{dM}\sqrt{N_{ci}}\right)^2}{\kappa_{c1}K_{SM}^2}$$

$$K_{\Omega1}>K_{\Omega3}+\frac{N_\Omega}{\kappa_{\Omega1}},\, K_{\Omega3}>\frac{2N_\Omega}{\kappa_{\Omega1}}-1-3\frac{\left(A_{dM}\sqrt{N_{ci}}\right)^2}{\kappa_{c1}K_{SM}^2},$$

$K_{Sm}>\dfrac{\Pi_M^2}{K_{Km}}+2$ and if one of the following inequalities holds:

$$\left\|\tilde{X}_{\xi i}\right\|>\sqrt{\frac{\eta_{UAVi}}{K_{SM}^2\left(\left(\kappa_{o1}\left(K_{o1}-K_{o3}\right)-2N_o\right)/2\kappa_{o1}\right)}} \quad \text{or}\quad \left\|e_{Si}\right\|>\sqrt{\frac{2\eta_{UAVi}}{\left(K_{Sm}-\frac{\Pi_M^2}{K_{Km}}-2\right)}}$$

$$\left\|e_{Ki}\right\|>\sqrt{\frac{2\eta_{UAVi}}{K_{Km}}} \quad \text{or}\quad \left\|\tilde{\Theta}_i^d\right\|>\sqrt{\frac{\eta_{UAVi}}{K_{SM}^2\left(K_{\Omega1}-K_{\Omega3}-\frac{N_\Omega}{\kappa_{\Omega1}}\right)}} \quad \text{or}\quad \text{or}\quad \left\|\tilde{W}_{\Omega i}\right\|_F>\sqrt{\frac{4\eta_{UAVi}}{\kappa_{\Omega1}K_{SM}^2}} \quad \text{or}$$

$$\left\| \tilde{V}_i \right\| > \sqrt{K_{SM}^2 \frac{\eta_{UAVi}}{\left(K_{o3} - \dfrac{2N_{oi}}{\kappa_{o1}} - 1 - 3\dfrac{\left(A_{dM}\sqrt{N_{ci}} \right)^2}{\kappa_{c1}K_{SM}^2} \right)}{2}} \quad \text{or} \quad \left\| \tilde{V}_{n\xi i} \right\| > \sqrt{\frac{\eta_{UAVi}}{\dfrac{K_{SM}^2}{2}\left(K_{o3} - \dfrac{2N_o}{\kappa_{o1}} \right)}} \quad \text{or}$$

$$\left\| \tilde{w}_i^d \right\| > \sqrt{\frac{\eta_{UAVi}}{\dfrac{K_{SM}^2}{2}\left(K_{\Omega 3} - \dfrac{2N_{\Omega i}}{\kappa_{\Omega 1}} - 1 - 3\dfrac{\left(A_{dM}\sqrt{N_{ci}} \right)^2}{\kappa_{c1}K_{SM}^2} \right)}} \quad \text{or}$$

$$\left\| \tilde{W}_{ci} \right\|_F > \sqrt{\frac{6\eta_{UAVi}}{\kappa_{c1}}} \quad \text{or} \quad \left\| \tilde{W}_{oi} \right\|_F > \sqrt{\frac{4\eta_{UAVi}}{\kappa_{o1}K_{SM}^2}} \quad .$$

Since the stability region can be made arbitrarily large, all the error signals are SGUUB [13]. By showing the individual Lyapunovs (205) are negative in the given bounds, one can easily conclude that the combined Lyapunov (204)is also negative.

5. SIMULATION RESULTS

To illustrate the effectiveness of the proposed controller, a group of four followers and a leader UAV are utilized in the simulation section. The Leader UAV is controlled to track a desired trajectory while the followers do not have knowledge about the desired trajectory and are controlled through consensus based formation controllers.

Initial positions, orientations, reference positions, linear and angular velocities are selected as

$$\begin{bmatrix} xL(0) & x1(0) & x2(0) & x3(0) & x4(0) \end{bmatrix} = \begin{bmatrix} 0 & -1.2 & -3.5 & -1.3 & 5.1 \end{bmatrix}$$

$$\begin{bmatrix} yL(0) & y1(0) & y2(0) & y3(0) & y4(0) \end{bmatrix} = \begin{bmatrix} 0 & -1.4 & -3 & -1.2 & 5.1 \end{bmatrix}$$

$$\begin{bmatrix} zL(0) & z1(0) & z2(0) & z3(0) & z4(0) \end{bmatrix} = \begin{bmatrix} 0 & 0 & 0 & 0 & 0 \end{bmatrix},$$

$$\rho_l^d = \begin{bmatrix} 0.1 & 0.1 & 0.1 \end{bmatrix}, \rho_1^d = \begin{bmatrix} 0.1 & 0.4 & 0.1 \end{bmatrix}, \rho_2^d = \begin{bmatrix} -0.2 & -0.2 & 0.1 \end{bmatrix}$$

$$\rho_3^d = \begin{bmatrix} 0.5 & -0.2 & 0.1 \end{bmatrix}, \rho_4^d = \begin{bmatrix} 0.1 & -0.5 & 0.1 \end{bmatrix}.$$

The initial pitch, roll and yaw angles as well as the linear and angular velocities are selected as zero for all four followers and the leader.

The dynamics parameters of all the UAVs are selected as $m = 0.9 \,\mathrm{kg}$, J=diag$\{0.32, 0.42, 0.63\} \in \mathbb{R}^{3 \times 3}$, $g = 9.81$. The desired trajectory for the leader is selected as $x_l^d = A_x \cos(t * f_r)(1 - e^{-q_2 t^2}))$, $y_l^d = A_y \sin(t * f_r)(1 - e^{-q_2 t^2}))$, $z_l^d = A_z(1 - e^{q_1 t}))$ where $A_x = 5, A_y = 5, A_z = 10$, $q_1 = .25, q_2 = .05, f_r = 0.01\pi$. The controller gains are selected as $K_\delta = \mathrm{diag}\{0.01, 0.01, 0.03\}$, $K_{o1} = K_{o2} = \mathrm{diag}\{22, 60, 25\}$, $K_{\Omega 1} = 30, K_{\Omega 2} = 80, K_{\Omega 3} = 25$, $k_{\delta x} = 15, k_{\delta y} = 15, k_{\delta z} = 30$, $K_\Theta = \mathrm{diag}\{20, 20, 35\}$, $K_w = diag\{35, 35, 40\}$, and the gain

selections satisfy the controller gain constraints in the theorem statements. The NN

parameters are selected as $F_o = 0.1, \kappa_{o1} = 0, \kappa_{o2} = 0.01, \quad F_c = 0.1, \kappa_{c1} = 0, \kappa_{c2} = 0.01,$

$F_\Omega = 0.1, \kappa_{\Omega 1} = 0, \kappa_{\Omega 2} = 0.01$. All the time varying NN weights are selected as zero initially

and the hidden layer neurons are initiated randomly in the interval $[-0.5, 0.5]$.

In Figure 5.2, the trajectories of all four UAVs and the leader UAV is plotted. The

simulation took 90 seconds in total. During the first seven seconds, the Leader UAV, the

first and Second UAV moved only as it is shown on the communication topology graph,

left part of Figure 5.1. After the 7th second, the third and the fourth UAV joined the group

as it is shown in the right side of Figure 5.1. The first and the second UAVs communicate

directly with the leader UAV; however, the third UAV receives the second UAV's

information and the fourth UAV receives the first UAV's information. That is, the third

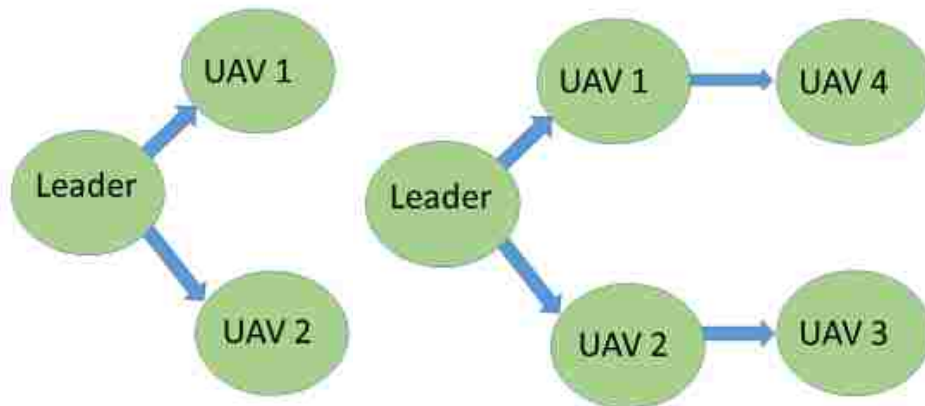and fourth UAVs do not directly communicate with the leader.

Figure 5.1 Communication topologies before and after the 7th second.

As it is shown in Figure 5.3 the first two UAVs quickly reach consensus with the leader UAV. Note that the formation errors of the third and fourth UAVs are initially large since they do not start moving until the 7th second of the simulation when they join the communication topology. As time progresses, each UAV achieves its required position within the formation with bounded error.
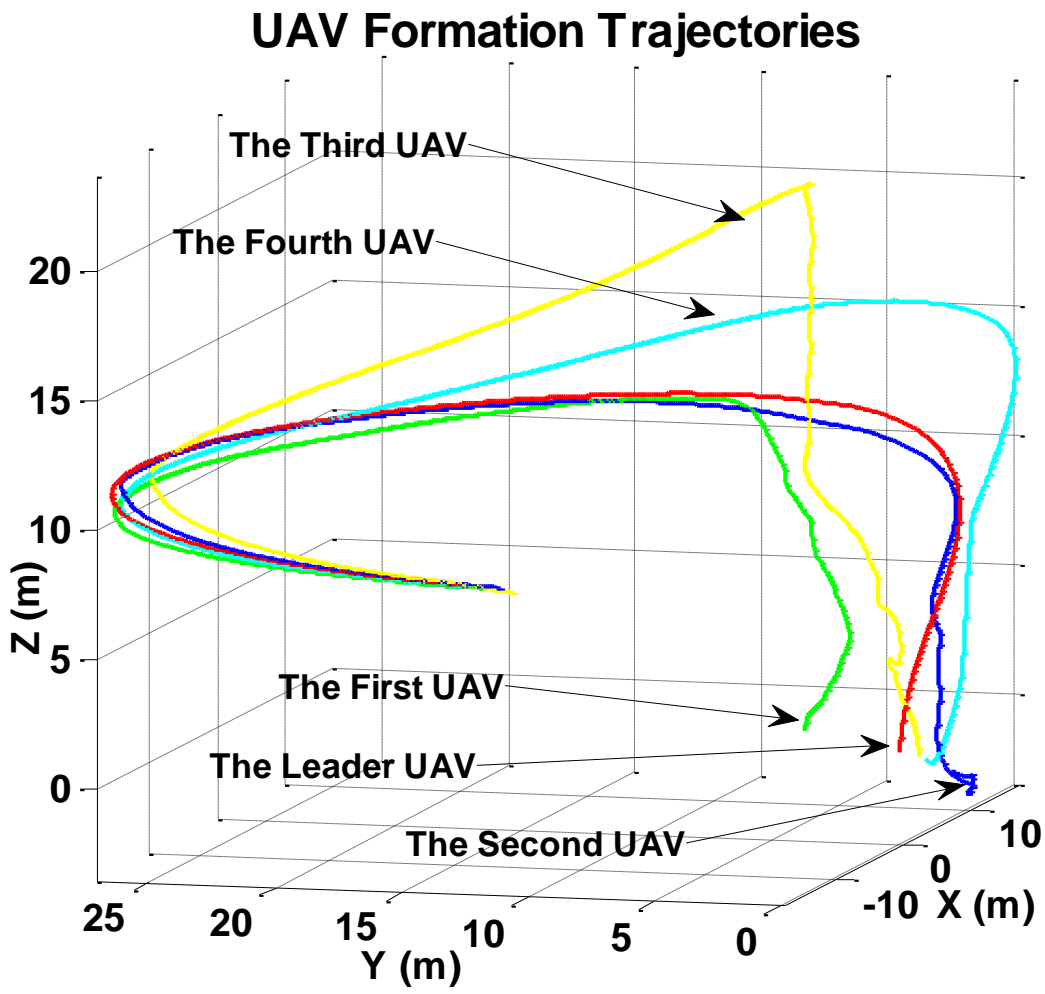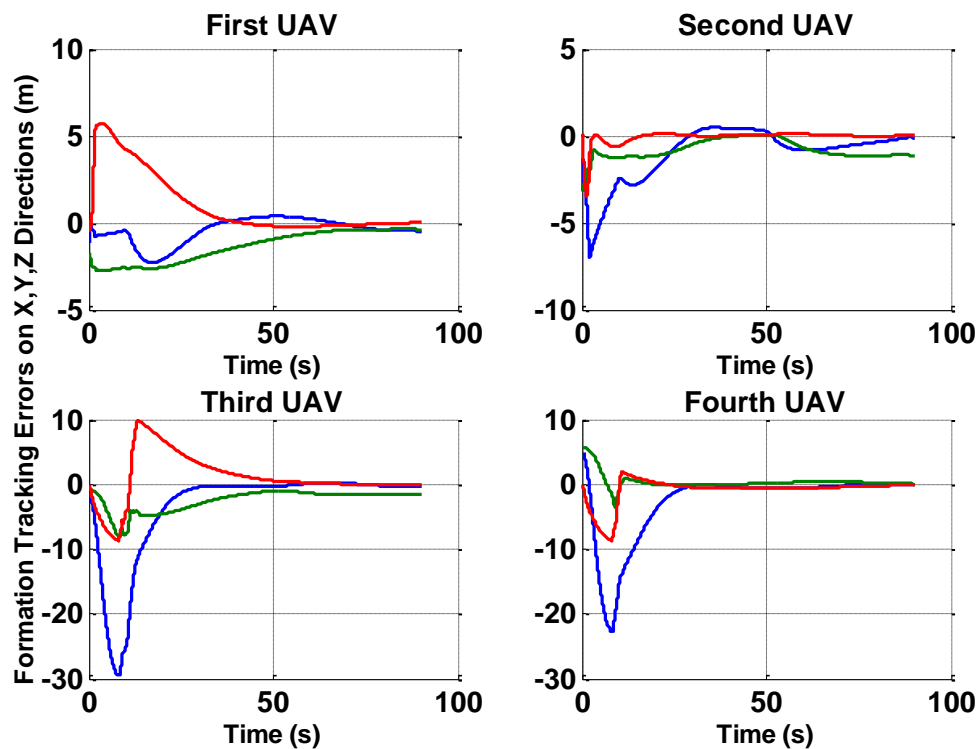

Figure 5.2 UAV trajectories.

Figure 5.3 Formation tracking errors on all three axes.

Figure 5.4 depicts the linear velocity observer estimation errors of all four follower UAVs on $x, y,$ and z directions. After an initial transient response, it is observed that the observer errors converge to the true values within a small bound as predicted by the theory. NN weight estimates are presented in Figure 5.5. As predicted by the theory, the steady state NN weights converge to bounded values.
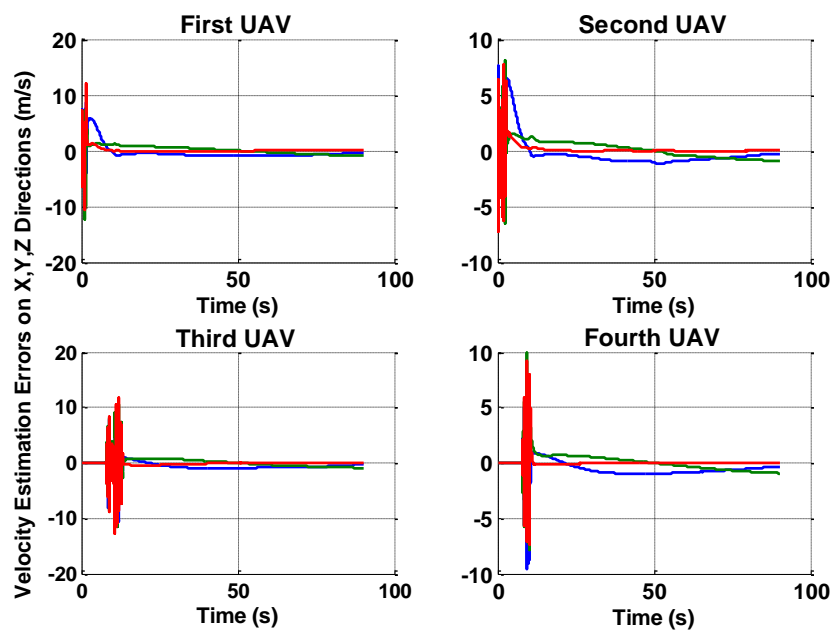
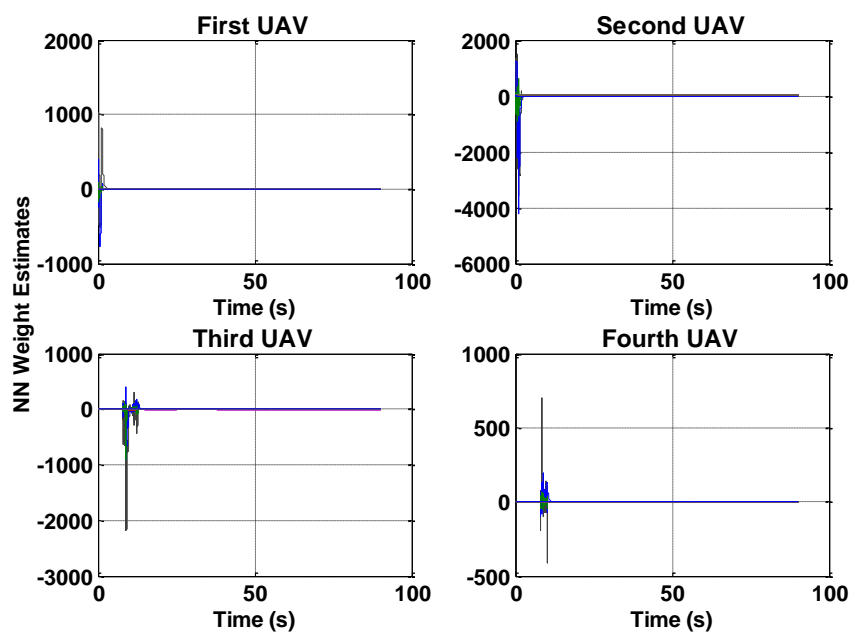Figure 5.4 Estimated linear velocity tracking errors of all four follower UAVs.

Figure 5.5 NN weight estimates of four UAVs.

6. CONCLUSION AND FUTURE WORK

A novel output feedback consensus based formation controller was developed for a group of underactuated quadrotor UAVs. The follower UAVs kept the desired formation by using their time varying neighbor's positions, orientations, and estimated velocities while the leader tracked a pre-defined trajectory. An NN-based adaptation was utilized to estimate velocities through positions and orientations as well as to learn the uncertain UAV dynamics, and a novel 'size reduction matrix' scheme was introduced which allowed for UAVs to join or leave the formation. Simulation results verified that the performance of the proposed output feedback controller was consistent with the theoretical conjectures developed within this paper.

Considering obstacle avoidance while keeping formation can be considered as a desirable future work. Optimal adaptive consensus-based formation control of quadrotor UAV formation can also be considered.

REFERENCES

[1]   T. Dierks and S. Jagannathan, "Neural network control of quadrotor UAV formations," *American Control Conference, 2009. ACC '09.* , June 2009, pp.2990-2996.

[2]   B. Zhao, B. Xian, Y. Zhang and X. Zhang, "Nonlinear Robust Adaptive Tracking Control of a Quadrotor UAV Via Immersion and Invariance Methodology," in *IEEE Transactions on Industrial Electronics,* , vol.62, no.5, pp.2891-2902.

[3]   B. J. Bialy, J. Klotz, K. Brink and W. E. Dixon, "Lyapunov-based robust adaptive control of a quadrotor UAV in the presence of modeling uncertainties," in *2013 American Control Conference (ACC),* pp.13-18, 17-19 June 2013.

[4]   Y. Kuriki and T. Namerikawa, "Formation control of UAVs with a fourth-order flight dynamics," *2013 IEEE 52nd Annual Conference on Decision and Control (CDC),* pp.6706,6711, Dec. 2013.

[5]   W. Yinqiu, W. Qinghe and W. Yao, "Distributed consensus protocols for coordinated control of multiple quadrotors under a directed topology," *IET Control Theory & Applications*, vol.7, no.14, pp.1780,1792, September 19 2013.

[6]   W. Yinqiu; W. Qinghe, W. Yao and Y. Di, "Consensus algorithm for multiple quadrotor systems under fixed and switching topologies," *Journal of Systems Engineering and Electronics,* vol.24, no.5, pp.818,827, Oct. 2013.

[7]   Y. Zhou, X. Dong, G. Lu and Y. Zhong, "Time-varying formation control for unmanned aerial vehicles with switching interaction topologies," *2014 International Conference on Unmanned Aircraft Systems (ICUAS),* pp.1203,1209, 27-30 May 2014.

[8]   Cheng Hui; Chen Yousheng; Wong Wing Shing, "Trajectory tracking and formation flight of autonomous UAVs in GPS-denied environments using onboard sensing," *Guidance, Navigation and Control Conference (CGNCC), 2014 IEEE Chinese* ,pp.2639,2645, 8-10 Aug. 2014.

[9]   Seo, J.H.; Back, J.; Kim, H.; Shim, H., "Output feedback consensus for high-order linear systems having uniform ranks under switching topology," *Control Theory & Applications, IET* , vol.6, no.8, pp.1118,1124, May 17 2012.

[10]   Huaqing Li; Xiaofeng Liao; Tingwen Huang, "Second-Order Locally Dynamical Consensus of Multiagent Systems With Arbitrarily Fast Switching Directed Topologies," *Systems, Man, and Cybernetics: Systems, IEEE Transactions on* , vol.43, no.6, pp.1343,1353, Nov. 2013.

[11] Jing Wang; Obeng, M.; Zhihua Qu; Tianyu Yang; Staskevich, G.; Abbe, B., "Discontinuous cooperative control for consensus of multiagent systems with switching topologies and time-delays," *Decision and Control (CDC), 2013 IEEE 52nd Annual Conference on*, vol., no., pp.7333,7338, 10-13 Dec. 2013.

[12] G. Hoffmann, H. Huang, S.Waslander, and C. Tomlin, "Quadrotor helicopter flight dynamics and control: Theory and experiment," in *Proc.AIAA Guid. Navigat. Control Conf Exhibit*, Aug. 2007, pp. 1–20.

[13] T. Dierks and S. Jagannathan, "Output feedback control of a quadrotor UAV using neural networks," IEEE Trans. Neural Netw., vol. 21, no. 1, pp. 50–66, Jan. 2010.

[14] W. Ren and E. Atkins, "Distributed multi-vehicle coordinated control via local information exchange," *International Journal of Robust and Nonlinear Control*, vol. 17, no. 10-11, pp. 1002–1033, 2007.

[15] R. Olfati-Saber and R. M. Murray, 'Consensus problems in networks of robot switching topology and time-delays', *IEEE Trans. on Automatic Control*, vol. 49, no. 9,pp. 1520–1533, Sep. 2004.

[16] C. Kecai, J. Bin, Y. Dong, "Distributed consensus of multiple nonholonomic mobile robots," *IEEE/CAA Journal of Automatica Sinica,* vol.1, no.2, pp.162-170, April 2014.

[17] D. Di Paola, D. Naso, B. Turchiano, "Consensus-based robust decentralized task assignment for heterogeneous robot networks," *American Control Conference (ACC), 2011*, June 2011, pp.4711-4716.

[18] X. Geng, "Consensus-reaching of Multiple Robots with Fewer Interactions," *2009 WRI World Congress on Computer Science and Information Engineering,* , March 2009, pp.249-253.

[19] F. L. Lewis, S. Jagannathan, and A. Yesilderek, *Neural Network Control of Robot Manipulators and Nonlinear Systems*. London, U.K.:Taylor & Francis, 1999.

[20] E. Semsar-Kazerooni and K. Khorasani, "Switching control of a modified leader-follower team of agents under the leader and network topological changes," in *IET Control Theory & Applications*, vol. 5, no. 12, pp. 1369-1377, August 2011.

SECTION

2. CONCLUSIONS AND FUTURE WORK

In this dissertation, consensus-based formation controller implementation for a network of mobile robots and UAVs is presented. A finite horizon optimal consensus-based formation controller, a novel hybrid regulation-formation controller was developed by using a novel blended velocity tracking error approach and an event-based formation controller implementation for a network of mobile robots. Additionally, a novel output feedback consensus-based formation controller was developed for a group of under-actuated quadrotor UAVs. The analytical results were verified using the simulation examples and the efficiency of the controllers' execution was demonstrated.

2.1   CONCLUSIONS

In this dissertation, first, a finite horizon optimal consensus-based formation controller was designed for mobile robot formation in the presence of uncertain robot dynamics. The consensus-based control was derived for a formation of mobile robots by taking into account their dynamics. Subsequently, the cost function derived as a function of regulation and formation errors was able to generate optimal inputs to each robot such that the entire formation can travel in consensus from an initial position to the goal position. An NN identifier generated the formation dynamics while the time-varying value function approximated the solution to the HJB equation. Simulation results confirmed the theoretical conclusions.

The results of the second paper provided controllers to the user to regulate a single robot to a desired posture and for a group of nonholonomic robots to reach consensus on their regulation errors to achieve a desired posture in a desired shape. This was accomplished through the development of two novel continuous time regulation and formation controllers for nonholonomic mobile robots. Then, a novel hybrid regulation-formation controller was developed by using a novel blended velocity tracking error approach. Time-varying Lyapunov functions were used to prove the stability of the hybrid approach, and simulation results verified the performance improvements of the proposed approach, which represents an improvement over traditional hard switched hybrid control architectures. The blended velocity tracking error approach reduced the size of the discontinuity at the switching conditions, which led to smaller peak velocity tracking errors and smaller peak required torques at the switching conditions. The blended hybrid controller is beneficial when multiple tasks need to be accomplished at the same time.

The third paper presents an event-based formation controller implementation for a network of mobile robots. The NN-based event-sampled torque control of mobile robots was able to bring the robots to consensus by stabilizing the formation as well as velocity tracking errors due to event sampled measurement errors, NN reconstruction errors and bounded disturbance. The event-sampling mechanism was able to generate additional events so that the formation error remains bounded and due to asynchronous mode, communication overhead is minimized. In the case of minimal communication, oscillatory behavior is observed initially although this improves over time while full communication is established with other robots thereby enhancing formation control. The event-sampling condition at each robot and the NN adaptation rules were derived using the Lyapunov

stability analysis. Analytical results were verified using simulation examples and the efficiency of the event-sampled controller execution was demonstrated in the presence of minimal communication information and with full communication overhead. It was observed that the robots reached consensus even in the presence of minimal communication. However, the consensus was reached much faster and the robots moved with much less oscillation when full communication was available to all the robots

A novel output feedback consensus-based formation controller was developed for a group of underactuated quadrotor UAVs. The follower UAVs kept the desired formation by using their time varying neighbor's positions orientations and estimated velocities while the leader tracked a pre-defined trajectory. NN-based adaptation was utilized to estimate velocities through positions and orientations as well as to learn the uncertain UAV dynamics.

2.2   FUTURE WORK

Considering obstacle avoidance while keeping formation can be considered as a desirable future work for both nonholonomic mobile robot and quadrotor UAV applications. In the hybrid analysis, obstacle avoidance controller can be added as a third task in addition to consensus seeking and regulation tasks.

REFERENCES

[1]   Hong Y, Hu J, Gao L. Tracking control for multi agent consensus with an active leader   and variable topology. *Automatic;*42(7):1177-1182, 2006.

[2]   Qu Z. Cooperative control of dynamics systems. *New York:Springer- Veriag,2009.*

[3]   Ren W, Beard R. Distributed consensus in multi-vehicle cooperative control. *New York: Springer-Veriag,2009.*

[4]   Tian Y, Liu C. Consensus of multi agent systems with diverse input and communication delays. *IEEE Transactions on Systems, Man, and Cybernetics-*Part B,40(2):362-370,2010.

[5]   Cao Y, Li Y, Ren W, Chen Y. Distributed coordination of networked fractional-order systems. *IEEE Transaction on Systems, Man and Cybernetics.-*Part B; 40(2):362-370, 2010.

[6]   Olfati-Saber R, Murray R M. Consensus problems in networks of agents with switching topology and time-delays. *IEEE Transactions on Automatic Control* 2004; 49(9): 1520-1513.

[7]   Long X, Jiang J. Information consensus in partial synchronous network of multi-robot systems. *CIMCA* 2008*, IAWTIC* 2008*, and ISE 2008.*

[8]   Ren W, Beard R. Consensus seeking in multiagent systems under dynamically changing interaction topologies. *IEEE Transaction on Automatic Control,* 50(5); 655-661, 2005.

[9]   Bauso D, Giarre L, Pesenti R. Consensus for networks with unknown but bounded disturbances. *SIAM journal of Control and Optimization* 48 (3) (2009) 1756-1770; Doi:10.1137/060678786.

[10]   Feng S, Zhang H. Formation control for wheeled mobile robots based on consensus protocol. *Information and Automation (ICIA), 2011 IEEE International Conference on* , vol., no., pp.696-700, 6-8 June 2011.

[11]   Listmann K D, Masalawala M V, Adamy J. Consensus for formation control of nonholonomic mobile robots. *IEEE International Conference on Robotics and Automation, 2009. ICRA '09,* pp.3886-3891, 12-17 May 2009.

[12]   Sheng L, Pan Y J, and Gong X. Consensus formation control for a class of networked multiple mobile robot systems. *Journal of Control Science and Engineering,* 2012, Article ID 150250, 12 pages, 2012; doi:10.1155/2012/150250.

[13]   Guzey H M, Jagannatan S. Adaptive neural network consensus based control of robot formations. *Proceedings of SPIE* Vol. 8741, 87410M (2013).

[14]   Semsar-Kazerooni E, Khorasani K. Optimal consensus algorithms for cooperative team of agents subject to partial information. *Automatica*, vol. 44, no. 11, pp; 2766–2777,2008.

[15]   Heydari A, Balakrishan S N. Finite-horizon control-constrained nonlinear optimal control using single network adaptive critics. *IEEE Trans. on Neur. Net. and Learni. Syst.*, vol. 24, pp. 145–157, 2013.

[16]   Vrabie D, Vamvoudakis K, Lewis F. Adaptive optimal controllers based on generalized policy iteration in a continuous-time framework. *Proc. of the IEEE Mediterranean Conf. on Control and Automation*, pp. 1402-1409, June 2009.

[17]   Frihauf P, Krstic M, Basar T. Finite horizon LQ control for unknown discrete-time linear systems via extremum seeking. *Proc. of IEEE Contr. Decision Conf.*, pp. 5717-5722, 2012.

[18]   Dierks T, Jagannathan S. Online optimal control of affine nonlinear discrete-time systems with unknown internal dynamics by using time-based policy update. *IEEE Trans. Neural Networks*, vol. 23, pp. 1118–1129, 2012.

[19]   Beard R. Improving the closed-loop performance of nonlinear systems. *Ph.D. dissertation*, Rensselaer Polytechnic Institute, USA, 1995.

[20]   P. Tabuada, 'Event-triggered real-time scheduling of stabilizing control tasks,' *IEEE Transactions on Automatic Control,* 52(9), pp.1680-1685, 2007.

[21]   A. Sahoo, H. Xu, and S. Jagannathan, 'Near optimal event-triggered control of nonlinear discrete-time systems using neuro-dynamic programming,' *IEEE Transactions on Neural Networks and Learning systems*, (In press), 2015.

[22]   M. Guinaldo, D. Lehmann, J. Sanchez, S. Dormido and K. H. Johansson 'Distributed event-triggered control with network delays and packet losses,' *IEEE 51st Annual Conference on Decision and Control (CDC),* December, pp. 1-6, 2012.

[23]   X. Wang, and M. D. Lemmon, 'Event-triggering in distributed networked control systems,' *IEEE Transactions on Automatic Control*, 56(3), pp.586-601, 2011.

[24]   T. Dierks, S. Jagannathan, "Neural network control of quadrotor UAV formations," *American Control Conference, 2009. ACC '09.* , June 2009, pp.2990-2996.

[25]   B. Zhao, B. Xian, Y. Zhang and X. Zhang, "Nonlinear Robust Adaptive Tracking Control of a Quadrotor UAV Via Immersion and Invariance Methodology," in *IEEE Transactions on Industrial Electronics, ,* vol.62, no.5, pp.2891-2902.

[26]   B. J. Bialy, J. Klotz, K. Brink and W. E. Dixon, "Lyapunov-based robust adaptive control of a quadrotor UAV in the presence of modeling uncertainties," in *2013 American Control Conference (ACC),* pp.13-18, 17-19 June 2013.

[27]   Y. Kuriki and T. Namerikawa, "Formation control of UAVs with a fourth-order flight dynamics," *2013 IEEE 52nd Annual Conference on Decision and Control (CDC),* pp.6706,6711, Dec. 2013.

[28]   W. Yinqiu, W. Qinghe and W. Yao, "Distributed consensus protocols for coordinated control of multiple quadrotors under a directed topology," *IET Control Theory & Applications*, vol.7, no.14, pp.1780,1792, September 19 2013.

[29]   Y. Zhou, X. Dong, G. Lu and Y. Zhong, "Time-varying formation control for unmanned aerial vehicles with switching interaction topologies," *2014 International Conference on Unmanned Aircraft Systems (ICUAS),* pp.1203,1209, 27-30 May 2014.

[30]   Cheng Hui; Chen Yousheng; Wong Wing Shing, "Trajectory tracking and formation flight of autonomous UAVs in GPS-denied environments using onboard sensing," *Guidance, Navigation and Control Conference (CGNCC), 2014 IEEE Chinese* , vol., no., pp.2639,2645, 8-10 Aug. 2014.

[31]   Seo, J.H.; Back, J.; Kim, H.; Shim, H., "Output feedback consensus for high-order linear systems having uniform ranks under switching topology," *Control Theory & Applications, IET* , vol.6, no.8, pp.1118,1124, May 17 2012.

[32]   Huaqing Li; Xiaofeng Liao; Tingwen Huang, "Second-Order Locally Dynamical Consensus of Multiagent Systems With Arbitrarily Fast Switching Directed Topologies," *Systems, Man, and Cybernetics: Systems, IEEE Transactions on* , vol.43, no.6, pp.1343,1353, Nov. 2013.

[33]   Jing Wang; Obeng, M.; Zhihua Qu; Tianyu Yang; Staskevich, G.; Abbe, B., "Discontinuous cooperative control for consensus of multiagent systems with switching topologies and time-delays," *Decision and Control (CDC), 2013 IEEE 52nd Annual Conference on* , vol., no., pp.7333,7338, 10-13 Dec. 2013.

[34]   G. Hoffmann, H. Huang, S.Waslander, and C. Tomlin, "Quadrotor helicopter flight dynamics and control: Theory and experiment," in *Proc.AIAA Guid. Navigat. Control Conf Exhibit*, Aug. 2007, pp. 1–20.

[35]   T. Dierks and S. Jagannathan, "Output feedback control of a quadrotorUAV using neural networks," IEEE Trans. Neural Netw., vol. 21, no. 1,pp. 50–66, Jan. 2010.

[36]   S. Feng and H. Zhang, "Formation control for wheeled mobile robots based on consensus protocol," *IEEE International Conference on Information and Automation (ICIA),* June 2011, pp.696-700.

[37]   M. S. Branicky, "Multiple Lyapunov functions and other analysis tools for switched and hybrid systems," *IEEE Trans. on Automatic Control*, vol.43, no.4, pp.475-482, Apr. 1998.

VITA

Haci Mehmet Guzey was born in Yozgat, Turkey in 1984. He earned his bachelor's degree in Electronics Engineering from Ankara University, Ankara Turkey in 2007. He received a fellowship from Turkish Ministry of Education for graduate education in the USA.

He started his master's degree in Mechanical Engineering at Drexel University in Philadelphia in September 2009 and earned his degree in June 2011. In August 2011 he started his Doctorate of Philosophy in Electrical Engineering at Missouri University of Science and Technology. He worked as a research assistant with Dr. Jagannathan Sarangapani and Dr. Acar. His work was based on adaptive consensus based formation control of unmanned vehicles. He received the degree of Doctor of Philosophy in Electrical Engineering from Missouri University of Science and Technology in December 2016.